

The Role of DNA Methylation in the Regulation of Skeletal Muscle Atrophy, Hypertrophy and Epigenetic ‘Memory’

Robert Arthur Elliston Seaborne
BSc (Hons), MSc, AFHEA

A thesis submitted in partial fulfilment of the requirements of
Liverpool John Moores University

for the degree of
Doctor in Philosophy

May 2018

Authors Declaration

I declare that the work presented in this thesis was performed in accordance with regulations of Liverpool John Moores University and has not been concurrently used for application of any other form of degree or professional qualification at this same University, or any other institute.

Except where otherwise stated by reference and acknowledgement, the work presented in this thesis is entirely my own. Where I have consulted or discussed the published findings of other authors, these have clearly been attributed.

Parts of the work presented here have been published in peer-reviewed journals. Where this is the case, acknowledgements are given to all contributing authors of publications.

List of Submitted, Accepted and Published Work

* Indicates co-primary authorship

Journal Articles:

Sharples, A. P., Stewart, C. E. & **Seaborne, R. A.** (2016). Does skeletal muscle have an ‘epi’-memory? The role of epigenetics in nutritional programming, metabolic disease, aging and exercise. *Aging Cell*. 15, 603-616

Fisher, A. G*, **Seaborne, R. A***, Hughes, T. M., Gutteridge, A., Stewart, C., Coulson, J. M., Sharples, A. P. & Jarvis, J. C. (2017). transcriptomic and epigenetic regulation of disuse atrophy and the return to activity in skeletal muscle. *The Official Publication of the Federation of American Societies of Experimental Biology (FASEB J)*, 31, 5268-5282.

Seaborne, R. A., Strauss, J., Cocks, M., Shepherd, S., O’Brien, T. D., van Someren, K. A., Bell, P. G., Murgatroyd, C., Morton, J. P., Stewart, C. E. & Sharples, A. P. (2018). Human skeletal muscle possesses an epigenetic memory of hypertrophy. *Scientific Reports*, 8, 1898.

Seaborne, R. A., Strauss, J., Cocks, M., Shepherd, S., O’Brien, T. D., van Someren, K. A., Bell, P. G., Murgatroyd, C., Morton, J. P., Stewart, C. E., Mein, C.A. & Sharples, A. P. (2018). Methylome of human skeletal muscle after acute & chronic resistance exercise training, detraining & retraining. *Scientific Data*. Accepted for Publication.

Book Chapters:

Sharples, A. P., **Seaborne, R. A.** & Stewart, C. E. (2018). Epigenetics of Skeletal Muscle Aging. In Moskalev, A., & Vaiserman, A. M. (eds.) *Epigenetics of Aging and Longevity*. Cambridge: MA, Elsevier, page 389-416.

Turner, D. C., Kasper, A. M., **Seaborne, R. A.**, Brown, A. D., Close, G. L. *et al.*, (2018). Exercise Bioengineered Skeletal Muscle in Vitro: Biopsy to Bioreactor. In Rønning, S. B. (eds.) *Myogenesis: Methods and Protocols*, Methods in Molecular Biology. *In Print*.

Note. Only published (as of September 2018) journal articles available in thesis appendix

Abstract:

Skeletal muscle mass is vitally important for the maintenance of health and quality of life into old age, with a plethora of disorders and diseases linked to the loss of this tissue. As a consequence, molecular biologists have extensively investigated both atrophying and hypertrophying skeletal muscle, in order to understand the molecular pathways that are induced to evoke both loss and growth of skeletal muscle. Despite huge progressions in the field, a full understanding of the molecular mechanisms that orchestrate growth and loss in skeletal muscle, remain elusive. In this regard, epigenetics, referring to alterations in gene expression via structural modifications of DNA without fundamental alterations of the DNA code, have recently become a promising area of research, specifically for its role in modulating genetic expression. However, the field of skeletal muscle epigenetics is in its infancy, and as such, there is currently a distinct paucity of research investigating this biological phenomenon. Herein, a genomic approach was utilised to examine the role DNA methylation plays in modulating the response, at both a genetic and phenotypic level, of mammalian skeletal muscle. The methodological and analytical approaches utilised in this thesis identify a number of important, novel and impactful findings. Firstly, it is identified that DNA methylation displays a distinct inverse relationship with gene expression during both muscular atrophy and hypertrophy, these findings are furthered by work identifying that DNA methylation alterations may precede functional changes in gene expression during skeletal muscle hypertrophy. This thesis also elucidated that skeletal muscle possesses an epigenetic memory that creates an enhanced adaptive response to resistance load induced hypertrophy, when the same stimulus was previously encountered. Finally, in human subjects, a number of novel and previously

unstudied gene transcripts were identified that display significantly positive correlations with changes in skeletal muscle mass, as evoked by resistance training.

The data in this thesis demonstrates an important role for DNA methylation in regulating skeletal muscle mass during periods of both muscle atrophy and hypertrophy, respectively. The work presented here may allow for further work to be conducted, expanding our understanding of epigenetics in skeletal muscle and best facilitating the development of therapeutics that may alleviate the detrimental effects observed during periods of skeletal muscle atrophy.

Acknowledgements and Personal Comments:

First, to Dr. Adam Sharples. Your knowledge, support and sheer passion has been a real source of inspiration throughout this process. I hope you look back on this period fondly, and look forward to some exciting work together in the future! To my co-supervisors, Prof. Claire Stewart and Prof. James Morton. You have both been enormous role models for me, and are two people I will aspire to emulate.

I would like to acknowledge the help and support from everyone at LJMU, especially all office and lab staff (specifically George, Gemma, Dean, Emily and Louise). The unrelenting work rate, team-effort and selfless nature of everyone in the department is the primary reason behind its success. A department with a very special culture!

To all of my many friends in Liverpool, of which there are too many to mention, you made the last 6-7 years of my life the best yet. So thank you. Special thank you to my friends from home. It is rare we get to spend time together, but when we do, it feels as if nothing ever changes! A special thanks to my best mate Tom, you are more like a brother than a friend!

To my father, mother and sisters. You mean more to me than I will ever truly be able to express, and wherever I am and whatever I am doing, you will always be the people I care for most! I hope that this work has given you something to be as proud of me, as I am of you – even if you have no idea what it is about!

Finally, a special comment to all those going through a similar process. This thesis is something I am truly proud of. As a person who has never been academically outstanding, I think this work proves that you don't have to be the most intelligent nor the most gifted to succeed, you simply need the personal determination and ambition to pursue your passion - and a mind-set that facilitates it!

Dedication:

To my mother and father. You have both taught me so much about life. You have allowed me to become the man I am today; someone I hope you are, and will forever be, proud of. You mean more to me than I will ever be able to explain.

For everything you have done for me, thank you!

Table of Contents

Author Declaration	1
List of Submitted, Accepted and Published Work	2
Abstract	3
Acknowledgements and Personal Comments	5
Dedication	6
Chapter 1	
1. Introduction	21
1.1. General Introduction	22
1.2. Overview of Skeletal Muscle Structure and Response to Catabolic and Anabolic Stimuli	24
1.2.1. Skeletal muscle structure: gross anatomy and cytoskeletal structure	24
1.2.2. The cascade of events that initiate skeletal muscle contraction	26
1.2.3. Satellite cells and the skeletal muscle specific stem cell niche	27
1.2.4. Physiological and Morphological response of skeletal muscle during hypertrophy and atrophy stimuli	30
1.3. The adaptive response of mammalian gene expression to orchestrate adaptive response during periods of skeletal muscle perturbation	35
1.3.1. Transcription, Translation and Biology of Gene Expression	36
1.3.2. Key Regulatory Signalling Pathways and Transcripts Associated with Skeletal Muscle Hypertrophy	36
1.3.3. Key Regulatory Signalling Pathways and Target Transcripts Identified as Pivotal in Muscle Atrophy	40
1.3.3.1. Ubiquitin-Proteasome Pathway Inducing Muscle Atrophy	41
1.4. Skeletal Muscle Epigenetics	44
1.4.1. Chromatin, Histone and DNA	45
1.4.2. Epigenetics and DNA Methylation	47
1.4.3. Alteration to DNA Methylation in Mammalian Skeletal Muscle	51
1.5. Epidemiological Evidence that Mammalian Skeletal Muscle Possesses a Memory of Earlier Stimulus	56
1.5.1. Early Life Encounters Effect Long Term Skeletal Muscle Phenotypes	56
1.5.2. Evidence of a Cellular Skeletal Muscle Memory	58
1.5.3. Skeletal Muscle Cells Remember the Niche in Which they are Derived	59
1.5.4. The Role of DNA Methylation in Skeletal Muscle Memory	60
1.6. Thesis Research Project	61
1.6.1. Research Project Aims	61
Chapter 2	
2. Materials and Methodologies	64

2.1.	Tetrodotoxin Exposure of the Tibialis Anterior Muscle in Rodents	65
2.1.1.	Wistar Rats	65
2.1.2.	Implantation of TTX Delivery Unit and Common Peroneal Nerve Block Model	65
2.1.3.	Muscle Harvesting Procedure	66
2.2.	Human Skeletal Muscle Resistance Training Studies	66
2.2.1.	Participants	66
2.2.2.	Experimental Design	67
2.2.3.	Resistance Exercise Protocols for Acute Loading & Chronic Loading and Unloading and Reloading	68
2.3.	Histological and Morphological Measurements of Muscle Mass Atrophy in Rodents	71
2.3.1.	Heamatoxylin and Eosin Staining for Fibre Cross Sectional Area and Tibialis Anterior Muscle Mass Analysis	71
2.4.	In-Vivo Assessment of Chains in Skeletal Muscle Strength and Mass in Human Studies	72
2.4.1.	Dual Energy X-Ray Absorptiometry	72
2.4.2.	Maximal Isometric Voluntary Contraction of the Quadriceps Muscle	72
2.5.	Muscle Harvesting and Tissue Handling	73
2.6.	RNA Isolation, q-RT-PCR for Gene Expression Analysis	74
2.6.1.	Homogenisation of Muscle Samples for Gene Expression Analysis	74
2.6.2.	Procedures of RNA Isolation	75
2.6.3.	Measurement of Quality and Quantity of Isolated RNA	76
2.6.4.	Quantitative Real Time Polymerase Chain Reaction Experiments	78
2.6.4.1.	One Step PCR Reaction	78
2.6.4.2.	First-Strand cDNA Synthesis and PCR	79
2.6.5.	Microarray Analysis of Rodent Muscle	80
2.6.5.1.	Rodent Muscle Preparation for Microarray Analysis	80
2.6.5.2.	Transcript Wide Analysis Via Transcriptome Analysis Control Software	80
2.7.	DNA Isolation, Epigenome-Wide Analysis and Loci-Specific DNA Methylation Experiments	81
2.7.1.	Preparation of Muscle Sample for DNA Isolation	81
2.7.2.	Isolation of Deoxyribonucleic Acid	81
2.7.3.	Quantification of DNA Quantity and Quality	82
2.7.4.	Bisulfite Conversion of Isolated DNA	83
2.7.4.1.	EZ DNA Methylation Kit Protocol	83
2.7.4.2.	InnuConvert Bisulfite Conversion Kit Protocol	85
2.7.5.	Methylome-Wide Bead Chip Arrays and Analysis	86
2.7.5.1.	Methylome Wide CpG DNA Methylation Assays	86
2.7.5.2.	Computational Data Handling and Quality Control Procedures	89

2.7.5.3.	Partek Genomic Suite for Hierarchical Clustering Dendrogram, Gene Ontology and KEGG Pathway Analysis	91
2.7.6.	Loci-Specific DNA Methylation Analysis	92
2.7.6.1.	Loci-Specific Pyrosequencing for Analysis of Rodent Muscle Atrophy	92
2.7.6.2.	High Resolution Melting (HRM) Polymerase Chain Reaction for Total DNA Methylation of Rodent Muscle Atrophy	93
2.8.	Statistical Analysis	94

Chapter 3

3.	Transcriptome and Epigenetic Regulation of Disuse Atrophy and the Return to Activity in Skeletal Muscle	95
3.1.	Introduction	96
3.2.	Methodology	98
3.2.1.	Experimental Design	98
3.2.2.	Morphological and Histological Analysis of Muscle Adaptation	99
3.2.3.	Transcriptome-Wide Analysis via Micro Array	100
3.2.4.	RNA Isolation and rt-qRT-PCR	101
3.2.5.	DNA Isolation and Methylation Analysis	102
3.2.6.	Statistical Analysis	105
3.3.	Results	106
3.3.1.	Disuse Atrophy Produces Significant Wasting of Skeletal Muscle	106
3.3.2.	Microarrays Identify Important Gene Regulatory Networks That Orchestrate Rodent Skeletal Muscle Atrophy	109
3.3.3.	Microarray and Significance Ranking Identifies Important Regulatory Genes During Atrophy	111
3.3.4.	DNA Methylation is Inversely Associated with Gene Expression of the Identified Genes During TTX Atrophy and Recovery	114
3.4.	Discussions of Findings	117
3.4.1.	DNA Methylation Inversely Correlates with Important Changes in Skeletal Muscle Gene Expression After Atrophy and the Return to Habitual Activity	118
3.5.	Summary, Conclusions and Future Chapter Directions	120

Chapter 4

4.	Human Skeletal Muscle Possesses an Epigenetic Memory of Hypertrophy	122
4.1.	Introduction	123
4.2.	Methodology	125
4.2.1.	Experimental Design	125
4.2.2.	Resistance Exercise Induced Muscle Hypertrophy: Loading, Unloading, Reloading	126
4.2.3.	In-Vivo Assessment of Lean Mass and Strength in Humans	128
4.2.4.	Muscle Biopsy Preparation	129

4.2.5. Isolation and Analysis of DNA for Methylome and CpG DNA Methylation Via EPIC Methylome Bead Array	129
4.2.6. Isolation and Analysis of RNA for Gene Expression	130
4.2.7. Statistical Analysis	133
4.3. Results	133
4.3.1. Lean Leg Mass and Muscle Strength is Increased After Loading, Returns Towards Baseline During Unloading and is Further Increased After Reloading	133
4.3.2. Exposure to Reloading Stimulus Evokes the Largest DNA Hypomethylated State Across the Genome in Human Muscle	136
4.3.3. Genome-wide Analysis Identified Two Distinct Temporal Clusters of Altered DNA Methylation that Provides Initial Evidence of an Epigenetic Induced Muscle Memory	145
4.3.4. Identification of Gene Expression Clusters Inversely Associated with CpG DNA Methylation	147
4.3.4.1. Cluster A: Increased expression after loading, return to baseline after unloading and enhanced expression upon reloading, mirrored by inverse changes in DNA methylation	149
4.3.4.2. Cluster B: Initial and progressive increase in gene expression from loading through unloading and reloading, met with an inverse profile of DNA methylation	150
4.3.5. Identification of a Number of Novel Genes at the Expression Level Correlates with Adaptations in Skeletal Muscle Mass	153
4.3.6. The E3 Ubiquitin Ligase, UBR5, has Enhanced Hypomethylation and Largest Increase in Gene Expression Upon Secondary Exposure to Load Induced Stimulus	156
4.4. Discussions of Findings	159
4.4.1. Secondary Exposure to Resistance Load Stimulus Induces Largest Hypomethylated Profile Met with Largest Increase in Skeletal Muscle Hypertrophy	159
4.4.2. Hypomethylation is Maintained from Earlier Load Induced Hypertrophy Even During Unloading Where Muscle Mass Returns Back Towards Baseline and is Inversely Associated with Gene Expression	160
4.4.3. Identification of Novel Genes with the Largest Hypomethylated Profile After Secondary Exposure to Load Stimulus, that are Associated with Enhanced Gene Expression	164
4.5. Summary, Conclusion and Future Chapter Directions	169

Chapter 5

5. DNA is Hypomethylated After a Single Bout of Exercise That is Retained After Continuous Periods of Loading and Reloading: Case for Sensitive DNA Methylation as a Biomarker for Adaptation	171
5.1. Introduction	172

5.2. Methodology	173
5.2.1. Experimental Design	173
5.2.2. Acute Exposure to Resistance Exercise Stimulus	173
5.2.3. Muscle Biopsy Preparation	174
5.2.4. Isolation of DNA and analysis for DNA methylome and CpG methylation	174
5.2.5. Isolation of RNA and Down Stream rt-qRT-PCR	175
5.2.6. Statistical Analysis	176
5.3. Results	177
5.3.1. Acute Resistance Exercise Rapidly Remodels the Human Methylome and Preferentially Favours a Hypomethylated Response	177
5.3.2. Cross-Comparison Analysis Reveals 27 Differentially Regulated CpG Sites Following Acute, Loading and Reloading Resistance Exercise	181
5.3.3. Altered CpG DNA Methylation Profile Following Acute Resistance Exercise Are Retained after Loading and Reloading	182
5.3.4. Dynamic and Sensitive Changes in DNA Methylation After Acute RE, Precede Observed Changes in Gene Expression After Loading and Reloading	184
5.4. Discussion of Findings	189
5.4.1. Summary	189
5.4.2. The Human Methylome is Rapidly Altered Following Single Exposure to RE to a Preferentially Hypomethylated State	190
5.4.3. DNA Methylation Profiles Following Acute RE are Identical to Those Observed Following Loading and Reloading: Highlighting Potential DNA Methylation Biomarkers for Later Adaptation	192
5.5. Summary and Concluding Remarks	196
 Chapter 6	
6. Thesis Conclusion	197
6.1. Thesis Aims	198
6.2. DNA Methylation is Modified Following Catabolic and Anabolic Exposure: Acute and Chronic Response of Mammalian DNA Methylation	200
6.3. DNA Methylation Displays an Inverse Mirrored Relationship with Changes in Gene Expression During Loss and Growth in Mammalian Skeletal Muscle	203
6.4. Retention and Memory of DNA Methylation in Mammalian Skeletal Muscle	206
6.5. DNA Methylation May Act as an Early Biological Marker for Later Adaptation	210
6.6. Future Direction	211
6.6.1. Elucidating Whether DNA Methylation Modifications Precede Those Observed in Gene Expression During Skeletal Muscle Adaptation	211

6.6.2. Do Repeated Exposures to a Catabolic Event Induce an Epigenetic Muscle Memory	212
6.6.3. Elucidating the Role of the Newly Identify E3 Ubiquitin Ligase Gene, UBR5, in Skeletal Muscle	214
6.7. Experimental Limitations	215
6.8. Final Conclusion	217
Chapter 7	
7. References	218
Chapter 8	
8. Appendix	237
Appendix 1. Does Skeletal Muscle Have an ‘Epi’-Memory? The Role of Epigenetics in Nutritional Programming, Metabolic Disease, Aging and Exercise.	238
Appendix 2. The Transcriptomic and Epigenetic Regulation of Disuse Atrophy and The Return To Activity In Skeletal Muscle.	251
Appendix 3. Human Skeletal Muscle Possesses an Epigenetic Memory of Hypertrophy	268

List of Figures

Figure 1.1	Gross anatomical structure of mature mammalian skeletal muscle	25
Figure 1.2	Schematic representation of the contraction-relaxation cycle.	26
Figure 1.3	Overview of the Satellite Cell Myogenic Differentiation Programme that Enables Skeletal Myofibre Repair and Regeneration	30
Figure 1.4	Cell signalling pathway for activation of mammalian target of rapamycin complex 1 by growth factor, hormone and amino acid activation.	40
Figure 1.5	Schematic representation of the cellular mechanisms induced upon skeletal muscle atrophy.	44
Figure 1.6	Composition and Structure of Chromosome, Chromatin, Nucleosome and DNA Network in Mammalian Cells	47
Figure 1.7	Biochemical reactions that create hypo- or hyper-methylated DNA at CpG genomic loci	50
Figure 1.8	Research interest into skeletal muscle epigenetics	56
Figure 2.1	Overview of resistance exercise training protocol for acute loading and chronic loading, unloading and reloading stimuli in human subjects	70
Figure 2.2	Process of RNA Isolation from Skeletal Muscle Samples and Reaction Tube Setup for Reverse-Transcription Quantitative Real Time Polymerase Chain Reaction Analysis	76
Figure 2.3	Overview of the Process for DNA Isolation from Muscle Tissue Samples	82
Figure 2.4	Schematic representation of modifications to DNA strands during bisulfite conversion treatment and PCR amplification.	86
Figure 2.5	Initial quality control analysis of human samples utilised for down-stream methylome wide bead arrays	90
Figure 3.1	Schematic representation of TTX muscle atrophy model and subsequent muscle sample preparation for morphologic, transcriptomic, and epigenetic analysis	99
Figure 3.2	Gene map of CpG islands for loci-specific pyrosequencing for quantitation of DNA methylation for transcripts.	103
Figure 3.3	Quantification of changes in muscle mass in vivo after TTX-induced nerve block.	107
Figure 3.4	Muscle fibre cross-sectional area after TTX-induced atrophy and recovery	109

Figure 3.5	Transcriptomic analysis indicates a highly dynamic gene expression response to progressive muscular disuse-induced atrophy, that upon recovery, returns to expression levels observed in control	111
Figure 3.6	Relative fold change in gene expression and DNA methylation displaying an inverse and transiently active relationship across experimental time-course, in a subset of identified and analysed gene transcripts	116
Figure 4.1	Schematic representation of experimental condition and types of analyses undertaken across the time-course.	126
Figure 4.2	Weekly total volume of resistance exercise undertaken by human participants during loading, unloading and reloading resistance exercise training	128
Figure 4.3	Skeletal muscle mass changes in human participants across resistance exercise and exercise cessation time-course	135
Figure 4.4	Skeletal muscle strength changes in human participants across resistance exercise and exercise cessation time-course	135
Figure 4.5	Frequency analysis of statistically differentially regulated CpG sites identified via Infinium MethylationEPIC Bead Chip array	138
Figure 4.6	Gene ontology analysis of the human methylome during loading, unloading and reloading	139
Figure 4.7	Representation of the DNA methylation modifications that occurred within the PI3K/AKT KEGG signalling pathway	141
Figure 4.8	Heat map depicting unsupervised hierarchical clustering of the top 500 statistically differentially regulated CpG loci	145
Figure 4.9	Genomic location of the top 100 statistically differentially regulated CpG sites across conditions	146
Figure 4.10	Relative changes in gene expression and representative schematic of CpG DNA methylation and gene expression relationship for genes in cluster A	149
Figure 4.11	Relative changes in gene expression and representative schematic of CpG DNA methylation and gene expression relationship for genes in cluster B	150
Figure 4.12	Relative fold changes in gene expression, correlation between gene expression and skeletal muscle mass across experimental conditions and a schematic representation of relationship between mRNA expression and CpG DNA methylation	153
Figure 4.13	Schematic representation of changes in gene expression and CpG DNA methylation in the E3 ubiquitin ligase gene, UBR5	155
Figure 4.14	Representation and characterisation of the DNA methylation modifications that occurred along the ubiquitin mediated proteolysis signalling pathway across all conditions	156

Figure 5.1	Response of the methylome after acute resistance exercise (acute RE) compared to baseline	176
Figure 5.2	Gene ontology analysis generated from EPIC BeachChip array confirms an enhanced hypomethylated profile	178
Figure 5.3	Cross-comparison analysis of acute RE methylome data and methylome data derived following chronic loading and reloading	179
Figure 5.4	Modifications of DNA methylation following acute RE are maintained following loading and reloading	181
Figure 5.5	Analysis of CpG DNA methylation changes following acute RE correlated with changes in CpG DNA methylation evoked following loading and reloading.	181
Figure 5.6	Relative fold changes in gene expression and CpG DNA methylation in all 12 gene transcripts identified from comparative analysis of acute RE and loading and reloading.	186
Figure 5.7	Representative schematic identifying early epigenetically modified genes after acute RE, that are associated with enhanced gene expression following reloading	187

List of Tables

Table 3.1	Gene primer sequences for rodent muscle atrophy experiment	101
Table 3.2	Detailed description of targeted DNA methylation assays for loci-specific pyrosequencing analysis	104
Table 3.3	Primer design for HDAC 4 for analysis of DNA methylation via HRM-PCR	105
Table 3.4	Top 20 most statistically differentially regulated gene transcripts across all conditions of rodent disuse-induced atrophy and return to activity, identified via gene expression microarrays, and ranked according to significance	113
Table 4.1	Gene primer sequences for human muscle memory experiment	131
Table 5.1	Gene primer sequences for acute human RE experiment	174
Table 5.2	Genomic location of 18 CpG sites that overlap in comparisons between acute RE, chronic load and chronic reload methylome data sets	182

Abbreviations

5hmC	5-hydroxy-methyl-cytosine
5mC	5-methyl-cytosine
A ^{vy}	Agouti viable yellow
Acetylcholine	ACh
ADSSL1	Adenylosuccinate synthase like 1
AFF3	AF4/FMR2 family member 3
Akt	Protein kinase B
Ampd 3	Adenosine monophosphate deaminase 3
AMPK α 2	AMP-activated protein kinase alpha 2
APLP1	Amyloid beta precursor like protein 1
ART3	ADP-Ribosyltransferase 3
ATG	Translational start codon
Atg12	Ubiquitin-like protein ATG12
ATP	Adenosine triphosphate
bHLH	Basic helix-loop-helix
BICC1	BicC family RNA binding protein 1
BNIP3	BCL2/adenovirus E1B 19 kDa protein-interacting protein 3
C11orf24	Chromosome 11 open reading frame 24
C12orf50	Chromosome 12 open reading frame 50
C8B	Complement C8 beta chain
Ca ²⁺	Calcium
CACNA1H	Calcium voltage-gated channel subunit alpha 1
CAMK4	Calcium/calmodulin dependent protein kinase IV
CDS	Coding DNA sequence
Chrna 1	Acetylcholine receptor subunit alpha precursor
CPED1	Cadherin like and PC-esterase domain containing 1
CpG	Cytosine-phosphate-Guanine
CPT1A	Carnitine Palmitoyltransferase 1
CRISPR	Clustered regulator interspaced short palindromic repeats
CSA	Cross-sectional area
CTNAP2	Contactin associated protein-like 2
DEXA	Dual energy x-ray absorptiometry
DMX	Dexamethasone
DNA	Deoxyribonucleic acid
DNMT1	DNA methyltransferase 1
DNMT3a	De-novo methyltransferase 3a
DNMT3b	De-novo methyltransferase 3b
eIF3b	Eukaryotic translation initiation factor 3 subunit B
ERICH1-AS1	ERICH1 antisense RNA 1
ERK	Extracellular signal-regulated kinases
FABP3	Fatty acid-binding protein 3

FBXL17	F-box and leucine rich repeat protein 17
FBXO32	F-box only protein 32
FKBP2	FK506 binding protein like
Foxo	Forkhead box O
FoxO3	Forkhead box O3
FREM2	FRAS1 related extracellular matrix protein 2
GAS7	Growth arrest-specific 7
GO	Gene Ontology
GRIK2	Glutamate receptor, ionotropic kainate 2
GSKb	Glycogen synthase kinase 3 beta
H3K4	Histone 3, lysine 4
H4K36	Histone 3, lysine 36
hCpG	Hemi-methylated CpG
HDAC4	Histone deacytelase 4
HEG1	Heart development protein with EGF like domains 1
HOXB1	Homeobox B1
HRM-PCR	High resolution melt polymerase chain reaction
HSPD1	Heat shock protein family D member 1
HYD	Hyperplastic discs
IGF-1	Insulin growth factor 1
IGF2BP3	Insulin like growth factor 2 binding protein 3
IGFbp-3	Insulin like growth factor binding protein 3
IKD	Isokinetic dynamometry
IL-1	Interleukin-1 family
IL-10	Interleukin 10
IL13ra2	Interleukin 13 receptor subunit alpha 2
IL19	Interleukin 19
JNK	Jun amino terminal kinases
Jumpy/MTMR14	Myotubularin related protein 14
KLHDC1	Kelch domain containing 1
LC3	Microtubule-associated proteins 1A/1B light chain 3B
LTB	Lymphotoxin beta
MAFbx/Fbxo 32	F-box only protein 32
MBD	Methyl binding domain
MeCP	Methyl CpG binding protein
MEF 2	Myocyte enhancer factor 2
MPB	Muscle protein breakdown
MPC	Muscle precursor cells
MPS	Muscle protein synthesis
mRNA	Messenger RNA
MRTF	Myocardin-related transcription factor
MTFR1L	Mitochondrial fission regulator 1 like
mTOR	Mammalian target of rapamycin

mTORc1	Mammalian target of rapamycin complex 1
MuRF1/Trim 63	Muscle RING finger protein-1
MVC	Maximal voluntary contraction
Myf 5	Myogenic factor 5
Myf 6	Myogenic factor 6
MYHC	Myosin heavy chain
MYO10	Myosin X
MYO16	Myosin XVI
MyoD	Myogenic differentiation 1
MyoG	Myogenin
nAchR	Nicotinic acetyl choline receptor
NF-κB	Nuclear factor kappa-light-chain-enhancer of activated B cells
Nm	Newton meters
NR2F6	Nuclear receptor subfamily 2 group f member 6
NUB1	Negative regulator of ubiquitin like proteins 1
NUP205	Nucleoporin 205
ODF2	Outer dense fibre of sperm tails 2
P38 MAPK	P38 mitogen activated protein kinase
P70-S6 Kinase-1	P70S6K
PAPD7	Poly(A) RNA polymerase D7
Pax 7	Paired box protein
PDK4	Pyruvate dehydrogenase lipoamide kinase isozyme 4
PGC1- <i>a</i>	Peroxisome proliferator activated receptor gamma co-activator 1-alpha
PI3K	Phosphoinositide 3-kinase
PLA2G16	Phospholipase A2 group XVI
POLR2a	DNA-directed RNA polymerase II subunit RPB1
PTH1R	Parathyroid hormone 1 receptor
qRT-PCR	Quantitative reverse transcription polymerase chain reaction
RN18s	18s ribosomal RNA
RNA	Ribonucleic acid
RPIIb	RNA polymerase II subunit B
RPL13a	Ribosomal protein L13a
RPL35a	Ribosomal protein L35a
RSU1	Ras suppressor protein 1
rt-qRT-PCR	Real time qRT-PCR
RUNX1	Runt related transcription factor 1
SAH	S-adenosyl homocysteine
SAM	S-adenosyl methionine
SD	Standard deviation
SEM	Standard error of the mean
SETD3	SET domain containing 3
SIN3a	SIN3 transcriptional regulator family protein member A

STAG1	Cohesin subunit SA-1
STIM1	Stromal interaction molecule 1
T2D	Type II diabetes
TA	Tibialis anterior
TAC	Transcriptome analysis console
TET1	Ten-eleven translocation methylcytosine dioxygenase 1
TFAM	Mitochondrial transcription factor A
TM6SF1	Transmembrane 6 superfamily member 1
TNF- <i>α</i>	Tumour necrosis factor alpha
TOR	Target of rapamycin
TRAF1	TNF receptor associated factor 1
TRD	Transcriptional repressor Domain
Trim63	Tripartite motif containing 63
TSC	Tuberous sclerosis complex
TSS	Transcriptional start site
TTX	Tetrodotoxin
UBR5	Ubiquitin protein ligase E3 component N-recognin 5
UNC45a	Protein unc-45 homolog A
URT	Untranslated region
VPS34	Phosphatidylinositol 3-kinase VPS34
WNT7b	WNT family member 7b
ZFP2	Zinc finger protein 2
ZNF56	Zinc finger protein 56

Chapter 1:

Introduction

Portions of the introduction of this thesis have been utilised in a literature review published in the peer-reviewed journal, *Aging Cell*:

Sharples, A. P., Stewart, C. E., Seaborne, R. A. (2016). Does skeletal muscle have an ‘epi’-memory? The role of epigenetics in nutritional programming, metabolic disease, aging and exercise. *Aging Cell*, 15, 603-616.

1.1 General Introduction

Skeletal muscle is the largest and most abundant tissue in the mammalian body, playing a fundamental role in locomotive performance, physiological function, metabolic homeostasis and maintenance of health across the organism life span. Despite homo-sapiens possessing almost identical genetic codes (Levy et al., 2007), large variations in skeletal muscle mass and functionality are observed, that may, in part, be due to encounters with environmental stimuli such as physiological behaviour (e.g. activity level) and nutrient availability (Sharples et al., 2016c). An observed increase in muscle mass, referred to as hypertrophy, is obtained following chronic periods, such as embryonic development and mammalian maturation/puberty, or repeated encounters with anabolic stimuli, in which the muscle is in a growth state. Most applicably, for example, this hypertrophic response is observed following resistance exercise (RE) in a fed state, where muscle protein synthesis (MPS) is increased orchestrating a positive net protein balance. Conversely, during periods of catabolism (fasting, sedentary behaviour, limb immobilization, disease states) the muscle decreases in size, known as atrophy, where muscle protein breakdown (MPB) is higher than MPS, leading to a negative net protein balance and muscle loss. One of the most prolific causes of atrophy, is the gradual loss in muscle observed with age, a condition known as sarcopenia (Narici and Maffulli, 2010). In young, healthy humans, muscle protein balance remains either in a state of synthesis or equilibrium, resulting in the sufficient development and turnover of skeletal muscle up until the age of ~ 40. However, for reasons that are not yet fully characterised, nor understood, this balance shifts towards a predominantly catabolic state with advancing age. Past the 4th decade, ~ 0.8% of muscle mass in humans is lost annually (Paddon-Jones and Rasmussen, 2009), with the rate of atrophy rising even further to 1-2% by the age of

50 (Hughes et al., 2001). In sedentary individuals this condition is exacerbated, with the onset of natural muscle atrophy occurring as early as 25 years of age, with a total reduction of 10% observed in skeletal muscle by the age of 40, rising to 40% by the age of 70 (Porter et al., 1995). Additionally, repeated exposure to acute periods of skeletal muscle atrophy (bed-rest, hospitalisation, injury) exacerbates the progression of sarcopenia, a phenomenon deemed *acute sarcopenia* (Wall et al., 2013a, Wall et al., 2013b). Collectively, this has important ramifications, as muscle mass is strongly linked with an increase in a number of debilitating conditions and health-impacting pathologies that ultimately lead to earlier life morbidity and mortality (Rennie et al., 2010).

Despite progressions in the field of molecular biology, the precise mechanisms that orchestrate muscle atrophy and hypertrophy are still poorly and inadequately described. It is of significant importance for scientists to elucidate the cause of muscle hypertrophy and atrophy in order to aid in the development of therapeutics that may help in alleviating the reduction in muscle mass during acute and chronic catabolic events. This may aid in the reduction of muscle loss associated pathologies and illnesses, and aid in promoting greater human health and quality of life into old age.

With this in mind, this thesis was performed to help develop the scientific communities understanding of the molecular regulation of skeletal muscle atrophy and hypertrophy. As such, it is important to understand the current knowledge base of skeletal muscle adaptation during periods of anabolism and catabolism. Further, given that muscle perturbation is observed at a whole body, cell and gene level, the review of literature will briefly focus upon the adaptive response of tissue during periods of

atrophy and hypertrophy. It will then aim to describe known genes and proteins that are regularly and commonly induced in differing models of muscle atrophy and hypertrophy, respectively, where their role is regarded as pivotal in these cellular processes. Finally, given the aim of this thesis, the majority of the literature review will focus on our current understanding of epigenetics as a biological mechanism. It will then move onto describing the current opinion for the role of epigenetics in skeletal muscle adaptation, before identifying areas of research that warrant investigation in this thesis.

1.2 Overview of Skeletal Muscle Structure and Response to Catabolic and Anabolic Stimuli

1.2.1 Skeletal muscle structure: gross anatomy and cytoskeletal structure

Skeletal muscle makes up a large portion (~ 40%) of the mature human body, and is constantly in a state of protein synthesis and degradation, equating to ~ 30-50% of whole-body tissue turnover. Only ~ 20% of skeletal muscle itself is made up of protein, with the majority of the tissues mass being comprised of water (~ 75%) and the remaining portion (~ 5%) made up of other biological substances such as carbohydrates, fats, minerals and salts (MacLaren and Morton, 2011). Skeletal muscle is made up of a multitude of mature single muscle cells known as myofibers that are arranged into bundles, which are themselves surrounded by a connective tissue known as the perimysium. Muscle fibers themselves contain large amounts of protein (~ 80 %) that are responsible for the cytoskeletal structure and integrity, homeostatic regulation and contractile performance of the tissue (Hoppeler et al., 1973). Each individual muscle fibre, approximately 100 µm in diameter and up to 100 mm in

length, is itself made up of a further bundle of protein dense muscular structures referred to as myofibrils (Figure 1.1 and 1.2). Myofibrils are predominantly (~ 70-80%) made up of the myofilament proteins actin and myosin, that when uniformly assembled, create a sarcomere which is the basic unit of contractile apparatus in mature skeletal muscle. At rest, these two myofilaments overlap and repeat along the myofibril structure, running in parallel with other localised myofibrils, a formation that gives rise to the striated appearance of skeletal muscle under microscopic analysis (Frontera and Ochala, 2015). A number of important organelles, macromolecular structures, proteins and elements are contained within, and on the periphery of, the sarcoplasm of skeletal muscle cells. Most notably, this includes axons, synaptic end bulbs, the neuromuscular junction and the sarcoplasmic reticulum, that all play a fundamental role in skeletal muscle contraction. Given the role of skeletal muscle contraction in initiating hypertrophy, via repair and regeneration processes, it is best to first detail the process of contraction, before proceeding.

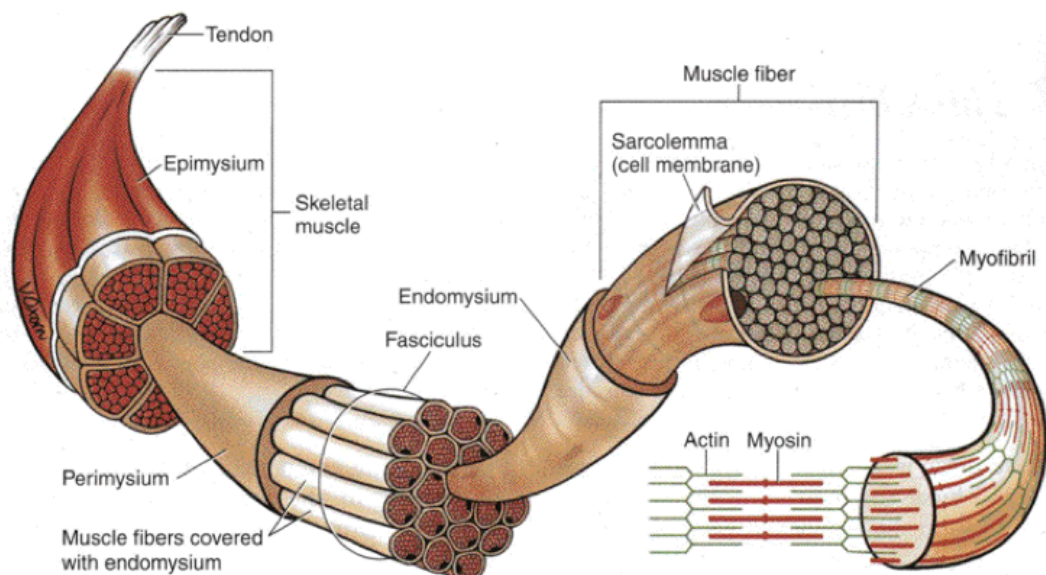


Figure 1.1. Gross anatomical structure of mature mammalian skeletal muscle. Taken from Kraemer et al. (2012).

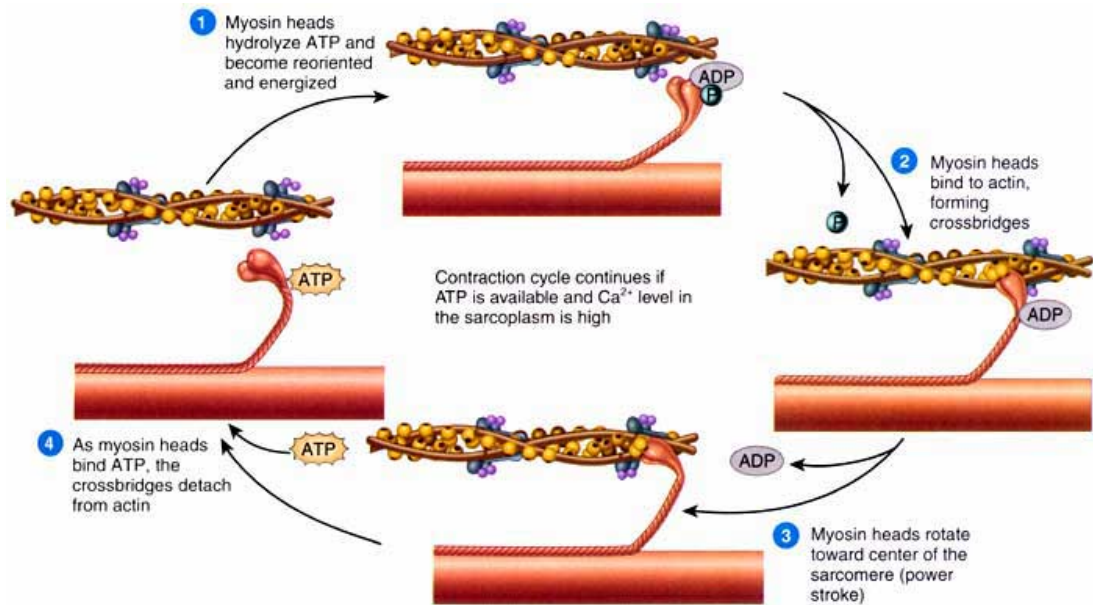


Figure 1.2. Schematic representation of the contraction-relaxation cycle. Taken from Tortora and Grabowski (2003)

1.2.2 The cascade of events that initiate skeletal muscle contraction

The sarcomere is a complex biological structure that, via a cascade of reactions and events starting from a neural impulse arriving from the motor complex and ending with the sliding filament mechanism, is responsible for the contractile properties of mammalian skeletal muscle (Figures 1.1 and 1.2). Briefly, the action of muscular contraction begins with a nerve impulse generated from the motor cortex that runs through the nervous system to the muscle of interest. A series of events subsequently occur that rely on the release and binding of acetylcholine (ACh) to its receptors within the myofiber structure. The binding of ACh to its receptors causes a voltage-gate ion channel to open allowing the influx of sodium and the efflux of potassium that renders the interior of the muscle fiber positively charged and depolarizes the sarcoplasmic reticulum (MacLaren and Morton, 2011). An action potential is then triggered via this event, that runs along the sarcolemma and into the T-tubules and

then propagates along the transverse tubule which allows for release and uptake of calcium ions, initiating the contractile apparatus. Cytosol-specific calcium causes the removal of the troponin-tropomyosin complex that, in basal non-contractile muscle, blocks the binding of myosin heads to actin receptors. Finally, in the presence of adenosine triphosphate (ATP), the myosin heads bind to actin receptors to form cross-bridges, a crucial biological step that is dysregulated in a number of pathologies and conditions (Frontera and Ochala, 2015). ATP is subsequently broken down into ADP and a phosphate group, the latter of which is released, tilting the myosin head and sliding the actin filament across the body of the myosin filament, causing contraction. This process, under the continued presence of ATP, is then repeated (figure 1.2) for each contraction. At microscopic level damage occurs to the myofiber structures during contraction that require repair in order for the muscle to regenerate. The next section of this literature review will focus on the role that a unique form of stem cells plays in this repair process.

1.2.3 Satellite cells and the skeletal muscle stem cell niche

Myofibers are established during gestation and therefore, during adulthood, are a stable post-mitotic tissue with infrequent turnover of myonuclei. The maintenance of mammalian myofibers is to conserve the number, size and cross-sectional area as well as the integrity of the cytoskeletal structure. During day-to-day activity, minor lesions are adequately repaired by the myofilament structure, without the causation of cell death, inflammatory responses or any major morphological adaptations. For example, plasma membrane damage caused by day-to-day activity can be effectively repaired by the incorporation of local blood vesicles that can fill the damaged plasma membrane (Bansal et al., 2003). However, more serious damage to the myofilament

structure warrants a greater repair and regenerative process. The first step of muscle regeneration is myofiber necrosis. Necrosis initiates a cascade of events that include the increased influx of calcium (Ca^{2+}) and/or increased Ca^{2+} release from the sarcoplasmic reticulum. In turn, this activates proteolysis and promotes skeletal muscle degeneration (Alderton and Steinhardt, 2000, Armstrong, 1990). Furthermore, necrosis also initiates skeletal muscle inflammation. Upon damage, two distinct sets of macrophages invade the tissue and secrete proinflammatory cytokines, such as tumour necrosis factor alpha (TNF- α) and the interleukin family member, IL-1, that reside within the tissue and peak at the protein level by \sim 24 hours post injury (Chazaud et al., 2009). Subsequently, a new population of macrophages invades and resides within the damaged muscle tissue. The new macrophages secrete anti-inflammatory cytokines, such as interleukin 10 (IL-10), and reside in the damaged tissue until the inflammation period terminates. These macrophages are the reported trigger for initiating the activation, proliferation and differentiation of a set of skeletal muscle-specific stem cells (Cantini and Carraro, 1995, Lescaudron et al., 1999, Al-Shanti et al., 2014). Residing beneath the basal lamina is a subset of skeletal muscle-specific stem cells, aptly named satellite cells. Muscle precursor cells (MPC) become activated following autocrine, paracrine and endocrine interactions of cytokines and progress through the stages of myogenic differentiation, a process governed by the expression of two myogenic regulatory factors, myogenic factor 5 (Myf 5) and myogenic differentiation 1 (MyoD; a schematic overview of the myogenic programme is represented in figure 1.3) (Tajbakhsh et al., 1996). A crucial stage of this differentiation pathway is the process of division in which the activated MPCs will undergo either symmetric or asymmetric division (figure 1.3). Asymmetric division is considered a hallmark of the myogenic differentiation process due to its

ability to divide an MPC into two distinctly different cells with two different fates. This division process, shown to be largely regulated by the mitogen-activated protein kinase (MAPK) P38 (Bernet et al., 2014, Troy et al., 2012), produces one terminally differentiated myoblast that expresses both paired box protein (Pax7) and MyoD, but also a stem cell that does not express MyoD and which returns to the quiescent stem cell pool niche, thereby maintaining the progeny pool (Zammit et al., 2004). Such events have been extensively confirmed by explorative work, such as that by Rudnicki's group (Kuang et al., 2007). Following multiple rounds of proliferation and entrance of the myogenic differentiation program, human satellite cells fuse to damaged regions of the existing tissue to help regenerate the muscle fibre. Satellite cells migrate and fuse to aid in repair and regeneration, with this process being governed by a number of myogenic regulatory factors including, and most notably, Myogenin and Myogenic Factor 6 (Myf6, otherwise referred to as Mrf4) (Cornelison et al., 2000, Cornelison and Wold, 1997).

The process of skeletal muscle regeneration, the maintenance and the efficiency of the satellite cell pool, and the conservation of the niche in which satellite cells reside is integral to the morphological adaptation of muscle mass. The following series of sections will focus on the morphological response of skeletal muscle upon insult to either anabolic or catabolic stimulus. In order to do so, findings presented hereafter are taken and interpreted from a number of different approaches, in which different mammalian organisms and different experimental models are utilised, and thus, must be taken into consideration when interpreting these data.

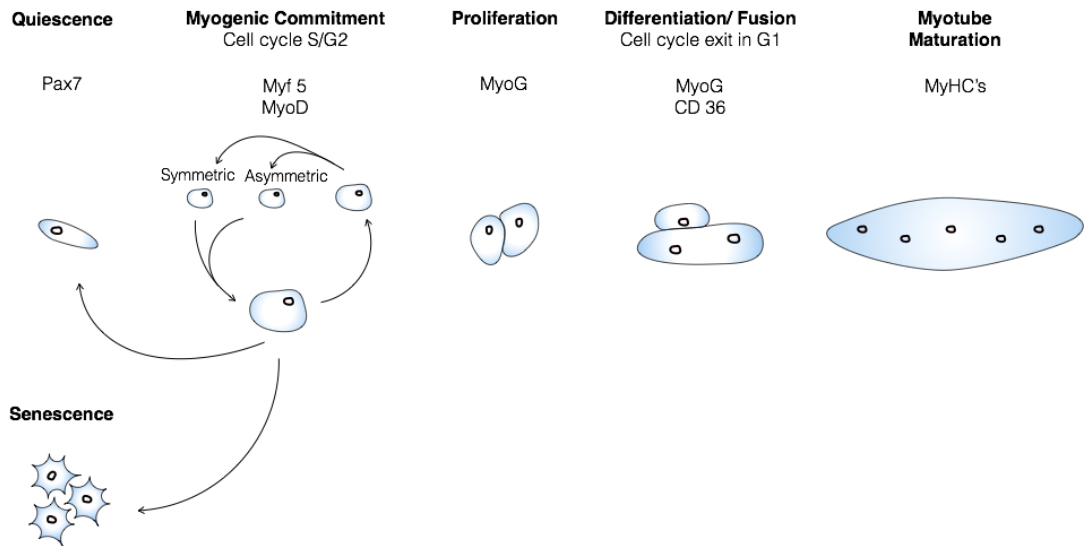


Figure 1.3. Overview of the Satellite Cell Myogenic Differentiation Programme that Enables Skeletal Myofiber Repair and Regeneration.

1.2.4 Physiological and Morphological Response of Skeletal Muscle During Hypertrophy and Atrophy Stimuli

As previously suggested, skeletal muscle makes up a large proportion of the mature human bodily structure, that is dependent on the balance between synthesis and degradation. A multitude of factors such as nutritional behaviour, hormonal regulation, physical activity and disease state, alter the balance between MPS and MPB and therefore the structural integrity of the proteins incorporated into fibres and therefore the functional capacity of myofibrils.

Muscle atrophy is defined by a reduction in muscle fibre cross sectional area, length and total muscle mass, but not in reduction in number (Nicks et al., 1989). On the contrary, sarcopenia, muscle atrophy relating to the gradual loss in muscle as a result of the aging process, also occurs via a reduction in fibre number (Lexell et al., 1988). Fundamentally, skeletal muscle atrophy occurs via a shift towards a greater muscle

protein breakdown, either via increased MPB itself, or via concomitant reduction in MPS and increased MPB. This process leads to a significant reduction or dysregulation of skeletal muscle organelles, cytoplasm and importantly, sarcomeric related proteins, and thus a reduction in fibre cross-sectional area and mass (Frontera and Ochala, 2015). It is also to be noted that alongside a reduction in fibre cross-sectional area and mass, a reduced functional capacity is also evident during muscle atrophy. For example, during bed rest periods, force, velocity and power are all significantly reduced in both type I and type II skeletal muscle fibres (Trappe et al., 2004). This observation is likely due to the reduction in number of contractile units within the myofibril and a dysregulation in the actin-myosin cross-bridge that orchestrates contraction (Stevens et al., 2013). Muscle atrophy is a multi-faceted phenomenon that is evoked by a number of different stimuli, including age-related decline in muscle (sarcopenia), disease-induced muscle loss (cachexia), disuse-induced muscle loss (e.g. bed rest or inactivity) and nutrient deprivation. To investigate the morphological outcomes of these stimuli, a wide-range of *in-vitro* and *in-vivo* models of atrophy have been used, as previously reviewed (Romanick et al., 2013, Frontera and Ochala, 2015). Indeed, the cross-sectional area (CSA) response of skeletal muscle following hind-limb suspension and/or immobilisation has extensively been studied across species, unequivocally showing a significant atrophic response. For example, 7, 14, 21 and 35 days of hind limb suspension in rodent models induced percentage reductions of 36, 40, 45 and 63%, in type I fibres of the soleus muscle, respectively (Desplanches et al., 1987, Hauschka et al., 1988, Templeton et al., 1986, Simard et al., 1987). Classical immobilisation studies agree with these findings. Indeed, time course analysis of immobilised soleus muscle in mice (induced via plaster cast of the muscle in the shortened position) across 7, 10 and 14 days

induced a progressive reduction in muscle fibre CSA of 19, 25 and 39%, respectively (Williams and Goldspink, 1984). With similar time course findings being reported across multiple species, including rat (Boyes and Johnston, 1979, Nicks et al., 1989), guinea pig (Maier et al., 1976) and cat (Cooper, 1972), as reviewed previously (Appell, 1990). To examine this process in a more tightly regulated model, the catabolic toxin, tetrodotoxin (a toxin obtained from *Tetraodontiformes* species, function of which is described in chapter 3), has been administered into rodents and has been reported to induce tibialis anterior muscle mass reductions of 19% after only 7 days (Dupont Salter et al., 2003), and 39% after 21 days of denervation (Adhihetty et al., 2007). The reduction in muscle mass was unequivocally confirmed by a number of intricate studies by Bodine et al. (2001a), where they mapped the percentile change in muscle mass at 3, 7 and 14 days in rodents treated via hind-limb suspension, immobilisation or denervation. Collectively, these findings confirm a rapid and maintained rate of muscle mass loss following a number of different atrophy-inducing stimuli. Human studies report similar findings, where after 5 and 14-days of limb-cast immobilisation, male subjects reported a 3.5 and 8% reduction respectively in muscle cross sectional area of the quadriceps in the treated limb (Dirks et al., 2014, Wall et al., 2013a). Similar reductions in cross sectional area have been found in models of unilateral knee immobilisation (14 days induced 5% reduction) (Glover et al., 2008) and lower limb suspension (14 days suspension induced a reduction of 5.2%) in humans.

On the contrary, muscle anabolism induces skeletal muscle hypertrophy via a shift towards a net positive protein balance, where MPS out-weighs breakdown. In this instance, a series of events take place that lead to an increase in this size and

abundance of myofibrillar proteins, actin and myosin, an increase in paralleled and uniform sarcomeres and a resulting increase in skeletal muscle fibre cross sectional area (Schoenfeld, 2010). The process of muscular hypertrophy is also met with the activation, migration and fusion of satellite cells, by which the addition of these cells results in an increased myonuclei number of the existing muscle fibres (Bruusgaard et al., 2010). It is suggested that the addition of new myonuclei to the existing myofiber plays a positive role in the promotion of skeletal muscle hypertrophy in mammals (Phillips, 2014). Nuclei possess a domain in which they regulate the activity of the cytoplasm within the cell, a cytoplasmic territory that is believed to be $\sim 2000 \mu\text{m}^2$ (Petrella et al., 2008). The nuclear domain theory states that an increase in muscle fiber cross-sectional area is met with a complementary increase in myonuclei number per fiber (Bazgir et al., 2017), suggesting a positive relationship between nuclei addition and fiber size. Despite this theory, the reliance on myonuclei for skeletal muscle hypertrophy and the elucidation of cause or effect of their behaviour during muscle fiber remodelling, has historically been controversial (Yin et al., 2013), and further work is required to elucidate this theory.

Muscle fibre cross-sectional area is a hallmark of muscular hypertrophy, with the increase in fibre cross-sectional area being well documented and reviewed previously (Schoenfeld, 2010, Schoenfeld, 2012). For example, 8-weeks (2 session per week for first 4 weeks, and 3 sessions per week thereafter) of either high or intermediate intensity resistance exercise (RE) (4 sets of 3-5 reps of rep max or 3 sets of 9-11 reps of rep max) produced an increase of $\sim 12.5 \%$, 19.5% and 26% in type I, type IIa and type IIx fibres, respectively (Campos et al., 2002). More explorative morphological analysis reports that in young males, 9 weeks of high-intensity leg-extensor training

increased quadriceps physiological cross-sectional area by 6%, fascicle penetration angle by 5% and quadriceps femoris activation by 3%, all of which reported as significant (Erskine et al., 2010b). Further, these authors report a significant increase (31% increase in torque production compared to baseline) in quadriceps femoris strength by measure of maximal voluntary contraction. Indeed, the association between increases in skeletal muscle strength as a result of RE stimulus has been observed previously (Schoenfeld, 2010, Schoenfeld, 2012). Importantly, the relationship between increased cross-sectional area and skeletal muscle strength has been implied. Where, in older adults, just 6-weeks of RE significantly increased the cross-sectional area of the vastus lateralis by 7.4%, with significant increases in physiological cross-sectional area of the quadriceps muscle showing a significant relationship to increases in strength (Scanlon et al., 2014). Finally, and important to note, that strength responses of skeletal muscle to RE has been suggested to be associated with large inter-individual differences (Erskine et al., 2010a).

Fundamentally, the balance of muscle morphology is as a result of periods of anabolism and catabolism that tilt the balance between protein synthesis and breakdown, respectively. At the molecular level, it is known that accompanying these periods of anabolism and catabolism is a vast, complex and multi-faceted cascade of events that orchestrate the signalling activity of a number of important proteins and pathways. The abundance (via protein translation in the ribosome) and ultimately the activity of these proteins (via phosphorylation, acetylation etc.) is altered only after changes that occur at the DNA level, via transcription of a messenger RNA (mRNA) molecule (or gene) in the nucleus preceding its translocation into the ribosome to produce the functional protein. Therefore, the next section will briefly detail the

current understanding for the role of gene transcription during periods of skeletal muscle atrophy and hypertrophy.

1.3 The Adaptive Response of Mammalian Gene Expression to Orchestrate Adaptive Responses During Periods of Skeletal Muscle Perturbation

While it is observed that periods of MPS or MPB orchestrate a number of distinct physiological and morphological adaptations at the myofiber level, the molecular mechanisms that support these changes lie, in-part, at a cellular level. Upon acute signal, such as an RE stimulus, the expression of key gene transcripts are attenuated or augmented compared to baseline expression levels (Perry et al., 2010). The commonly accepted molecular mechanisms that govern skeletal muscle adaptation revolve around the acute, temporal changes in gene expression that occur following exposure to a specific stimulus. Upon chronic and repeated exposures of the same or similar stimulus, regular increases or decreases in gene expression orchestrate a gradual adaptation in protein content and enzyme activity and result in functional changes and remodelling of skeletal muscle (Perry et al., 2010, Egan and Zierath, 2013). In accordance with this, during periods of skeletal muscle anabolism and catabolism, a number of distinct transcript targets have been regularly cited as having pivotal roles in orchestrating functional changes in muscle mass. The following sections provide an overview of the process of gene transcription and ultimately translation into the protein, before discussing our current understanding of important genes involved in skeletal muscle growth and loss.

1.3.1 Transcription, translation and biology of gene expression

Ribonucleic acid (RNA) polymerase binds to the promotor region of a gene strand and dissociates the nucleotide pairings, creating two open helical deoxyribonucleic acid strands. The RNA polymerase molecule copies the nucleotide sequence creating a messenger RNA (mRNA) which encodes for a specific protein of interest. The copying process ends when the RNA polymerase molecule reaches the termination region of the gene. A complex protein structure, the spliceosome, removes the mRNA strand of all non-coding introns and provides a 5' and 3' cap onto the mRNA sequences. The mRNA strand then travels into the cytoplasm of the skeletal muscle cell, where it encounters ribosomes and the initiation of protein translation will begin. As previously mentioned, acute environmental stimuli (such as RE) results in either an increase or decreased expression (from normal basal levels) in key gene transcripts. Upon regular and repeated exposure to similar stimuli, such as a chronic period of RE, the basal level of gene expression can then increase (Perry et al., 2010) in order for there to be a consistently higher abundance of protein to facilitate morphological adaptations.

1.3.2 Key regulatory signalling pathways and transcripts associated with skeletal muscle hypertrophy

In order to elucidate a list of candidate genes whose differential expression (upon hypertrophic stimulus) is commonly associated with positive changes to skeletal muscle mass, studies have employed and compared transcriptome wide (RNAseq and/or microarrays) analyses during a variety of muscular hypertrophy models. In contrast to those findings found in muscular atrophy models (see below), a list of gene targets whose gene expression is commonly up- or down-regulated during skeletal

muscle hypertrophy, remains somewhat elusive. Indeed, when correlative analysis was performed on the transcriptome of the vastus lateralis muscle tissue in both young and aged individuals before and following a 12-weeks RE programme (3 sessions per week at 3 sets of 10 reps at 70-75% 1RM; biopsies taken pre and 4h post first and last training session), it was identified that >660 gene transcripts correlated with changes in skeletal muscle size and strength (Raue et al., 2012). When young participants were segregated for analysis, the same authors identified that >1,100 gene transcripts that were differentially regulated following a single bout of REX (4h post first training session) and 524 gene transcripts that were significantly differentially regulated following the final training session (Raue et al., 2012). Similar findings of an extensively dysregulated transcriptome following in-vivo REX has been shown in a more prolonged exercise programme of 20 weeks training (Phillips et al., 2013). Cross-comparative analysis of muscle hypertrophy transcriptomes following models of muscular hypertrophy, to identify a candidate list of genes associated with muscle mass and strength changes, has, however, shown divergent results (Pereira et al., 2017). Using models of post-natal growth (2 and 4 weeks old), Akt over-expression and over-load in extensor digitorum longus (EDL) muscle in mice, the authors failed to identify a list of commonly differentially regulated gene transcripts responsible for muscular hypertrophy (Pereira et al., 2017). Instead, through western-blot analysis of the same tissue, the authors conclude that all models of skeletal muscle hypertrophy induced an increase in mammalian target of rapamycin (mTOR) signalling, and that phosphorylation of the ribosomal protein S6 kinase 1 (P70S6k1/S6K1) was increased across all but one time point within the models of muscular hypertrophy (Pereira et al., 2017). From these data analyses, the authors collectively suggest that skeletal muscle hypertrophy is not, per se, associated with a common set of differentially

regulated transcripts. Rather, the authors suggest that muscle hypertrophy stimulus induces activity changes to the key mTOR signalling pathway, and that translation (given changes in ribosomal biogenesis activity) rather than transcriptional changes are a hallmark of hypertrophying skeletal muscle (Pereira et al., 2017). Further work is required to develop a consensus of gene transcripts that are commonly differentially regulated during periods of skeletal muscle hypertrophy.

Despite the elusiveness of a ‘fingerprint’ profile of candidate genes that are commonly differentially regulated during skeletal muscle hypertrophy, a distinct cellular pathway has been identified (Figure 1.4). Indeed, binding of both endogenous ligands, insulin and insulin-like growth factor 1 (IGF-1), to their respective receptors on the cellular membrane initiate a cascade of events, triggering multiple down-stream targets, most notably phosphoinositide 3-kinase (PI3K), protein kinase B (Akt), and the mammalian/mechanistic target of rapamycin complex 1 (mTORC1; Figure 1.4) (Bodine et al., 2001b, Rommel et al., 2001, Sandsmark et al., 2007). Following resistance exercise stimulus (electrically evoked isometric contraction of the gastrocnemius muscle of Sprague-Dawley rats), muscle specific expression of IGF-1 significantly increased 1h and remained elevated through to 3h post REX (Kido et al., 2016). Similar findings have also been shown in time-course analysis in human subjects, with multiple IGF-1 isoforms/splice variants (IGF1-ea, IGF-1Eb and IGF-1Ec/MGF) showing significant increases in transcriptional expression following a maximal knee-extensor eccentric muscle protocol (Philippou et al., 2009). Importantly, cell signalling work suggests that IGF-1 binding to its targeted receptor brings about activity changes in a cascade of kinases downstream of the cellular membrane, that, eventually leads to an increased activity of Akt (Bodine et al., 2001b,

Rommel et al., 2001). Both direct and indirect targets of activated Akt include mTOR, P70S6K1 and 4E binding protein 1 (4eBP1), that are important proteins involved in translation and muscle protein synthesis (Laplante and Sabatini, 2012, Cross et al., 1995, Nave et al., 1999, Scott and Lawrence, 1998).

A paucity currently exists within the literature for a conclusive list of candidate gene markers that are commonly differentially regulated during periods of muscular hypertrophy, and the role these targets play in regulating muscle protein synthesis. On the contrary, cellular and molecular response of skeletal muscle during periods of hypertrophy has generally focussed around the activity of known kinases and protein complexes (figure 1.4).

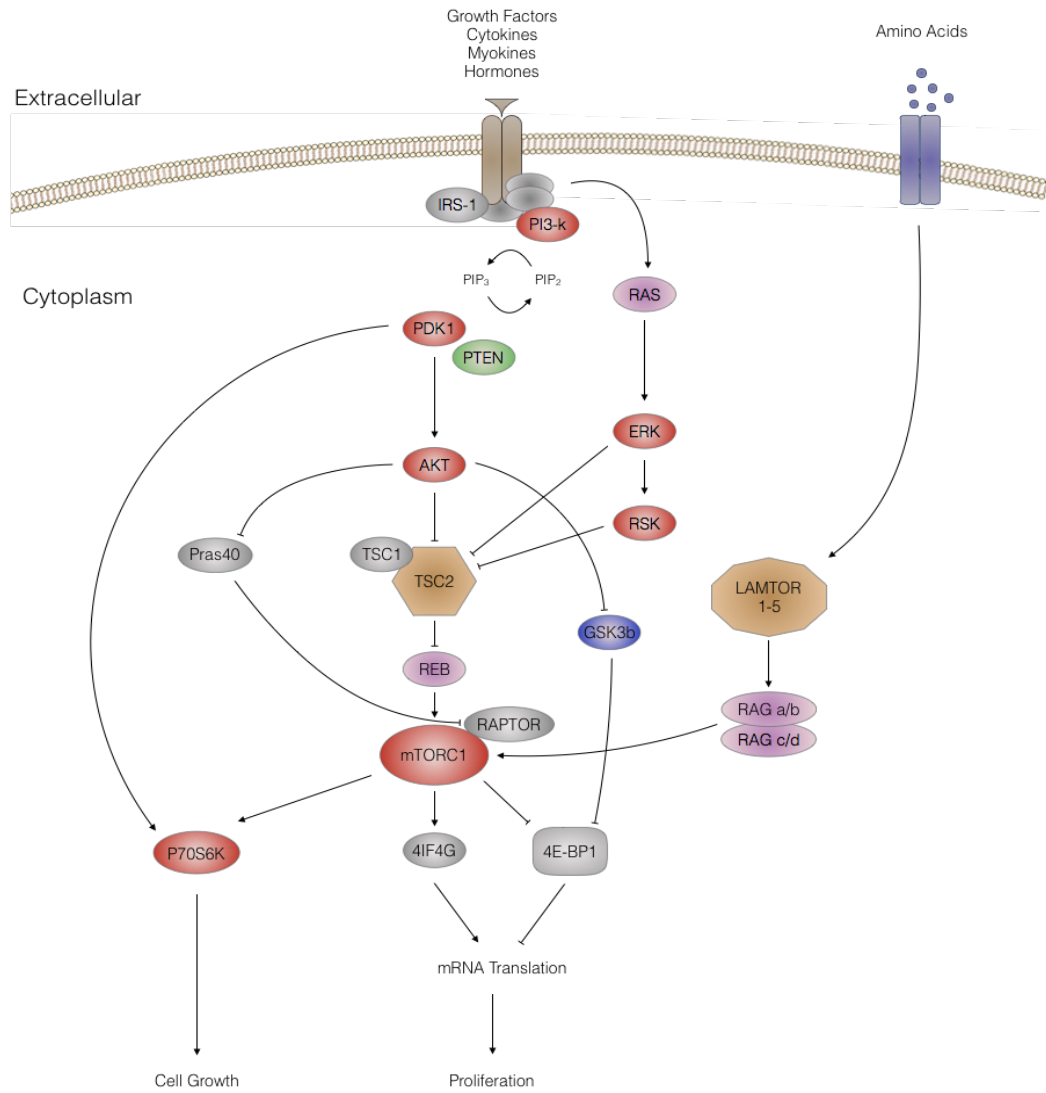


Figure 1.4. Cell signalling pathway for activation of mammalian target of rapamycin complex 1 by growth factor, hormone and amino acid activation.

1.3.3 Key regulatory signalling pathways and target transcripts identified as pivotal in muscle atrophy

Transcriptomic work examining the regulatory response during periods of skeletal muscle atrophy has received large amounts of scientific attention. Developments in scientific technology, assay quality, reliability and feasibility have allowed for increased amounts of research focussing on the transcriptomic response to atrophy, with a number of genes and gene pathways being elucidated (Bodine, 2013, Bodine et al., 2001a, Gomes et al., 2001, Lecker et al., 2004). Among the commonly identified

genes are transcripts relating to the ubiquitin-proteasome pathway. The alteration in the regulatory behaviour of these identified genes at the protein level are thought to bring about the destruction, degradation and loss of muscle specific components, and thus are commonly referred to as ‘atro-genes’ (Lecker et al., 2004).

1.3.3.1 Ubiquitin-proteasome pathway inducing muscle atrophy

The ubiquitin-proteasome pathway is responsible for removing sarcomeric related structures from myofibres during periods of skeletal muscle turnover, remodelling and atrophy. The rate limiting step in the process of ubiquitin-proteasome dependent muscle fibre degradation is the E3 enzymes. Over 600 E3 protein members have been identified (Deshaies and Joazeiro, 2009), with a small cluster of ligases being identified as ‘muscle-specific’ and regularly being up-regulated during periods of muscle atrophy. Muscle RING finger protein-1 (MuRF1) and F-box protein only 32 (MAFbx; Figure 1.5), otherwise known as Trim63 and Fbxo32 respectively, were the first two E3-ubiquitin ligases to be commonly associated with a loss of muscle mass during periods of atrophy. Indeed, mice lacking MuRF1 and MAFbx are resistant to muscle atrophy induced via denervation and exposure to the corticosteroid dexamethasone (DMX) (Bodine et al., 2001a, Baehr et al., 2011), and knockdown of MAFbx allows fasting mice to become resistant to muscle wasting (Cong et al., 2011). The role and expression characteristics of these two E3-ubiquitin ligases was unravelled in a series of intricate studies by Bodine et al. (2001a). Indeed, the authors unequivocally report the upregulation of these genes during periods of muscle atrophy evoked via denervation, DMX exposure, immobilization and unloading in rodents (Bodine, 2013, Bodine et al., 2001a), systematically confirming the induction of these two atro-genes during a number of models of muscle loss. The common up-stream

regulator of both MuRF1 and MAFbx is the muscle specific basic helix-loop-helix (bHLH) transcriptional factor and a member of the myogenic regulatory factors (MRFs), myogenin (MyoG; figure 1.5). Previous work has identified a regulatory link between MyoG induction and the increased expression and activity of the downstream E3 ubiquitin ligases, MuRF1 and MAFbx (Cohen et al., 2007). MyoG is a highly conserved muscle specific protein that is commonly associated with the coordination of skeletal muscle development/myogenesis or skeletal muscle regeneration, and specifically the differentiation/fusion of skeletal muscle cells (Le Grand and Rudnicki, 2007). The expression of MyoG is required for maximal activation of MuRF1 and MAFbx, and is therefore suggested as having a dual role in the regulation of muscle (Moresi et al., 2010). Forkhead box O (Foxo) is a sub complex of transcripts to the larger forkhead transcription factor family, whose activity has been implicated in apoptosis and skeletal muscle atrophy and closely linked to the E3 ubiquitin ligases MuRF1 and MAFbx (figure 1.5). In skeletal muscle, Akt phosphorylates the three known mammalian isoforms of Foxo attenuating their translocation into the nucleus and therefore inhibiting their contact with target genes for normal transcription processes (Brunet et al., 1999). This is confirmed by targeted dephosphorylation of Foxo isoforms that permits its nuclear entry, increasing the transcriptional expression of MuRF1 (Sandri et al., 2004) and the upregulation of apoptosis (Ramaswamy et al., 2002). The importance and necessity of Foxo isoforms in producing skeletal muscle atrophy was demonstrated in a series of *in-vitro* studies examining their role in fasting, diabetes, uraemia and cancer related muscle atrophy (Lecker et al., 2004, Sandri et al., 2004, Furuyama et al., 2003).

A large amount of research has investigated the altered expression of a number of target transcripts and activity of key cellular pathways during periods of muscular anabolism and catabolism. Despite the vast amount of research, the precise mechanisms that regulate these processes are still poorly understood and inadequately described. Furthermore, recent breakthroughs in the field of skeletal muscle epigenetics has elucidated an important and as yet under-reported role for epigenetics in regulating gene expression involved in the regulation of muscle metabolism and mass. Given the aim of this thesis project, the remaining literature review sections will focus on our current understanding of epigenetics, its role in skeletal muscle and the potential role of epigenetics in skeletal muscle programming or ‘memory’.

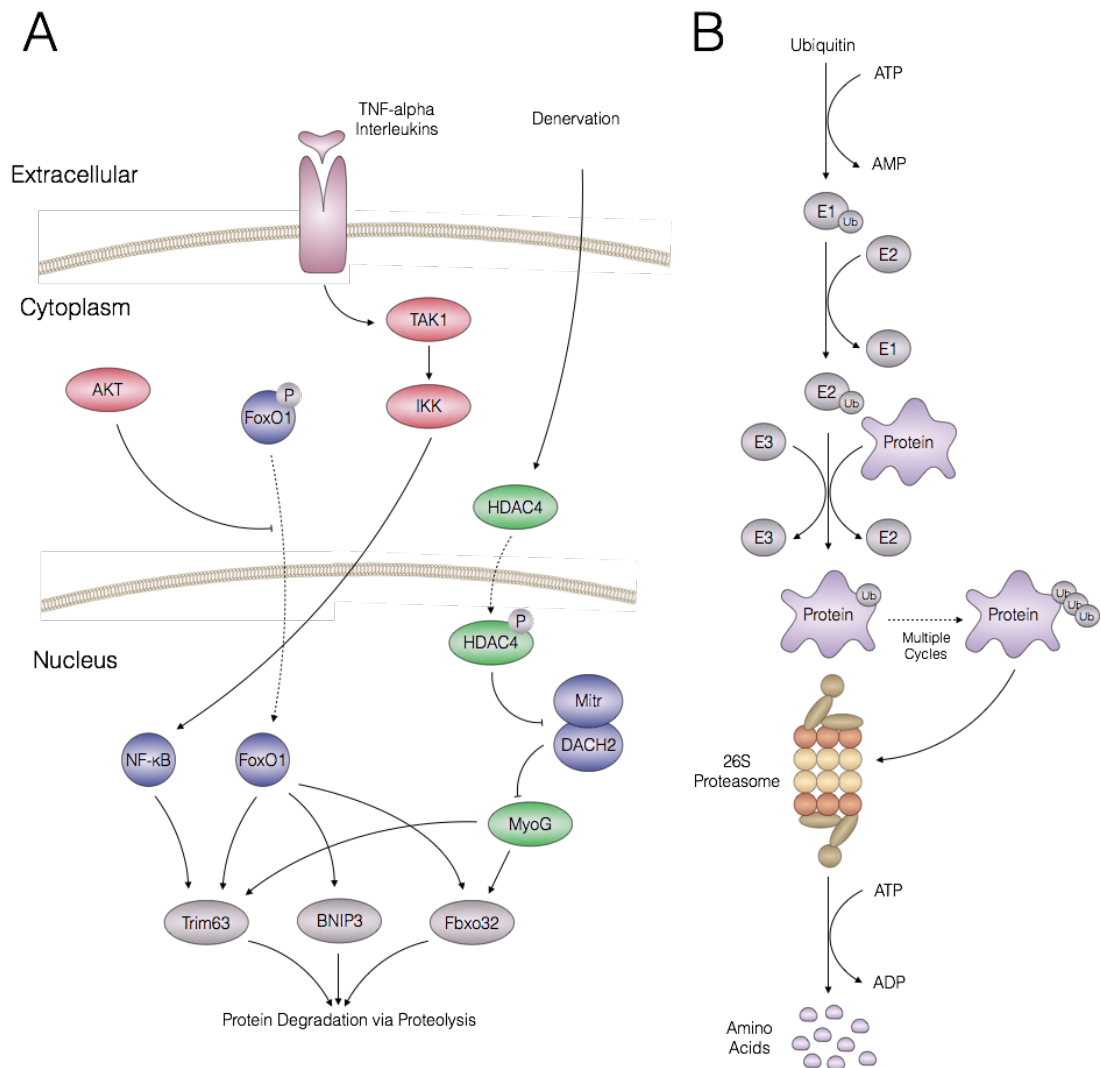


Figure 1.5. Schematic representation of the cellular mechanisms induced upon skeletal muscle atrophy. A. Cell signalling pathways of transcripts that are known to play an important role in protein degeneration, as activated via TNF-alpha, interleukins and denervation. B. The molecular process of proteolysis via the ubiquitin ligases (E1, E2 and E3) and the 26S proteasome complex. Regulatory networks are detailed in section 1.3.3.

1.4 Skeletal Muscle Epigenetics

The study of epigenetics has rapidly developed over the last 50 years; before which it was a generic term referring to the development of the original fertilized zygote

through to the mature mammalian organism (Waddington, 1953). However, through scientific development, the field of epigenetics has taken a more uniform and finite domain. Indeed, our current understanding of epigenetics has led to the working definition that is mitotically and/or meiotically heritable changes in gene behaviour that are not due to changes in DNA sequence, however this definition is, itself, continuing to evolve (Berger et al., 2009). Epigenetics is a biochemical process that occurs in a number of macromolecular loci within the mammalian genome, that serves to chemically modify these loci, and in doing so, alters gene expression. In order to review the current literature focusing on epigenetics and its role in skeletal muscle, a narrative is given of the basic biological structure of chromatin, histones and DNA, the location in which epigenetic regulation predominantly occurs.

1.4.1 Chromatin, histone and DNA

All eukaryotic cells contain a nucleus that houses all the molecular blueprints required to create a living cellular structure. Skeletal muscle cells, like other eukaryotic cells, contain 23 paired chromosomes. Chromosomes are DNA and histone based molecules that include all of the genetic material of an organism's genome. The chromosome consists of a chromatin fibre that, itself, is made up of multiple amounts of macromolecule complexes known as nucleosomes (Figure 1.6). The nucleosome is a compound of histones in an octamer like structure that allow the DNA to wrap around the outer side of its structure to condense the DNA strand down into tightly packed units. Histone tails disperse from the individual histone units and running a number of amino acids long which creates a site for epigenetic modification (Bannister and Kouzarides, 2011). The chromatin structure resides into two major functional states. Euchromatin translates to a more open and transcriptionally active chromatin state, in

which the nucleosome structures open apart from one another, allowing the binding of transcriptional proteins to specific strands of DNA (Allis and Jenuwein, 2016). Conversely, heterochromatin conveys a more closed chromatin state, in which DNA strands are protected from transcriptional or modifying machinery (Allis and Jenuwein, 2016). The process of inducing either a euchromatin or heterochromatin state has been identified to be a highly conserved phenomenon, in which epigenetics has, in part, been suggested to play an important regulatory role (Bannister and Kouzarides, 2011, Allis and Jenuwein, 2016).

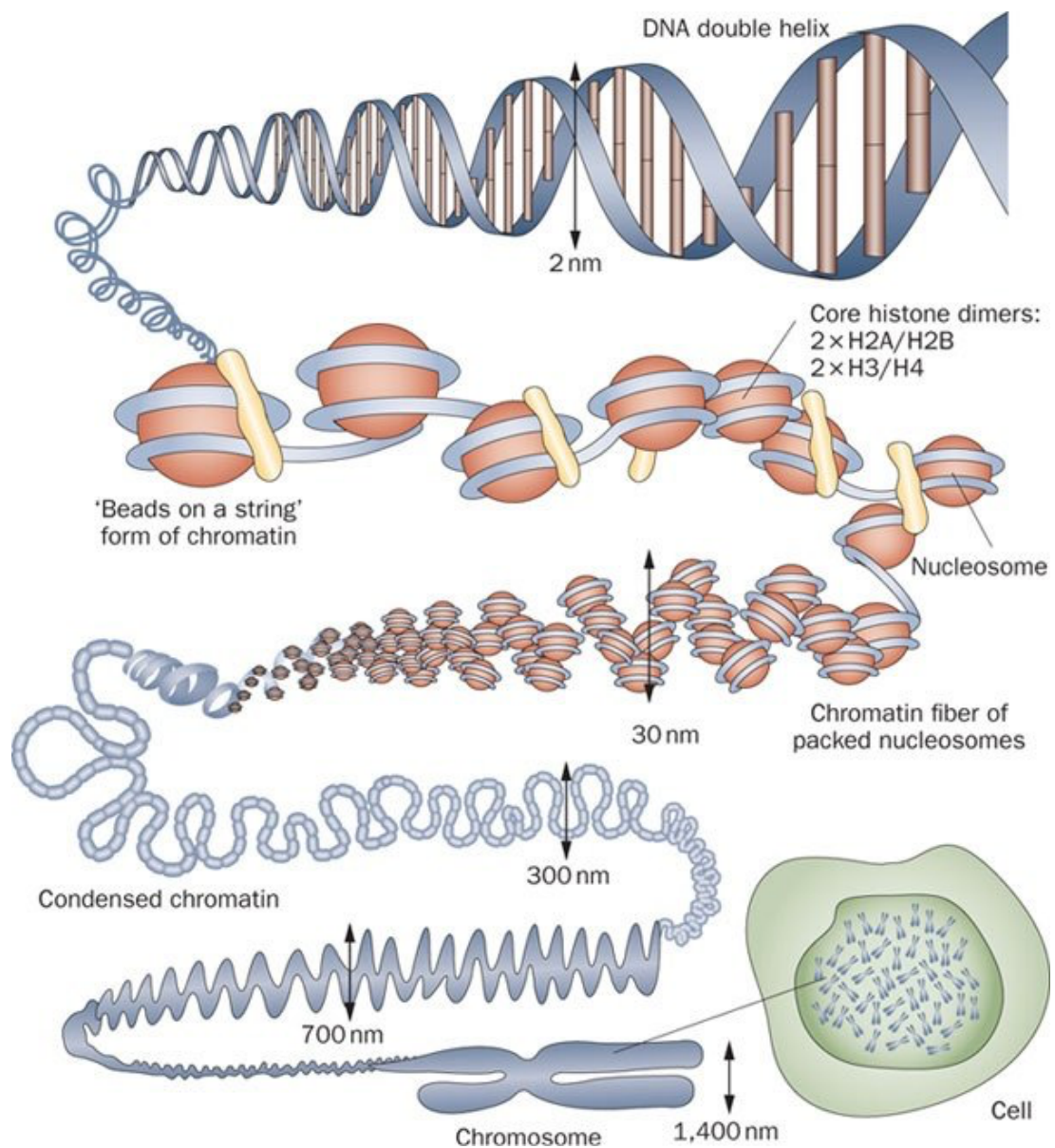


Figure 1.6. Composition and Structure of Chromosome, Chromatin, Nucleosome and DNA Network in Mammalian Cells. Taken from Tonna et al. (2010).

1.4.2 Epigenetics and DNA methylation

Epigenetics, translated means ‘above genetics’, and by definition is the study of mitotically and/or meiotically heritable changes in gene behaviour that are not due to changes in DNA sequence (Bird, 2007, Bird, 2002, Jaenisch and Bird, 2003). These modifications occur on multiple sites within the cell nucleus, most important of which are at histone and DNA loci. The amino acid N-terminal tails that protrude from the core histones means they are readily available for epigenetic modifications such as methylation (increased methylation state; hypermethylation), demethylation (decreased methylation state; hypomethylation), acetylation, deacetylation, phosphorylation, sumoylation, ubiquitination, ADP-ribosylation and citrullination (Bannister and Kouzarides, 2011). Alternatively, epigenetic modifications that occur at the DNA level are more limited, with the most characterised and biologically prominent modification being DNA methylation (Bird, 1986).

DNA methylation attaches a methyl molecule to the 5' position of a cytosine nucleotide located at a cytosine-phosphate-guanine (CpG) dinucleotide pairing, creating a 5-methyl-cytosine (5mC) residue (Figure 1.7). When hypermethylation occurs (increased DNA methylation) in important regulatory regions of a gene transcript, this type of epigenetic modification commonly leads to a reduction in its expression, via two known methods. Attachment of a methyl-molecule co-attracts the addition of CpG methyl binding proteins (MBD) to the promotor region of the gene,

blocking the binding of RNA polymerase and subsequently attenuating the transcription phase of gene expression (Bogdanovic and Veenstra, 2009). The second process is via the incorporation of chromatin remodelling protein methyl CpG binding protein (MeCP1/ MeCP2) that, via binding with the transcriptional-repressor domain (TRD) and co-incorporation of SIN3 transcriptional regulator family member A (SIN3a) and histone deacetylases, leads to a heterochromatin structure (Nan et al., 1997, Nan et al., 1998, Jones et al., 1998) suppressing the expression of genes. Therefore, where strands of DNA are hypermethylated or hypomethylated, it would suggest that the genes effected by this epigenetic modification have reduced or enhanced expression, respectively. Other DNA methylation sites have been uncovered, notably, intragenic DNA methylation, however their role in modulating gene expression is less well understood. The process of DNA methylation is orchestrated via a group of enzymes called DNA methyltransferases. De-novo methyltransferases 3a and 3b (DNMT3a/3b, respectively) are able to methylate non-methylated cytosine residues via the donation of a methyl group from s-adenosyl methionine (SAM), producing 5mC and s-adenosyl homocysteine (SAH; Figure 1.7) (Trasler et al., 2003). To remove the cytosine modification (Figure 1.7), the ten-eleven translocation methylcytosine dioxygenase 1 (TET 1) enzyme and other members of the TET protein family, catalyse the conversion of 5mC to 5-hydroxy-methylcytosine (5hmC) via oxidation of 5mC in an iron and alpha-ketoglutarate dependent reaction (Ito et al., 2010). Importantly, DNMT 3a/b are largely considered *de novo* by nature and induce an epigenetic modification that is considered to be relatively transient. Whereas, DNA methyltransferase 1 (DNMT 1) is considered the stabilising methylation modification enzyme, whereby during DNA replication DNMT1 localises to replication foci and hemi-methylated DNA strands are synthesised. Upon

selective binding to specific hemi-methylated CpG (hCpG) loci, DNMT1 replicates the exact epigenetic modification that preceded at this site, prior to DNA replication (Pradhan et al., 1999, Ramsahoye et al., 2000, Leonhardt et al., 1992). Via this process, DNMT 3a/b are considered *de novo* in which they orchestrate initial DNA methylation, and DNMT1 is considered the enzyme that creates a stabilised modification sufficient to be passed onto daughter generations of cells (Probst et al., 2009). Interestingly however, recent evidence suggests that the clear definitive role of the DNMT 1, 3a and 3b is somewhat ambiguous. Indeed, evidence is apparent that DNMT 1 may also play a role in *de novo* methylation of genomic DNA (Egger et al., 2006), and that DNMT 3a may also play a role in maintaining the cytosine modification (Riggs and Xiong, 2004). Further work is needed to fully characterise the roles the enzymes play in initiating and stabilising DNA epigenetic modifications.

Cytosine 5-Methyl-Cytosine 5-Hydroxymethyl-Cytosine

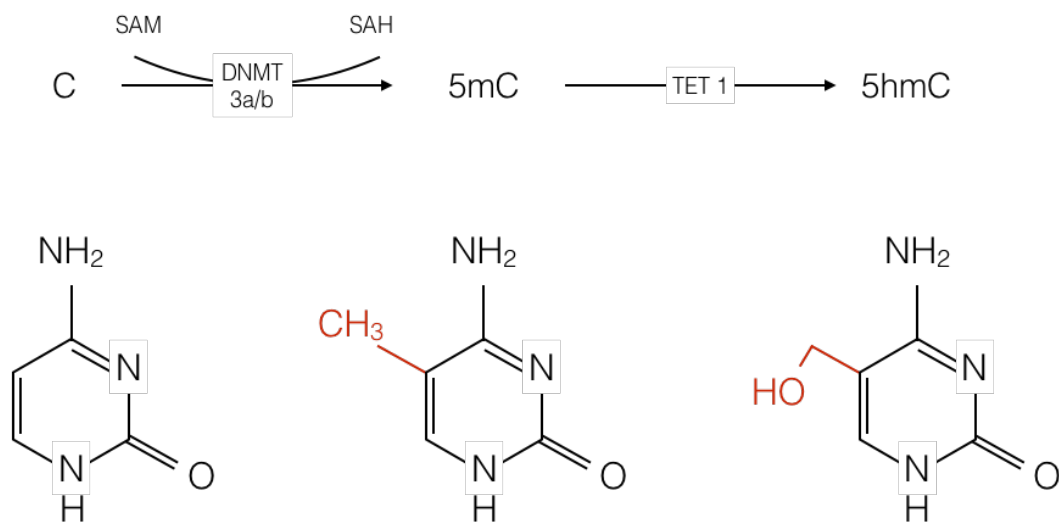


Figure 1.7. Biochemical reactions that create hypo- or hyper-methylated DNA at CpG genomic loci. Briefly, DNMT3a/b attach a methyl-molecule to 5th position of the cytosine nucleotide, via donation from s-adenylmethionine (SAM), rendering 5-methyl-cytosine (5mC) and therefore resulting in DNA methylation. Through the

Ten-Eleven-Translocase 1 enzyme (TET1), 5mC is converted in 5-hydroxymethyl-cytosine and undergoes DNA de-methylation through base excision repair processes.

DNA methylation has previously been shown to play a regulatory role in a number of biological and pathological processes, most prominent of which is X chromosome inactivation, tumorigenesis and cancer progression (Jones and Baylin, 2007, McCabe et al., 2009, Jin et al., 2008, Jin et al., 2009, Gopalakrishnan et al., 2008, Robertson, 2005). However, more recently, its role in modulating muscle specific gene expression has become of significant interest, with findings suggesting that DNA methylation may play a role in regulating gene expression and is associated with alterations in physiological response in skeletal muscle to environmental stress.

1.4.3 Alterations to DNA methylation in mammalian skeletal muscle

The association of DNA methylation alterations in response to exercise have been explored in a number of biological tissues (Voisin et al., 2015). However, with respect to skeletal muscle, the field of epigenetics is still very much in its infancy. The investigative work that has been performed has focused mainly on the adaptive response to either acute/ chronic aerobic exercise. Indeed, following on from findings suggesting that hypermethylation of the peroxisome proliferator activated receptor gamma co-activator 1-alpha (*PGC1- α*) resulted in a reduced mitochondrial content in patients suffering from type II diabetes (T2D) (Barres et al., 2009), the same authors report aberrant DNA methylation patterns in the promotor regions of important mitochondrial related genes, following acute aerobic exercise (Barres et al., 2012). Indeed, acute aerobic exercise at 80% of maximal aerobic capacity, induces significant hypomethylated profiles of genes *PGC1- α* , mitochondrial transcription

factor A (TFAM) and pyruvate dehydrogenase lipoamide kinase isozyme 4 (PDK4) immediately following the termination of exercise, and a reduction in PPAR- δ DNA methylation 3 hrs post exercise. This reduction in DNA methylation corresponded with a time-dependent reduction in gene expression (Barres et al., 2012). In support of this work, Lane et al. (2015) report that after 120-min of steady state aerobic exercise (60 % VO_2 peak), an increased DNA methylation profile of fatty acid-binding protein 3 (FABP3) 4h into recovery corresponded to a reduction in gene expression (Lane et al., 2015). These data collectively suggested that aerobic exercise is sufficient to induce alterations to DNA methylation, that coincide with changes in gene expression, of important metabolic transcripts. Similarly, chronic exposure to aerobic based training stimuli have been reported to have a significant effect on DNA methylation patterns in the mammalian genome. A six-month training intervention, consisting of predominantly aerobic based exercises, 3 times a week for 1-hour per session, produced 134 differentially methylated genes, with 115 of these genes showing significantly decreased DNA methylation profiles (Nitert et al., 2012). Suggesting that chronic exposure to aerobic based training interventions induces large-scale changes in the human epigenome, preferentially favouring a hypomethylated modification.

DNA methylation changes have also been observed at specific CpG site loci, independent to global methylation changes in the gene of interest. Indeed, an initial experiment by King-Himmelreich et al. (2016), undertook 4 weeks of aerobic based exercise training (5 days per week, comprising of jogging, Nordic walking and climbing) in humans and demonstrated significant changes in loci-specific CpG sites of the gene alpha 2 subunit of the AMP-activated protein kinase (*AMPK α 2*) (King-

Himmelreich et al., 2016). In continuation of this initial work, the same authors exposed male *C57BL/6* mice to a bout of acute exercise (1 hour at a running speed of 10.2m/ min to all subjects), before analysing skeletal muscle for epigenetic, transcript and protein profiles, 30-mins following exercise termination. Interestingly, the authors report that 3 out of the 7 CpG sites analysed within the first exon of the *AMPK α 2* gene presented greater DNA methylation when compared to un-exercised controls (King-Himmelreich et al., 2016). The increased DNA methylation of specific sites of the *AMPK α 2* exon corresponded with attenuated gene transcript expression, and protein abundance via qRT-PCR and Western Blot analysis, respectively (King-Himmelreich et al., 2016). Importantly, this work identifies that changes in DNA methylation at a small number of CpG sites of a transcript are sufficient to produce alterations in gene and protein expression, findings that have also been identified elsewhere in rodents (Laker et al., 2014). Where, a maternally fed high fat diet (60% caloric intake in fat) induced a hypermethylated profile of CpG site -260 within the promotor region of *PGC-1 α* , detected at birth and persisting to 12-months of age in offspring, that correlated with a trend for reduction in *PGC-1 α* gene expression (Laker et al., 2014).

In attempts to understand greater the role DNA methylation plays in modulating the mammalian genome, research studies have begun to utilise epigenome wide approaches during periods of exercise or nutrient manipulation. For example, a 6-month aerobic exercise intervention in healthy male subjects and male subjects who had hereditary T2D, demonstrated that 17,975 individual CpG sites displayed a significantly differentially regulated methylation signature (Ronn et al., 2013), from DNA samples obtained from adipose tissue. The same authors report that 18 and 21

gene transcripts displayed significantly altered DNA methylation profiles for obesity and type 2 diabetes respectively, with a number of these candidate genes displaying inverse relationships with gene expression (Ronn et al., 2013). Further work has overlapped the epigenome and the transcriptome to elucidate the response to a period of exercise training. Following 3 months of aerobic exercise training in one leg, muscle samples from the vastus lateralis were analysed for their epigenomic and transcriptomic profiles (Lindholm et al., 2014). The authors reported a significant alteration in DNA methylation of intergenic regions, motifs and enhancer regions of gene transcripts, that inversely corresponded to gene expression and enhanced performance (greater average wattage compared to control limb) during a 15-min maximal one-legged performance cycle test (workload was modified throughout to keep a continued cadence of 60 rpm). Collectively, the authors suggest that following continuous exposure to aerobic stimulus, highly correlative modifications in the human epigenome and transcriptome orchestrate functional changes in skeletal muscle that bring about enhanced performance at a whole tissue level (Lindholm et al., 2014). Finally, investigative work has shown that even relatively acute periods of external stimuli are sufficient to produce large scale adaptations of the epigenome. Indeed, after only 5 days of high fat feeding (50% extra calories of which 60% came from fat) altered the DNA methylation profile of 6,508 genes of the 14,475 studied (Jacobsen et al., 2012). More interestingly, the authors demonstrated a slow return of DNA methylation profiles of the most differentially regulated candidate genes when the high fat diet was removed. Where, out of 10% of the genes previously studied during the high fat diet, 66% displayed a methylation pattern whose direction of change (i.e. hypo- or hypermethylated) reverted back towards control levels. Of these however, only 5% reported a significant change in methylation pattern, suggesting a

slow reversibility in the profile of DNA methylation during exposure to a high-fat diet (Jacobsen et al., 2012). Furthermore, the authors identified that following the initial encounter with a high fat diet (5 days overfeeding), the gene expression of the methyltransferase enzymes, DNMT1 and 3a (*de novo* and maintenance of methylation respectively), were significantly elevated. Together, these studies suggest that both acute and chronic high fat diets lead to large and significant alterations to the epigenome that correlate closely to alterations in gene expression.

It is clear that a strong association exists for DNA methylation in modulating the adaptive response of mammalian skeletal muscle, in response to a number of different environmental stimuli. However, the field of skeletal muscle epigenetics is in its infancy. For example, before 2009 there has been no official publications recorded when searching for the terms of “skeletal muscle and epigenetics” (Figure 1.8A) in the National Centre for Biotechnology Information ‘PubMed’ database. Interestingly however, when refining the terminology to “skeletal muscle and DNA methylation” a slightly greater number of publications is reported (Figure 1.8B), but even here, prior to 2009 a total of 103 papers (in a 25-year period) had been published when searching for these terms, averaging just over 4 papers annually between the years of 1984 and 2008 (Figure 1.8B). What is also interesting is that this area of research is rapidly expanding, with a clear exponential increase in the sheer number of publications (both search criteria) from 2011 onwards. Indeed, 2016 saw a ~445% increase in the amount of publications published when searching for skeletal muscle epigenetics, and a ~180% increase when searching for skeletal muscle DNA methylation, when compared to publications in the year 2011 (Figure 1.8A and 1.8B, respectively). Nonetheless, distinct paucities exist in our current understanding of

skeletal muscle epigenetics and specifically the role of DNA methylation. For example, it has recently been hypothesised that skeletal muscle may be programmable or possess a ‘memory’, defined by (Sharples et al., 2016b) as: ‘*The capacity of skeletal muscle to respond differently to environmental stimuli in an adaptive or maladaptive manner if the stimuli have been previously encountered.*’ This concept has been ascribed, in part, to epigenetic modifications. Therefore, the next part of this literature review will focus on the potential role of epigenetic modifications in retaining the biological information generated from earlier periods of muscle atrophy and hypertrophy – in analogous to a memory effect.

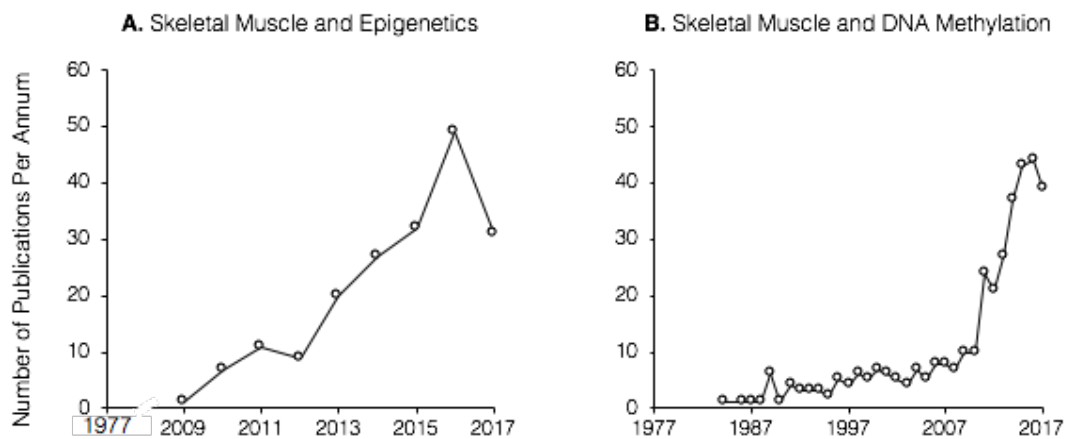


Figure 1.8. Research interest into skeletal muscle epigenetics (A) and skeletal muscle DNA methylation (B) as indicated via number of publications annually. Data acquired from PubMed (National Centre for Biotechnology Information) searches for terms ‘skeletal muscle and epigenetics’ and ‘skeletal muscle and DNA methylation’. Data accurate as of 2017-11-09.

1.5 Epidemiological Evidence That Mammalian Skeletal Muscle Possesses a Memory of Earlier Stimulus

1.5.1 Early life encounters effect long term skeletal muscle phenotypes

Epidemiological evidence suggests there is a distinct association between low-birth weight and deleterious outcomes in skeletal muscle functionality and morphology. Indeed, low birth weight in humans has regularly been associated with reductions in later life grip strength, as a marker for muscle functionality (Inskip et al., 2007, Sayer et al., 2008, Sayer et al., 2004). Grip strength itself has further been associated with overall health, with reductions in grip strength being linked with heart disease, type II diabetes and deleterious metabolic conditions (Rantanen, 2003, Rantanen et al., 2002, Rantanen et al., 1999). Furthermore, low-birth weight has been associated with significant reductions in skeletal muscle mass into later-life. Indeed, large cohort analysis of >900 male subjects found that a reduction of 1kg in birth weight correlated to a 4.1kg reduction in skeletal muscle mass, later on in life (Yliharsila et al., 2007). Collectively, these findings suggest that the early life phenotype, may have a long-lasting effect on the development of the mammalian organism. In agreement with these conclusions, *in-utero* nutrient manipulation during gestation has been shown to alter the development of the off-spring into later life, a phenomenon termed *foetal programming*. Indeed, at the tissue level, reduction of 60% of total calorie consumption in adult guinea pigs resulted in significant reductions in the offspring's birth weight together with a reduction of 20% myofiber number in biceps brachii (Dwyer and Stickland, 1992, Ward and Stickland, 1991). Similar findings were identified in a rat model, where 50% reductions in body and organ weight were

observed following a 50% reduction in gestational nutrient availability during day 7 – 21 (Garofano et al., 1998). As well as total weight, *in-utero* nutrient manipulation has also been shown to have a large impact on the fibre type composition in skeletal muscle. As evident in new born rats exposed to a 30% reduction in calories during gestation, resulting in significantly fewer fast type muscle fibres in both the soleus and lumbrical muscle groups of the progeny, when compared to controls (Wilson et al., 1988). Interestingly, re-feeding of the mothers during lactation was unable to rescue the fibre composition alterations in the soleus muscle, suggesting that altered programming was sufficient to be retained even upon reversal of nutrient availability (Wilson et al., 1988). Furthermore, work in ewes has reported that a global reduction of 50% maternal nutrition (between days 30-70 of gestation) resulted in a fibre compositional alteration, favouring an increase in slow twitch fibres and a reduction in fast twitch fibres, 14 days after birth (Fahey, 2005). These data collectively suggest that *in-utero* manipulation of total calorie availability leads to altered responses in the skeletal muscle in the offspring. Similar conclusions have also been identified during protein restriction during gestation (Mallinson et al., 2007, Hales and Barker, 1992, Snoeck et al., 1990).

1.5.2 Evidence of a cellular skeletal muscle memory

Seminal *in-vivo* work from Egner and colleagues identified that skeletal muscle retains myonuclei following a period of earlier muscle growth (Egner et al., 2013). Using a mouse model, following a period of exercise induced overload they reported a retention of myonuclei number in mice during the ensuing period of denervation-induced atrophy (Bruusgaard et al., 2010). The follow up work administered testosterone to provide a hypertrophic stimulus to increase muscle mass size, in which

an increased myonuclei number accompanied the increase in muscle mass. Similar to the previous work, a retention of this myonuclei number was observed during a subsequent period of muscle wasting, where removal of steroidal exposure reduced muscle mass back towards baseline. Importantly however, when the rodents that had experienced the early testosterone encountered a later period of mechanical overload, they were able to increase muscle mass size more efficiently and rapidly compared to rodents who had not experienced the earlier encounter with testosterone, thereby acting as relevant controls (Egner et al., 2013). Indeed, the rodents that were exposed to both the early (testosterone) and late (overload) anabolic stimuli, presented a 31 % increase in muscle fibre cross-sectional area over a period of 6 days compared to controls, who showed no significant increase in the same time period. Importantly, these studies suggest that skeletal muscle has the capability to increase myonuclei number following earlier hormone induced hypertrophy, and retain this number even during periods when muscle returns to baseline levels following stimulus withdrawal. Following, this adaptation at the level of the myonuclei therefore provides the opportunity for skeletal muscle to hypertrophy more quickly when encountering later muscle growth stimuli. This is suggestive, given the earlier definition of a skeletal muscle memory. Given that retention of epigenetic modifications can occur in skeletal muscle, such as 30 days after the termination of a 5 day high fat diet discussed above (Jacobsen et al., 2012), it is feasible that epigenetic modifications to the DNA of cell nuclei can be retained following earlier periods of growth, even during periods when muscle returns to a pre-growth amount.

1.5.3 Skeletal muscle cells remember the niche in which they are derived

Together with the above work identifying a cellular retention in skeletal muscle, there have been important *in-vitro* based studies that show skeletal muscle cells retain information from the *in-vivo* niche in which they were derived, a process where epigenetics has begun to be elucidated as an important factor. It was first revealed by members of my supervisory team, that skeletal muscle stem cells isolated from patients suffering from cancer exhibit inappropriate proliferation compared to age-matched healthy control cells (Foulstone et al., 2003a). Importantly, at the cellular level, it was identified that the gene encoding for insulin like growth factor binding protein 3 (IGFBP-3) displayed impaired expression resulting in dysregulated cell retrieval in the cells derived from cancer patients (Foulstone et al., 2003a). Since this work, further studies have confirmed the findings that cells derived from different patients retain altered behavioural characteristics when cultured *in-vitro*. Indeed, myotubes grown from muscle-derived stem cells isolated from obese patients exhibit an altered relocation of the fatty acid translocase protein, resulting in a greater intramyocellular lipid content (Aguer et al., 2010). Further work in satellite cells derived from obese patients suggests that upon lipid over-supply *in-vitro*, these cells display a differential gene expression compared to those of cells isolated from healthy humans (Maples and Brault, 2015). Morphologically, muscle-derived cells from *in-utero* growth-restricted foetuses demonstrate weaker proliferative capabilities vs. controls (Yates et al., 2014). Furthermore, cells taken from nutrient-restricted prenatal mice or a postnatal high-fat diet (60 % of total caloric intake) exhibit a significant reduction in the number of derived precursor cells, with these cells displaying an attenuated ability to regenerate post trauma (induced via 5s dry-ice exposure to belly of TA muscle) (Woo et al., 2011). Collectively, these studies suggest that at a

morphological, behaviour and cellular level, skeletal muscle derived stem cells remember the niche in which they were isolated from and demonstrate altered responses when encountering different environmental insults *in-vitro* vs. relevant control cells. However, the precise mechanisms by which this retention of their environmental niche is poorly understood and require further elucidation.

1.5.4 The role of DNA methylation in skeletal muscle memory

To the author's knowledge, only one study has investigated the hypothesis as to whether skeletal muscle possesses an epigenetic memory (Sharples et al., 2016a). The authors utilised an *in-vitro* model, in which murine myoblasts were cultured in the presence or absence of the inflammatory cytokine, TNF- α , cultured for 30 population doublings before experiencing a secondary stimulus of the same cytokine. Importantly, at the morphological and biochemical level, it was reported that cells exposed to both early and late TNF- α treatments displayed significantly reduced myotube number and reduced creatine kinase activity compared to control cells that only experienced the late dosage. It was further reported that epigenetic modifications of the myogenic regulatory factor, MyoD, that were generated following acute early life exposure to TNF- α , were retained even after 30 population doublings in specific CpG regions (Sharples et al., 2016a). Collectively, these data suggest that murine myoblasts retain biological information acquired from early life encounters with the catabolic cytokine, with this retention manifesting into a higher susceptibility to myofiber size reductions upon later life TNF- α exposure. It also suggests that even after an acute early life exposure (24-hrs) and extensive replicative aging (30 population doublings) that DNA methylation tags are able to be retained. It is to be

noted that upon secondary exposure to TNF- α no further adaptations in MyoD gene expression nor DNA methylation were observed.

Nonetheless, this work was the first to directly explore the concept of ‘epigenetic muscle memory’, reporting intriguing findings. As yet however, no further work has explored this concept *in-vivo*, and thus, further investigative work is warranted.

1.6 Thesis Research Project

1.6.1 Research project aims

Given that skeletal muscle cells seem to undergo epigenetic modifications in atrophic conditions we first wished to identify the epigenetic modifications that occur during muscle atrophy *in-vivo*. Therefore, we aimed to:

1. Investigate the role of DNA methylation in skeletal muscle atrophy using an *in-vivo* tetrodotoxin nerve silencing system in rodents to model disuse atrophy over a period of 14 days.

Furthermore, because epigenetic modifications have been shown to be retained for a significant period of time following atrophic exposures, we aimed to:

2. elucidate whether these epigenetic modifications were retained or returned to normal with 7 d of full active recovery in the same animals.

We next wished to explore the concept of epigenetic retention in skeletal muscle of human participants and the role DNA methylation played in orchestrating this phenomenon, especially given previous work elucidating a cellular based phenomenon in rodents, as described above. We therefore aimed to;

3. Investigate whether an epigenetic muscle memory of hypertrophy occurs in human skeletal muscle *in-vivo*, using chronic resistance exercise (loading), followed by cessation of exercise (unloading), and finally a subsequent later chronic resistance exercise programme (reloading), thus allowing the elucidation of the underlying epigenetic alterations that occur after muscle hypertrophy (loading), a return of muscle back to baseline size (unloading) and a secondary anabolic encounter (reloading), respectively.

Finally, given evidence described above that epigenetic modifications are dynamically altered post-acute aerobic exercise stimulus, we wished to elucidate the extent to which acute resistance exercise modifies the human methylome and whether these modifications may exist as early biological markers of later life adaptation to resistance exercise induced muscle hypertrophy. Therefore, we aimed to;

4. Explore modifications to genome wide DNA methylation following a single bout of resistance exercise in previously untrained human subjects (acute RE), and correlate these modifications to changes in the DNA methylation and gene expression following chronic resistance exercise induced hypertrophy (loading) and later life reloading induced muscle growth (data derived in aim 3 above).

The overarching aim of this thesis was to produce novel data in the field of skeletal muscle epigenetics in order to aid in the development of our current understanding of the epigenetic mechanisms that govern skeletal muscle adaptations.

Chapter 2

Materials and Methodologies

2.1 Tetrodotoxin Exposure of the Tibialis Anterior Muscle in Rodents

2.1.1 Wistar rats

Wistar rats from Fisher (2012) weighing between 350 – 450 g were utilised for experimentation, and housed in controlled conditions of 20°C, 45% relative humidity

with food and water available ad libitum. Rats were grouped into five experimental conditions including one control group (CON), three groups were exposed to tetrodotoxin (TTX) administered to the peroneal nerve in one hind limb (detailed below) for 3, 7 and 14-days (d). A final group was exposed for 14-d to TTX followed by TTX removal and 7 days of habitual physical activity. The rats' general welfare was routinely checked and their mobility was minimally affected during experimentation.

2.1.2 Implantation of TTX delivery unit and common peroneal nerve block model

In rats exposed to TTX, a mini-osmotic pump (Mini Osmotic Pump 2002, Alzet, Cupertino CA, USA) was implanted subcutaneously in the scapular region, as previously described (Jarvis and Salmons, 1991, Fisher, 2012). Delivery tubes were then subcutaneously channelled to a silicone rubber cuff that was carefully placed around the common peroneal nerve of the left hind limb of the rodent. Implantation was performed as an in house modification of previous work (Michel and Gardiner, 1990). The osmotic pump efficiently delivered 0.5 μ l/hr of TTX (350 μ g/ml in sterile 0.9 % saline) to the delivery cuff unit allowing the common peroneal nerve to be exposed to TTX at a consistent rate. TTX exposure resulted in the ankle dorsiflexor muscles (tibialis anterior and extensor digitorum longus) to be silenced, but normal voluntary plantarflexion was maintained. Following correct assembly of TTX delivery apparatus, rats were subjected to 3, 7 or 14 days (d) of TTX exposure, with a further group under-going 14d TTX exposure with a subsequent 7d of TTX cessation where normal habitual physical activity resumed. At the end of each experimental time course, all animals were humanely euthanized with increasing CO₂

concentration and cervical dislocation, in accordance with the Animals (Scientific Procedures) Act 1986.

2.1.3 Muscle harvesting procedure and treatment

Following termination of the animals, the TA muscle was harvested, placed on a sterile petri dish and dissected into adequate sections for downstream histological, gene expression and DNA analysis. For histological analysis, samples were mounted and frozen onto cork in isopentane before being stored at -80 °C. Samples required for downstream molecular analysis of RNA and DNA (microarray, RT-PCR and pyrosequencing), were snap frozen in liquid nitrogen before being stored in -80 °C, ready for further analysis.

2.2 Human Skeletal Muscle Resistance Training Studies

2.2.1 Participants

Eight healthy males gave written, informed consent to participate in the study, following successful completion of a readiness to exercise questionnaire and a pre-biopsy screening as approved by a physician. Inclusion criteria for all human studies were:

- i. Male volunteers - to avoid changes in muscle function as a consequence of menstrual cycle (Sarwar et al., 1996) and the known variability between genders in the response to resistance exercise training (Ivey et al., 2000, Tracy et al., 1999)
- ii. Aged 18 – 40
- iii. Free from known medical conditions

- iv. Having not previously taken part in any form of structured resistance exercise
- v. Able to successfully pass both readiness to exercise questionnaire and pre-biopsy medical screening.

One participant withdrew from the study at experimental week 17 of 21, for reasons unrelated to this investigation. However, consent allowed samples to be analysed prior to withdrawal, therefore for this participant this included all conditions excluding the final reloading condition (described below). Ethical approval was granted by the NHS West Midlands Black Country, UK, Research Ethics Committee (NREC approval no. 16/WM/0103).

2.2.2 Experimental design

Using a within subject design eight previously untrained male participants (27.6 ± 2.4 yr, 82.5 ± 6.0 kg, 178.1 ± 2.8 cm, means \pm SEM) completed an acute bout of resistance exercise (acute RE), followed by 7 weeks (3d/week) of resistance exercise (training), 7 weeks of exercise cessation (detraining) and a further period of 7 weeks (3d/week) resistance exercise (retraining). Graphical representation of experimental design is provided in Figure 2.1. Whole-body fan beam dual-energy x-ray absorptiometry (DEXA), strength of the quadriceps via dynamometry and muscle biopsies from the vastus lateralis for RNA and DNA isolation were obtained at baseline, after 7 weeks training (beginning of week 8), 7 weeks detraining (end of week 14) and 7 weeks retraining (beginning of week 22). A muscle biopsy was also obtained 30 minutes after acute RE prior to 7 weeks resistance exercise/training.

2.2.3 Resistance Exercise Protocols for Acute Loading & Chronic Loading, Unloading and Reloading

Untrained male subjects initially performed an exercise familiarization week, in which participants performed all exercises with no/low load to become familiar with the exercise movements (detailed below). In the final session of the familiarization week, the load that participants could perform 4 sets of 8-10 repetitions for each exercise was assessed. Due to participants being un-customized to resistance exercise, assessment was made on competence of lifting technique, range of exercise motion and verbal feedback. Subsequently, starting load was set for each participant on an individualised basis. Three to four days later, participants then undertook a single bout of lower limb resistance exercise (acute RE) followed by biopsies 30-mins post exercise. Following this single bout of acute RE they then began a chronic resistance exercise program (training), completing 60-min training sessions (Monday-Wednesday-Friday), for 7 weeks, with 2 sessions/week focusing on lower limb muscle groups (Monday and Friday) and the third session focusing on upper body muscle groups (Wednesday). Lower limb exercises included, behind head barbell squat, leg press, leg extension, leg curl, Nordic curls, weighted lunges and calf raises. Upper limb exercises included, flat barbell bench press, machine shoulder press, latissimus dorsi pull down, bent over dumbbell row and triceps cable extension. To ensure progression in participants with no previous experience of resistance exercise, a progressive volume model was adopted (Peterson et al., 2011) in which investigators regularly assessed competency of sets, reps and load of all exercises. Briefly, exercises were performed for 4 sets of 10 reps in each set, ~90-120s in between sets and ~3 mins between exercises. When participants could perform 3 sets of 10 repetitions without assistance and with the correct range of motion, load was increased

by ~5-10% in the subsequent set and participants continued on this new load until further modification was required. Where subjects failed to complete 10 full repetitions (usually for their final sets), they were instructed to reduce the load in order to complete a full repetition range for that set or the subsequent set. Total weekly volume load was calculated as the sum of all exercise loads;

$$\text{Total Exercise Volume (kg)} = (\text{Exercise Load} * \text{No. of Reps}) * \text{No. of Sets}$$

Equation 1. Equation to identify the total exercise volume undertaken by human participants during the resistance loading programmes.

The acute RE session resulted in a total load of 8,223 kg (± 284). Thereafter, the loading and reloading phases resulted in a progressive increase in in training volume (\pm SEM) of $2,257 \pm 639$ kg and $2,386 \pm 222$ kg respectively per week. Loading and reloading programs were conducted in an identical manner, with the same exercises, program layout (same exercises on same day), sets and repetition pattern, as well as rest between sets and exercises. During the 7 week detraining phase, participants were instructed to return to habitual pre-intervention exercise levels and not to perform any resistance training. Regular verbal communication between researcher and participant ensured subjects followed these instructions. A trainer was present at all resistance exercise sessions to enable continued monitoring, provide verbal encouragement and to ensure sufficient progression. No injuries were sustained throughout the exercise intervention.

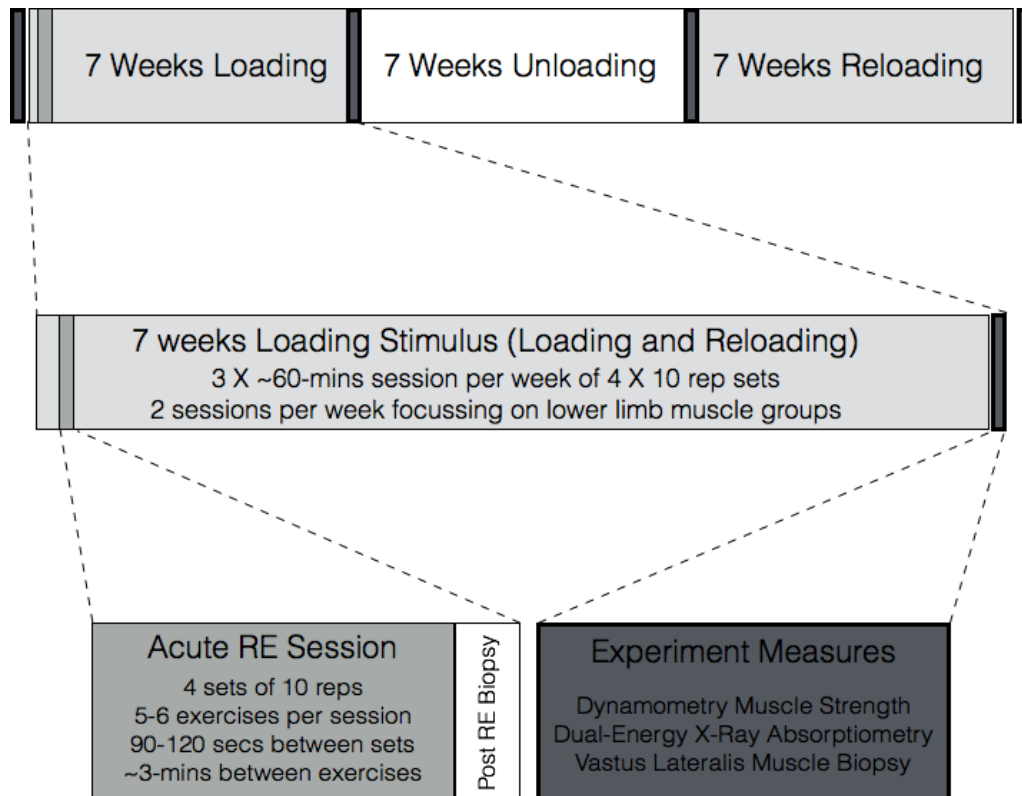


Figure 2.1. Overview of resistance exercise training protocol for acute loading and chronic loading, unloading and reloading stimuli in human subjects. Light grey (loading) and white box (unloading) indicate training programme. Medium grey box with black outline identifies the acute RE condition, with biopsy occurring immediately (> 30 mins) post RE. Dark grey box with solid black outline details the experimental measures taken for analysis of *in-vivo* muscle mass and strength adaptations and acquisition of muscle sample for down-stream RNA/DNA analysis.

2.3 Histological and Morphological Measurements of Muscle Mass Atrophy in Rodents

2.3.1 Haematoxylin and eosin staining for fibre cross sectional area and tibialis anterior muscle mass analysis

For morphological and histological purposes, muscle was harvested from control and experimental groups (n = 6 per group), weighed, and divided into pieces, and a transverse portion from the mid-belly of the muscle was frozen in melting isopentane,

cryostat sectioned (10 μm), and stained with haematoxylin and eosin, as previously described (Fisher, 2012). To perform staining, samples were removed from -80°C and left to stand at room temperature for 30 mins before being rehydrated in water. Sections were placed in haematoxylin solution for 3 mins, washed in warm-water for 3 mins, placed in Eosin solution for 1-min and subsequently washed in warm water for 10 secs. Finally, the sections were dehydrated through incremental exposures to molecular grade alcohol solutions at 50, 70, 90 and 100% purity, cleared in xylene and mounted using Dibutyl phthalate in xylene (VWR, Lutterworth, UK). For each muscle sample, 5 images were obtained at random. By using ImageJ 1.45i software (National Institutes of Health, Bethesda, MD, USA), each photograph was overlaid with an 8 X 8 grid with which to make an unbiased selection of fibres. Ten fibres were selected for counting for each field of view at the first 10 intersections of the grid that fell within a fibre. Magnification of each section was calibrated from an image of a stage graticule. Cross-sectional area (CSA) was estimated from precise diameter measurements that were taken by selecting 2 points across the minimum diameter and assuming a circular cross-section. Mean TA mass for all control and experimental groups were expressed as a percentage of whole animal body mass to normalize for inter-individual differences in animal size ($n = 6$). Mean CSA of TA muscle fibre of the treated (left) limb was expressed as percent change from the untreated contralateral control (right) limb for each animal ($n = 6$).

2.4 In-Vivo Assessment of Changes in Skeletal Muscle Strength and Mass in Human Studies

2.4.1 Dual energy X-Ray absorptiometry

A whole-body fan beam dual-energy x-ray absorptiometry (DEXA; Hologic QDR Series, Discovery A, Bedford, MA, USA) scan was performed at baseline (control) and after loading, unloading and reloading conditions to assess lower limb changes in lean mass. All scans were performed and analysed (QDR for Windows, version 12:4:3) by the same trained operator, according to Hologic guidelines. The DEXA scan was automatically analysed via the QDR software before the operator confirmed areas of interest including lower limb positions. Lean muscle mass (kg) was calculated and analysed on absolute values for each condition, and presented as a relative percentage change compared to baseline. Furthermore, to assess whether reloading induced adaptations in skeletal muscle mass compared to loading alone, absolute values of lean mass were normalised to appropriate conditions to account for residual starting mass. Where, loading condition was normalised to baseline, and reloading was normalised to unloading for each participant, with change in lean mass presented as percentage change to the normalised condition.

2.4.2 Maximal isometric voluntary contraction of the quadriceps muscle

To assess quadriceps muscle strength, *in-vivo* isometric knee extension maximal voluntary contractions (MVC) were performed using an isokinetic dynamometer (IKD; Biodex, New York, USA) to measure peak joint torque. Data is presented as percentage increase to baseline (%) using absolute values (Nm), unless otherwise stated. The participants were seated on the dynamometer chair with the hip flexed to

90°, the lateral femoral condyle of the right leg aligned with the dynamometer axis of rotation during contraction and the tibia strapped to the dynamometer lever arm proximal to the malleolus. Inextensible straps harnessed participants into the chair at the hip, distal end of the thigh and the chest to minimize compensatory movements. Following a progressive warm-up of submaximal through to maximal contractions (e.g. a 5-10% increasing in rate of perceived exertion of each sequential repetition, climaxing to performing 1-2 maximum efforts), participants performed two or three isometric MVCs at the 'optimum' knee angle for torque production. This angle was identified as that at which peak torque was recorded during a prior isokinetic knee extension at a constant speed of 30°/s (through a full range of motion). The optimum ranging between 70° – 90°. A rest period of 90 – 120 s was allowed between efforts. Verbal and visual (real-time trace of torque motion) feedback as well as verbal encouragement were given throughout all MVC efforts. Joint torques and angles were recorded and filtered with a low-pass 500 Hz filter (AcKnowledge Version 4.4) to omit background noise. The highest peak joint torque recorded from all isometric trials was taken forward for analysis. Data are presented as percentage increase to baseline (%) using absolute values (Nm), unless otherwise stated.

2.5 Muscle Harvesting and Tissue Handling

At all experimental time points, muscle biopsies were obtained from the right vastus lateralis (VL) muscle of human participants, using conchotome instruments. Subjects were asked to relax on a pre-sterilised hospital bed, whilst the biopsy area of the VL was prepared. Avoiding immediate areas of previous incision, the site was shaved, washed with an alcohol swab and washed again with Hydrex surgical scrub (ECOLAB Ltd. Leeds, UK), before a sterile sheet was placed around the site of

interest and participants were informed to avoid direct contact with the surgical area. A local anaesthetic (bupivacaine hydrochloride; Kays Medical Supplies, Liverpool, UK) was administered to the incision site, at a concentration of 5 mg.ml (~ 1.5 – 2 ml), to anaesthetise the area. A sterile, one-use, disposable scalpel (needle size 10; Swann-Morton, Mu-Care Ltd., Bedfordshire, UK) was used to make an incision, penetrating the skin and muscle fascia. An autoclaved sterilised conchotome biopsy tool was used to retrieve a muscle sample from the vastus lateralis muscle of subjects. Surgically sterile tweezers and a scalpel were used to dissect the obtained muscle sample on an irradiated sterile petri-dish for preparation of down-stream analysis (see below). In the unlikely event of the biopsy containing any fibrous/fat tissue this was removed using a scalpel, leaving only lean tissue. Post-incision treatment and follow-up aftercare was given to all participants in alignment with our laboratories operating procedures.

2.6 RNA Isolation, q-RT-PCR for Gene Expression Analysis

2.6.1 Homogenisation of muscle samples for gene expression analysis

A schematic representation of RNA isolation procedure is given in Figure 2.2 The following procedures were all performed on ice to attenuate the activity of endogenous RNases, allowing for the maintenance of RNA integrity. Samples were withdrawn from -80°C storage and immediately immersed in 1 ml of TRIzol (Thermo Fischer Scientific, UK), before being spun for 40 s at 6,000 rpm (MagNA Lyser Instrument, Roche Life Sciences, UK) in MagNA Lyser (Green Top) Beaded tubes filled with 1.4 mm ceramic beads and left to stand on ice for 5-

mins. This step was performed 3 times, or until whole muscle sample was visibly homogenised.

2.6.2 Procedures for RNA isolation

Two hundred μ l of Chloroform was added to each 1 ml working sample and shaken vigorously to encourage sufficient mixing indicated by a cloudy pink colour. Samples were left to stand for 2-3 mins at room temperature before being centrifuged at 12000 g for 15 mins at 4°C. Following centrifugation, samples were separate into three distinct sections; (i) a lower red organic component that comprises TRIzol, protein and lipid, (ii) a thin milky interphase layer that contains DNA, and (iii) a clear aqueous phase that contains RNA and chloroform (Figure 2.2). The final layer, the clear RNA component, was carefully extracted and placed in new RNA-free tubes (Ambion[®] RNase-free, Ambion[™]). These samples were then supplemented with isopropanol in a 1:1 ratio with the amount of original TRIzol used to lyse sample, before being vortexed and left to stand at room temperature for 10 mins. Centrifugation for 10 mins at 12,000 g and 4°C created an RNA pellet, the excess isopropanol was then removed via pipette as not to dislodge the RNA pellet (Figure 2.2). To clean the RNA pellet from any residual isopropanol, 1 ml of molecular grade ethanol (75 %: 25% molecular grade RNA free water) was added to the RNA pellet which was gently agitated to remove from the side of the tube in order to clean the entire pellet. The sample was then centrifuged again at 7500 g for 8 mins at 4°C. Excess ethanol was then pipetted off and RNA pellets were left to stand at room temperature until ethanol had evaporated and the pellet had dried (usually indicated by the pellet turning from cloudy white to translucent). As soon as the pellet turned translucent the samples were immediately resuspended in 20-30 μ l of RNA storage solution (Ambion[®] RNA

Storage Solution, Ambion™), thoroughly vortexed and left on a 35°C heating block for 10 mins.

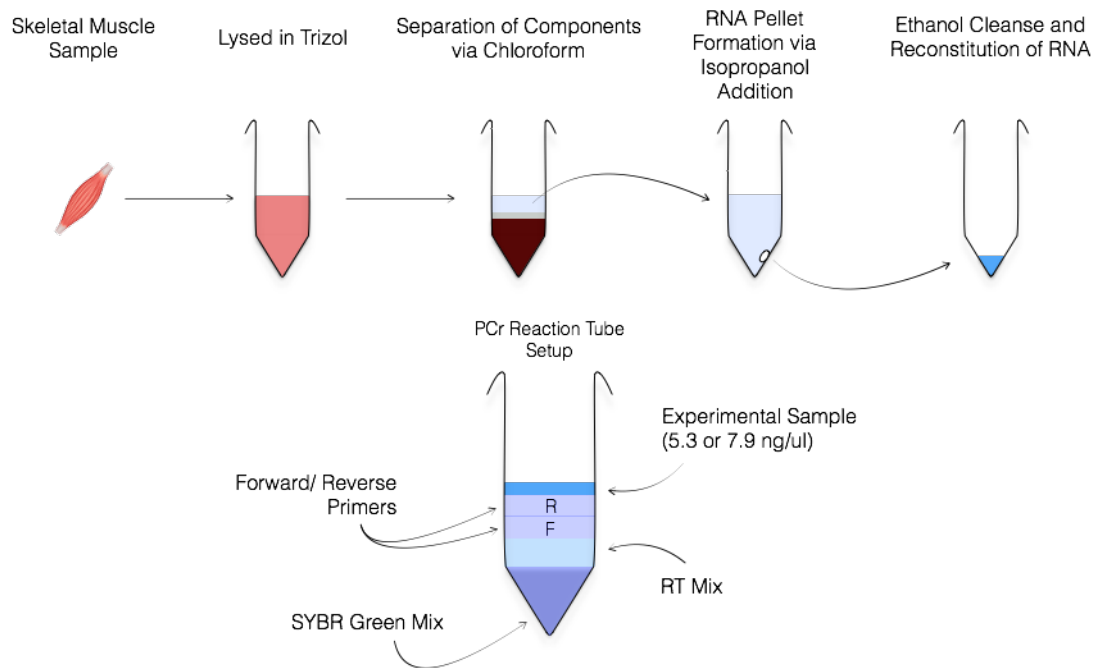


Figure 2.2. Process of RNA isolation from skeletal muscle samples and reaction tube setup for reverse-transcription quantitative real time polymerase chain reaction analysis.

2.6.3 Measurement of quality and quantity of isolated RNA

A measurement of isolated RNA concentration and purity was done via use of a Nanodrop spectrophotometer (Nanodrop 2000, Nanodrop, Thermo Scientific). The concentration of RNA was made under the assumption that nucleotides absorb a UV light in specific patterns. A UV light, at a wavelength of 260 nm, was emitted and passed through 1µl of experimental sample. A photo-detector measured the amount of UV light that passed through the sample, and therefore the absorbency of the targeted suspension. Utilising the Beer-Lambert law (modified for analysis of oligonucleotides; see below for equation 3) of optical density, and prior knowledge of

the absorbance (A), the wavelength-dependent extinction coefficient (ϵ) and the path length of emission (b), it is possible to identify the concentration (C) of suspension. Where the known wavelength-dependent extinction coefficient for RNA is $40 \text{ ng-cm}\cdot\mu\text{l}^{-1}$.

$$C = \frac{(A * \epsilon)}{b}$$

Equation 2. The modified Beer-Lambert Law of absorbance. The equation allows for detection of quantity (C) for both RNA via the identification of absorbance (A), and the known properties of extinction-coefficient (ϵ) and path length (b).

The purity of the suspension was measured via the 260:280 ratio of absorbance, given that protein absorbs maximally at 280 nm, it can identify protein contamination. RNA is considered to be purest with a reading of around 1.9 - 2.1. To further confirm purity of isolated RNA suspension, absorbance of UV light emitted at wavelengths of 260 and 230 nm (260:230 ratio) were analysed. The 260:230 of nucleic acids are often higher than the 260:280 counter-part for the same sample, however, readings will usually lie in the range of 1.8-2.2. If considerably different to these targets, it would indicate the presence of residual amounts of phenol, guanidine or proteins. Average \pm standard deviation for 260:280 ratios for samples are described in the methods for experimental chapters, where applicable.

2.6.4 Quantitative real time polymerase chain reaction experiments

2.6.4.1 One step PCR reaction

To analyse gene expression for all genes in chapters 4 and 5, and Ampd3 and POLr2a in chapter 3, QuantiFast™ SYBR® Green RT-PCR one-step kit was utilised with reactions setup as follows; 9.5 µl RNA sample (7.3 ng/µl = 70 ng total RNA in the reaction or 5.3 ng/ µl = 50 ng total), 0.15 µl of both forward and reverse primers (100 µM stock suspension, 0.2 µl of RT mix and 10 µl of SYBR® Green, totalling 20 µl reactions (Figure 2.2). For all human gene expression analysis, PCR reactions were set up as 50 ng reactions, and rodent work set up as 70 ng reactions. Reverse transcription cycles were completed before subsequent PCR performed as follows: hold 50°C for 10 min (reverse transcription/cDNA synthesis), followed by 95°C for 5 min (transcriptase inactivation and initial denaturation step), before 40 - 45 PCR cycles of; 95 °C for 10 s (denaturation), 60 °C for 30 s (annealing and extension). Finally, a melt curve step was performed to identify any primer dimer formation or non-specific amplification. All relative mRNA expression was quantified using the comparative Ct ($\Delta\Delta\text{Ct}$) method (Schmittgen and Livak, 2008) against a known reference gene. Primer sequences were designed by the current Ph.D applicant via use of the Primer-Blast software on National Centre of Biotechnology (<https://www.ncbi.nlm.nih.gov/tools/primer-blast/>). All primers were subsequently sent for manufacturing from Sigma-Aldrich, before being purchased and re-suspended in TE buffer (pH 8.0: TE Buffer, Ambion®, Invitrogen, California, USA). All primer sets for gene expression can be found in relevant experimental chapters, along with average Ct value, standard deviation and percentage variation of housekeeper utilised within each experiment.

2.6.4.2 First-strand cDNA synthesis and PCR

Analysis of a sub-set of genes in chapter 3 (Myog, Fbxo32, Trim63, Chrna1 and Hdac4) was performed previously by Dr. Andrew Fisher using a cDNA and end-point PCR method, as described here (Fisher, 2012). One μg of RNA was taken forward (addition of RNase free water to equate a 12 μl suspension), and 1 μl of oligo dT primer (Invitrogen, Thermo Fisher Scientific, California, United States) was added to the suspension before being incubated at 70°C for 10-mins. A reaction mix containing 4 μl of 5X buffer, 2 μl of dithiothreitol (DTT) and 1 μl of deoxynucleotide triphosphates (dNTPs; all products Invitrogen), was added to each RNA sample and incubated at 42°C for 2 mins. Superscript II Reverse Transcriptase (Invitrogen) was added (1 μl) and suspension was incubated for a further 50 mins at the same temperature, before being incubated for 15 mins at 70°C to inhibit the reaction. Reverse-transcription PCR (HotStar Taq Master Mix; Qiagen, Crawley, UK), performed on a Px2 Thermocycler (ThermoFisher, Scientific), was setup as follows; 3 μl of cDNA, 15 μl HotStar Taq Master Mix, 1.5 μl of forward and reverse primers (20 μM) and 9 μl of RNase free water, to total a 30 μl reaction. PCR cycles began with 1 cycle of 95°C for 10 mins, before 40 cycles of denaturation (94°C for 30 s), annealing (55-65°C for 30 s) and extension (72°C for 1 min) were performed, and a final polishing hold was performed (72°C for 10 mins). For real-time qPCR using HotStar Taq Master Mix Kit on the iQ5 Thermocycler, reactions were as follows: 3 μl cDNA, 15.396 μl of RNase-free water, 7.5 μl 2X SYBR Green Supermix (BioRad, Hemel Hempstead, UK) and 0.27 μl of forward and reverse primers (20 μM). Relative gene expression was subsequently analysed and performed as previously described (section 2.6.4.1).

2.6.5 Microarray Analysis of Rodent Muscle

2.6.5.1 Rodent muscle sample preparation for microarray analysis

Frozen muscle samples were sent to AROS Applied Biotechnology for processing and preparation for downstream analysis, this included N=4 for all conditions of sham control, 3-D, 7-D, 14-D TTX exposed and 14-D TTX plus 7-D of active recovery conditions. AROS Applied Biotechnology performed all homogenisation, nucleic acid isolation, quality control and array analysis. Over 30,000 rat transcripts and 28,000 variants were examined via Affymetrix GeneChip® Rat Genome 230 2.0 Array (Affymetrix, High Wycombe, UK).

2.6.5.2 Transcript wide analysis via transcriptome analysis control software

Raw data files were analysed by the current Ph.D applicant for the elucidation of differentially regulated transcripts across experimental conditions. Raw data files (.CEL) were normalised via the MAS 5.0 signal method (Irizarry et al., 2003a, Irizarry et al., 2003b) and .CHP files were subsequently analysed for significantly differential gene expression from microarray data (Transcriptome Analysis Console; TAC, Affymetrix, High Wycombe, UK). TAC software was used to create hierarchical clustering heatmaps of the most differentially expressed genes and lists of the most frequently differentially regulated transcripts across experimental comparisons. Specific heatmap details can be found in figure legends within experimental chapters.

2.7 DNA Isolation, Epigenome-wide Analysis and Loci-Specific DNA Methylation Experiments

2.7.1 Preparation of muscle sample for DNA isolation

Samples were withdrawn from -80°C storage and immediately stored on ice, before being immersed in 200 µl of DNA homogenate buffer (180 µl of ATL buffer and 20 µl of proteinase k; DNA Blood and Muscle Kit, Qiagen, Manchester, UK), before being spun for 40 s at 6,000 rpm (MagNA Lyser Instrument, Roche Life Sciences, UK) in MagNA Lyser (Green Top) Beaded tubes filled with 1.4 mm ceramic beads, and left to stand on ice for 5 mins. This step was repeated 3 times, or until whole muscle sample was visibly homogenised (Figure 2.3).

2.7.2 Isolation of deoxyribonucleic acid

All samples were isolated using a commercially available DNA isolation kit (DNeasy Blood and Tissue Kit; Qiagen, United Kingdom) in accordance with manufacturers' instructions. Samples were collected from -80°C and immediately kept on ice before being immersed in 200 µl of DNA homogenate buffer (180 µl of ATL buffer and 20 µl of proteinase k) and homogenised at 6,000 rpm 40 s (MagNA Lyser Instrument, Roche Life Sciences, UK). This step was repeated 3 times with 5 mins on ice between homogenisations, to ensure total disruption of muscle cells, and the release of genomic DNA while avoiding its degradation. Suspension was supplemented with 200 µl of AL buffer before being incubated at 56°C for 10 mins. Molecular grade ethanol (200 µl of > 96 % pure) was subsequently added to the suspension before being briefly vortexed and aliquoted into spin columns placed in 2 ml collection tubes (DNeasy Mini Spin Colum, DNeasy Kit, Qiagen). Spin columns were centrifuged at 6,000 g

for 1 min, flow through discarded and 500 μ l of buffer AW1 was added to the spin column and centrifuged at 6,000 g for 1 min. Buffer AW2 was then added to the spin column and centrifuged at 20,000 g for 3 min. All flow through was discarded and spin columns were placed in new RNA/DNA free tubes (RNase-free Microfuge Tubes, Ambion™, ThermoFisher Scientific, United States), before 50 μ l of elution reagent (buffer AE) was added directly to the spin column and centrifuged at 6,000 g for 1 min. The elution step was repeated to yield a total DNA suspension of 100 μ l per original sample. Samples were then frozen (-20°C) in this form until further downstream analysis. This process is schematically represented in Figure 2.3.

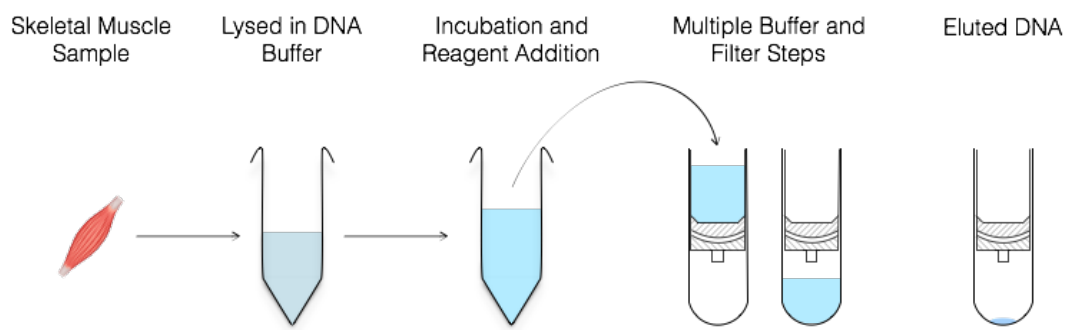


Figure 2.3. Overview of the Process for DNA Isolation from Muscle Tissue Samples.

2.7.3 Quantification of DNA quantity and quality.

Isolated DNA was analysed for quality and quantity via UV spectroscopy (Nanodrop 2000, ThermoFisher Scientific, United States), in identical fashion to that described for RNA analysis (see section 2.6.3). However, double stranded DNA has a known wavelength-dependent extinction coefficient of 50 $\text{ng}\cdot\text{cm}\cdot\mu\text{l}^{-1}$ and single-stranded DNA (that best represents bisulfite converted DNA, see below) has a coefficient of

33 ng-cm. μl^{-1} . The optimum absorbency ratio for isolated DNA is 2.0 for 260/280 wavelengths, and in the range of 1.8-2.2 for 260/230 ratio.

2.7.4 Bisulfite conversion of isolated DNA

Once isolated DNA was quantified, downstream bisulfite conversion was required in order to allow for detection of unmethylated and methylated loci (Frommer et al., 1992). This methodology works on the principle of generating an artificial single nucleotide polymorphism (SNP) where methylated CpG sites maintain cytosine uniformity upon bisulfite treatment, whereas un-methylated CpG locus are modified into uracil and read as a thiamine upon PCR amplification. Thus, an artificial SNP is rendered at the site of un-methylated CpG and is detectable upon down-stream analysis (Figure 2.4). In all experiments, bisulfite treatment was accomplished via use of EZ-DNA methylation kit (Zymo Research, California, United States), or InnuConvert Bisulfite Basic kit (AJ Innuscreen GmbH, Berlin, Germany) and were performed in accordance with manufacturer's instructions.

2.7.4.1 EZ DNA methylation kit protocol

The EZ DNA methylation bisulfite conversion protocol was performed using Zymo-Spin™ IC Columns (pyrosequencing method of DNA methylation detection, chapter 3) and a Silicon-A™ Binding Plate for higher throughput of conversion (DNA methylation BeadChip Array, chapter 4 and 5). Both protocols are performed identically, unless otherwise stated. Five micro-litres of M-Dilution Buffer was added to 500 ng of isolated DNA, and distilled water (dH2O) was added where applicable, to yield a total suspension of 50 μl , before samples were incubated for 15 mins at 37

°C. In each sample 100 µl of prepared CT Conversion Reagent was added, and incubated overnight (16 hrs) at 50 °C. CT Conversion Reagent is light sensitive and thus, the incubation period was performed overnight and in the dark to limit exposure, where possible. Following incubation, samples were moved onto ice for 10 mins. Four-hundred µl of M-Binding Buffer was added to a Zymo-Spin™ IC Column or a Silicon-A™ Binding Plate, before the experimental sample suspension was added and mixed via inversion. Spin columns were spun at either maximum speed for 30 s (spin column) or at 3,000 g for 5 mins (silicon plate) and flow through discarded. For spin column-based conversion, a series of wash buffer stages followed, where all steps included a 30 s spin at maximum speed; i. 100 µl of M-Wash Buffer, ii. 200 µl M-Desulphonation Buffer (incubation for 15-20-mins at room temperature), iii. 200 µl of M-Wash Buffer, iv. 200 µl of M-Wash Buffer. Finally, 10 µl of M-Elution Buffer was added directly to spin column matrix and centrifuged for 30 s at maximum speed to elute DNA. For conversion performed on the Silicon-A™ Binding Plate, a series of wash buffer stages were performed. Five-hundred µl of M-Wash Buffer was added and centrifuged at 3,000 g for 5 mins. M-Desulphonation Buffer (200 µl) was added to the suspension and left to incubate at room temperature for 15-20 mins before being centrifuged at 3,000g for 5 mins. Two wash buffer stages were then performed, where 500 µl of M-Wash Buffer was added to the suspension and centrifuged at 3,000 g for 5 and 10 mins, respectively. To elute the sample, the silicon plate was placed onto an Elution Plate and 30 µl of M-Elution Buffer was added directly to the matrix of each well and spun at 3,000 g for 3 mins

2.7.4.2 InnuConvert bisulfite conversion kit protocol

To generate bisulfite converted DNA for use in down-stream high resolution melt polymerase chain reaction (HRM-PCR; described in section 2.7.6.2), as utilised in chapter 3, isolated DNA was converted using the InnuConvert bisulfite conversion kit, as described. A bisulfite conversion suspension was created containing 70 μl of Conversion Reagent and 30 μl of Conversion Buffer, and was added to 50 μl of isolated DNA, before being vortexed and incubated at 85 °C for 45 min with suspension being vortexed every 15 mins, throughout the incubation. 700 μl of Binding Solution GS was added to incubated suspension, vortexed briefly and added to a spin column and receiver tube system and spun at 14,000 g for 1 min. A six-step protocol of washing and buffer reagents ensued, in which all reagents were spun at 14,000 g for 1 min; i. 200 μl Washing Solution BS, ii. 700 μl Desulphonation Buffer (10 min incubation), iii. 500 μl Washing Solution C, iv. 650 μl Washing Solution BS, v. 650 μl ethanol absolute, vi. 650 μl ethanol absolute. The remaining substance in the spin filter was then incubated for 10-min to air dry, then incubated for a further 1-min in the presence of 25 μl of Elution Buffer and spun at 8,000 g for 1 min. The eluted suspension was aliquoted out, and this final step was performed for a second time, resulting in a total yield of 50 μl of bisulfite converted DNA.

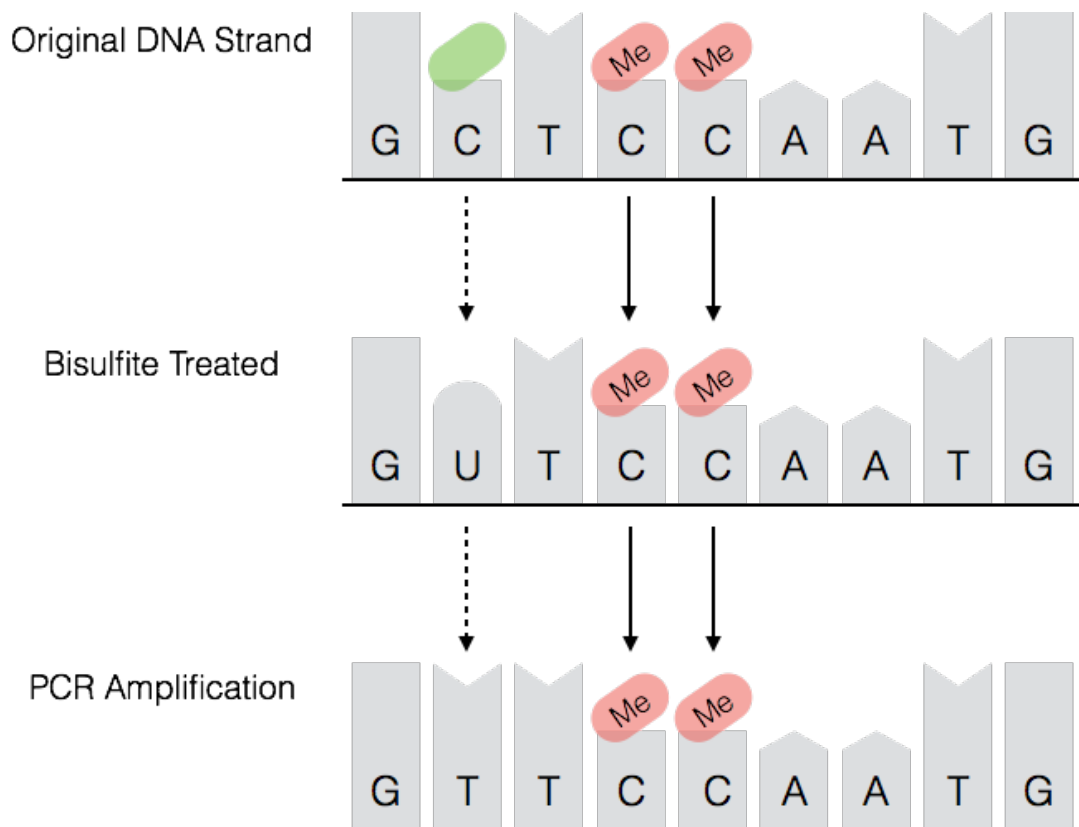


Figure 2.4. Schematic representation of modifications to DNA strands during bisulfite conversion treatment and PCR amplification. Briefly, methylated cytosine residues (depicted as ‘C’ with red methylation (Me) modification) maintain cytosine uniformity during bisulfite modification. Conversely, unmethylated cytosine residues (depicted as ‘C’ with a green empty modification) are modified into uracil residues (rounded nucleotide; U) and once amplified via PCR, are read as thymine (inverted nucleotide; T). Solid black arrows indicate unmodified base during bisulfite and amplification processes. Dashed arrow indicates modification of the base nucleotide during the same processes.

2.7.5 Methylome-wide bead chip arrays and analysis

2.7.5.1 Methylome Wide CpG DNA Methylation Assay

Isolated DNA and bisulfite converted samples, as outlined previously, from all human *in-vivo* studies were sent to The Genome Centre at Barts and the London School of Dentistry of Queens Mary University London for analysis of the Illumina Infinium

MethylationEPIC array that examines over 850,000 CpG sites of the human epigenome (Infinium MethylationEPIC BeadChip, Illumina, California, USA). The EPIC array covers 99% of the reference sequence of promoters and includes targets of the FANTOM5 and ENCODE methylated sites previously identified (Bibikova et al., 2011). In a 3 stage process, the EPIC Infinium array was performed in accordance with Illumina standard operating procedures, as described here.

2.7.5.1a Genomic DNA Bisulfite Conversion and Amplification:

Four μl of bisulfite converted DNA (BCD; section 2.7.4.1) was transferred from the bisulfite conversion plate in to corresponding wells of a MSA4 plate and 20 μl of MA1, 4 μl of 0.1N NaOH were added before plate was vortexed (1600 rpm for 1-min), pulse centrifuged (280 g) and left to incubate at room temperature (RT) for 10-mins. Samples within this place then had 68 μl of RPM and 75 μl of MSM added before a further round of vortex and centrifugation was performed (identical to above). Samples were subsequently left in a 37°C hybridization oven overnight (20-24 hrs) to allow for amplification.

2.7.5.1b Fragmentation, Precipitation and Resuspension of Amplified DNA:

FMS (50 μl) was added to each well of the MSA4 before being vortexed (1600 rpm for 1-min), centrifuged (280 g) and incubated (37°C for 1-hr) to fragment DNA. An endpoint fragmentation was used to avoid over-fragmentation. Following incubation, 100 μl of PM1 and 300 μl of 2-propanol were added to each well interspersed with vortexing (1600 rpm for 1-min), incubation (37°C for 5-mins) and centrifugation (280 g for 1-min). MSA4 plate was subsequently mixed via inversion (at least 10 times) incubated at 4°C for 30-mins, centrifuged at 3000 g at 4°C for 20-mins, supernatant

liquid decanted out of wells and left at room temp for 1 hour to dry pellet. Following precipitation, each pellet in each well was resuspended in 46 μ l of RA1 incubated at 48°C for 1-hour, vortexed for 1-min (at 18000 rpm) and pulse centrifuged at 280 g.

2.7.5.1c Hybridization to BeadChip, Extension and Staining:

Fragmented DNA residing on the MS4A plate was incubated at 95°C for 20-mins to denature experimental samples before being left to stand at RT for 30-mins and pulse centrifuged at 280 g, and subsequently prepared for transfer and precisely loaded onto a working BeadChip. BeadChips were loaded into the Illumina Hyb Chamber and placed for over-night incubation at 48°C for 16-hrs, before being washed (gentle agitation in 200 ml of PB1) and readied for BeadChip staining. Assembled flow-through chambers were loaded into a chamber rack where single based-extension occurred of each flow through assembly. Single base-extension was performed at 44°C via the addition of the following reagents: 150 μ l of RA1 with incubation of 30-secs (repeated 5 times), 450 μ l of XC1, 450 μ l of XC2, 200 μ l of TEM and 450 μ l of 95% formamide/1 mM EDTA (repeated). Each flow-through assembly was incubated for 5-mins, before 450 μ l of XC3 was added (repeated). Staining of assemblies was performed in 5 repeated cycles of the following: addition of 250 μ l of STM to each flow-through assembly (10-mins incubation), 450 μ l of XC2 incubated for 1-min (repeated) and left to stand for 5-mins. To wash staining reagents, BeadChips were gently submerged and agitated initially in PB1 (310 ml per 8 BeadChips), and then in XC4 (same total amount of reagent), with a 5-min delay in between the use of both cleaning buffers. Finally, washed BeadChips were left to dry for 50-55-mins before being taken for BeadChip imagery, using the Illumina iScan® System (Illumina, United States).

2.7.5.2 Computational data handling and quality control procedures

Raw data files (.IDAT) were returned and normalised via subset-quantile within array normalisation (SWAN) method, as previously described (Maksimovic et al., 2012) within the genome package, Partek Genomics Suite V.6.6 (Partek Inc. Missouri, USA). Subsequent data sets represent SWAN-normalised β -values that correspond to the percentage of methylation at each CpG site, calculated as the ratio of methylated to unmethylated probes via the formula (equation 4);

$$\beta \text{ value} = \frac{\text{Methylated Signal}}{(\text{Methylated Signal} + \text{Unmethylated Signal}) + 100}$$

Equation 3. Calculation for Identifying the Percentage Methylation at Each Individual CpG Site Following Methylome Wide Bead Array Analysis.

Where a β value of 1 indicates total methylation and a value of 0 represents a completely unmethylated CpG site (Pidsley et al., 2016). Initial quality control steps, Principal Component Analysis (PCA) and normalisation histograms, were undertaken to detect for arrays/samples that were identified as being outliers. Differential methylation was subsequently detected across all experimental conditions, and between conditions to identify statistically differentially regulated CpG sites. All analysis of methylation data and statistical analysis was performed using Partek Genomic Suite V.6.6 software (Partek Inc., Chesterfield, Missouri, USA).

Quality control analysis of principal component and intensity frequency histogram were plotted for identification of outliers (Figure 2.5). This analysis revealed two

outliers, while all other samples were reported as consistent between conditions. Down-stream analysis was therefore performed on the remaining samples and these two samples disregarded for downstream analysis.

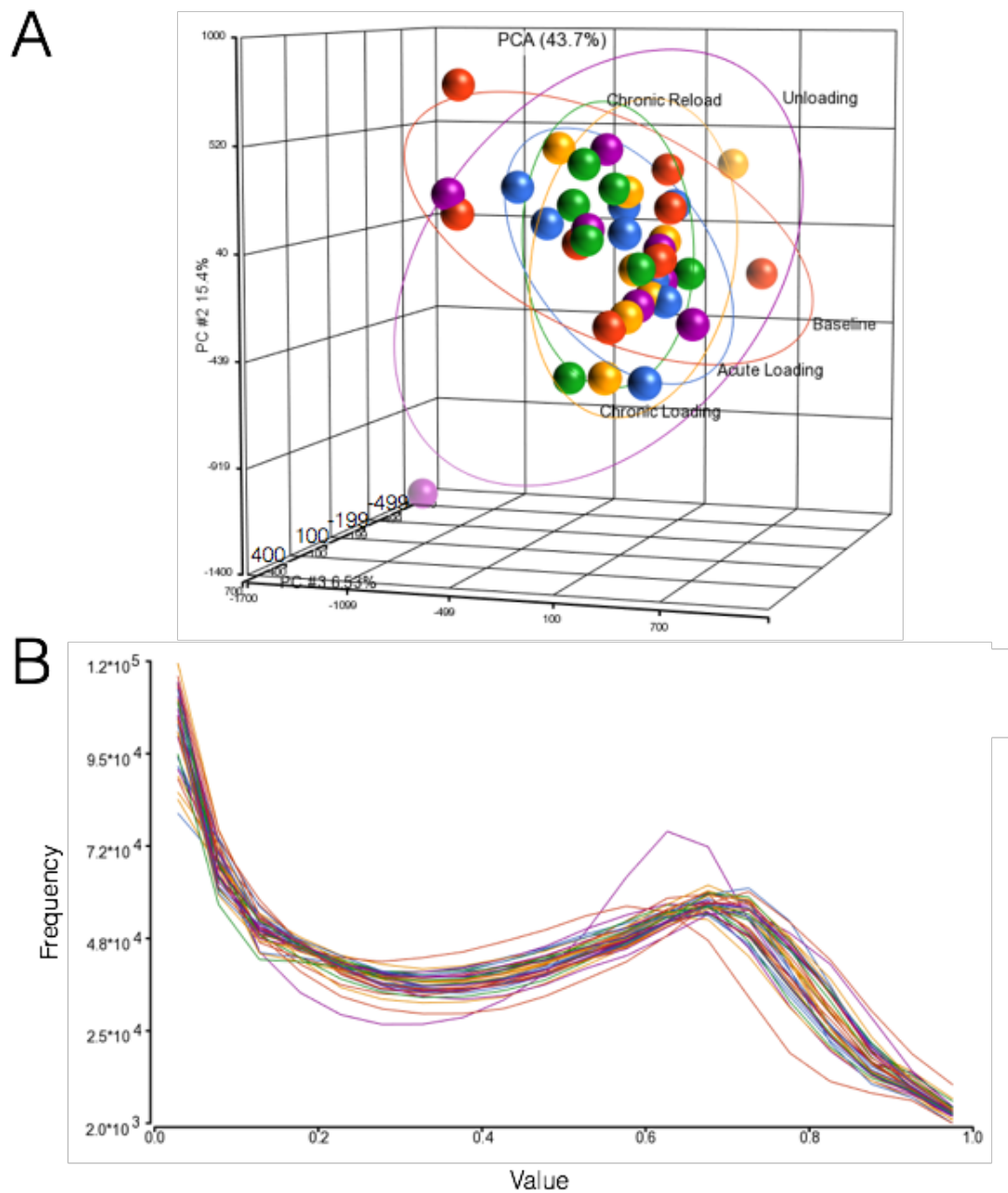


Figure 2.5. Initial quality control analysis of human samples utilised for down-stream methylome wide bead arrays. 13A. Figure displaying the average methylation profile across all detected CpG loci allowing for analysis of variability using three-dimensional principal component analysis (PCA), where each sample is represented by a dot and ellipses for each condition. 13B. Histogram plot representing the

distribution of intensity for each probe allowing for detection of aberrant samples. Two samples are identified as being outliers (X) from both quality control procedures and were subsequently removed from down-stream analysis.

2.7.5.2 Partek genomic suite for hierarchical clustering dendrogram, gene ontology and KEGG pathway analysis

Unadjusted p-value significance ($P < 0.05$) was used to create a CpG site marker list of standardized beta-values across arrays of interest. A standardized expression normalisation was performed to shift CpG sites to mean of zero and scale to a standard deviation of one. Unsupervised hierarchical clustering was performed and a dendrogram was constructed to represent differentially methylated CpG loci and statistical clustering's of experimental samples. Heatmaps represent the modification of CpG loci, where regulated sites that possess reduced methylation (hypomethylated) are represented in green, increases in methylation (hypermethylated) in red, and unchanged sites are represented in black. Statistically differentially regulated CpG sites were analysed via Fishers exact test ($FDR < 0.05$) in Partek Genomic Suite and Gene Ontology Browser, for molecular function, cellular component and biological process. An enrichment score of greater than 3 indicated a significantly enriched/altered functional group. In similar approach, Kyoto Encyclopaedia of Genes and Genomes (KEGG) pathways were examined for identification of transcripts with associated significantly differentially regulated CpG sites (Kanehisa et al., 2017, Kanehisa and Goto, 2000, Kanehisa et al., 2016). Statistically differentially regulated CpG sites were analysed via Fishers exact test ($FDR < 0.05$) in Partek Genomic Suite and exported to the software, Partek Pathway (Partek Inc., Missouri, USA). To ascertain differential methylation, configuration by fold-change

of conditions was applied, and represented by colour intensity, where green indicates hypomethylation, red hypermethylation and grey unchanged. The strength of colour indicates a greater fold change.

2.7.6 Loci-specific DNA methylation analysis

2.7.6.1 Loci-specific pyrosequencing for analysis of rodent muscle atrophy

Assays for pyrosequencing were purchased from EpigenDX (Hopkinton, MA, USA). Following bisulfite conversion, PCR reactions were designed depending on the specific DNA methylated region of interest and the size of the product, as per manufacturer's instructions. However, a typical reaction was performed as follows; 3 μ l of 10X PCR buffer (containing 15 mM $MgCl_2$), 0.2 μ l of 10 mM dNTPs, 1.8 μ l of 25 mM $MgCl_2$, 0.6 μ l of 10 mM dNTPs, 0.15 μ l HotStar Taq Polymerase, 1 μ l of bisulfite treated DNA and 0.2 μ M of forward and reverse primer. One primer was biotin-labelled and HPLC purified in order to facilitate purification of the final PCR product using sepharose beads. Following an initial denaturation incubation at 95°C for 15-min, 45 cycles of denaturation at 95°C for 30 s; 63°C for 30 s (annealing), 68°C for 30 s (extension) were performed, with all PCR cycles followed by a final 5 minutes at 68°C. PCR products were then bound to Streptavidin Sepharose HP (GE Healthcare Life Sciences), after which the immobilized PCR products were purified, washed, denatured with a 0.2 μ M NaOH solution and rewashed using the Pyrosequencing Vacuum Prep Tool (Pyrosequencing, Qiagen, Manchester, UK), as per the manufacturer's instructions. Following annealing with 0.5 μ M sequencing primer, the purified single stranded PCR products were then sequenced using the PSQ96 HS System (Qiagen) following the manufacturer's instructions. The methylation status of each CpG site was determined individually as an artificial C/T SNP using QCpG

software (Qiagen). The methylation level at each CpG site was calculated as the percentage of the methylated alleles divided by the sum of all methylated and unmethylated alleles. The mean methylation level was calculated using methylation levels of all measured CpG sites within the targeted region of each gene. Each experiment included non-CpG cytosines as internal controls to detect incomplete bisulfite conversion of the input DNA. In addition, a series of unmethylated and methylated DNA strands were included as controls after each PCR. Furthermore, PCR bias testing was performed by mixing unmethylated control DNA with methylated DNA at different ratios (0%, 5%, 10%, 25%, 50%, 75%, and 100%), followed by bisulfite modification, PCR, and Pyrosequencing analysis.

2.7.6.2 High resolution melting (HRM) polymerase chain reaction for total DNA methylation of rodent muscle atrophy

HRM-PCR for CpG methylation was performed in accordance with protocols previously described (Sharples et al., 2016a). Briefly, 20 ng of isolated and bisulfite treated DNA was subjected to HRM-PCR using EpiTect HRM-PCR kits and Rotorgene 3000Q (Qiagen, Crawley, UK) with Rotorgene software (Hercules, CA, USA). All primer concentrations for gene CpG assays and EpiTect HRM master mix volumes were used in accordance with the manufacturer's instructions. HDAC4 (Qiagen) was designed to amplify a product length of 140 to 190 bp. PCR cycles were performed as follows; 10 s at 95 °C (denaturation), 30 s at 55 °C (annealing), 10 s at 72 °C (extension) for a maximum of 55 cycles. Following PCR, a high-resolution melt (HRM) analysis was performed with 0.1 °C increments from 65 to 95 °C. Fluorescence versus melt temperature was used to create a standard curve using rat methylated DNA standards representing 100, 75, 50, 25, 10, 5 and 0 % methylation.

All samples were run in duplicate normalised to 0% methylated control and averaged to produce a single curve. The relationship between the area under the curve, determined via each standard curve, and the corresponding percentage methylation curve of specific gene loci was determined via the best fitting fourth-order polynomial relation. This relationship was subsequently used to quantify the % methylation from the integrated raw melt curves of experimental samples. The calculations were performed using an in-house developed Python-based program, MethylCal.

2.8 Statistical Analysis

Statistical analysis was performed via MiniTab Statistical Software (v. 17.2.1; MiniTab Inc, Pennsylvania, USA) or a statistical package for the social sciences software for Microsoft (SPSS, v. 22.0 and v 23.0; IBM Corporation, New York, USA). All genome-wide data sets (Rat Transcriptome and Human MethylomeEPIC array) were analysed for significance via the use of the genomic software Transcriptome Analysis Console (TAC) or Partek Genomic Suite software (version 6.6). Statistical values were considered significant at the level of $P \leq 0.05$.

Chapter 3:

Transcriptomic and Epigenetic Regulation of Disuse Atrophy and the Return to Activity in Skeletal Muscle

Fisher, A. G. (Primary Author), Seaborne, R. A. (Primary Author), Hughes, T. M., Gutteridge, A., Stewart, C., Coulson, J. M., Sharples, A. P (Corresponding Author) and Jarvis, J. C (Corresponding Author). 2017. Transcriptomic and epigenetic regulation of disuse atrophy and the return to activity in skeletal muscle. *Official Publication of the Federation of American Societies for Experimental Biology*. 31 (12). 5268 - 5282.

Please note that this chapter extends work by Dr. A. Fisher and Professor, J. Jarvis. Muscle mass and cross-sectional area analysis was performed and published previously (Fisher, 2012), with raw data being provided to the current Ph.D applicant by Dr. Fisher. Muscle mass and cross-sectional area were re-analysed by the current applicant, with all figures produced by the current Ph.D applicant. Raw microarray files were donated to the current Ph.D applicant who performed all bioinformatic analysis for the derivation of data in this thesis. The PhD candidate also ran all of the HRM DNA methylation and pyrosequencing experiments and analysis, as well as created all graphs, figures and schematics for the epigenetic (DNA methylation) data presented in the current chapter.

3.1 Introduction

Skeletal muscle is the most abundant tissue in the mammalian body, whose maintenance is pivotal for the health and life longevity. However, the precise molecular mechanisms that regulate skeletal muscle mass remain elusive. In chapter 1, we identified that skeletal muscle cells *in-vitro* undergo significant epigenetic modifications during catabolic conditions (exposure to the cytokine TNF- α) (Sharples et al., 2016a). Despite these preliminary findings, further work examining the role of DNA methylation during periods of skeletal muscle atrophy *in-vivo* remain scarce. Furthermore, the findings by Sharples et al. (2016a) suggest that epigenetic modifications incorporated following exposure to an atrophic stimulus, may be retained for a substantial period of time (30 population doublings *in-vitro*) once the stimulus is removed. Again, however, the exploration of this work since these findings has not been performed, and thus it is unknown as to whether modifications of the DNA will persist following removal/reversal of the atrophying stimuli, *in-vivo*.

In order to investigate the underlying time-course and molecular mechanisms responsible for skeletal muscle atrophy, molecular biologists have commonly implemented models such as denervation (Tang and Goldman, 2006, Batt et al., 2006), limb suspension (de Boer et al., 2007), space flight (Nikawa et al., 2004) and joint immobilisation (Yasuda et al., 2005). Within these models, large alterations in gene regulatory networks have been identified to orchestrate the altered balance between protein synthesis and degradation during muscle atrophy (Bonaldo and Sandri, 2013). Indeed, previous investigative work has uncovered key pathways, such as the ubiquitin-proteasome pathway (Eddins et al., 2007, Sandri et al., 2004, Lecker et al., 2004), and key gene transcripts, such as Trim63 (MuRF1) and Fbxo32 (MAFbx)

(Bodine et al., 2001a), that converge to promote the breakdown of skeletal muscle proteins, as described in chapter 1. However, there are currently no studies that investigate the epigenetic modifications that occur during skeletal muscle atrophy *in-vivo*. Furthermore, current *in-vivo* models are not without limitations. For example, during limb cast immobilisation, systemic stress response factors are released, due to the muscle still being able to contract but without generating any movement, that have the potential to interfere with down-stream molecular events, such as gene expression and DNA methylation (Midrio, 2006, Holecek, 2012).

With this in mind, the aim of this chapter was to investigate the role of DNA methylation in skeletal muscle atrophy, and, for the first time, characterise DNA modifications that are associated with skeletal muscle mass perturbation *in-vivo*. To do so, we used an *in-vivo* osmotic pump and nerve cuff apparatus that would administer tetrodotoxin (TTX) to the peroneal nerve and silence the neural input to the muscles of the hind limb. Importantly, because this model also allowed for successful cessation of TTX administration following a specific time-course, the hind limb of the same animal could be recovered and normal physical activity could be established (Fisher, 2012). Therefore, the second aim of this chapter was to elucidate whether any of the epigenetic modifications identified after atrophy were retained following a return to normal physical activity levels in the same animals. It was hypothesized that TTX-induced atrophy would be coupled with an inverse relationship between DNA methylation and corresponding changes in gene expression. Where reduced (hypo)methylation of promoter regions of genes would lead to increases in gene expression and increased (hyper)methylation would lead to gene silencing. It was also hypothesized that these DNA methylation modifications

would be dynamic in nature and was therefore sort to exploratively elucidate this behaviour.

3.2 Methodology

3.2.1 Experimental design

As described previously (Fisher, 2012), the tibialis anterior muscle of Wister rats was subjected to either 3, 7 or 14 days (D) worth of tetrodotoxin (TTX) or 14D of TTX plus 7D worth of activity induced recovery, via an assembled osmotic pump and nerve cuff apparatus that would deliver treatment in a continuous manner (see sections 2.1.1 – 2.1.2 for details). Following termination, the TA muscle group from both control and experimentally treated limbs of rodents were harvested and either mounted and frozen for histological purposes, or snap frozen for gene expression and DNA methylation assays (see methodology section 2.1.1 – 2.1.2). For details of experimental procedures see methodology section 2.1. Schematic representation of experimental design is given in Figure 3.1.

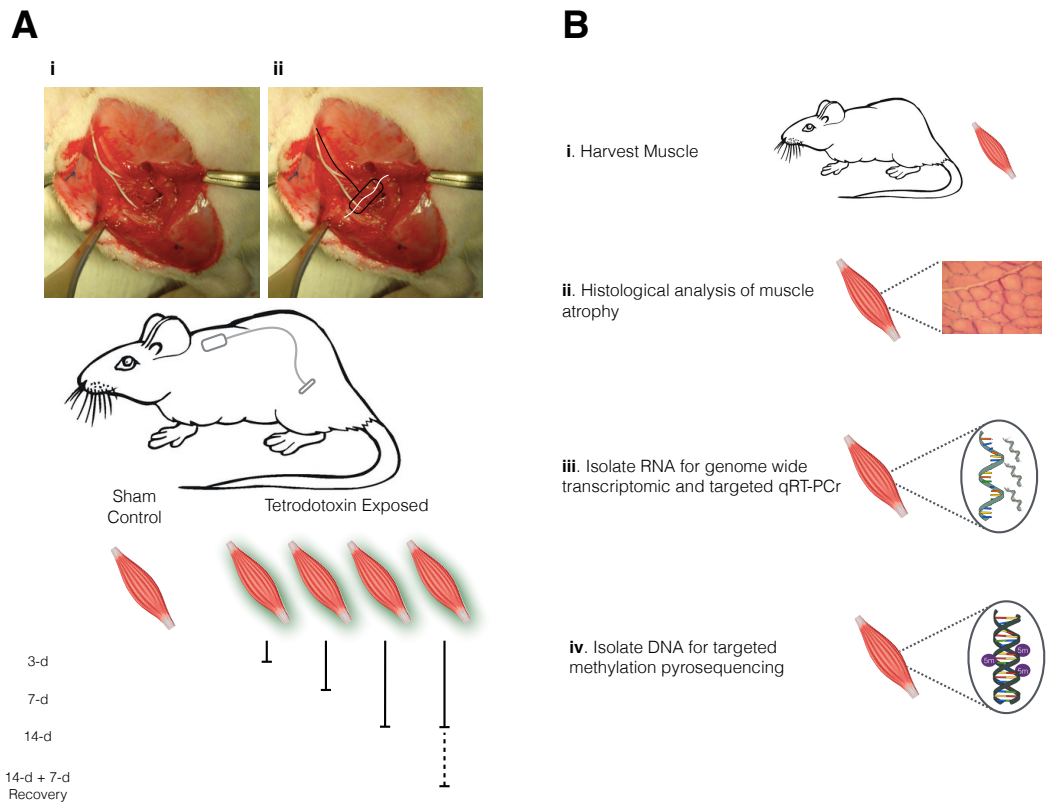


Figure 3.1. Schematic representation of TTX muscle atrophy model and subsequent muscle sample preparation for morphologic, transcriptomic, and epigenetic analysis.

A. Display of physiological location of TTX administration pump. (i) Real image of osmotic pump location and assembly with the left hind limb of the rodent, originally defined in Fisher (2012). A representative overview of the osmotic pump assembly (ii; black lines show osmotic pump unit and delivery tube to nerve cuff unit and white line displays the synaptic nerve; real morphology images (Ai & ii) **B.** Muscle sample preparation for downstream analysis: treated (left) and untreated contralateral control (right).

3.2.2 Morphological and histological analysis of muscle adaptation

Following cessation of experimental procedures, all animals were humanely euthanized via increasing CO₂ concentration and cervical dislocation. Muscle samples

were harvested from both the control and experimentally treated groups (N=6), weighed and divided into pieces for down-stream analysis of muscle size and fibre cross-sectional area, as previously described (section 2.1.3). Data for muscle mass of the tibialis anterior (TA) for all control and experimentally treated groups was expressed as a percentage of whole animal body mass (428 ± 45 g) to normalise for inter-individual differences in animal size. Mean CSA of the tibialis anterior (TA) muscle fibres were expressed as a percentage change from the untreated contralateral control limb for each animal. All data are presented as means \pm SD, unless otherwise stated.

3.2.3 Transcriptome-wide analysis via microarray

Microarray analysis of the rodent genome was performed to elucidate transcript expression changes in experimental compared to control groups. All analysis was performed as previously described (2.6.5). Briefly, samples were sent to AROS Applied Biotechnology, who performed RNA isolation (AROS Standard Operating Procedures) and microarray analysis via Affymetrix GeneChip Rat Genome 230 2.0 Array (Affymetrix, High Wycombe, UK). Raw data files were subsequently analysed by the current Ph.D applicant utilising the freely available genomic software, Transcriptome Analysis Console (TAC; Affymetrix). Raw data files (.CEL) were normalised via the MAS 5.0 signal method (Irizarry et al., 2003b, Irizarry et al., 2003a) and CHP files were subsequently analysed for significantly differential gene expression, compared to baseline and within pairwise comparisons of experimental groups. TAC software was utilised to create clustering heatmaps.

3.2.4 RNA isolation and rt-qRT-PCR

Gene expression was performed previously by Dr Andrew Fisher and presented in his Ph.D thesis (Fisher, 2012), with raw data provided to, and statistically reanalysed by, the current Ph.D applicant. The current Ph.D applicant isolated further RNA and qRT-PCR (as described in methodology) for the gene of interest (Ampd3) and reference gene (POLR2a) for analysis of their expression. RNA was isolated, and quantity and quality analysis was performed via protocols outlined in sections 2.6.1 – 2.6.3. All relative gene expression was quantified by using the $\Delta\Delta$ Ct method against known references genes of (POLR2a) and/or RN18s. Average Ct values for POLR2a and RN18s were 20.08 (\pm 0.59) and 15.80 (\pm 0.39), respectively, across all experimental conditions. Primer sets for transcripts analysed for gene expression are given in table 3.1. All data for fold change in gene expression is presented as mean \pm SD, unless otherwise stated (N=6).

Table 3.1. Gene primer sequences for rodent muscle atrophy experiment. All primers were used the same cycling conditions.

Gene Name	Accession No.		Primer Sequence	Primer Length	Product Length
Trim63	NM_080903	F	GGAGGAGTTTACTGAAGAGG	20	180
		R	GACACACTTCCCTATGGTGC	20	
Fbxo32	NM_133521	F	CTTGTCTGACAAAGGGCAGC	20	184
		R	TGAAAGTGAGACGGAGCAGC	20	
Ampd3	NM_031544	F	ACGCTTGCTGGTCGGTTTAG	20	96
		R	TGGCTTCCTTCTGTCCGATG	20	
Hdac4	XM_343629.4	F	GCAGCCAAACTTCTCCAGCA	20	212
		R	TTGACATTGAAACCCACGCC	20	
MyoG	NM_017115.2	F	GCCATCCAGTACATTGAGCG	20	267
		R	CATATCCTCCACCGTGATGC	20	
Chrna1	NM_024485.1	F	TGTCATCAACACACACCACC	20	269
		R	CTGCAATGTACTTCACACCC	20	
RN18s	X01117	F	TTGACGGAAGGGCACCACCAG	21	131
		R	GCACCACCACCCACGGAATCG	21	
POLR2a	XM_001079162.5	F	GCTGGACCTACTGGCATGTT	20	102
		R	ACCATAGGCTGGAGTTGCAC	20	

3.2.5 DNA isolation and methylation analysis

DNA was isolated and subsequently analysed for quantity and quality in protocols described in section 2.7.1 – 2.7.3, from control and experimental conditions (N=3). DNA methylation of identified transcripts was detected via two methods. Bisulfite treatment for analysis of DNA methylation via loci-specific pyrosequencing was performed via the Zymo EZ Methylation Kit (Zymo Research, Irvine, CA, USA) using the protocol previously described (section 2.7.4.1). DNA methylation detection via high-resolution melt PCR (HRM-PCR) utilised a bisulfite treatment performed via the InnuConvert All-in-One Bisulfite Conversion Kits (AJ Innuscreen GmbH, Berlin, Germany) using methods previously described (2.7.4.2). The use of bisulfite treatment for detection for down-stream DNA methylation analysis has previously been described within this thesis (section 2.7.4) and previously (Frommer et al., 1992). Both DNA methylation analysis methods were performed as previously described (2.7.6). Transcript primers for loci-specific DNA methylation analysis is presented in Figure 3.2 and table 3.2, and via HRM-PCR given in table 3.3.

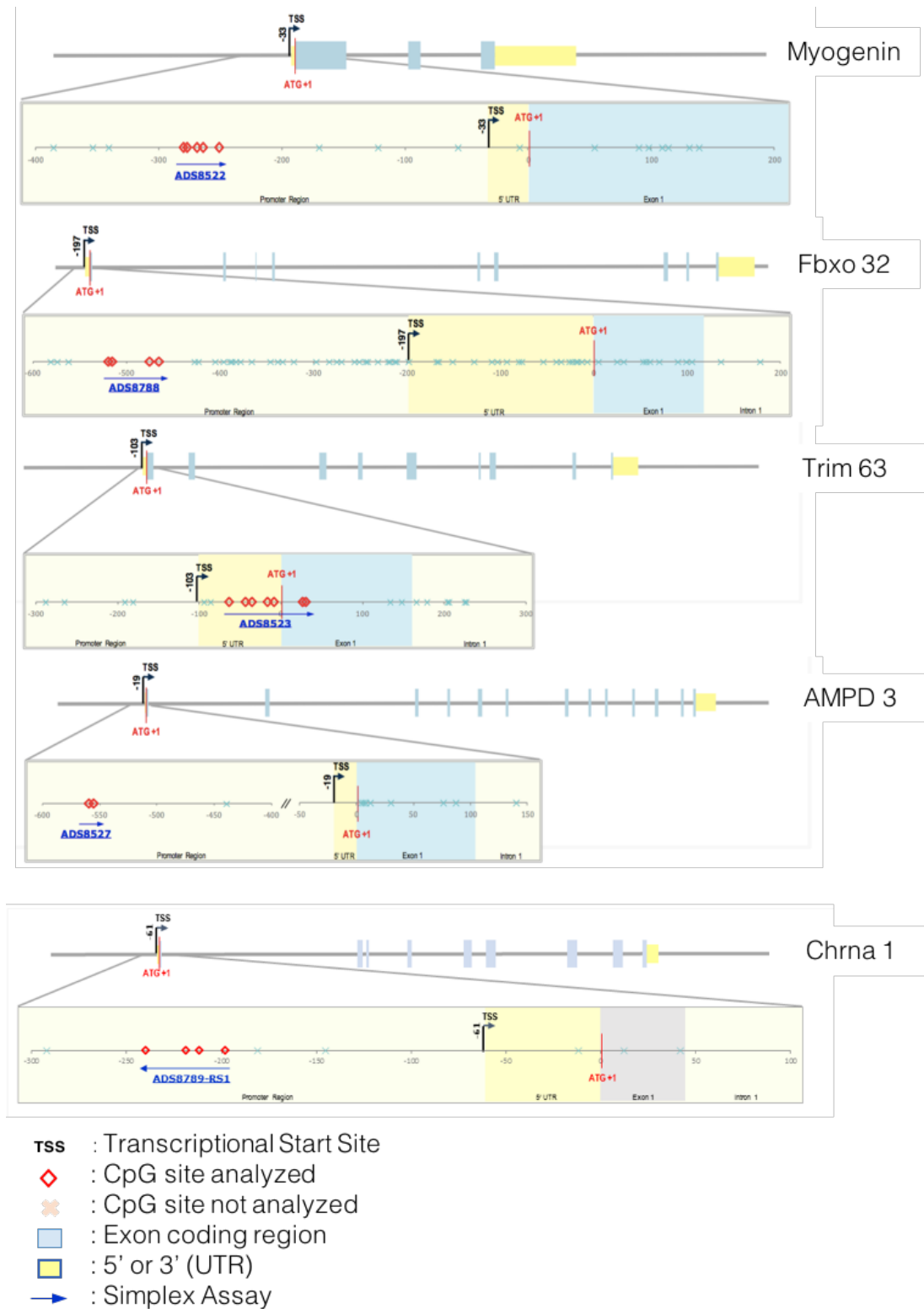


Figure 3.2. Gene map of CpG islands for loci-specific pyrosequencing for quantitation of DNA methylation for transcripts. In descending order: MyoG, Fbxo32 (MAFbx), Trim63 (MuRF1), Ampd3 and Chrna1. UTR untranslated region.

Table 3.2. Detailed description of targeted DNA methylation assays for loci-specific pyrosequencing analysis. Where Y and R bases indicate cytosine residues in CpG sites, depending on whether a reverse (Y base) or forward (R base) biotinylated primer is used (Delaney et al., 2015).

Gene	CpG	Pos. from ATG	Pos. from TSS	Chromatin Location	Assay Sequence
MyoG	CpG-9	-280	-247	Chr13:51126212	AGTYGAYGGTTTTTYGATTYG TGTATAGGAGTYGTTTGGG
	CpG-8	-277	-244	Chr13:51126215	
	CpG-7	-269	-236	Chr13:51126223	
	CpG-6	-264	-231	Chr13:51126228	
	CpG-5	-251	-218	Chr13:51126241	
Trim63	CpG-5	-64	40	Chr5:152533388	ATTYGAGTGGGATTTTTTTTA TTYGGTGTGAYGTAGGTGGA AGAGATAGTYGTAGTTYGA AGTAATATGGATTATAAATTT GGTTTGATTTYGGAYGGAAT G
	CpG-4	-44	60	Chr5:152533408	
	CpG-3	-36	68	Chr5:152533416	
	CpG-2	-17	87	Chr5:152533435	
	CpG-1	-9	95	Chr5:152533443	
	CpG1	26	129	Chr5:152533447	
	CpG2	30	133	Chr5:152533481	
Ampd3	CpG-10	-559	-540	Chr1:175585557	GYGGGYGTATGGGTG
	CpG-9	-555	-536	Chr1:175585561	
Fbxo32	CpG-49	-519	-322	Chr7:98098590	TAYGTTYGATAGGGGAGTAG GGGAGGTGTAAGAGGTGTTA GGGTATYGAGGGTTAGYGGG ATATTTGG
	CpG-48	-515	-318	Chr7:98098586	
	CpG-47	-475	-278	Chr7:98098546	
	CpG-46	-465	-268	Chr7:98098536	
Chrna1	CpG-7	-240	-179	Chr3:60460903	TCRACTCATATTAACRTAAA CCRTATAAAAATCTACATAAA TCRTAAACCAAAAAC
	CpG-6	-219	-158	Chr3:60460882	
	CpG-5	-212	-151	Chr3:60460875	
	CpG-4	-198	-137	Chr3:60460861	

Table 3.3. Primer design for HDAC 4 for analysis of DNA methylation via HRM-PCR

Gene Name	CpG No.	Gene Globe Cat No.	Chromatin Location	Primer Sequence	Length
Hdac4	1	PM00599046	Chr9:9138915 1-91391341	GGGCGCGCAAGAGCG CAGACTGTGACGGGG GCCCCGT	190
	2	PM00599053	Chr9:9139007 7-91391147	GCGCCCGCGAAGCGG GGGTGGCTGTTGGGCT ATTGTAGGGCGGA	138
	3	PM00599060	Chr9:9138905 2-91391220	GCTAGCGCCTGGAGA GTCCTCGGTACGCCCC GC	168
	4	PM00599067	Chr9:9138947 7-91391621	GCTTTGGGTCGCCGCC ACCGCGTCCCGGT CGTTGCTGTGGCGGAG	144
	5	PM00599074	Chr9:9138947 2-91391621	GTGTAGGCTTTGGGTC GCCGCCACCGCGTCCC G	149

3.2.6 Statistical analysis

Analysis of morphologic data were performed previously (Fisher, 2012) and confirmed by the current Ph.D applicant in SPSS (v. 22.0; SPSS, Chicago, IL, USA). Gene array analysis was performed using Transcriptome Analysis Console (TAC; Affymetrix) described in full (section 2.6.5.2). Morphological comparisons between experimental and control conditions were assessed via 1-way between-groups ANOVA. Microarray data were analysed for statistical comparison via 1-way between-group ANOVA within the freely available genomic software (TAC). Targeted rt-qRT-PCR was analysed by using a 1-way between-group ANOVA (with Tukey's post-hoc test). DNA methylation data sets were analysed via a 2-way between-group ANOVA (with Tukey's post-hoc test) which allowed for comparison

of experimental conditions and individual CpG islands. A follow-up 1-way ANOVA between CpG islands at each experimental condition was used to identify significant differences in the DNA methylation states of each individual CpG island within the same experimental condition. Finally, Student's t tests were used to identify significant differences in CpG methylation between experimental conditions and control. All statistical analyses for DNA methylation were performed on absolute percentage values, with figures representing the fold change (means \pm SD) to relevant control. Differences were considered statistically significant at values of $P \leq 0.05$.

3.3 Results

3.3.1 Disuse atrophy produces significant wasting of skeletal muscle

Cross-sectional area and muscle weight were analysed and presented for thesis examination previously (Fisher, 2012), with raw data being given to, and statistically reanalysed by, the current Ph.D who subsequently modified/redrew all figures for the purpose of this thesis. Tetrodotoxin (TTX) produced an average of $7.0 \pm 2.4\%$ loss in TA muscle weight at 3D, $28.7 \pm 5.1\%$ at 7D and $50.7 \pm 2.7\%$ loss following 14D that resulted in statistical significance at all time points versus the untreated control TA ($P < 0.001$; Figure 3.3) and a significant difference between paired comparisons of 3 and 7D, 3 and 14D, 7 and 14D ($P < 0.001$). In the experimental group that received 7D of recovery (habitual activity patterns) following 14D of TTX exposure, muscle significantly recovered by 51.7% vs. 14D of denervation ($P = 0.001$). Muscle weight, however, did not completely recover to baseline control levels as there was still a significant reduction in the recovery group when compared to control ($P < 0.001$; Figure 3.3). Interestingly muscle weight in the recovery group was equivalent to that

of the 7D TTX atrophy group, suggesting that rates of recovery of a 7D period were similar to rates of loss over the same period of time. Collectively, these data suggest a significant and progressive reduction in TA muscle weight following disuse-induced atrophy, that is significantly, albeit partially, recovered following disuse cessation and normal habitual activity is resumed.

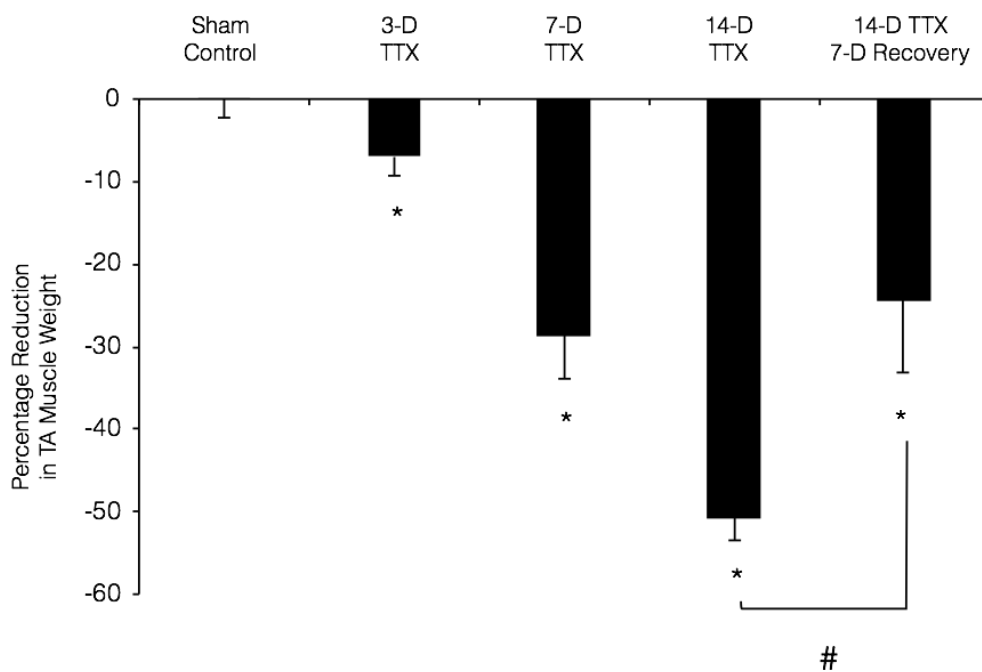


Figure 3.3. Quantification of changes in muscle mass *in vivo* after TTX-induced nerve block. Data shown for 3, 7 and 14D of treatment, and TTX nerve block for 14D plus 7D of active recovery (14D TTX 7D recovery). Mean TA mass is expressed as a percentage difference of whole animal body mass (428 ± 45 g) to normalise for inter-individual differences in animal size. All data are presented as means \pm SD for N = 6. * Statistically significant vs. sham control ($P < 0.05$); # statistically significant vs. 14D TTX ($P < 0.05$). Figures adapted/redrawn from raw data provided by Dr. Andrew Fisher (Fisher, 2012) and statistically re-analysed by the current PhD candidate.

Exposure to TTX produced a progressive reduction in mean muscle fibre CSA of $17.95 \pm 12.06\%$ at 3D, $42.09 \pm 6.17\%$ at 7D and $68.94 \pm 2.97\%$ at 14D of TTX exposure, with 7D and 14D TTX exposure being significantly reduced versus the control ($P = 0.003$; $P < 0.001$, respectively; Figure 3.4). Similarly, to TA muscle weight, upon TTX cessation, the 14D TTX + 7D recovery group muscle CSA significantly recovered compared to 14D TTX alone, with an increase of 62.6% in CSA compared with 14D TTX alone ($p = 0.002$; Figure 3.4). Therefore, there was significant atrophy of individual skeletal muscle fibres in the TA muscles following denervation and a 51.7% recovery of muscle weight and 62.6% recovery of muscle CSA following 7D cessation of the TTX administration and normal habitual physical activity (Figure 3.4).

The presented morphological data reports the successful induction of severe disuse-induced atrophy across time-course. It is also observed that 7D of normal habitual physical activity, where 14D of TTX had previously induced significant atrophy, was sufficient to induce significant, albeit partial, recovery of skeletal muscle mass.

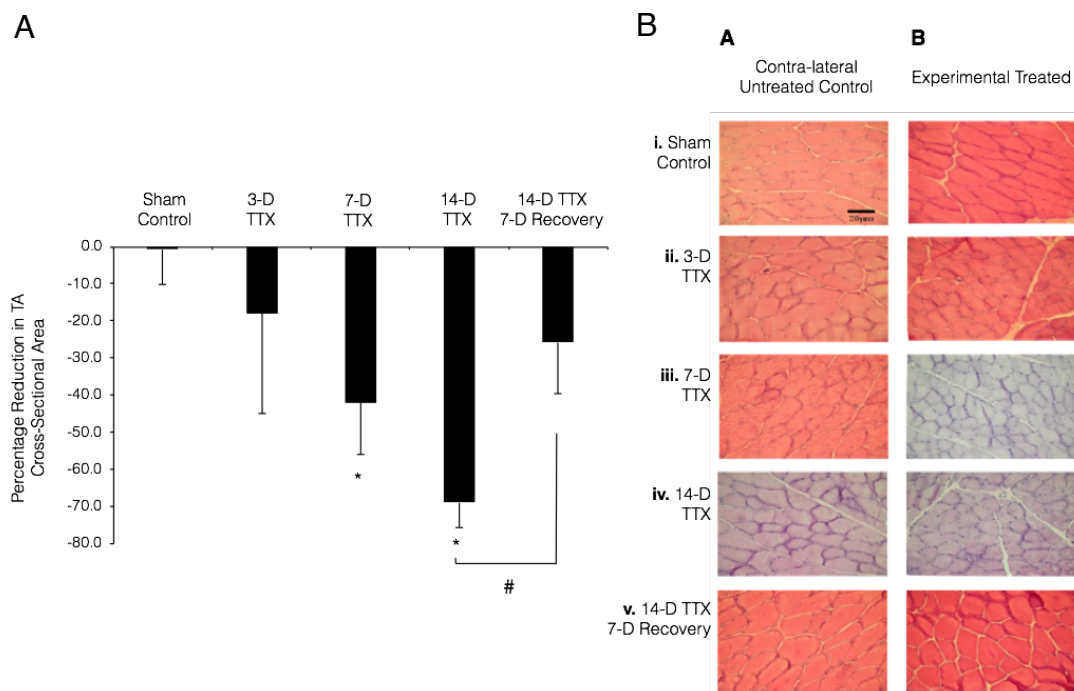


Figure 3.4. Muscle fibre cross-sectional area after TTX-induced atrophy and recovery.

A). Mean cross sectional area of the TA muscle was expressed as a percentage change from untreated contralateral control limb for each animal. B). Haematoxylin and eosin-stained sections of untreated (A) and treated (B) TA muscle of control (i), 3D TTX (ii), 7D TTX (iii), 14D TTX (iv) and 14D TTX plus 7D recovery (v) conditions. * Statistically significant vs. sham control ($P < 0.05$); # statistically significant vs. 14D TTX ($P < 0.05$). Figures adapted/redrawn from raw data provided by Dr. Andrew Fisher (Fisher, 2012) and statistically re-analysed by the current Ph.D candidate.

3.3.2 Microarrays identify important gene regulatory networks during rat skeletal muscle atrophy

After confirming a significant reduction and subsequent recovery in muscle mass, the temporal transcriptome profile accompanying muscle atrophy was investigated (N=4). For comparison, treated TA muscle samples from sham, 3D, 7D, 14d TTX and 14D TTX plus 7D recovery groups were sent for microarray analysis. 30,000 rat

transcripts and 28,000 variants were examined via Affymetrix GeneChip® Rat Genome 230 2.0 Array and subsequently analysed for statistically differentially regulated transcripts.

The representative dendrogram from the hierarchical clustering analysis of probe sets across the genome identified 3,714 genes that were significantly differentially expressed ($P \leq 0.001$; Figure 3.5 A). It also demonstrated that there was a strong clustering of data sets for the 3, 7 and 14D TTX atrophy groups, which showed a clear and separate differentially regulated transcriptome compared to the recovery and sham control groups. This suggests that disuse-induced atrophy evoked a significant alteration on a large number of gene sets, that, following 7D worth of recovery, returned to baseline levels. To explore these findings further, the top 20 most differentially regulated probe sets across all comparisons were investigated, producing an unsupervised hierarchical clustering (Figure 3.5 B). These findings display a similar pattern of gene expression, reporting that 3, 7 and 14D of disuse-induced atrophy show clear differentially regulated gene activity compared to recovery and sham control groups.

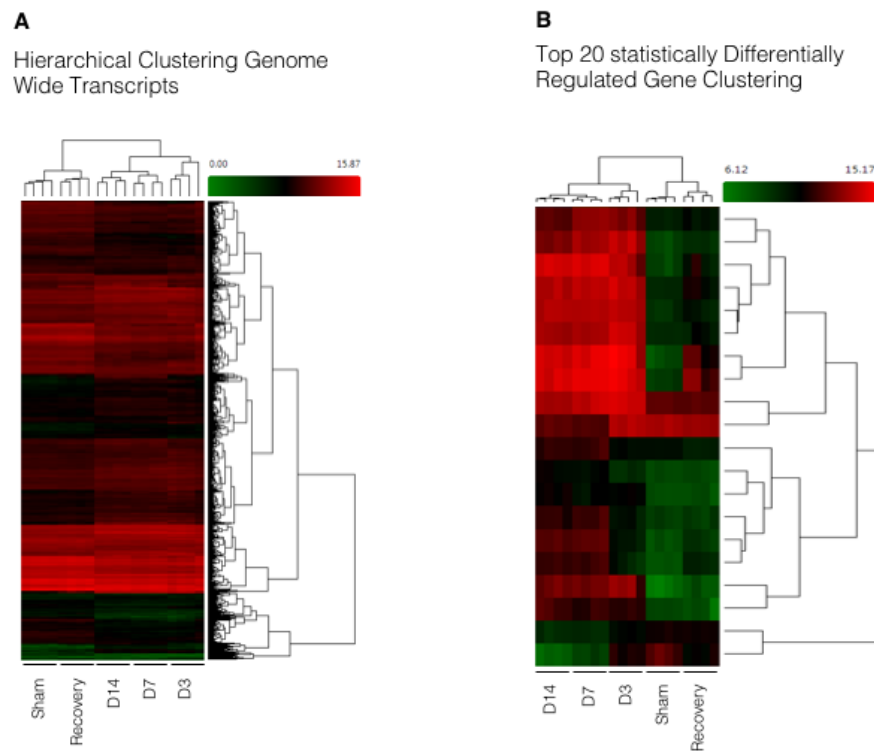


Figure 3.5. Transcriptomic analysis of disuse atrophy and recovery in rats. A. Hierarchical clustering heatmaps of probe set expression across the rodent genome identified 3714 genes that were highly and significantly differentially regulated ($P \leq 0.001$) across all conditions. Clustering analysis displays conditions 3, 7 and 14D to be significantly differentially regulated compared to sham control and 14D TTX and 7D recovery. B. This analysis was confirmed in the top 20 statistically differentially expressed genes across all conditions. Similar clustering occurred that segregated TTX only exposure groups to sham control and 14D TTX and 7D of recovery.

3.3.3 Microarray and significance ranking identifies important regulatory genes during atrophy

In order to decipher what genes were important in the regulation of skeletal muscle atrophy and subsequent recovery, transcriptome wide data sets were analysed to produce six separate pairwise comparisons (sham vs, 3D, 7D and 14D, and recovery vs. 3D, 7D and 14D), revealing a list of genes that were most statistically altered within these experimental parameters. Trim63 (MuRF1), Myogenin (MyoG) and

Ampd3 were identified as being the most frequently occurring highly differentially regulated genes across all pairwise comparisons, who all also appeared in the top 20 most statistically differentially regulated genes across all probe set comparison (table 3.4). Previous work has identified Ampd3 as playing a pivotal role in protein degradation in C2C12 murine myotubes (Davis et al., 2015). The E3 ubiquitin ligase Trim 63, has regularly been shown to be a key transcript in orchestrating the loss of skeletal muscle in a number of catabolic situations, as has its protein family members, Fbxo 32 (Cohen et al., 2009, Cohen et al., 2007, Tang and Goldman, 2006, Tang et al., 2009, Tang et al., 2015). This justification led for an extended analysis of these three genes for confirmation of transcript behaviour and elucidation of epigenetic profile during muscular atrophy and recovery. The basic helix-loop-helix myogenic factor, MyoG has been shown to play a crucial role in denervation-dependent skeletal muscle atrophy (Macpherson et al., 2011, Tang et al., 2009). Importantly, the MyoG upstream regulator, Hdac4, also appeared in the top 20 most statistically differentially regulated genes and was the most highly differentially regulated when comparing sham control to 3d TTX atrophy. The class II histone deacetylase has previously been shown to play an important role in the regulation of MyoG activity (Moresi et al., 2010, Tang et al., 2009), and thus both genes warranted further analysis. Additional NMJ associated genes that were significantly altered and appeared in the top 20 most differentially regulated genes included the acetylcholine receptor subunit alpha 1 (Chrna1; table 3.4). This gene also appeared in 2 out of 6 paired comparisons of most differentially regulated genes. Chrna1 plays a crucial role in acetylcholine binding and channel gating activity, within the neuromuscular junction pathway (Yu and Hall, 1991) and has been previously been identified via transcriptome analysis as the most differentially regulated gene in skeletal muscle loss observed in age-related muscle

loss/denervation (Ibebunjo et al., 2013).

Table 3.4. Top 20 most statistically differentially regulated gene transcripts across all conditions of rodent disuse-induced atrophy and return to activity, identified via gene expression microarrays (N=4), and ranked according to significance. Transcript ID identifies multiple transcript variants. Two unknown transcripts were identified and removed from this table (ranked at positions 3 and 15, respectively). Highlighted cells indicate those run for further down-stream analysis.

Gene Symbol	Ranked	Gene Description	ANOVA P-Value	Transcript ID
Runx1	1	Runt-related transcription factor 1	6.60E ⁻¹⁰	Rn.11201.1
Ampd3	2	Adenosine Monophosphate Deaminase 3	6.60E ⁻¹⁰	Rn.11106.1
Atf4	4	Activating Transcription Factor 4	7.43E ⁻⁹	Rn.2423.1
Myog	5	Myogenin	1.96E ⁻⁸	Rn.9465.1
Adig	6	Adipogenin	2.59E ⁻⁸	Rn.17645.1
Gadd45a	7	Growth Arrest and DNA-damage-inducible alpha	2.59E ⁻⁸	Rn.17645.1
Runx1	8	Runt-related transcription factor 1	3.17E ⁻⁸	Rn.31927.1
Trim63	9	Tripartite Motif Containing 63/ Murf1	4.10E ⁻⁸	Rn.40636.1
Sat1	10	Spermidine	4.10E ⁻⁸	Rn.40636.1
Hdac4	11	Histone Deacetylase 4	5.98E ⁻⁸	Rn.23483.1
Ankrd1	12	Ankyrin Repeat Domain 1	6.62E ⁻⁸	Rn.3789.1
Pdhx	13	Pyruvate Dehydrogenase Complex, Component X	6.62E ⁻⁸	Rn.2260.1
Reps1	14	RALPBP1 Associated Eps Domain Containing 1	1.19E ⁻⁷	Rn.12867.1
Adam19	16	ADAM Metallopeptidase Domain 19	3.01E ⁻⁷	Rn.904.1
Hdac4	17	Histone Deacetylase 4	3.72E ⁻⁷	Rn.20628.1
Ankrd1	18	Ankyrin Repeat Domain 1	3.96E ⁻⁷	Rn.3789.1
Chrna1	19	Cholinergic Receptor, Nicotinic alpha 1	4.07E ⁻⁷	Rn.44633.1
Mxra7	20	Matrix-Remodelling Associated 1 (uncharacterised)	5.65E ⁻⁷	Rn.12266.1

3.3.4 DNA methylation is inversely associated with gene expression of the identified genes during TTX atrophy and recovery

Following 3D TTX exposure there was a significant reduction (0.85 ± 0.04 , $P = 0.011$) in DNA methylation (hypomethylation; 3D, $40.2 \% \pm 2.6$) in the promotor region of the myogenic regulatory factor, MyoG (Figure 3.6 A), compared to baseline control (sham control, $33.9 \% \pm 6.8$). This reduction in DNA methylation coincided with a significant ($P = 0.011$) increase in gene expression (33.08 ± 33.71) at the same time point (Figure 3.6 B). Interestingly, following this time point both DNA methylation and gene expression profiles of this gene returned towards baseline control levels during TTX only exposure (i.e. 7 and 14D TTX; Figure 3.6 A and 3.6 B). The DNA methylation profile of the cholinergic receptor nicotinic alpha 1-subunit (Chrna1) portrayed a progressive hypomethylation from sham control through to 14D of TTX exposure, with 7D ($41.5 \% \pm 1.5$, representing a fold change of 0.93 ± 0.04) and 14D ($39.4 \% \pm 2.1$, representing a fold change of 0.89 ± 0.04) attaining significance compared to control ($44.4 \% \pm 0.7$; $P = 0.035$ and $P < 0.001$, respectively; Figure 3.6 A). This progressive reduction in DNA methylation was met with a progressive increase in gene expression across the same time points (7D, 133.55 ± 38.73 ; 14D, 177.52 ± 205.19 ; Figure 3.6 B), where it attained a significance value at 14D TTX exposure ($P = 0.016$). In similar fashion to Chrna1, Trim63 showed a significant reduction in DNA methylation status at both 7D ($32.4 \% \pm 2.3$) and 14D ($31.7 \% \pm 3.7$) of TTX exposure ($P = 0.035$ and $P < 0.001$, respectively) (Figure 3.6 A), which coincided with a stable increase in mRNA expression at the same time points (7D, 2.70 ± 1.73 ; 14D, 1.52 ± 2.14). Trim63's protein family member, Fbxo32, showed a decreasing trend in DNA methylation over the 14D period which attained significance at 14D of exposure ($0.4 \% \pm 0.4$, representing a fold change of 0.30 ± 0.21 ; $P = 0.021$),

when compared to control ($1.1 \% \pm 0.4$). mRNA expression of the *Fbxo32* gene showed significant increases compared to control at both 3D (3.03 ± 2.5 ; $P = 0.037$) and 7D of atrophy (3.03 ± 2.3 ; $P = 0.038$).

Interestingly, in genes *Fbxo32*, *Trim 63* and most notably *Chrna1*, TTX cessation and 7D worth of recovery caused DNA methylation profiles to become methylated once more and return to sham control levels ($P > 0.05$; Figure 3.6 A). Importantly, the return of DNA methylation status to resemble that of sham control levels, was met with a concomitant return of gene expression towards baseline levels. Schematic representation of the correlation between DNA methylation and gene expression profiles is given in Figure 3.6 B. No statistically significant observations were noted in the behaviour of *Ampd3* methylation following disuse-induced atrophy or return to activity in skeletal muscle. Furthermore, following initial screening of the gene *Hdac4* for total percentage methylation within the amplicon/ product via HRM PCR, methylation above that of the 0% control was undetectable and therefore loci-specific pyrosequencing of this gene was not performed.

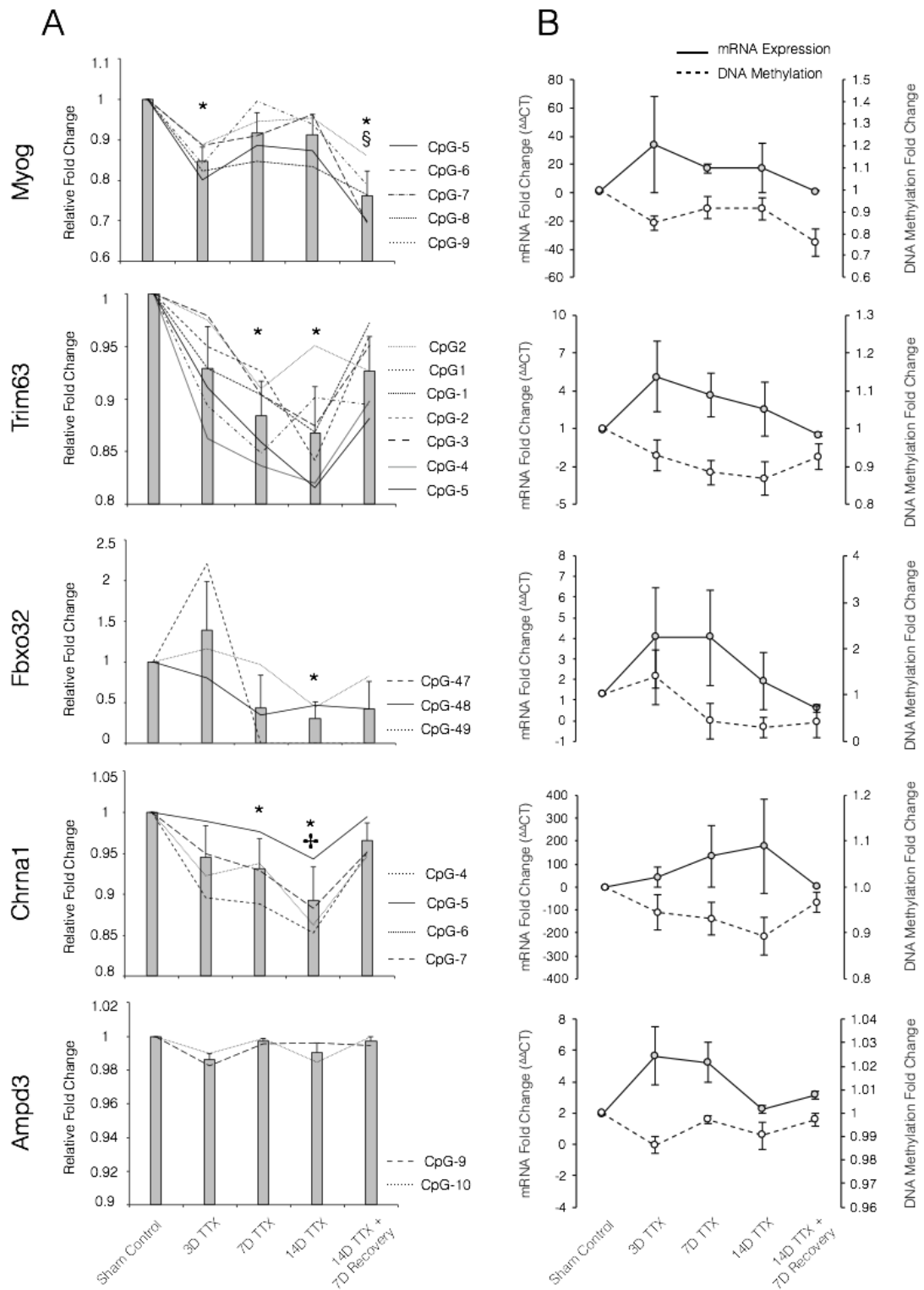


Figure 3.6. Relative fold change in gene expression and DNA methylation displaying an inverse and transiently active relationship across experimental time-course, in a subset of identified and analysed gene transcripts. A. DNA methylation data presented as relative fold change compared with sham control for all genes previously reported (except Hdac 4). Mean data (histogram bars) are the average taken from each CpG

island of the respective gene transcript, analysed via loci-specific pyrosequencing. Individual CpG island methylation percentages are visualised as individual lines and annotated in graph specific indents. Data presented as means \pm SD for N = 3. Statistically significant reductions compared with control group represented by *; reduction compared to 3 d TTX represented by †; and § represents significance compared to 7 and 14 d TTX atrophy. B. An overlap representative schematic of the relationship between changes in gene expression (thick black line; mean fold change to baseline \pm SD) and DNA methylation (black dashed line) of key transcripts.

3.4 Discussion of Findings

The aim of this chapter was to, for the first time, investigate the role of DNA methylation in skeletal muscle atrophy using an *in-vivo* implanted osmotic pump and nerve cuff apparatus that would administer tetrodotoxin (TTX) to the peroneal nerve and silence the neural input to the muscles of the hind limb. We also wished to elucidate whether any epigenetic modifications identified after atrophy were retained or returned to normal following a return to normal physical activity levels in the same animals. The findings in this chapter support the first hypothesis, whereby epigenetic modifications to the promotor region of important genes are concomitant with functional changes in gene expression, during a progressive muscle atrophy model. Contrary to the second hypothesis however, upon cessation of the atrophic stimulus, we observed that promotor methylation in the majority of gene transcripts returned towards baseline, showing no statistical difference compared to control, suggesting that these genes did not retain epigenetic modifications.

3.4.1 DNA methylation is inversely mirrored with important changes in skeletal muscle gene expression after atrophy and the return to habitual activity

The observed changes in DNA methylation profiles of muscle specific regulatory gene targets is inversely reflected with altered expression of a number of key target transcripts previously identified as playing a significant role in orchestrating muscular atrophy in a disuse or denervated milieu. The bHLH transcriptional factor and member of the MRFs, MyoG, is commonly associated with having an important role in the process of skeletal muscle development/myogenesis and the repair and regeneration process of myofibres following injury, specifically the differentiation and fusion process (Le Grand and Rudnicki, 2007). Counterintuitively, we observe a marked increase in gene expression upon disuse-induced atrophy (Figure 3.6 B), that may reflect a compensatory mechanism in an unsuccessful attempt by the organism to halt the atrophy process. However, novel data is reported here to suggest that DNA hypomethylation is met with increases in gene expression observed over the atrophy time-course.

Two well categorised down-stream transcriptional targets of the MyoG protein are the E3 ubiquitin ligases Trim63 and Fbxo32, that have both previously been identified as being highly regulated during periods of muscle loss caused by denervation, immobilization and unloading in rodents (Bodine et al., 2001a, Bodine and Baehr, 2014). Trim63 is an E3 ubiquitin ligase and member of the RING zinc finger family of proteins, and is responsible for the polyubiquitination of proteins to target them for proteolysis (Bodine et al., 2001a, Gomes et al., 2001). Upon catabolic stimuli, such as diabetes, glucocorticoid treatment, cytokine treatment, unloading and denervation, the expression of Trim63 has consistently been reported to increase, confirming its

action in atrophying skeletal muscle (Goldberg, 1969, Bodine et al., 2001a). At a protein level, northern blot analysis reported a significant increase of both Trim63 and Fbxo32 proteins at 3 and 7 days of denervation induced atrophy (Bodine et al., 2001a). Here, it is reported that DNA hypomethylation of these ubiquitin ligases is decreased at specific time points during disuse-induced atrophy time-course, that was coupled with time specific increases in gene expression (Figure 3.6 B). Interestingly, upon TTX cessation and 7 d of active recovery, DNA methylation of these two E3 ubiquitin ligase genes, increases back towards control levels, which coincides with a reduction in gene expression (Figure 3.6 B). Collectively, these data suggest a distinct role for DNA methylation in modulating gene expression of the two ubiquitin ligases proteins during progressive disuse atrophy and subsequent physical activity induced muscle mass recovery.

Chrna 1, the major component of the muscle specific nicotinic acetyl choline receptor (nAChR) in adult skeletal muscle (Giniatullin et al., 2005), plays an integral role in initiating the opening of the nAChR channel allowing for the transfer of positively charged ions through the cell membrane (Beker et al., 2003). Interestingly, given its role in muscle contraction, we observe a progressive and significant increase in gene expression which is met with an equally progressive reduction in DNA methylation, culminating at 14 d of TTX exposure. Following 7d of active recovery, DNA methylation returns to sham control levels, which coincides with a significant reduction of gene expression, back to control levels also. The gene expression and DNA methylation profile of the gene Chrna1 shows interesting temporal behaviour through the 14 d atrophy time-course and subsequent 7 d of recovery. Chrna1 is one of five isoforms found in human skeletal muscle, and the most dominant in the nAChR

cluster. All five isoforms function to create an acetylcholine cluster surrounding the neuromuscular central pore, in which they house target binding sites, predominantly located on the alpha subunit. Upon contact of a chemical messenger to one of the target binding sites, all present subunits undergo a conformational change resulting in the channel gate opening, and the potential passing of positively charged ions (Colquhoun and Sivilotti, 2004). Given the specific model of denervation in this chapter, in which no action potential signals reach these subunits, it is possible that the observed reduction in DNA methylation and concomitant progressive increase in gene expression is a compensatory mechanism to form new end plates and enable the successful opening of the nAChR channel.

3.5 Summary, Conclusions and Future Chapter Directions

Analysis of individual CpG sites within the promoter region of key target transcripts (Myog, Trim63, Fbxo32, Chrna1, Ampd3) during skeletal muscle atrophy and recovery in rodents, identified a potential relationship with gene expression. Where hypomethylation of DNA, especially within promotor regions as studied here, has been well characterised to promote increased gene expression. Overall, suggesting an important role for the epigenetic control of these genes during disuse atrophy. Furthermore, upon recovery of skeletal muscle, DNA methylation of the same genes were methylated once more and returned back to normal levels concomitantly with a reduction in gene expression back towards normal levels. This also suggested that epigenetic changes in these genes, via DNA methylation, were transient and reversible after recovery from atrophy.

After targeted analysis of DNA methylation of genes identified to be important during atrophy and recovery, demonstrating muscle size reductions are sufficient to induce epigenetic modifications skeletal muscle, we wished to explore whether during muscle mass increases (hypertrophy) we identified similar changes. Furthermore, we wanted to elucidate whether such epigenetic modifications, were retained or reversed (similar to findings in the present chapter) during a subsequent later period of skeletal muscle hypertrophy in order to investigate the concept of epigenetic muscle memory, as speculated in chapter 1.

Chapter 4:

Human Skeletal Muscle Possesses an Epigenetic Memory of Hypertrophy

The work contained within this chapter has recently been published;

Seaborne, R. A., Strauss, J., Cocks, M., Shepherd, S., O'Brien, T. D., van Someren, K. A., Bell, P. G., Murgatroyd, C., Morton, J. P., Stewart, C. E. & Sharples, A. P. (2018). Human skeletal muscle possesses an epigenetic memory of hypertrophy. *Scientific Reports*, 8,1898.

4.1 Introduction

In chapter 3, significant epigenetic modifications (in the form of DNA hypomethylation) in the promotor region of genes increased at the expression level during skeletal muscle atrophy were identified. Furthermore, via re-introduction of habitual physical activity, it was possible to identify a reversal of DNA methylation during recovery that was associated with gene expression returning to normal control levels. Therefore, contrary to our original hypothesis, these DNA methylation modifications were not retained and instead, returned back towards control levels. In order to explore these concepts further, we sought to elucidate the role DNA methylation plays in modulating skeletal muscle growth (hypertrophy) following a period of chronic resistance exercise in humans (RE). Further, via the implementation of an experimental design whereby following earlier hypertrophy, RE was completely ceased for a period of time retuning muscle mass to baseline levels and then re-introduced to evoke later hypertrophy, we aimed to identify if there was an epigenetic retention or simply a reversal of DNA modifications that occurred during earlier hypertrophy. Furthermore, if a retention of epigenetic information did occur during cessation of RE and later RE (following a period of earlier hypertrophy), if this was associated with advantageous gene expression and larger muscle mass during subsequent hypertrophy.

Indeed, there is a distinct paucity of work identifying the large-scale epigenetic modifications that occur following RE in the mammalian organism. In skeletal muscle, acute RE (3 sessions, $4 \times 8-10$ reps, 3 exercises, 2-days rest between sessions) induced significant DNA methylation changes to 474 regions of DNA isolated from

the vastus lateralis muscle (Laker et al., 2017). Furthermore, when exploring the relationship between the methylome and transcriptome, the authors identified 54 genes as demonstrating a significant relationship between modifications in DNA methylation and gene expression (Laker et al., 2017). However, interpretation of these findings was somewhat limited given were consuming a high-fat diet in addition to undertaking RE (3.9 g fat/kg fat free mass, equating to 77% of total caloric intake) in an attempt to compare with a high fat diet alone control group, with no basal comparison. Thus, it is still unknown as to the basal response of the human methylome following a period of RE-induced muscle hypertrophy. There are currently no investigations in skeletal muscle tissue that identify the DNA methylation changes after chronic RE. The only data included DNA methylation changes in leukocytes following 8-wks of chronic RE (3 times per week, 3×10 -12 reps at 80% 1RM). Where analysis of the human methylome via BeadChip array identified 57,384 CpG sites as portraying a significantly differentially modified profile, with the same number of DNA sites being identified to be hypomethylated (28,987) vs. hypermethylated (28,397) (Denham et al., 2016).

Therefore, the aim of this was to elucidate the response of the human methylome following exposure to chronic RE, and to identify whether these modifications are retained or reversed over a period of exercise cessation and if further modified following exposure to a secondary RE stimulus. In order to investigate these aims, an *in-vivo* RE model was utilised, where human subjects were exposed to an initial 7-weeks of RE (loading), a subsequent 7-weeks of exercise cessation (unloading), and a final, secondary 7-week period of RE loading (reloading). Furthermore, to determine if there was retention or a reversal of epigenetic modifications following muscle mass increases, a methylome array was utilised to examine over 850,000 CpG sites of the

human genome after all conditions (baseline, loading, unloading and reloading).

Following identification that DNA methylation plays a role in muscle mass regulation, in chapter 3, it was first hypothesised that large-scale modifications to the human methylome would occur following 7-weeks of RE induced hypertrophy in humans. Furthermore, it was hypothesised that a distinct number of these modifications would be retained during 7-weeks unloading, and would aid in generating a further enhanced (e.g. enhanced gene expression) response of the human methylome following secondary exposure to RE.

4.2 Methodology

4.2.1 Experimental design

Using a within subject design, eight previously untrained male participants (27.6 ± 2.4 yr, 82.5 ± 6.0 kg, 178.1 ± 2.8 cm, means \pm SEM), completed a 7 week chronic and progressive resistance exercise training programme (3d/week; loading), 7 weeks of exercise cessation (unloading) and a subsequent 7 weeks (3d/week) of resistance exercise loading (reloading). Exercise protocol is detailed previously (section 2.2.2), and experimental design is schematically represented in Figure 4.1. Whole-body fan beam dual-energy x-ray absorptiometry (DEXA), isometric voluntary contraction to assess quadriceps strength and muscle biopsy samples from the vastus lateralis for down-stream RNA and DNA analysis were obtained at baseline and experimental weeks 8, 14 and 22, respectively (detailed in Figure 4.1). Genome wide DNA methylation analysis was performed via Illumina EPIC array for participants (N=8 baseline, loading, unloading; N=7 reloading) across all conditions. Follow up gene

expression was subsequently performed on identified transcripts of interest.

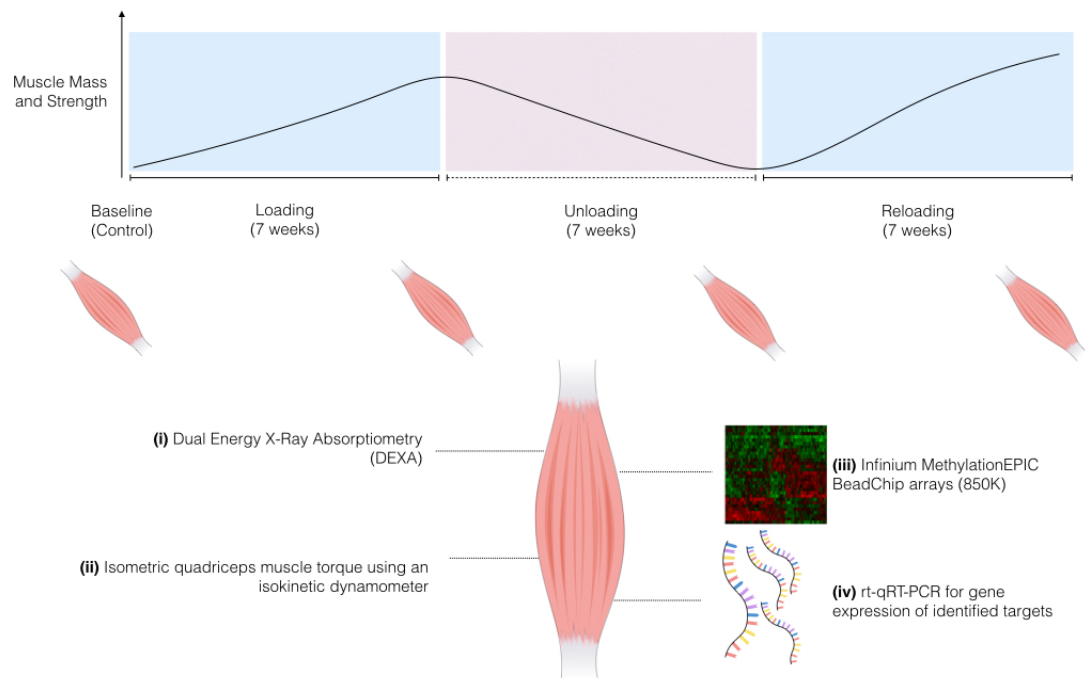


Figure 4.1. Schematic representation of experimental condition and types of analyses undertaken across the time-course. Muscle schematic represents data collection time, where analysis of muscle size (i. DEXA) and muscle strength (ii. IKD) were performed. Muscle samples were obtained at the same experimental time points and down-stream analysis of methylome wide bead array (iii) were performed on isolated and treated DNA. Finally, gene expression was analysed on muscle samples via rt-qRT-PCR (iv).

4.2.2 Resistance exercise-induced muscle hypertrophy: loading, unloading, reloading

Complete description of resistance load induced hypertrophy programme is detailed in methodology section 2.2.2. Briefly, following a familiarization week which accustomed previously novice participants to the required lifting techniques, range of motions and exercise, exercise loads were set via an ability assessment and verbal feedback (participant). Participants performed 3 sessions (~ 60mins per session) per week for 7 weeks of resistance exercise training constituting of two lower limb

sessions and one upper body focused session (section 2.2.2). Due to participants being unaccustomed to exercise training modality, an overall progression model was utilised, similar to that previously described (Baechle et al., 2008, Peterson et al., 2011). Full descriptive of exercises, sets, reps and progression model utilised are given in section 2.2.2. Following 7 weeks of resistance training, participants were instructed to return to habitual pre-intervention exercise levels (unloading) and not to perform any form of resistance training. Regular verbal communication between researcher and participant ensured subjects followed these instructions. Participants subsequently began a secondary period of 7 weeks of resistance training (reloading). In the first session of this training phase (reloading), participants performed sets, reps and load that resembled week 1 of loading training. All exercises, sets, reps and progression were performed and monitored in identical to fashion to that of the loading phase (section 2.2.2). Total weekly volume load was calculated as the sum of all exercise loads;

$$\text{Total Exercise Volume (kg)} = (\text{Exercise Load} * \text{No. of Reps}) * \text{No. of Sets}$$

This model of progression and resistance training, resulted in a progressive increase in training volume (\pm SEM) of $2,257 \pm 639$ kg and $2,386 \pm 222$ kg respectively per week (Figure 4.2), with the reloading phase displaying a significant ($P = 0.043$) increase in average load.

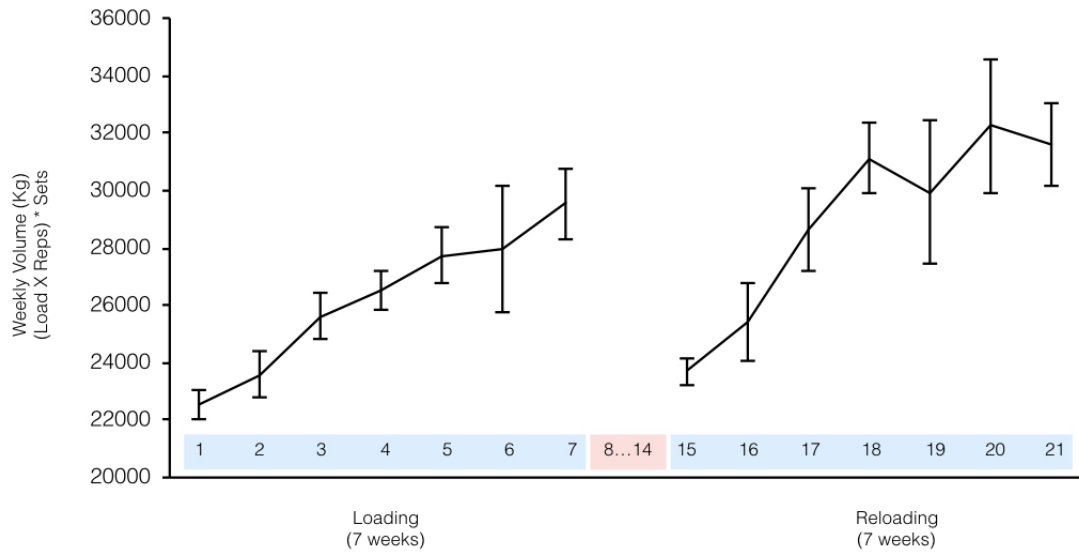


Figure 4.2. Weekly total volume of resistance exercise undertaken by human participants (N=7) during first 7 weeks of resistance exercise period (loading), followed by 7 weeks' exercise cessation period (weeks 8-14), and the later secondary period of 7 weeks' resistance exercise loading (reloading).

4.2.3 In-vivo assessment of lean mass and strength in humans

At experimental time points (Figure 4.1), DEXA and knee-extensor MVC measured were taken from participants (N=7) for analysis of changes in skeletal muscle mass of the lower limbs, and muscular strength changes in the quadriceps femoris of the right leg. Protocols for analysis of lean mass via DEXA and muscular strength via isokinetic dynamometer (IKD) are provided in sections 2.4.1 and 2.4.2, respectively. Lean mass of the combined lower limb values were analysed via QDR software, calculated on absolute values for each condition, and presented as percentage change compared to baseline. Furthermore, to assess whether later reloading altered lean mass, loading was normalised to baseline, and reloading was normalised to unloading data to account for residual starting mass in both conditions. Quadriceps femoris measure of strength was analysed using absolute values (Nm) as a percentage change to baseline (%). Furthermore, to assess whether later reloading altered quadriceps

femoris strength, loading was normalised to baseline, and reloading was normalised to unloading data to account for residual starting strength in both conditions.

4.2.4 Muscle biopsy preparation

At baseline, 7 weeks loading (beginning of week 8), 7 weeks unloading (end of week 14) and 7 weeks reloading (beginning of week 22) (Figure 4.1), a muscle sample was obtained from the vastus lateralis muscle of the right leg from each participant, avoiding areas of immediate proximity to previous incisions, before being carefully dissected using a sterile scalpel on a sterile (gamma-irradiated) petri dish. Separate samples were immediately snap frozen in liquid nitrogen before being stored at -80°C for down-stream analysis.

4.2.5 Isolation and analysis of DNA for methylome and CpG DNA methylation via epic methylome bead array

DNA was isolated and analysed for quality and quantity from skeletal muscle biopsy samples as previously described (section 2.7.1 to 2.7.3). Isolation of DNA yielded averages quantities of $8.0\ \mu\text{g}$ (± 4.2) and 260/280 quality ratio of 1.88 (± 0.09). Five hundred ng of prepared DNA was subsequently bisulfite converted using the EZ-96 DNA methylation kit (as described 2.7.4.1). Illumina MethylationEPIC BeadChip (Infinium MethylationEPIC BeadChip, Illumina, California, United States) array was then used to examine over 850,000 CpG sites of the human methylome (see section 2.7.5), and subsequent data files (.IDAT) were imported into Partek Genomic Suite for differential methylation analysis across all experimental conditions to identify differentially regulated CpG sites of experimental groups. Fold change in CpG

specific DNA methylation and statistical significance was performed using Partek Genomic Suite V.6.6 software, where statistical significance was obtained following ANOVA (with Bonferroni correction) analysis. Unadjusted p-value significance ($P < 0.05$) was used to create a CpG site marker list of standardized beta-values. Unsupervised hierarchical clustering was performed and a dendrogram was constructed to represent differentially methylated CpG loci and statistical clustering of experimental samples, and schematically represented in heatmaps (for further details see section 2.7.5). The same marker list was used to analyse gene ontology (GO) terms and KEGG signalling pathways, as previously described (section 2.7.5.2)

4.2.6 Isolation and analysis of RNA for gene expression

RNA was isolated, quantified, prepared and setup for rt-qRT-PCR as described in sections 2.6.1 to 2.6.4. All primer sequences for analysis of genes of interest are provided in table 4.1. Gene expression analysis was performed on at least $n = 7$ for all genes, unless otherwise stated. All relative gene expression was quantified using the comparative Ct ($\Delta\Delta$ Ct) method (Schmittgen and Livak, 2008). Individual participants' own baseline Ct values were used in $\Delta\Delta$ Ct equation as the calibrator using RPL13a as the reference gene. The average Ct value for the reference gene was consistent across all participants and experimental conditions; 20.48 (± 0.64 , SD) with low variation of 3.17%, and an average efficiency of 82.5 % (± 7.1 , SD) and low percentage variation 3.9.

Table 4.1. Gene primer sequences for human muscle memory experiment. All primers used the same cycling conditions.

Gene	Accession No.		Primer Sequence	Primer Length	Prod. Length
RPL13a	NM_01242 3	F-	GGCTAAACAGGTAAGTCTGGG	21	105
		R-	AGGAAAGCCAGGTAAGTCAACTT	23	
ERICH1-AS1	NM_00134 6810.1	F-	AATGGGCAATTCGAGTCCGT	20	105
		R-	GCTGTGACTCCTTGTTCCGA	20	
CACNA1H	NM_00100 5407.1	F-	AGCGCCGGCCCTACT	15	119
		R-	CATGGTGTGACGTTGACACAG	22	
GAS7	NM_20143 2.1	F-	GAACCTGGGATCCTCATCGC	20	79
		R-	GTGAGGGAACGTCACACAGT	20	
FBXL17	NM_00116 3315.2	F-	TTGCACAGAGCAGCAAGTCT	20	76
		R-	TGTTCCACCGTCACTTCGTT	20	
CPT1A	NM_00103 1847.2	F-	CAGGCCGAAAACCCATGTTG	20	104
		R-	AGGCCTCACCGACTGTAGAT	20	
STAG1	NM_00586 2.2	F-	GCATTTTTAGCAACTTCTACCAGC	24	115
		R-	AACTTGAATTTGGCAGGGCA	20	
AFF3	NM_00228 5.2	F-	AACGGGAGCTGAGAGCTGAT	20	70
		R-	GGGTGTCGACTTCAAACCTTG	21	
STIM1	NM_00127 7962.1	F-	TGGACGATGATGCCAATGGT	20	110
		R-	CTCACCATGGAAGGTGCTGT	20	
AXIN1	NM_00350 2.3	F-	AAGGTCCCGAGGCTACTCAG	20	112
		R-	GCATTTCTTTTGCACGCCAC	20	
MTRF1L	NM_00109 9625.1	F-	CAACCTACCCTTGAAGCCGT	20	89
		R-	TGGGGGCACATCTCTCAAAC	20	
ODF2	NM_15343 6.1	F-	TTGTGGCGCACCCAGTGTA	20	71
		R-	GCACATTCACAGTGTCCCCT	20	
GRIK2	NM_00116 6247.1	F-	CACATACAGACCCGCTGGAA	20	110
		R-	GGTCTAAAATGGCACGGCTG	20	
CAMK4	NM_00132 3377.1	F-	AGCTCTGCTGTGGGTTTTGA	20	91
		R-	AAATGCCGGTGTGGCTTC	20	
CPED1	NM_02491 3.4	F-	GCCGAAGGGCCATACTCTAC	20	106
		R-	TCTTCAGCGATGACAACCGT	20	
NUB1	NM_00124 3351.1	F-	GGATCATGCGGCCACTCATA	20	102
		R-	AACCTGATGTTCTCGAGGCG	20	
APLP1	NM_00102 4807.2	F-	CATCTGGGACAGCAGTTGGT	20	87
		R-	CCTCCTCTTCCTCGTCCTCA	20	
PAPD7	NM_00117 1805.1	F-	CATGAAAGCCATGACCAGCG	20	120
		R-	TCGAAGACCTGCTTCACCTG	20	
IL19	XM_01150 9450.2	F-	CCATCGGCCTCCTGATATGG	20	84
		R-	TGGGAGAGGTTCTCCACAGT	20	
UNC45A	NM_00103 9675.1	F-	GAGATGTTGGGGTTCCAGG	20	118
		R-	AGCTGAAGAGCAGCAGTAGC	20	
CNTNAP2	NM_01414 1.5	F-	CACTTGGTGGGTTGGCAAAG	20	105
		R-	GGATCTGTGCAGTTGCGTTC	20	
MYO10	NM_01233 4.2	F-	CACTGAGTGTGACTTCAAGAAAGC	24	110
		R-	TTTGGGGCTGACATAGGGGA	20	
TM6SF1	NM_00114 4903.1	F-	CCATCCCGGTCACCTATGTC	20	101
		R-	CAGCAGTGCTACCAGGAACA	20	

NUP205	NM_00132	F-	CTGGAGAGCATCAACAGCCA	20	85
	9434.1	R-	ATGCATCGCTTTCCATCCCA	20	
HOXB1	NM_00214	F-	TACCCACTCTGTAACCGGGG	20	100
	4.3	R-	ATAGCTGTCAACCGCCTGAG	20	
C8B	NM_00127	F-	TGCCAAGGAAATGGAGTCCC	20	91
	8544.1	R-	AGGAGACCTCACAGGCTAGG	20	
KLHDC1	NM_17219	F-	TGGTGGGAGCAAAGATGACT	20	102
	3.2	R-	TCAAGGCATGACCTGAGTAGTG	22	
MYO16	NM_01501	F-	AGTCTCAGGACAGCATCCCT	20	85
	1.2	R-	TTTGGGGCAGGAGGCATTAG	20	
C11orf24	NM_00130	F-	CCAGCTCACCCACAAGATGT	20	98
	0913.1	R-	AGTTGCGTGGATCGTTGGAT	20	
FREM2	NM_20736	F-	GAGAAGGGGCTAATGCCACA	20	102
	1.5	R-	TCCATGCCCAATTCAGACGA	20	
ADSSL1	NM_15232	F-	ACTTCATCCAACCTGCACCGT	20	71
	8.4	R-	ACGTCACCTATGTTCTGCGG	20	
RPL35A	NM_00099	F-	TAACTCGGGCCCATGGAAAC	20	76
	6.2	R-	TGTCCAATGGCCTTAGCAGG	20	
SETD3	NM_03223	F-	GACCCATCCTCATGCCAACA	20	77
	3.2	R-	CAGAAGAGACTGCCACCTG	20	
TRAF1	NM_00119	F-	GGAAGCTGCGTGTGTTGAG	20	97
	0947.1	R-	AGCTGGCTCTGGTGGATAGA	20	
ART3	NM_00113	F-	AGGAGGTTATACCCGGAGGT	20	80
	0017.2	R-	GATCAGCACTGGCAGCAAAC	20	
NR2F6	NM_00523	F-	TCCAGGATGGAGGGTCCAAT	20	74
	4.3	R-	CCCACCATCCCACAAGTTCA	20	
C12orf50	NM_15228	F-	GCAACCACTTTCAGCGTTTCT	21	71
	9.1	R-	GCCTCTTCACAGTGTTCGGAA	20	
BICC1	NM_00108	F-	GGCCATGTTACAAGCTGCTG	20	97
	0512.2	R-	TGGCCAAGCAATCTGCGTAT	20	
ZFP2	NM_03061	F-	TTCCACAGCCAGCATCTCAC	20	99
	3.3	R-	TCAGTAATAACCCGGCTTCGG	20	
FKBPL2	NM_02211	F-	CTCCTGTCAGGCTCACACTG	20	78
	0.3	R-	GGGCTTCCTTCTCGCTAGTC	20	
RSU1	NM_01242	F-	TGCCGCCAGATATTGGGAAG	20	78
	5.3	R-	CCTTAGGCAGCGAGATCAGG	20	
IGF2BP3	NM_00654	F-	ACTCGGTCCCAAAAAGGCAA	20	107
	7.2	R-	CCAGCACCTCCCCTGTAAAT	21	
UBR5	NM_00128	F-	AGGCAACACCTTAGGAAGCC	20	81
	2873.1	R-	GCTCCAGCTGATGACCTACC	20	
LTB	NM_00234	F-	TCACCCCGATATGGTGGACT	20	87
	1.1	R-	TCGCACCACGCACTCATATT	20	
PTH1R	NM_00031	F-	CAAGGGATGGACATCTGCGT	20	85
	6.2	R-	GTCCTCCTCAGACTCAGGGT	20	
HEG1	NM_02073	F-	AACGTTGATCGCTGGGATT	20	73
	3.1	R-	TGGTCGCTGGAAGTCCTTTG	20	
HSPD1	NM_00215	F-	GGTGGTGCAGTGTGGGAGA	20	118
	6.4	R-	TGGCATCGTCTTTGGTCACA	20	
ZNF562	NM_00112	F-	GTGTGCACAAGGAAGCCTCT	20	89
	0021.1	R-	CACAGCAAGGCCTGGAGTTA	20	
PLA2G16	NM_00112	F-	GATGACAAGTACTCGCCGCT	20	81
	8203.1	R-	CTTGTAGAGCACCTCCTGCC	20	

4.2.7 Statistical analysis

Analysis of in-vivo data (N=7) was performed via a one-way repeated measures ANOVA in SPSS (v.23.0), with follow up analysis of change in mass and strength as a result of loading or reloading (when normalized to relevant baseline or unloading control to account for residual starting mass or strength) performed via a pairwise T-test in SPSS. In MiniTab Statistical Software (MiniTab v.17.2.1), MANOVA analysis was used for gene expression of relevant transcript clusters to detect for significance across time with a follow up ANOVA performed for analysis of time, within each transcript cluster. Correlation analysis of gene expression to percentage change in leg lean mass was performed via a Pearson correlation coefficient with significance ascertained via two-tailed test (SPSS). All methylome-wide and CpG loci specific statistical analysis was performed in Partek Genomic Suite (v.6.6), as described in section 2.5. Statistical values were considered significant at the level of $P \leq 0.05$. All data represented as mean \pm SEM, unless otherwise stated.

4.3 Results

4.3.1 Lean leg mass and muscle strength is increased after loading, returns toward baseline during unloading and is further increased after reloading

Analysis of lower limb lean mass via DEXA, identified a significant increase of 6.5% ($\pm 1.0\%$; $P = 0.013$) in lean mass after 7-wks of chronic loading compared to baseline (20.74 ± 1.11 kg loading vs. 19.47 ± 1.01 kg baseline). Following 7-wks of unloading, lean mass significantly reduced by $4.6\% \pm 0.6\%$ ($P = 0.02$) vs. the 7 weeks loading, back towards baseline levels (unloading, 19.83 ± 1.06 kg), confirmed by no significant

difference between unloading and baseline. Subsequently, a significant increase in lean mass of the lower limbs was accrued after the reloading phase of $12.4 \pm 1.3\%$, compared to baseline (reloading, 21.85 ± 2.78 kg, $P = 0.001$, Figure 4.3), resulting in an increase of $5.9 \pm 1.0\%$ compared to the earlier period of loading ($P = 0.005$). Pairwise t-test analysis that corrected for any lean mass that was maintained during unloading demonstrated a significant increase in lean muscle mass in the reloading phase (unloading to reloading), compared to the loading phase (baseline to loading) ($P = 0.022$; Figure 4.3).

Analysis of muscle strength suggested a similar trend. Isometric peak torque increased by $9.3 \pm 3.5\%$ from 296.2 ± 22.1 Nm at baseline to $324.5 \text{ Nm} \pm 27.3$ Nm after 7-wks of loading, not attaining statistical significance ($P > 0.05$; Figure 4.4). Upon 7-wks of unloading, peak torque reduced by $8.3 \pm 2.8\%$ vs. loading, back towards baseline levels displaying no significant difference to baseline ($P > 0.05$). Upon subsequent reloading, a significant $18 \pm 3.6\%$ increase in isometric peak torque production (349.6 ± 27.7 Nm) was observed compared to baseline ($P = 0.015$; Figure 4.4). Pairwise t-test analysis that corrected for any residual quadriceps' strength maintained from unloading displayed no significant difference in strength of reloading phase (unloading to reloading), compared to the loading phase (baseline to loading) (Figure 4.4).

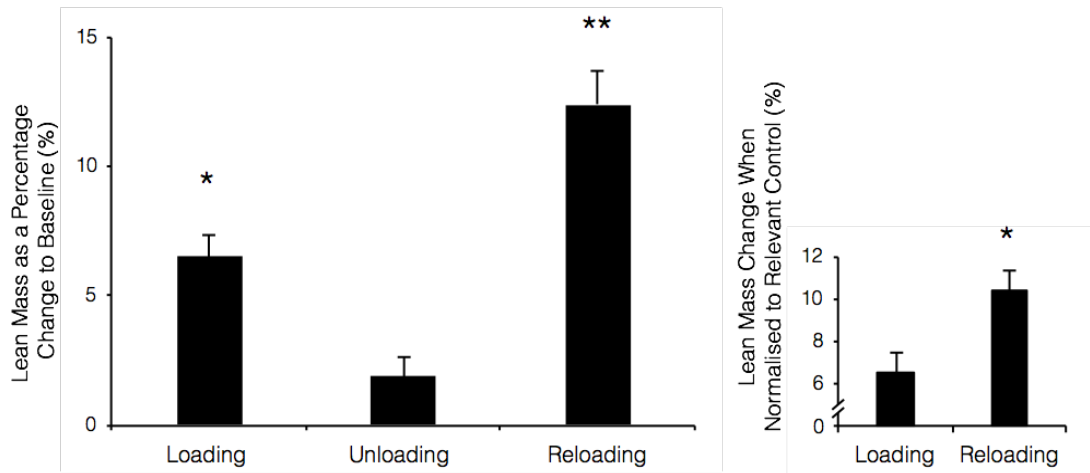


Figure 4.3. Skeletal muscle mass changes in human participants across resistance exercise and exercise cessation time-course. **A.** Lean mass changes in human subjects (N=7) after a period of 7 weeks resistance exercise (loading), exercise cessation (unloading) and a subsequent second period of 7 weeks resistance (reloading). Total limb lean mass was normalised to baseline and presented as a percentage change. Significant change compared to baseline represented by * and significant to all other conditions represented by **. **B.** Total lean mass percentage change when loading is normalised to baseline, and reloading normalised to unloading to account for starting lean mass in both conditions. Pairwise t-test of significance indicated by *. All data represented as mean \pm SEM.

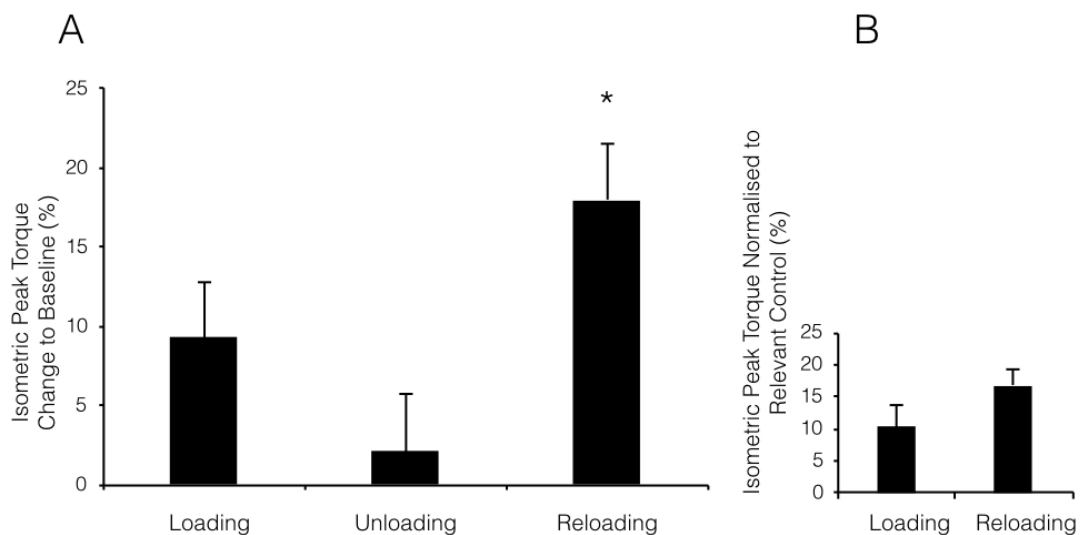


Figure 4.4. Skeletal muscle strength changes in human participants across resistance exercise and exercise cessation time-course. 4.4A. Isometric quadriceps peak torque

in participants (N=7) after a period of 7 weeks resistance exercise (loading), exercise cessation (unloading) and a subsequent second period of 7 weeks resistance exercise (reloading). Data was normalised back to baseline and represented as a percentage to the same. Significant change compared to baseline represented by *. 4.4B. Isometric peak force change when loading is normalised to baseline, and reloading normalised to unloading to account for starting lean mass in both conditions. Pairwise t-test of significance indicated by *. All data presented as mean \pm SEM (N=7).

4.3.2 Exposure to reloading stimulus evokes the largest DNA hypomethylated state across the genome in human muscle

The frequency of statistically ($P < 0.05$) differentially regulated CpGs in each condition was analysed (Figure 4.5), reporting 17,365 CpG sites as significantly ($P < 0.05$) differentially epigenetically modified following loading induced hypertrophy compared to baseline, with a larger number being hypomethylated (9,153) compared to hypermethylated (8,212 CpG sites; Figure 4.5). Interestingly, the frequency of hypomethylated epigenetic modifications was similar to loading after unloading (8,891) (Figure 4.5), where it was previously reported that lean muscle mass returned back towards baseline. Importantly, following reloading induced muscle growth, an increased number of epigenetically modified CpG sites (27,155) and an enhanced number of hypomethylated DNA sites (18,816; Figure 4.5) was observed. This increase in hypomethylation coincided with the largest increase in skeletal muscle mass in reloading, as previously described (Figure 4.3). By contrast, hypermethylation remained stable across conditions of loading, (8,212) unloading (8,638) and subsequent reloading (8,339 CpG sites).

To further analyse the reported increased frequency of hypomethylated genes across the genome following reloading, gene ontologies and KEGG signalling pathways were analysed for the frequency of hypo and hypermethylated CpG sites. In agreement with our above frequency analysis, the most statistically significant enriched GO terms identified an increased number of hypomethylated CpG sites following reloading, compared to baseline (Figure 4.6). Indeed, the most statistically significantly (FDR < 0.05) enriched GO terms were: 1) molecular function GO:0005488 encoding for genes related to 'binding', that displayed 9,577 (68.71%) CpG sites that were hypomethylated following reloading and 4,361 (31.29%) sites as hypermethylated compared to baseline (Figure 4.6 A), and: 2) Biological process GO:0044699 encoding for genes related to 'single-organism processes' that displayed 7,586 (68.57%) hypomethylated CpG sites compared to 3,493 (31.43%) sites profiled as hypermethylated after reloading compared to baseline (Figure 4.6 B). Finally, 3) cellular component, GO:004326 encoding for genes related to 'organelle' reported 7,301 hypomethylated CpG sites following reloading and 3,311 hypermethylated sites, compared to baseline, therefore favouring a majority 68.88% hypomethylated profile (Figure 4.6 C). Following confirmation that the largest alteration in CpG DNA methylation occurred upon reloading, we sought to elucidate how the serine/threonine AKT signalling pathway, a critical pathway involved in mammalian growth, proliferation and protein synthesis (Egerman and Glass, 2014, Schiaffino and Mammucari, 2011), was differentially regulated across experimental conditions. Intuitively, the PI3K/AKT signalling pathway was significantly enriched upon all pairwise comparisons of base vs. load, unload and reload, respectively ($P < 0.022$; figures 4.7 A-C), suggesting that the pathway was significantly epigenetically modified following periods of skeletal muscle perturbation. Importantly, frequency

analysis of statistically differentially regulated transcripts (Figure 4.7 D) attributed to this pathway, reported an enhanced number of differentially regulated CpG sites (444 CpG sites) following reloading (Figure 4.7 D), compared to loading and unloading alone (Figure 4.7 D). Furthermore, and in accordance with the previous findings from the genome-wide and GO analysis, the enhanced number of statistically differentially regulated CpG sites in this pathway upon reloading condition is attributed to an enriched number of hypomethylated (299 CpG sites, 67.3 %) compared to hypermethylated (145 sites, 32.7 %) CpG sites (Figure 4.7 E).

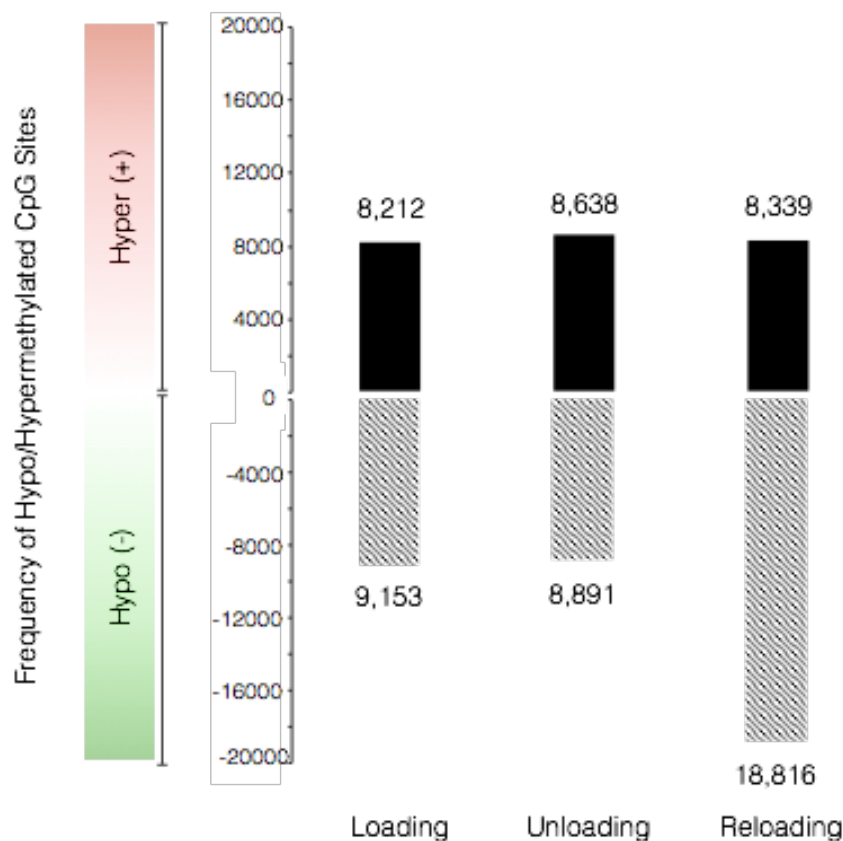


Figure 4.5. Frequency analysis of statistically differentially regulated CpG ($P < 0.05$) sites identified via Infinium MethylationEPIC Bead Chip array (850K CpG sites) of the human methylome during 7 weeks of chronic resistance exercise (loading), 7 weeks' exercise cessation (unloading) and a secondary period of 7 weeks of resistance training (reloading). Frequency analysis revealed large adaptations of the human

methylome upon initial exposure to resistance loading, with equal number of CpG sites being up- and down-regulated. This response was maintained following 7 weeks of exercise cessation. Upon secondary exposure of later reloading, a larger number of CpG sites were hypomethylated compared to hypermethylated within the reloading condition, but also compared to all other conditions.

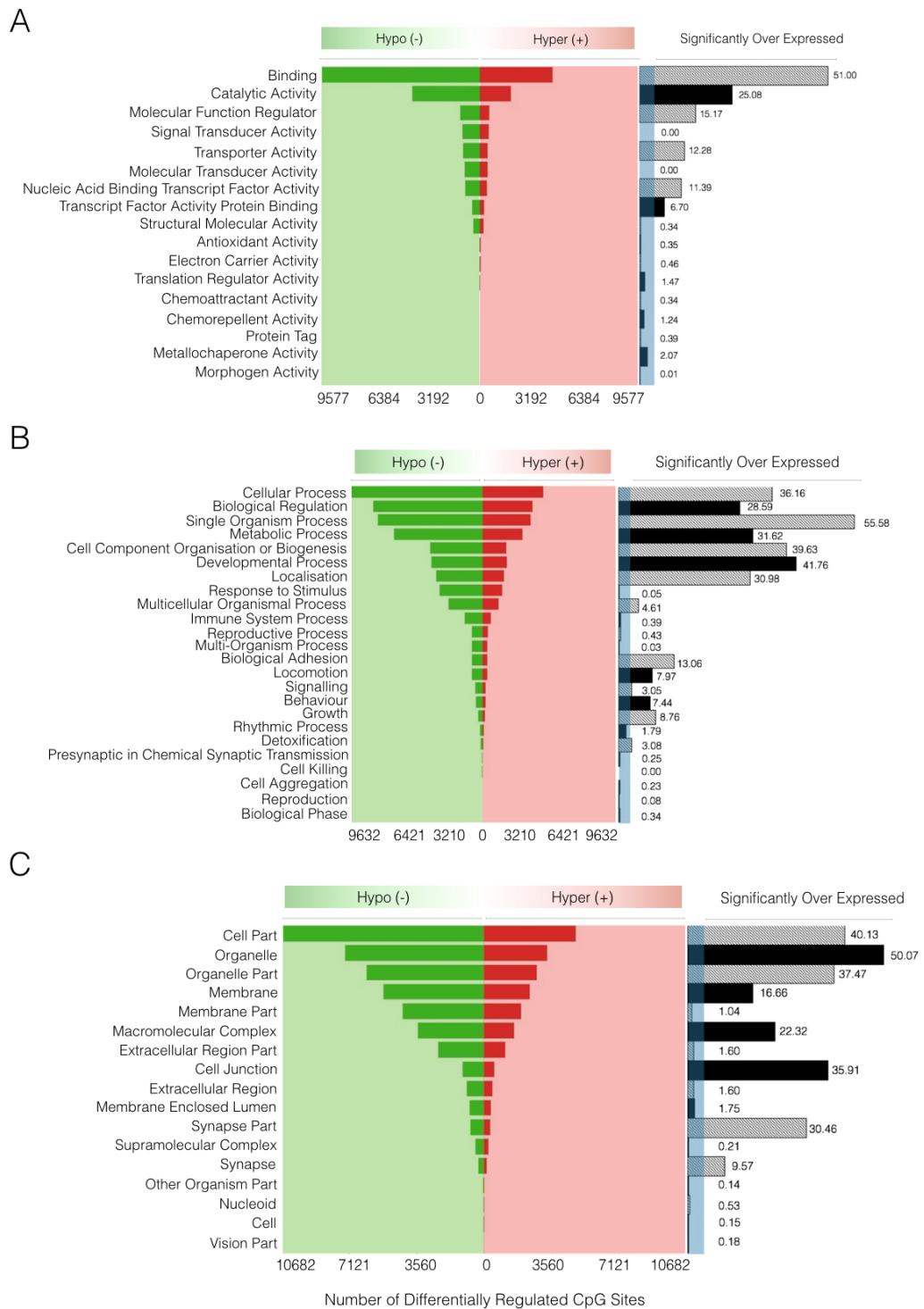
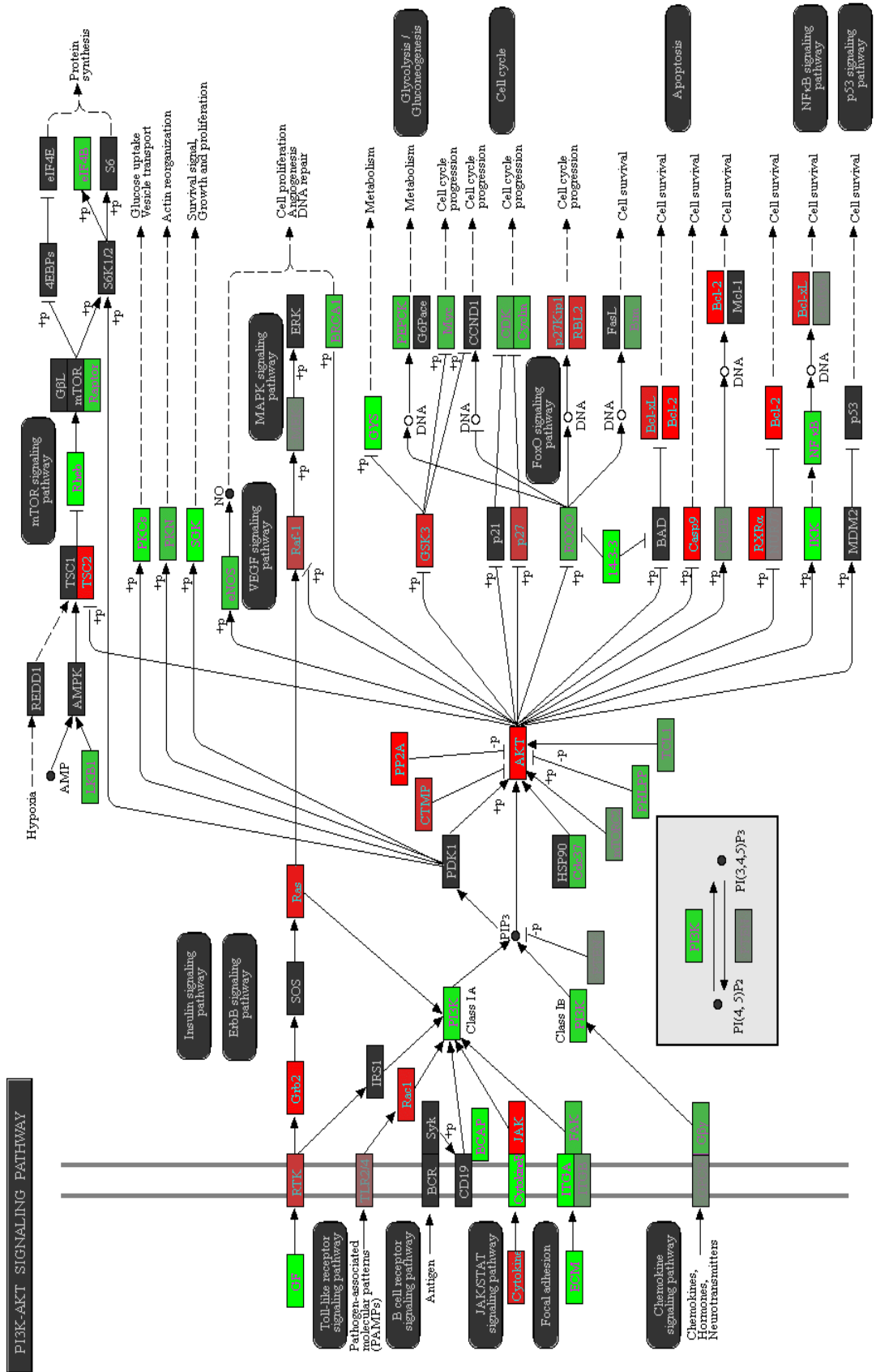


Figure 4.6. Gene ontology analysis generated from Infinium MethylationEPIC BeadChip array of 850,000 CpG sites of the human methylome. Analysis confirms an enhanced hypomethylated profile after reloading compared to baseline, as previously indicated via frequency analysis. Forest plot schematics represent the number of CpG sites hypo- or hyper-methylated in reloading versus control conditions across various functional groups in A). molecular function, B) biological processes and C) cellular components. Functional with a fold enrichment > 3 (as indicated via shaded blue region) represents statistically modified (termed overexpressed for visual purposes) KEGG pathways, $FDR < 0.05$.

B. Unloading – PI3/AKT Signalling Pathway



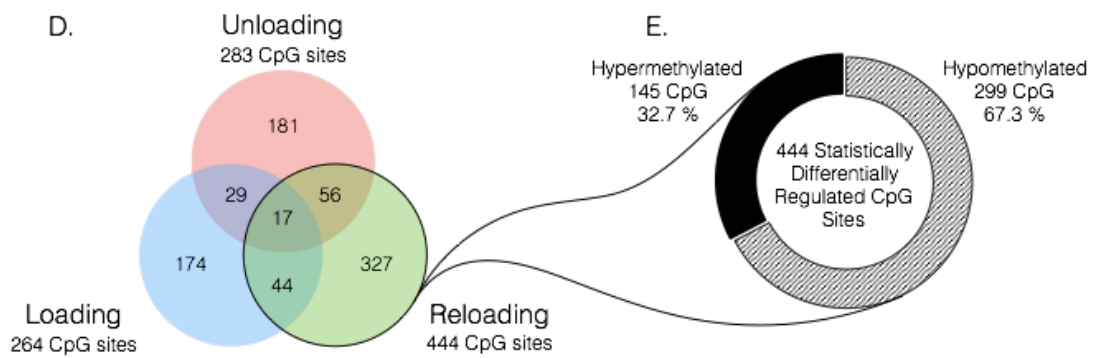


Figure 4.7. Representation of the DNA methylation modifications that occurred within the PI3K/AKT KEGG signalling pathway following 7 weeks of loading (A), unloading (B) and reloading (C) in human subjects. Signalling analysis performed on statistically differentially regulated CpG sites compared to baseline, with green indicating a hypomethylated fold change and red indicating a hypermethylated change, with strength of colour representing the intensity of fold change (Kanehisa and Goto, 2000, Kanehisa et al., 2017, Kanehisa et al., 2016). figure D. Venn diagram analysis of the statistically differentially regulated CpG sites attributed to the PI3K/AKT signalling pathway following loading, unloading and reloading, compared to be baseline. Ellipses reports number of commonly statistically differentially regulated CpG sites across each condition. Analysis confirms an enhanced number of differentially regulated CpG sites upon reloading condition. figure E. Analysis of hypo vs. hypermethylated profile of statistically differentially regulated CpG sites associated to the PI3K/AKT signalling pathway,

4.3.3 Genome-wide analysis identified two distinct temporal clusters of altered DNA methylation that provides initial evidence of an epigenetic induced muscle memory

Changes in genome-wide DNA methylation were analysed following loading, unloading and reloading induced muscle adaptation. A dendrogram of the top 500 most statistically epigenetically modified CpG sites across of each experimental condition compared to baseline, identified large alterations in DNA methylation profiles (Figure 4.8). A ranked unsupervised hierarchical clustering analysis demonstrated significant differences between the initial loading (weeks 1-7) vs. all other conditions (Figure 4.8). Closer analysis of the top 500 CpG sites across experimental conditions highlighted a clear temporal trend occurring within different gene clusters. The first cluster (named Cluster, A) displayed enhanced hypomethylation with earlier loading-induced hypertrophy. This cluster was methylated at baseline and became hypomethylated after loading, re-methylated with unloading (Figure 4.8), and, subsequently, hypomethylated after reloading. The second temporal trend (named Cluster B) also displayed an enhanced hypomethylated state across the top 500 CpG sites as a result of load induced hypertrophy. As with Cluster A, Cluster B genes were methylated at baseline and became hypomethylated after initial loading. In contrast to Cluster A however, Cluster B remained hypomethylated with unloading even when muscle mass and CSA returned to baseline levels and this hypomethylation was also maintained/ 'remembered' after reload induced hypertrophy (Cluster B, Figure 4.8). The third temporal trend, named Cluster C, revealed genes as hypomethylated at both baseline and after initial loading, suggesting no epigenetic modifications were retained or remembered after the first period of hypertrophy in these genes (Cluster C, Figure 4.8). During unloading, genes

were hypermethylated and remained in this state during reloading. The final cluster (Cluster D) of genes, were hypomethylated at baseline, became hypermethylated after loading (Cluster D, Figure 4.8), reverted back to a hypomethylated state with unloading and then maintained the hypomethylated state after reloading, reflecting the profile of the baseline targets in the same cluster (Cluster D, Figure 4.8). These two clusters (C&D) did report a maintenance of the DNA methylation profile from unloading to reloading conditions. Cluster C also reported a hypermethylated profile after unloading following a period of loading, that may therefore identify important CpG sites that are hypermethylated when muscle mass is reduced. Collectively, both clusters A and B identify a retention of modified epigenetic patterns following the initial resistance exercise loading period, where in contrast, both Cluster C&D suggest no retention of epigenetic modifications following the same stimulus.

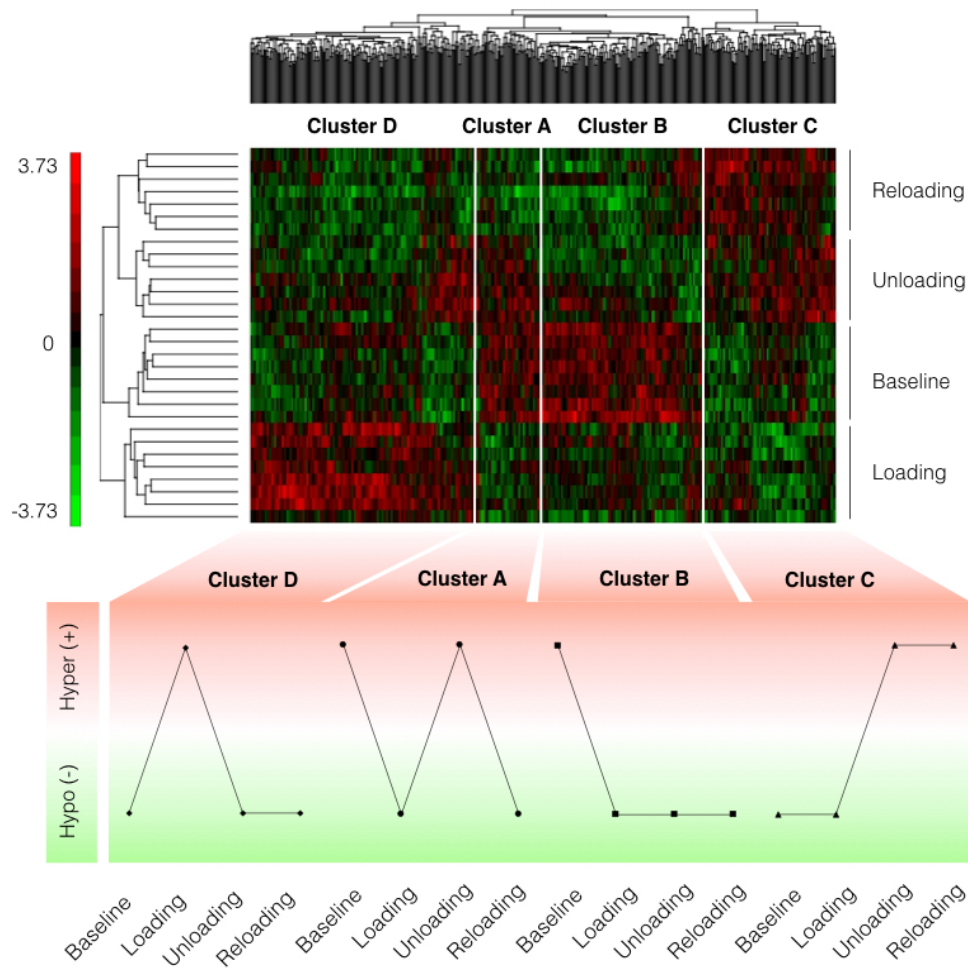


Figure 4.8. Heat map depicting unsupervised hierarchical clustering of the top 500 statistically differentially regulated CpG loci (columns; $P < 0.05$) and conditions (baseline, loading, unloading and reloading) in previously untrained male participants ($N=8$). The heat-map colours correspond to standardised expression normalised β -values with green representing hypomethylation, red representing hypomethylation and unchanged sites are represented in black. The temporal pattern of DNA methylation in each individually identified cluster is schematically represented beneath the heatmap for clarity.

4.3.4 Identification of gene expression clusters inversely associated with CpG DNA methylation

To assess whether the changes in DNA methylation affected gene expression, the 100 most significantly differentially modified CpG sites across all conditions were

identified and cross referenced with the most frequently occurring CpG modifications in pairwise comparisons of all conditions. Importantly, forty-six percent of the top 100 CpG sites were within gene promoter regions with 18% residing in intergenic regions, suggesting high biological relevance of the CpG sites of this candidate list (Figure 4.9). In total, 48 genes were analysed by rt-qRT-PCR to assess gene expression. Interestingly, gene expression analysis identified two distinct clusters of genes that had different transcript profiles, inversely mirroring the temporal patterns in DNA methylation of clusters already described.

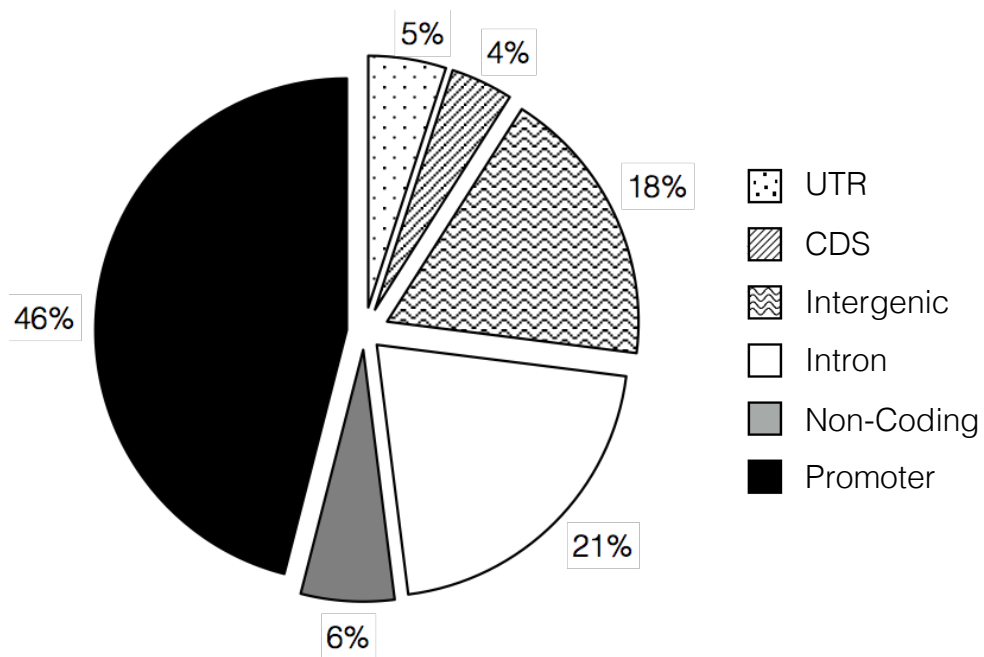


Figure 4.9. Genomic location of the top 100 statistically differentially regulated CpG sites across conditions, in the human methylome as identified via Infinium MethylationEPIC Bead Array. Coding DNA sequence (CDS), Untranslated region (UTR).

4.3.4.1 Cluster A: increased expression after loading, return to baseline after unloading and enhanced expression upon reloading, mirrored by inverse changes in DNA methylation

This first cluster (A) included RPL35a, C12orf50, BICC1, ZFP2, UBR5, HEG1, PLA2G16, SETD3 and ODF2 genes that displayed a significant main effect for time ($P < 0.0001$) after MANOVA analysis (Figure 4.10 A). Importantly, this first cluster displayed a mirrored (inverse) temporal pattern to those identified previously in Cluster A above for CpG methylation (in the top 500 differentially regulated CpG sites, Figure 4.8). Where, upon 7-wks of loading, gene expression of this cluster significantly increased (1.22 ± 0.09 , $P = 0.004$) and CpG methylation of the same genes was non-significantly reduced (hypomethylated) (0.95 ± 0.04 Figure 4.10 B). During unloading, methylation returned to baseline (1.03 ± 0.07), which was met by a return to baseline in gene expression (0.93 ± 0.05), as indicated by both CpG methylation and gene expression displaying no significant difference compared to baseline (Figure 4.10 A and B). Importantly, upon reloading, both CpG methylation and gene expression displayed an enhanced response compared to the baseline and loading time point, respectively. Indeed, upon reloading, this cluster became hypomethylated (0.91 ± 0.03 , $P = 0.05$, Figure 4.10 B). This was met with a significant enhancement (1.61 ± 0.06) in gene expression of the same cluster compared to baseline and loading ($P < 0.001$, Figure 4.10 A).

4.3.4.2 Cluster B: Initial and progressive increase in gene expression from loading through unloading and reloading, met with an inverse profile of DNA methylation

A second separate gene cluster was identified and included: AXIN1, GRIK2, CAMK4, TRAF1, NR2F6 and RSU1. Although together there was no significant effect of time via MANOVA analysis. ANOVA analysis reported that this cluster displayed increased gene expression after loading (1.19 ± 0.08) that then further increased during unloading (1.58 ± 0.13) resulting in statistical significance ($P = 0.001$) compared to baseline alone. Gene expression was then even further enhanced (1.79 ± 0.09) upon reload induced hypertrophy ($P < 0.0001$; Figure 4.11 A). This temporal gene expression pattern was inversely associated to CpG methylation observed in Cluster B (identified previously in the top 500 differentially regulated CpG sites, Figure 4.8). Closer fold-change analysis of CpG DNA methylation of this gene cluster, identified a potential association between methylation and gene expression of 4 out of 6 of the targets (AXIN1, GRIK2, CAMK4, TRAF1; Figure 4.11 B). Where, upon loading, these genes became significantly hypomethylated (0.78 ± 0.09 ; $P = 0.036$) compared to baseline, with this profile being maintained during unloading (0.84 ± 0.09) and reloading (0.83 ± 0.05) conditions, albeit non-significantly (Figure 4.11 B). Collectively, we report that a sustained hypomethylated state in 4 out of 6 of the genes in this cluster that were met with an increased transcript expression of the same genes (Figure 4.11 B).

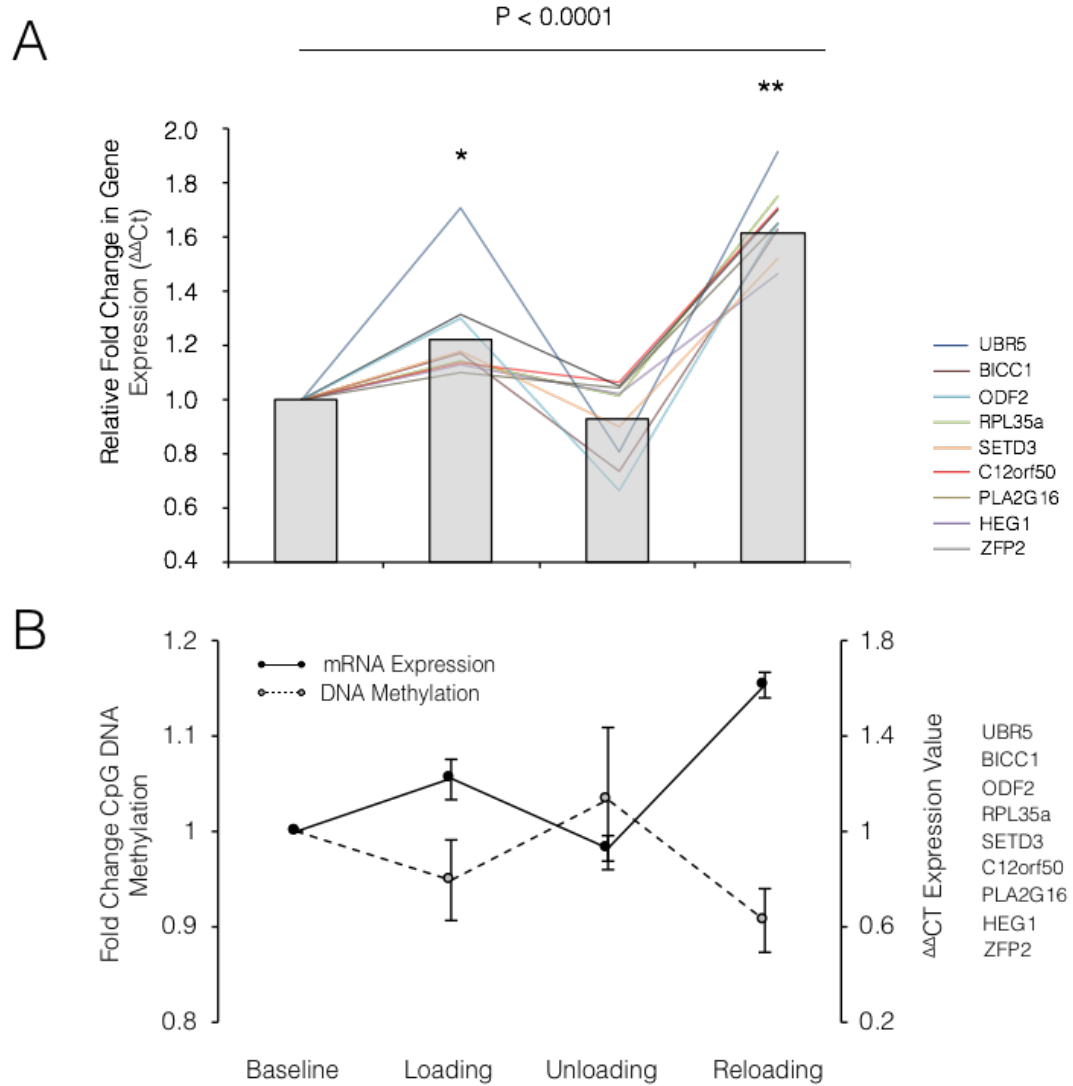


Figure 4.10. Relative changes in gene expression (A) and representative schematic of CpG DNA methylation and gene expression relationship (B) for genes in cluster A. A). Expression of genes that displayed significant increased compared to baseline (*) upon earlier loading, that returned to baseline during unloading, displayed enhanced expression after reloading (**). MANOVA analysis reported a significant effect over entire time course ($P < 0.0001$). B). Representative schematic displaying a potential relationship between gene expression (solid black lines) and CpG DNA methylation (dashed black lines) of grouped transcripts (RPL35a, C12orf50, BICC1, ZFP2, UBR5, HEG1, PLA2G16, SETD3 and ODF2). All data represented as mean \pm SEM for gene expression (N=7 for UBR5, PLA2G16, N=8 for all others) and CpG DNA methylation (N=8 for baseline, loading and unloading; N=7 for reloading).

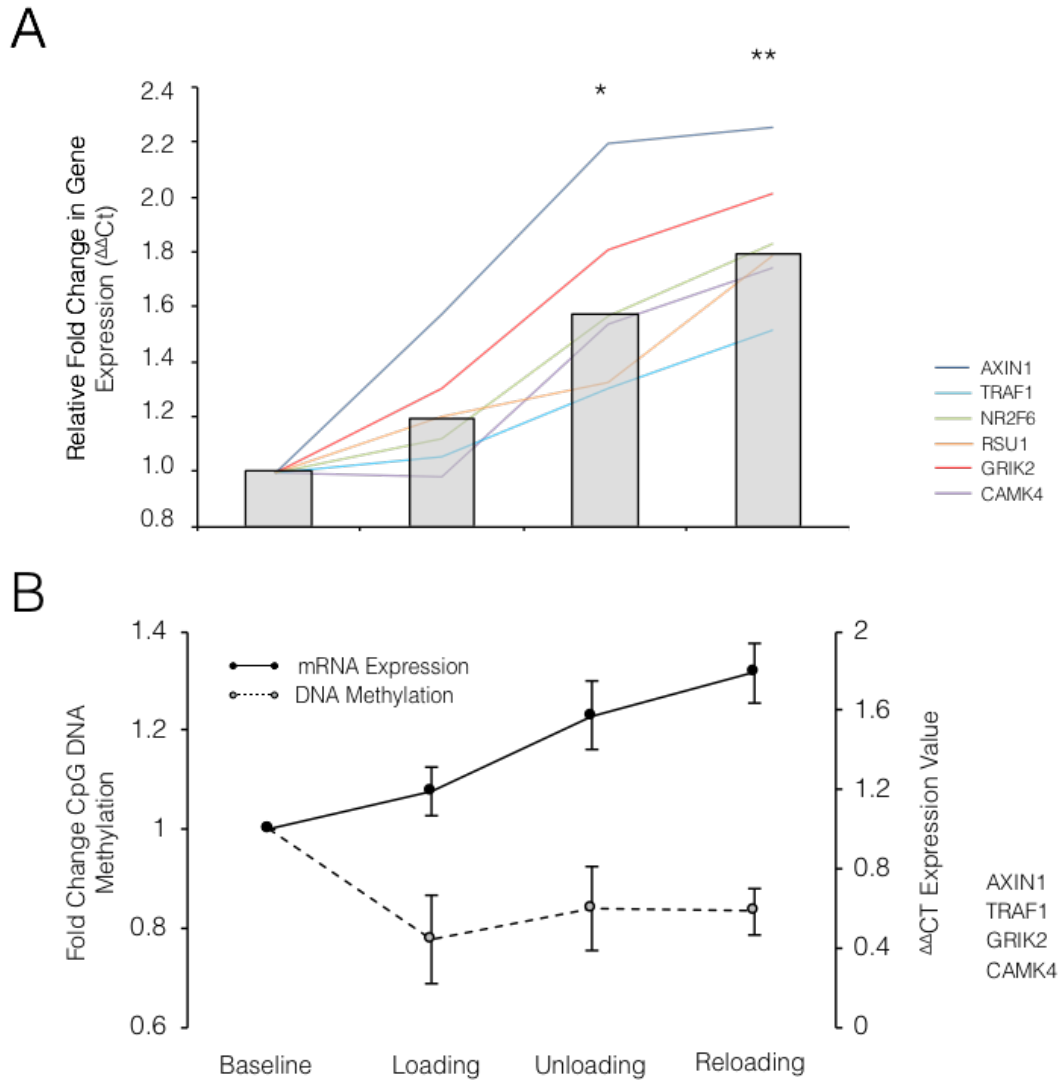


Figure 4.11. Relative changes in gene expression (A) and representative schematic of CpG DNA methylation and gene expression relationship (B) for genes in cluster B. A). Gene expression analysis of genes that portrayed an accumulative increase in expression after loading, unloading and reloading. With the largest increase in gene expression observed after reloading, compared to control. Culminating in significance in the unloading (compared to baseline, *) and reloading (compared to baseline, **). B) Representative schematic displaying a potential relationship between mean gene expression (solid black lines) and CpG DNA methylation (dashed black lines) of grouped transcripts (AXIN1, TRAF1, GRIK2 and CAMK4). All data represented as mean \pm SEM for gene expression (N=7 for AXIN1, GRIK2, N=8 for all others) and CpG DNA methylation (N=8 for baseline, loading and unloading; N=7 for reloading).

4.3.5 Identification of a number of novel genes at the expression level correlates with adaptations in skeletal muscle mass

To ascertain the importance and relationship of the identified transcripts, fold change in gene expression was plotted against percentage changes (to baseline) in leg lean mass. Interestingly, in the first cluster of genes identified above (RPL35a, C12orf50, BICC1, ZFP2, UBR5, HEG1, PLA2G16, SETD3 and ODF2), a significant correlation between gene expression and lean mass was observed for genes RPL35a, UBR5, SETD3, PLA2G16 and HEG1 (Figure 4.11 B). Following exposure to 7-wks of load induced hypertrophy, RPL35a gene expression displayed a non-significant increase compared to baseline (1.13 ± 0.23 ; Figure 4.11 Ai), that upon unloading returned back to the baseline levels (1.01 ± 0.21). Upon reloading, the expression of RPL35a increased to $1.7 (\pm 0.44$; Figure 4.11 Ai) compared to baseline ($P = 0.05$). This expression pattern across loading, unloading and reloading conditions corresponded to a significant correlation with percentage changes in skeletal muscle mass ($R = 0.6$, $P = 0.014$; Figure 4.11 Bi) with RPL35a accounting for 36% of the variation in muscle mass (assessed via DEXA) across experimental conditions. Both UBR5 and SETD3 displayed similar percentage accountability for the change in skeletal muscle mass across conditions. Indeed, UBR5 and SETD3 accounted for 33.64% and 32.49% of the variability in skeletal muscle mass, respectively, both portraying statistically significant correlation between their gene expression and the percentage change in lean leg mass (UBR5, $R = 0.58$, $P = 0.018$, Figure 4.11 Bii; SETD3, $R = 0.57$, $P = 0.013$, Figure 4.11 Biii, respectively). Additionally, UBR5 (1.65 ± 0.4 ; Figure 4.11 Aii) and SETD3 (1.16 ± 0.2 ; Figure 4.11 Aiii) both demonstrated non-significant increases in gene expression after 7-wks of loading ($P > 0.05$), with the expression of both genes, UBR5 (0.82 ± 0.27) and SETD3 (0.90 ± 0.15), returning to baseline levels

upon 7-wks of unloading (figures 4.11 Aii & Aiii, respectively). Furthermore, upon reloading UBR5 displayed its greatest increase in expression (1.84 ± 0.5 ; Figure 4.11 Aii), approaching significance when compared to baseline condition ($P = 0.07$), and a significant increase compared to unloading ($P = 0.035$). Whereas, SETD3 demonstrated a fold increase of $1.48 (\pm 0.25)$; Figure 4.11 Aiii), again, approaching significance compared to baseline ($P = 0.072$) and achieving significance compared to unloading ($P = 0.036$). PLA2G16 also demonstrated a significant correlation between its fold change in gene expression and the percentage change in skeletal muscle mass ($R = 0.55$; $P = 0.027$; Figure 4.11 Biv), with PLA2G16 accounting for 30.25% of the change in skeletal muscle. Interestingly, across conditions, PLA2G16 demonstrated the greatest significant changes in gene expression. Indeed, loading induced hypertrophy, PLA2G16 displayed a non-significant increase compared to baseline in expression (1.09 ± 0.17 ; Figure 4.11 Aiv), that upon unloading returned back to the baseline levels (1.04 ± 0.25). Importantly, upon reloading, the expression of PLA2G16 significantly increased (1.60 ± 0.18 ; Figure 4.11 Aiv) compared to baseline ($P = 0.026$) and unloading conditions ($P = 0.046$), as well as approaching a significant increase compared to the initial loading stimulus ($P = 0.067$ compared to load; Figure 4.11 Aiv). HEG 1 gene expression exhibited a significant correlation with skeletal muscle mass ($R = 0.53$, $P = 0.05$) with HEG 1 accounting for 28.09% of the changes in muscle mass. However, HEG1 did not demonstrate any significant fold changes in gene expression across the experimental conditions (Figure 4.11 Av). Furthermore, no significant correlation was observed for the other identified cluster of genes (AXIN1, GRIK2, CAMK4, TRAF1, NR2F6 and RSU1; $P > 0.05$). Collectively, these data suggest that RPL35a, UBR5, SETD3 and PLA2G16 all display a significantly enhanced gene expression upon reloading induced

hypertrophy. This suggests, that these genes have the ability to recall information generated from earlier load-induced hypertrophy, by displaying the largest fold increases in gene expression after reload-induced growth. Out of these identified 4 genes, UBR5 visually displayed temporal patterns in CpG methylation and gene expression of particular (Figure 4.12), after all experimental conditions.

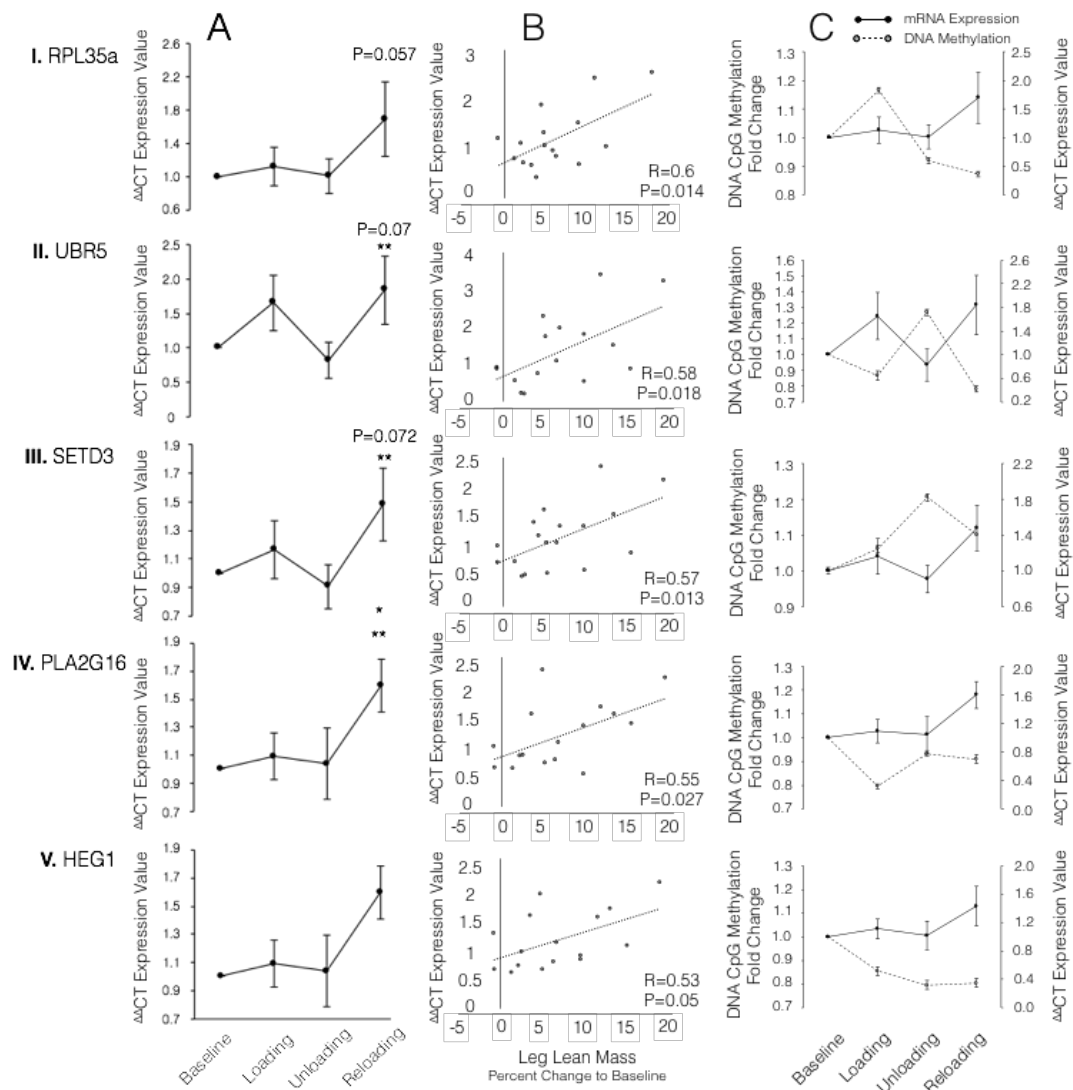


Figure 4.12. Relative fold changes in gene expression (A), correlation between gene expression and skeletal muscle mass across experimental conditions (B) and a schematic representation (C) of relationship between mRNA expression (solid black line) and CpG DNA methylation (dashed black line) for identified genes: RPL35a (I),

UBR5 (II), SETD3 (III), PLA2G16 (IV) and HEG1 (V). Statistical significance compared to baseline and unloading represented by* and** respectively. All significance taken as $P \leq 0.05$ unless otherwise stated on graph. All data presented as mean \pm SEM (n=7/8).

4.3.6 The E3 ubiquitin ligase, UBR5, has enhanced hypomethylation and largest increase in gene expression upon secondary exposure to load induced stimulus

The HECT E3 ubiquitin ligase gene, UBR5 (also known as EDD1; represented in its signalling pathway in Figure 4.14), for which the CpG identified is located on chromosome 8 (start 103424372) in the promoter region 546bp from the transcription start site, was identified as being within the top 100 most statistically differentially regulated CpG sites across all pair-wise conditions (load, unload and reload); but also the transcript that visually displayed the most distinctive temporal patterns in DNA methylation and gene expression (Figure 4.11), after every condition. Following the initial period of 7-weeks of load induced hypertrophy, there was a non-significant increase in UBR5 gene expression (1.65 ± 0.4) versus baseline, which was met with a concomitant (albeit non-significant) reduction in CpG DNA methylation (0.87 ± 0.03). Gene expression returned to baseline control levels after unloading (0.82 ± 0.27) demonstrated by a significant reduction vs. loading ($P = 0.05$) and non-significance versus baseline ($P = \text{N.S.}$; Figure 4.13). After the same unloading condition, we observed a significant increase in CpG DNA methylation compared to baseline (1.27 ± 0.02 ; $P = 0.013$; Figure 4.13). Importantly, upon reloading, UBR5 displayed its largest increase in transcript expression, significantly greater compared to unloading (1.84 ± 0.5 vs. 0.82 ± 0.27 , $P = 0.035$) and versus baseline levels (approaching significance, $P = 0.07$). Concomitantly, after the reloading condition,

we observed the largest statistically significant reduction in CpG DNA methylation (0.78 ± 0.02) compared to baseline ($P = 0.039$), and unloading ($P \leq 0.05$; figure 4.13 and 4.14).

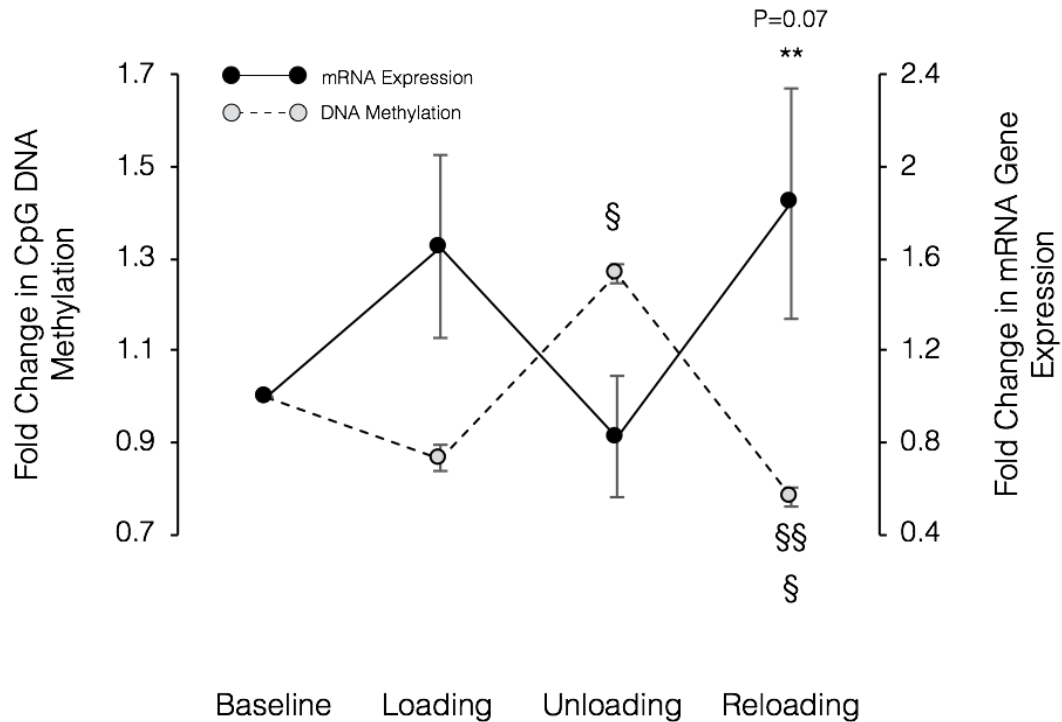


Figure 4.13. Schematic representation of changes in gene expression and CpG DNA methylation in the E3 ubiquitin ligase gene, UBR5. Representation demonstrates the inverse relationship between significant changes in gene expression (black lines; change compared to baseline, $P=0.07$; significant to unloading, **), and CpG DNA methylation (dashed lines; significantly different to baseline, §; to unloading, §§). All data presented as mean \pm SEM ($N=7/8$), with arbitrary units displayed in the y-axis.

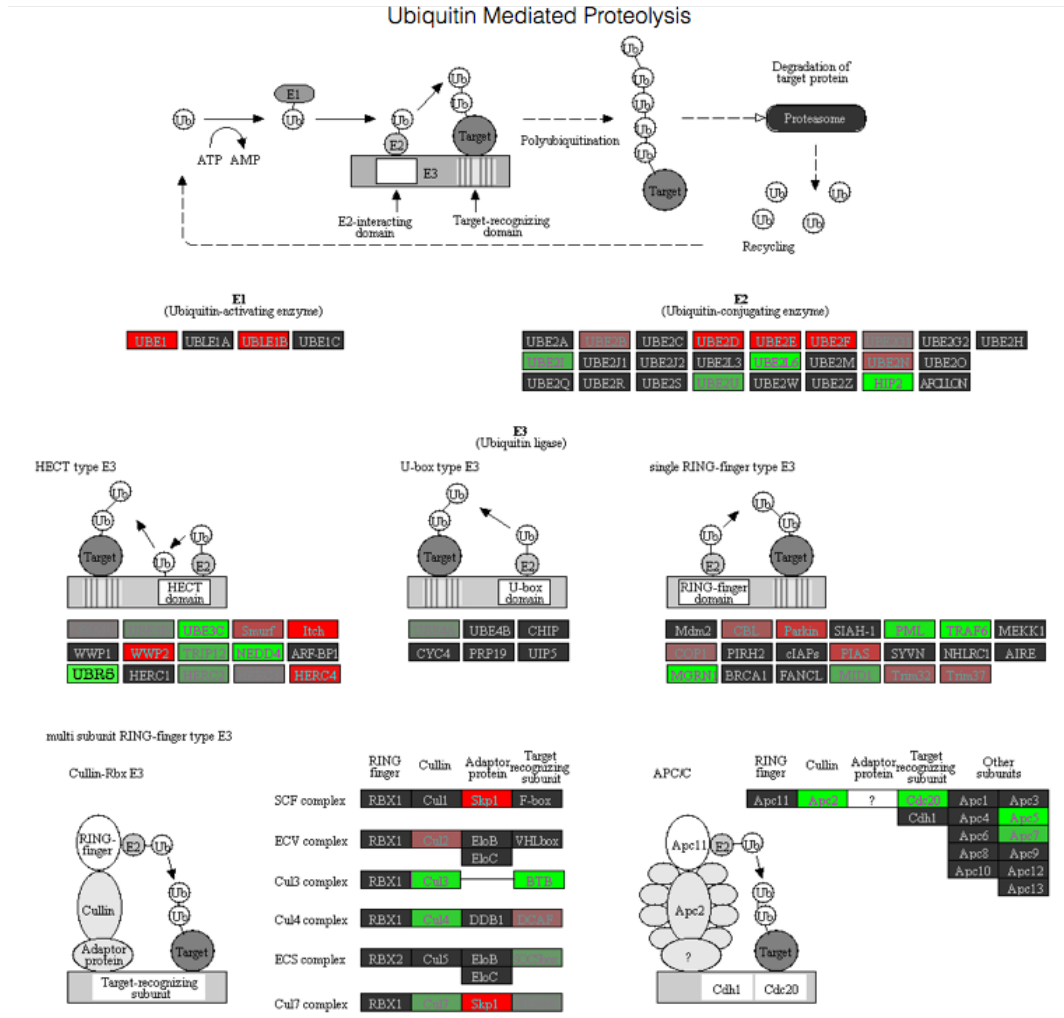


Figure 4.14. Representation and characterisation of the DNA methylation modifications that occurred along the ubiquitin mediated proteolysis signalling pathway across all conditions of loading, unloading and reloading compared to baseline (ANOVA). Signalling analysis performed on statistically differentially regulated CpG sites compared to baseline, with green indicating a hypomethylated fold change and red indicating a hypermethylated change, with strength of colour representing the intensity of fold change (Kanehisa and Goto, 2000, Kanehisa et al., 2017, Kanehisa et al., 2016). Importantly, the novel HECT-type E3 ubiquitin ligase, UBR5, displays a significantly hypomethylated state within this pathway following reloading.

4.4 Discussion of findings

We aimed to investigate the adaptive response of the human methylome following load induced skeletal muscle hypertrophy (loading and reloading) and the epigenetically induced retentive potential of human skeletal muscle in-vivo. As a continuation of the findings in chapter 3, we hypothesised that a chronic period of RE induced muscular hypertrophy would be met with large modifications in the human methylome. In this regard, our hypothesis was met as we identified large-scale remodelling of the human methylome following both the initial 7 weeks of loading (17,365 differentially regulated CpG sites) and a secondary period of loading (reloading; 27,165 CpG sites).

4.4.1 Secondary exposure to resistance load stimulus induces largest hypomethylated profile met with largest increase in skeletal muscle hypertrophy

We first confirmed that we were able to elicit an increase in lean mass of the lower limbs after 7 weeks loading, that returned back to baseline levels after 7 weeks unloading, with 7 weeks reloading evoking the largest increase in lean mass. Following DNA methylation analysis of over 850,000 CpG sites of the human methylome, we identified the largest frequency of hypomethylation (18,816 CpG sites) occurred after reloading where the largest lean mass occurred. Previous studies have suggested that hypermethylation of over 6,500 genes is retained, after a more acute stress of high fat intake (for 5 days) 8 weeks later despite removal of the high fat diet (Jacobsen et al., 2012), and hypermethylation occurs following early life inflammatory stress in muscle cells and is maintained for over 30 cellular divisions (Sharples et al., 2016a). The present study therefore also suggested hypomethylation was maintained during unloading (8,891 CpG sites) where muscle mass returned to

baseline having being subjected to an earlier period of load induced muscle growth (9,153 CpG sites), then upon reloading the frequency of hypomethylation was enhanced in association with the largest increases in lean mass. Furthermore, bioinformatic analysis of the PI3K/AKT signalling pathway across loading, unloading and reloading conditions, supports the findings of an enhanced hypomethylated state upon secondary exposure to resistance stimulus. Importantly, this pathway is identified as critical for cell proliferation/differentiation, muscle protein synthesis and therefore muscle hypertrophy (Schiaffino and Mammucari, 2011), and therefore, it is plausible that the enhanced hypomethylated state of the genes in this pathways would lead to enhanced gene expression and protein levels. However, further analysis is required to investigate the total protein or activity of these pathways in this model. Nonetheless, collectively, these results provide initial evidence for a maintenance of universal hypomethylation. The only other study to demonstrate a retention of prior hypertrophy in skeletal muscle was in rodents following earlier encounters with testosterone administration, where a preservation of myonuclei occurred even during testosterone withdrawal and a return of muscle to baseline levels (Bruusgaard et al., 2010), suggesting a memory phenomenon at the cellular level. However, these are the first studies to demonstrate that a memory occurs at the epigenetic level within skeletal muscle tissue. Collectively, these findings provide initial evidence for a potential maintenance/memory of universal hypomethylation.

4.4.2 Hypomethylation is maintained from earlier load induced hypertrophy even during unloading where muscle mass returns back towards baseline and is inversely associated with gene expression

Following the frequency analysis above, closer analysis of the top 500 most

significantly differentially modified CpG sites across all conditions, we identified two epigenetically modified clusters of interest (named Cluster A&B). Cluster B supported the frequency analysis above and demonstrated hypomethylation after load induced hypertrophy that was then maintained following unloading where muscle returned to baseline levels and this hypomethylation was then also maintained after reload induced hypertrophy. This maintenance of hypomethylation during unloading, suggested that the muscle retained biological information that occurred after an earlier period of load induced muscle hypertrophy, with this finding being an agreement with our original hypothesis. As reduced DNA methylation of genes generally leads to enhanced gene expression due to the removal of methylation allowing improved access of the transcriptional machinery and RNA polymerase that enable transcription, and also creating permissive euchromatin (Bogdanovic and Veenstra, 2009, Fuks et al., 2003, Lunyak et al., 2002, Rountree and Selker, 1997), this would be suggestive that the earlier period of hypertrophy leads to increased gene expression of this cluster of genes that is then retained during unloading to enable enhanced muscle growth in the later reloading period. To confirm this, in a separate analysis we identified the top 100 most significantly differentially modified CpG sites across all conditions and cross referenced these with the most frequently occurring CpG modifications in all pairwise comparisons of experimental conditions. From this we identified 48 genes that were frequently occurring in all pairwise comparisons and examined gene expression by rt-qRT-PCR. Interestingly, we identified two clusters of genes with distinct temporal expression after loading, unloading and reloading. One of the clusters included AXIN1, GRIK2, CAMK4, TRAF1, NR2F6 and RSU1. Importantly, the majority of these genes demonstrated a mirror/inverse relationship with DNA methylation of the CpG sites within the same genes. Where DNA

methylation reduced after loading and remained low into unloading and reloading, gene expression accumulated, demonstrating the highest expression after reloading where the largest increase in lean mass was also demonstrated. Overall, this suggested that these genes were increased after the earlier period of load induced hypertrophy, maintained during unloading due to methylation of these genes remaining low, and then upon exposure to a later period of reload induced hypertrophy, these genes were switched on to an even greater extent. Indeed, when analysing CpG methylation fold changes, significance was demonstrated across all pairwise comparisons for 4 out of 6 genes within this cluster (AXIN1, GRIK 2, CAMK4, TRAF1). Overall, this demonstrates that the methylation and collective responsiveness of these genes are important epigenetic regulators in allowing skeletal muscle to retain biological information.

Interestingly, AXIN1 is a component of the beta-catenin destruction complex, where in skeletal muscle cells AXIN1 has been shown to inhibit WNT/ β -catenin signalling and enable differentiation (Figeac and Zammit, 2015), where treatment with the canonical WNT ligand suppresses differentiation (Huraskin et al., 2016). Other studies suggested that AXIN2 not AXIN1 is increased after differentiation, however confirmed that the absence of AXIN1 reduced proliferation and myotube formation (Huraskin et al., 2016). Therefore, together with the present data, it suggests an important epigenetic regulation of AXIN1 involved in human skeletal muscle memory and hypertrophy, with this characteristic perhaps due to inhibition of WNT/ β -catenin signalling. GRIK2 (glutamate ionotropic receptor kainate type subunit 2, a.k.a. GluK2) belongs to the kainate family of glutamate receptors, which are composed of four subunits and function as ligand-activated ion channels (Han et al.,

2010). Although reportedly expressed in skeletal muscle, its role in muscle growth or cellular function has not been determined. CAMK4 is calcium/calmodulin-dependent protein kinase that via phosphorylation triggers the CaMKK-CaMK4 signalling cascade and activates several transcription factors, such as MEF2 (Blaeser et al., 2000). MEF2 has been previously associated with a switch to slow fibre types after exercise (Wu et al., 2000). While resistance exercise has been shown to preferentially increase the size of type II faster fibres, chronic innervation even at higher loads can lead to an overall slowing in phenotype (reviewed in (Fry, 2004) and therefore this epigenetically regulated gene, although not studied during hypertrophy maybe important in fibre type changes in the present study. However, it is unknown how DNA methylation affects the protein levels of CAMK4, and with its role in phosphorylation, would be important to ascertain in the future. Furthermore, fibre type properties were not analysed in the present study and require further investigation. TRAF1 is the TNF receptor-associated factor 1 and together with TRAF2 form the heterodimeric complex required for TNF- α activation of MAPKs, JNK and NF κ B (Pomerantz and Baltimore, 1999). In skeletal muscle, acute TNF exposure activates proliferation via activation of MAPKs such as ERK (Stewart et al., 2004, Sharples et al., 2010, Foulstone et al., 2004, Li, 2003, Al-Shanti et al., 2008, Serrano et al., 2008). Therefore, acutely elevated systemic TNF- α following damaging exercise such as resistance exercise correlates positively with satellite cell activation *in-vivo* after damaging exercise (Mackey et al., 2007, Mikkelsen et al., 2009, van de Vyver and Myburgh, 2012), yet chronic administration *in-vitro* inhibits differentiation, promotes myotube atrophy and evokes apoptosis (Meadows et al., 2000, Foulstone et al., 2001, Stewart et al., 2004, Al-Shanti et al., 2008, Saini et al., 2008, Sharples et al., 2010, Saini et al., 2012, Saini et al., 2010, Grohmann et al., 2005b, Foulstone et al., 2004,

Foulstone et al., 2003b, Grohmann et al., 2005a, Li et al., 2005, Li et al., 2003, Li and Reid, 2000, Jejurikar et al., 2006, Girven et al., 2016) and muscle wasting *in-vivo* (Li et al., 2005, Li and Reid, 2000). Indeed, exposure to early life TNF- α during an early proliferative age in mouse C2C12s results in maintenance of hypermethylation in the MyoD promoter after 30 divisions and an increased susceptibility to reduced differentiation and myotube atrophy when muscle cells encounter TNF- α in later proliferative life (Sharples et al., 2016a). This explorative *in-vitro* work suggests a role for DNA methylation in retention of earlier periods of high inflammation, where the association between RE and an increase in systemic circulation of TNF- α , as well as an increase at the protein level in muscle, is well documented (Mackey et al., 2007, Mikkelsen et al., 2009, van de Vyver and Myburgh, 2012). These data collectively suggest an interesting epigenetic role for TNF and TRAF1 in the epigenetic memory of earlier load induced muscle hypertrophy.

4.4.3 Identification of novel genes with the largest hypomethylated profile after secondary exposure to load stimulus, that are associated with enhanced gene expression

The second DNA methylation cluster determined in the top 500 differentially modified CpG sites across all conditions, identified a cluster of genes (named Cluster A) that was methylated at baseline and also became hypomethylated after loading (similar to Cluster B above), then, upon unloading, genes reverted back to a methylated state and after reloading switched back to hypomethylated. Therefore, while not demonstrating an epigenetic retention *per se*, if hypomethylation was further enhanced and was associated with enhanced gene expression in reloading versus loading would also support an epigenetic induced retention characteristic. Further

gene expression analysis identified a cluster of genes that demonstrated a mirror/inverse temporal pattern of gene expression versus their DNA methylation pattern. These genes included RPL35a, C12orf50, BICC1, ZFP2, UBR5, HEG1, PLA2G16, SETD3 and ODF2 and demonstrated hypomethylation of DNA after load induced growth and an increase in gene expression. Subsequently, then both DNA methylation and gene expression returned back to baseline levels (in opposite directions) and after reload induced muscle growth DNA was hypomethylated again with an associated increase in gene expression. Importantly, during reloading, gene expression was further enhanced versus loading, suggesting that an earlier period of load induced growth was enough to produce a larger gene expression when reload induced muscle growth was encountered later, again suggesting a skeletal muscle memory at both the epigenetic and transcript level. Statistical analysis identified a number of genes (RPL35a, UBR5, SETD3 and PLA2G16) as having significantly enhanced expression upon reloading. Importantly, these four genes, plus HEG1, displayed significant correlations between their gene expression and the percentage change in skeletal muscle mass, suggesting for the first time, an association for these four genes in regulating adult human load induced skeletal muscle growth. Interestingly, SET Domain Containing 3 (SETD3) is a H3K4/ H3K36 methyltransferase, is abundant in skeletal muscle, and has been shown to be recruited to the MyoG promoter, with MyoD, to promote its expression (Eom et al., 2011). Furthermore, overexpression of SETD3 in C2C12 murine myoblasts, evokes increases in MyoG, muscle creatine kinase, and Myf6 (or MRF4) gene expression. Inhibition via shRNA in myoblasts also impairs muscle cell differentiation (Eom et al., 2011), suggesting a role for SETD3 in regulating skeletal muscle regeneration. However, less is known regarding the role of PLA2G16 in skeletal muscle. PLA2G16

is a member of the superfamily of phospholipase A enzymes, whose predominant localization is in adipose tissue. PLA2G16 is known to regulate adipocyte lipolysis in an autocrine/paracrine manner, via interactions with prostaglandin and EP3 in a G-protein-mediated pathway (Jaworski et al., 2009). Indeed, ablation of PLA2G16 (referred to as *Adpla*), prevents obesity during periods of high fat feeding in mouse models, indicated via significantly less adipose tissue and triglyceride content, compared to relevant controls (Jaworski et al., 2009). However, to date no known research has elucidated the role of PLA2G16 in skeletal muscle and therefore, this requires future experimentation. Finally, HEG homology 1 (HEG1), initially reported as the *heart of glass* gene, is recognised for its role in regulating the zebrafish heart growth. HEG1 is a transmembrane receptor that has been reported to be fundamental in the development of both the heart and blood vessels (Gingras et al., 2012, Mably et al., 2003) (Kleaveland et al., 2009). However, a recent study reported a distinct role for HEG1 in regulating malignant cell growth (Tsuji et al., 2017). Tsuji et al. (2017) and colleagues reported that gene silencing of HEG1 in human MPM cell line, a cell lineage that develop mesothelioma tumours (Martarelli et al., 2006), significantly reduced the survival and proliferation of mesothelioma cells, suggesting a role for HEG1 in regulating cellular growth. However, no known research has examined the role of HEG1 in regulating adult skeletal muscle growth. In the present study, UBR5 visually displayed the most suggestive relationship between DNA hypomethylation and increased gene expression following loading and reloading conditions (Figure 4.13). With the largest increase in hypomethylation and gene expression after reloading where the largest increase in lean mass was also observed. UBR5 is a highly conserved homologue of the drosophila tumour suppressor hyperplastic discs (HYD), and in the mammalian genome refers to a protein that is a member of the E3 ubiquitin-

ligase family (Callaghan et al., 1998, Mansfield et al., 1994). E3 ubiquitin ligases play an integral role in the ubiquitin - proteasome pathway, providing the majority of substrate recognition for the attachment of ubiquitin molecules onto targeted proteins, preferentially modifying them for targeted autophagy/breakdown (Deshaies and Joazeiro, 2009, Buetow and Huang, 2016, Kuang et al., 2013). Indeed, extensive work has identified a distinct role of a number of E3 ubiquitin ligases such as MuRF1, MAFbx and MUSA1 in muscle atrophy (Baehr et al., 2011, Bodine, 2013, Bodine and Baehr, 2014, Bodine et al., 2001a, Fisher et al., 2017, Sartori et al., 2013). Furthermore, we have recently demonstrated that reduced DNA methylation and increased gene expression of MuRF1 and MAFbx are associated with disuse atrophy in rats following nerve silencing of the hind limbs via tetrodotoxin exposure (Fisher et al., 2017). A process that is reversed upon a return to habitual physical activity and a partial recovery of skeletal muscle mass (Fisher et al., 2017), suggesting a role for DNA methylation in regulating the transcript behaviour of a number of E3 ligases during periods of skeletal muscle atrophy and recovery. However, there have been no studies that the authors are aware of for UBR5 in skeletal muscle atrophy or growth. Given the role of ubiquitin ligases in skeletal muscle, counterintuitively, we report that the expression of the E3 ubiquitin ligase, UBR5, is increased during earlier periods of skeletal muscle hypertrophy and are even further enhanced in later reload induced muscle growth. We further report that the methylation profile of this E3 ubiquitin ligase portrays an inversed relationship with gene expression, supporting a role for DNA epigenetic modifications in regulating its expression, as previously suggested (Fisher et al., 2017). However, in support of its role in positively impacting on muscle, UBR5 has also been shown to promote smooth muscle differentiation through its ability to stabilize myocardin proteins (Hu et al., 2010). In confirmation,

silencing of UBR5 using siRNA in fibroblasts reduced myocardin-induced smooth muscle-specific gene expression and knockdown of UBR5 in smooth muscle cells also reduced smooth muscle-specific genes (Hu et al., 2010). Interestingly, when UBR5 was present myocardin protein degradation was reduced, resulting in increased total protein levels without changes in gene expression (Hu et al., 2010). While myocardin is only expressed in smooth and cardiac muscle, it is considered the master regulator of smooth muscle gene expression (Wang et al., 2003) and a known transcription factor that upregulates smooth muscle myosin heavy chains (MYHCs), actin and desmin. It therefore possesses a similar role to the myogenic regulatory factors Mrf5, MyoD and Myogenin in skeletal muscle. These genes enable the upregulation of slow and fast adult MYHCs, actin, desmin and titin and are expressed in a temporal fashion during early differentiation (Mrf5 and MyoD), during fusion (MyoG) and during myotube hypertrophy (adult MYHC's). Interestingly, it has previously been observed that myocardin-related transcription factors (MRTF) interact with the myogenic regulatory factor, MyoD, to activate skeletal muscle specific gene expression (Meadows et al., 2008), suggesting a cross-talk between muscle specific regulatory factors, enabling skeletal muscle adaptations (Meadows et al., 2008). However, reports suggest a complex bi-functional characteristic of myocardin as a transcriptional repressor of skeletal muscle differentiation in favour of smooth muscle differentiation (Long et al., 2007). Therefore, UBR5's expression throughout the time course of skeletal muscle cell differentiation and its role in myotube hypertrophy requires future attention. Finally, and confirming a role for UBR5 in growth, whole-exon sequencing identified strong gene amplifications of UBR5 in triple negative breast cancers that was confirmed via targeted mRNA and protein studies (Liao et al., 2017). Further, silencing of UBR5 via CRISPR/Cas9-

deletion in an *in-vivo* murine mammary carcinoma model of triple negative breast cancer reduced tumour growth and metastasis via reductions in blood vessel formation that was associated with tumour apoptosis, necrosis and growth arrest (Liao et al., 2017). Overall, this suggests that UBR5 is important in angiogenesis, blocking apoptosis and enabling growth in other cell types. Therefore, UBR5 may play a distinct role in skeletal muscle growth, however to determine this, future models of mammalian overexpression and knock-out of UBR5 are required to confirm its important function. Further work is needed to characterize UBR5, as well as other HECT-domain E3 ubiquitin ligase protein members identified in this work via signalling pathway analysis of the ubiquitin mediated proteolysis pathway, in the development of muscle growth to better understand its role in facilitating skeletal muscle hypertrophy.

4.5 Summary, Conclusion and Future Chapter Directions

This work furthers the claim that DNA methylation plays an important role in the regulation of human skeletal muscle during periods of muscle mass adaptation. These data also suggest that through retention of epigenetic modifications after earlier muscle hypertrophy, even following cessation of structured exercise interventions and muscle mass returning to baseline level, DNA methylation patterns are associated with a memory of earlier hypertrophy.

Here we identify an epigenetic retention of hypertrophy via retention of DNA methylation in this chapter and given the dynamic and sensitive nature of DNA methylation identified to muscle atrophy in chapter 3. We wished to ascertain how quickly and dynamically the human methylome was regulated after a single bout of

resistance exercise and therefore, and by comparing with data derived in chapter 4, if the epigenetics of target genes could be used as sensitive DNA methylation biomarkers that would be associated with enhanced gene expression and muscle hypertrophy when more chronically repeated. This would potentially identify genes that could be measured acutely in human skeletal muscle and predict future adaptation.

Chapter 5:

**DNA is Hypomethylated After a Single Bout of Exercise
That is Retained After Continuous Periods of Loading and
Reloading: Case for Sensitive DNA Methylation as a
Biomarker for Adaptation**

The work contained within this chapter has recently published:

Seaborne, R. A., Strauss, J., Cocks, M., Shepherd, S., O'Brien, T. D., van Someren, K. A., Bell, P. G., Murgatroyd, C., Morton, J. P., Stewart, C. E. & Sharples, A. P.

(2018). Human skeletal muscle possesses an epigenetic memory of hypertrophy. *Scientific Reports*, 8, 1898.

5.1 Introduction

After identifying that skeletal muscle retained hypomethylation signatures after earlier loading induced hypertrophy through to later reloading induced hypertrophy, it was next sought to ascertain how dynamic and transient DNA methylation of these identified genes was, after a single acute bout of resistance exercise (acute RE). It was aimed to identify methylation sensitive genes (to single acute resistance loading stimuli) that were still affected at the DNA methylation and gene expression levels after later chronic load and reload induced hypertrophy conditions. This would potentially identify important DNA methylation biomarkers after a single bout of exercise that would suggest if an individual was going to adapt advantageously (in terms of muscle size increases) to a more chronic exercise regime.

Following previous work suggesting that a single bout of exercise creates changes in promotor DNA methylation (Barres et al., 2012), and that short-term exposure to RE (3 sessions over 9 days) generates large modifications in the number of differentially methylated regions (DMRs) (Laker et al., 2017), we first hypothesized that the human methylome would undergo large-scale remodelling following a single bout of RE. We further hypothesised that modifications observed following acute RE may resemble those observed following continuous exposure to RE (i.e. chronic loading and reloading stimuli), and would therefore be acute DNA methylate biomarkers for skeletal muscle adaptation at later time points.

5.2 Methodology

5.2.1 Experimental design

All male subjects ($N = 8$; 27.6 ± 2.4 yr, 82.5 ± 6.0 kg, 178.1 ± 2.8 cm, means \pm SEM) enrolled in muscle memory study (chapter 4), performed an acute resistance exercise (acute RE) training session prior to loading, unloading and reloading. Skeletal muscle biopsies were obtained from the right vastus lateralis muscle, and down-stream analysis of RNA and DNA were compared to baseline biopsies (detailed in section 4.2). Genome wide DNA methylation analysis was performed via Illumina EPIC array to compare the human methylome immediately following single exposure to resistance load. Cross-comparison of differentially regulated CpG sites was performed with chapter 4 data to allude to CpG sites that were differentially regulated at both acute and chronic time-points. Follow-up gene expression was subsequently performed on identified transcripts of interest.

5.2.2 Acute exposure to resistance exercise stimulus

The resistance exercise protocol was performed in identical fashion to that previously explained (section 4.2.2), where a familiarization week was initially performed at no/low loads and a competency of lifting load assessment was performed. Three to four days following the familiarization week, subjects performed their first training session of their resistance exercise programme (section 4.2.2) that was used as the acute resistance exercise stimulus for analysis within this experiment. Exercise load was set and progression was applied in accordance with that previously described (section 4.2.2). Exercises for this acute resistance exercise session included over-head

squat, leg press, Nordic curls, leg press, leg extension and dumbbell weighted calf raises, with all exercises being performed bilaterally and in single or in a superset.

Total session load for the acute training stimulus was calculated as;

$$\text{Total Session Load (kg)} = (\text{No. of Reps} * \text{Exercise Load (kg)}) * \text{Sets}$$

This model evoked an average acute session load of 8223 kg (\pm 284).

5.2.3 Muscle biopsy preparation

Immediately following acute resistance exercise cessation (30mins), all participants gave a muscle biopsy sample from the vastus lateralis muscle of the right quadriceps, via conchotome method (section 2.5). Muscle samples were dissected on a sterile, gamma-irradiated petri-dish using sterile scalpels and immediately snap-frozen in liquid nitrogen before being stored at -80°C for RNA and DNA analysis.

5.2.4 Isolation of DNA and analysis for DNA methylome and CpG methylation

DNA was isolated and analysed for quality and quantity in methods as previously described (section 2.7). Isolation of acute muscle biopsies yielded an average quantity of 8.1 μg (\pm 0.03) and a 260/280 quality ratio of 1.86 (\pm 0.03). Five hundred ng of prepared DNA was bisulfite converted using EZ-96 DNA methylation kit (Zymo Research corp., CA, USA) (section 2.7 for details). Illumina MethylationEPIC BeadChip (Infinium MethylationEPIC BeadChip, Illumina, California, United States) and subsequently sent to The Genome Centre and Barts and The London School of Medicine and Dentistry where Illumina MethylationEPIC BeadChip (Infinium MethylationEPIC BeadChip, Illumina, California, United States) arrays were performed was then used to examine over 850,000 CpG sites of the human

methylome, and subsequent data files (.IDAT) were imported into Partek Genomic Suite for detection of differentially methylated CpG sites compared to baseline biopsy. Fold change in CpG specific DNA methylation and statistical significance was performed using Partek Genomic Suite V.6.6 software, where statistical significance was obtained following ANOVA (with Bonferroni correction) analysis. Unadjusted p-value significance ($P < 0.05$) was used to create a CpG site marker list of standardized beta-values. Unsupervised hierarchical clustering was performed and a dendrogram was constructed to represent differentially methylated CpG loci and statistical clustering of experimental samples, and schematically represented in heatmaps.

5.2.5 Isolation of RNA and down-stream rt-qRT-PCR

RNA was isolated, quantified, prepared and setup for rt-qRT-PCR as described in sections 2.6.1 – 2.6.3. All primer sequences for analysis of genes of interest are provided in table 5.1. Gene expression analysis was performed on at least $n = 7$ for all genes, unless otherwise stated. All relative gene expression was quantified using the comparative Ct ($\Delta\Delta\text{Ct}$) method (Schmittgen and Livak, 2008). Individual participants own baseline Ct values were used in $\Delta\Delta\text{Ct}$ equation as the calibrator using RPL13a as the reference gene. The average Ct value for the reference gene was consistent across all participants and experimental conditions $20.48 (\pm 0.53, \text{SDEV})$ with low variation of 2.60 %, and an average efficiency of 81.5 % ($\pm 8.9, \text{SD}$) with low percentage variation of 4.9 %.

Table 5.1. Gene primer sequences for acute human RE experiment. All primers used the same cycling conditions.

Gene	Accession No.		Primer Sequence	Primer Length	Prod. Length
FBXL17	NM_00116 3315.2	F –	TTGCACAGAGCAGCAAGTCT	20	76
		R –	TGTTCCACCGTCACTTCGTT	20	
STAG1	NM_00586 2.2	F –	GCATTTTTAGCAACTTCTACCAGC	24	115
		R –	AACTTGAATTGGCAGGGCA	20	
AFF3	NM_00228 5.2	F –	AACGGGAGCTGAGAGCTGAT	20	70
		R –	GGGTGTCGACTTCAAACCTGC	21	
STIM1	NM_00127 7962.1	F –	TGGACGATGATGCCAATGGT	20	110
		R –	CTCACCATGGAAGGTGCTGT	20	
AXIN1	NM_00350 2.3	F –	AAGGTCCCGAGGCTACTCAG	20	112
		R –	GCATTTCTTTTGCACGCCAC	20	
ODF2	NM_15343 6.1	F –	TTGTGGCGCACCCAGTGTA	20	71
		R –	GCACATTCACAGTGTCCCCT	20	
GRIK2	NM_00116 6247.1	F –	CACATACAGACCCGCTGGAA	20	110
		R –	GGTCTAAAATGGCACGGCTG	20	
NUB1	NM_00124 3351.1	F –	GGATCATGCGGCCACTCATA	20	102
		R –	AACCTGATGTTCTCGAGGCG	20	
KLHDC1	NM_17219 3.2	F –	TGGTGGGAGCAAAGATGACT	20	102
		R –	TCAAGGCATGACCTGAGTAGTG	22	
C11orf24	NM_00130 0913.1	F –	CCAGCTCACCCACAAGATGT	20	98
		R –	AGTTGCGTGGATCGTTGGAT	20	
ADSSL1	NM_15232 8.4	F –	ACTTCATCCAACCTGCACCGT	20	71
		R –	ACGTCACCTATGTTCTGCGG	20	
TRAF1	NM_00119 0947.1	F –	GGAAGCTGCGTGTGTTTGAG	20	97
		R –	AGCTGGCTCTGGTGGATAGA	20	
BICC1	NM_00108 0512.2	F –	GGCCATGTTACAAGCTGCTG	20	97
		R –	TGGCCAAGCAATCTGCGTAT	20	

5.2.6 Statistical analysis

All methylome and CpG DNA methylation statistical analysis was performed in Partek Genomic Suite via use of an in-software ANOVA. In SPSS (SPSS, version 23.0, SPSS Inc, Chicago, IL), a pairwise t-test was used to analyse gene expression following acute resistance exercise to baseline. For correlation analysis comparing

CpG DNA methylation values from acute, loading and reloading (data taken from chapter 4) of transcripts of interest, a Pearson correlation coefficient was calculated and significance ascertained via two-tailed test. Statistical values were considered significant at the level of $P \leq 0.05$. All data represented as mean \pm SEM unless otherwise stated.

5.3 Results

5.3.1 Acute resistance exercise rapidly remodels the human methylome and preferentially favours a hypomethylated response

We first sought to identify if CpG sites were globally hypo or hypermethylated across the human methylome following a single bout of RE. Herein, it was identified that 17,884 CpG sites of the human methylome display statistically differentially ($P < 0.05$) regulated DNA methylation profiles compared to baseline (Figure 5.1). Hierarchical clustering analysis confirmed a distinct differential regulation between all participant arrays (acute stimulus; Figure 5.1) compared to baseline. Further analysis revealed that exposure to acute RE preferentially modulates the human methylome into a greater hypomethylated state, where it was reported that 57.5% (10,284 sites) of the altered CpG sites were hypomethylated compared to 42.5% (7,600 sites) as hypermethylated.

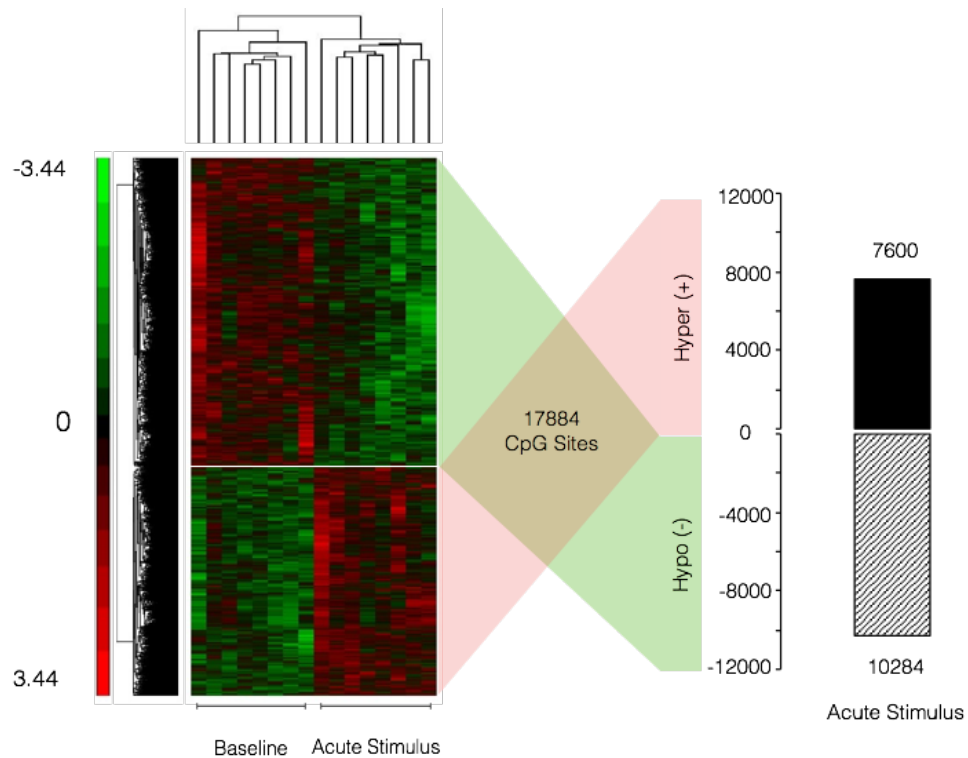


Figure 5.1. Response of the methylome after acute resistance exercise (acute RE) compared to baseline (N=8). Hierarchical cluster of significantly differentially regulated CpG sites (rows; $P \leq 0.05$) demonstrates an increased number of hypomethylated sites compared to hypermethylated. The heat-map colours correspond to standardised expression normalised β -values with green representing hypomethylation, red representing hypermethylation and unchanged sites are represented in black.

To further analyse the preferentially hypomethylated methylome following acute resistance exercise, GO terms were analysed to detect for most significantly enriched functional groups and frequency of hyper and hypomethylated CpG sites of these were compared. In agreement with the previous findings, the most statistically significantly enriched functional groups displayed a preferentially hypomethylated state following acute exposure to a resistance exercise stimulus. Indeed, the most significantly enriched functional group relating to biological processes was GO:0044699 encoding

for genes related to ‘single-organism processes’ that displayed 3491 CpG sites (56.8 %) as being hypomethylated compared to 2609 (43.2 %) as being hypermethylated, compared to baseline control (Figure 5.2 A). A similar pattern was observed for the most significantly enriched groups for molecular function and cellular component. Where the terms, GO:0005488 (binding; Figure 5.2 B) and GO:0044422 (organelle part; Figure 5.2 C), displayed 56.6 % (5267 CpG sites) and 57.2 % (3491 CpG sites) of their differentially regulated CpG sites as being hypomethylated. Collectively suggesting that, acutely, following exposure to a single resistance exercise stimulus a large adaptive response of the human methylome is exhibited in previously untrained subjects, that preferentially favours a greater hypomethylated response.

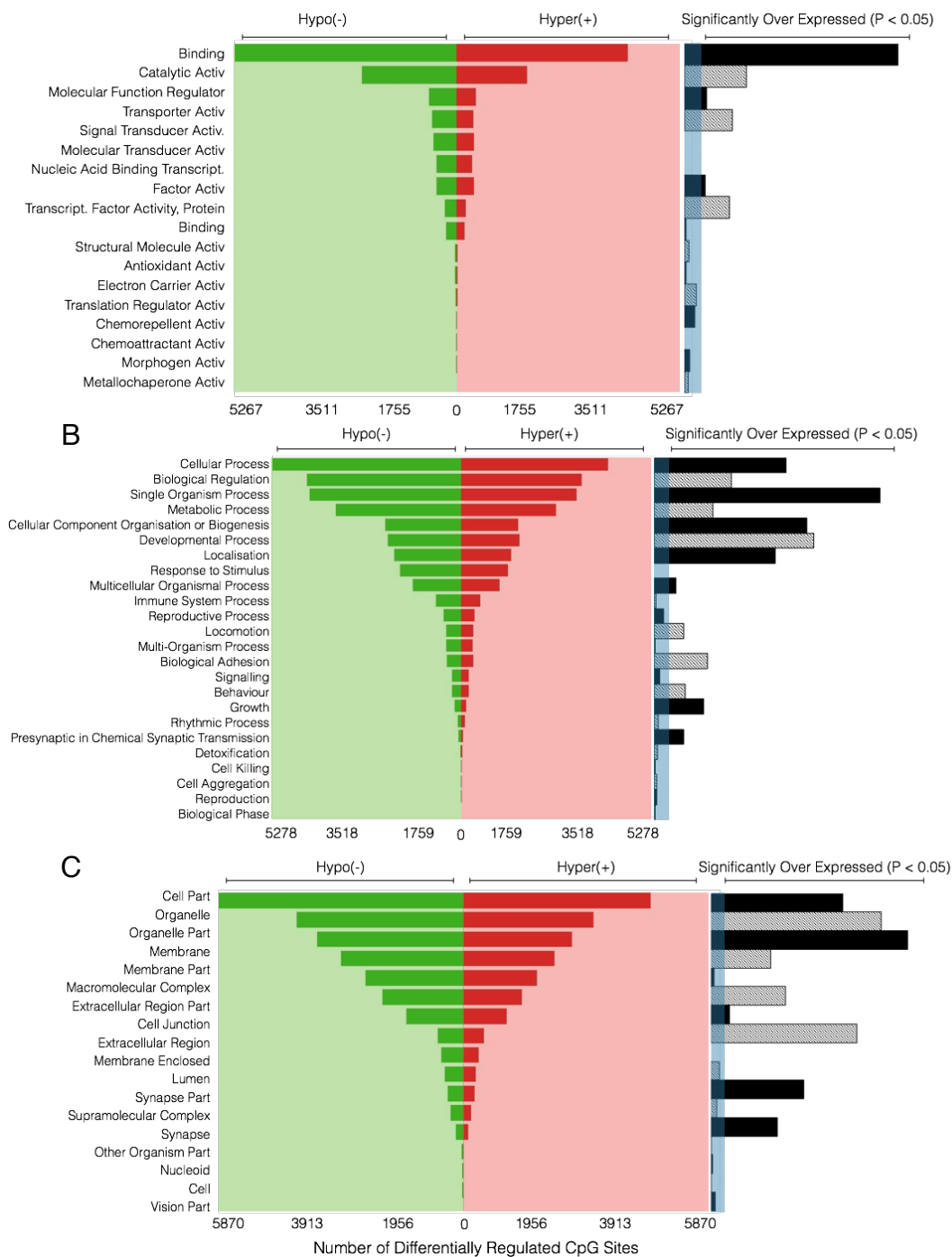


Figure 5.2. Gene ontology analysis generated from Infinium MethylationEPIC BeadChip array of 850,000 CpG sites of the human methylome. Analysis confirms an enhanced hypomethylated profile immediately following exposure to a single bout of resistance exercise training in previously untrained subjects. Forest plot schematics represent the number of CpG sites hypo- or hyper-methylated in reloading versus control conditions across various functional groups in A) molecular function, B) biological processes and C) cellular components. A fold enrichment > 3 (as indicated

via shaded blue region) represents statistically over expressed KEGG pathways, $FDR < 0.05$.

5.3.2 Cross-comparison analysis reveals 27 differentially regulated CpG sites following acute, loading and reloading resistance exercise

In order to identify if methylation sensitive genes (to single acute resistance loading stimuli) were still affected at the DNA methylation and gene expression levels after later chronic load and reload induced hypertrophy conditions, we undertook comparative DNA methylation analysis of acute RE conditions compared to chronic loading and reloading from chapter 4. Analysis of the top 100 differentially regulated CpG sites from chapter 4 and the significantly differentially regulated CpG sites from acute RE methylome analysis, revealed 27 CpG sites that were commonly differentially regulated (Figure 5.3) across all conditions. Location analysis of the identified 27 CpG sites reported that 9 CpG sites lie within regions that did not code for known genes. Of the 18 remaining CpG sites, 88% of sites were located within promotor or intron regions of the relevant gene transcript (Figure 5.3).

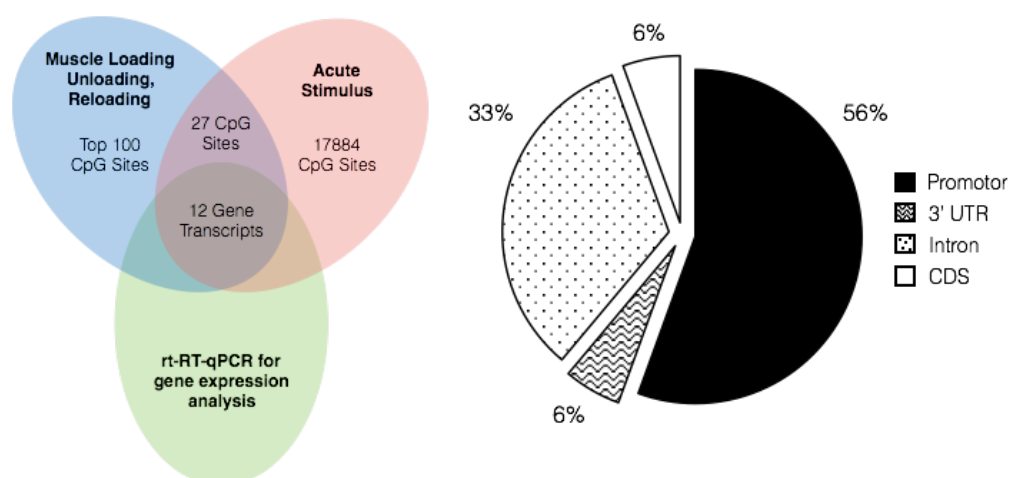


Figure 5.3. Cross-comparison analysis of acute RE methylome data and methylome data derived following chronic loading and reloading. Venn diagram depicts the number of CpG sites analysed for gene expression across acute, RE 7 weeks loading and 7 weeks reloading, respectively. Pie chart details the location of the top 18 gene transcripts identified in cross-comparison analysis of the human methylome. Coding DNA sequence (CDS).

5.3.3 Altered CpG DNA methylation profiles following acute resistance exercise are retained after loading and reloading

The fold change in CpG DNA methylation of the remaining 18 sites (table 5.2) displayed virtually identical regulation across conditions of acute RE, loading (7 weeks' resistance loading) and reloading (7 weeks loading, unloading and reloading, respectively; Figure 5.4). The majority of genes demonstrating a hypomethylated profile, demonstrated on Figure 5.4, (genes with a fold change less than 0), confirming earlier analysis that acute resistance exercise evokes a largely hypomethylated profile. Correlation analysis of CpG DNA methylation fold change confirmed these findings with acute RE compared to loading and reloading conditions reporting a strong positive and significant relationship ($R = 0.94$, $P < 0.0001$; Figure 5.5). Collectively suggesting that even after a single bout of acute resistance exercise, DNA methylation of the identified CpG sites remained hypomethylated even through loading, and reloading. Suggesting that these DNA methylation sites were extremely sensitive to acute exercise induced hypomethylation and associated with increases in lean muscle mass in loading and reloading conditions (identified in chapter 4).

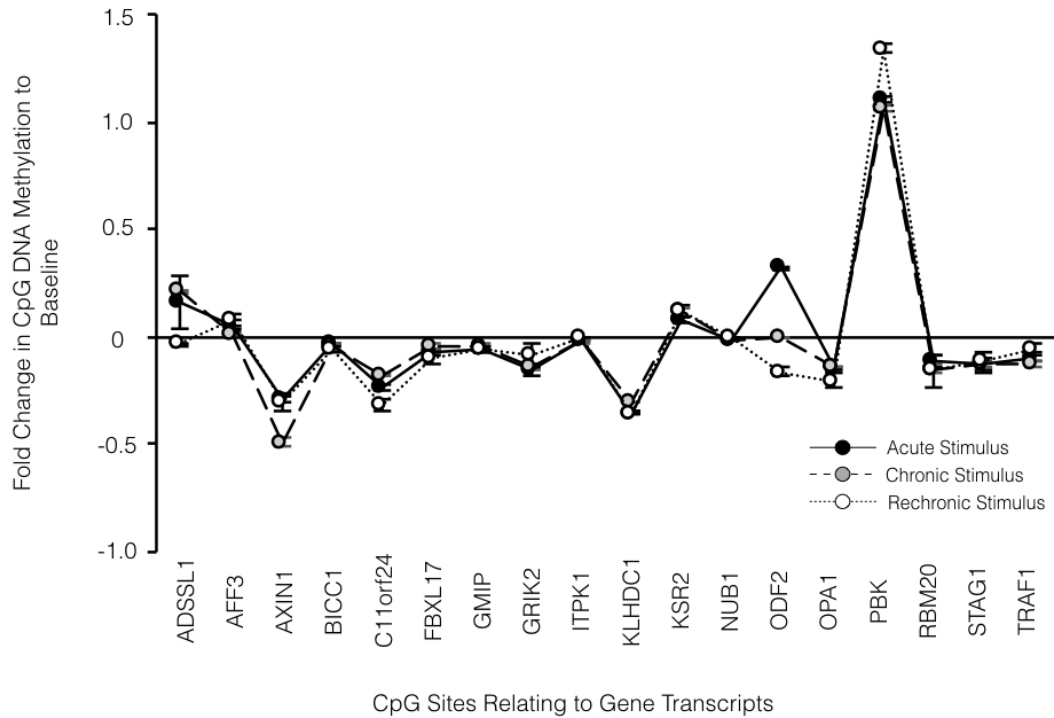


Figure 5.4. Modifications of DNA methylation following acute RE are maintained following loading and reloading. Temporal pattern of fold changes in CpG DNA methylation of the identified overlapping CpG sites that mapped to relevant gene transcripts as generated via cross-comparison analysis, figure 5.3. All data represented as mean \pm SEM (N=7/8).

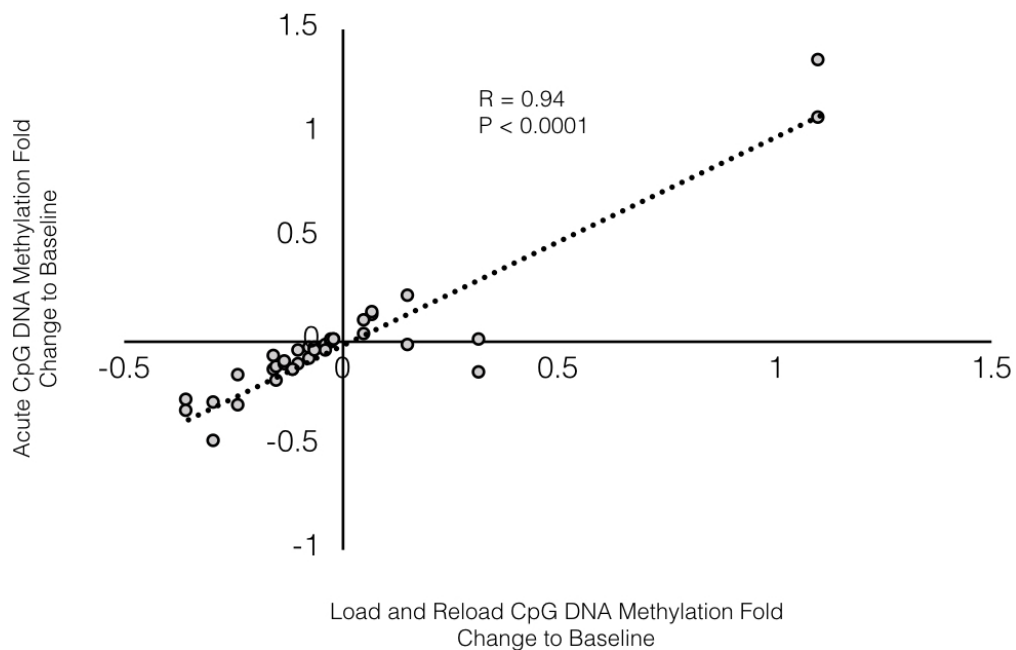


Figure 5.5. Analysis of CpG DNA methylation changes following acute RE correlated with changes in CpG DNA methylation evoked following loading and reloading,

respectively. DNA methylation reported as mean (N=7/8) methylation change to baseline, of identified transcripts generated via cross-comparison analysis, figure 5.3.

Table 5.2. Genomic location of 18 CpG sites that overlap in comparisons between acute RE, chronic load and chronic reload methylome data sets.

Gene	CpG ID	Chromosome Site	Transcript ID
ADSSL1	cg10797850	14: 105213611	NM_152328
AFF3	cg07349094	2: 100759014	NM_002285
AXIN1	cg04808813	16: 343299	NM_003502
BICC1	cg22557725	10: 60368369	NM_001080512
C11orf24	cg14870456	11: 68039143	NM_001300913
FBXL17	cg05426509	5: 107382801	NM_001163315
GMIP	cg16175206	19: 19744627	NM_001288998
GRIK2	cg14974622	6: 101886381	NM_001166247
ITPK1	cg09257735	14: 93581049	NM_001142594
KLHDC1	cg04707327	14: 50159532	NM_172193
KSR2	cg16953186	12: 118112000	NM_173598
NUB1	cg17067889	7: 151038703	NM_001243351
ODF2	cg21792562	9: 131218455	NM_153436
OPA1	cg01640444	3: 193311744	NM_015560
PBK	cg21734487	8: 27695307	NM_001278945
RBM20	cg18594033	10: 112524504	NM_001134363
STAG1	cg09094119	3: 136469223	NM_005862
TRAF1	cg20015583	9: 123681613	NM_001190945

5.3.4 Dynamic and sensitive changes in DNA methylation after acute RE, precede observed changes in gene expression after loading and reloading

In order to elucidate whether changes in CpG DNA methylation of the candidate gene list was met with altered expression of these genes, a sub-set of transcripts were analysed for fold-change following acute resistance exercise and compared with loading and reloading. Firstly, in this analysis, it was identified that significant changes in CpG DNA methylation following acute resistance exercise stimulus was not met with significant changes in gene mRNA expression. Indeed, all 12 CpG sites associated with genes ADSSL1, AFF3, AXIN1, BICC1, C11orf24, FBXL17, GRIK2, KLHDC1, NUB1, ODF2, STAG1 and TRAF1 all displayed significant alterations in

fold change of CpG DNA methylation compared to baseline (Figure 5.6 B; $P < 0.05$). This was met with no significant change in these gene transcript expression levels (Figure 5.6 A; $P > 0.05$), following acute load stimulus. However, upon continued loading (loading and reloading), significant changes in CpG DNA methylation were met with significant changes in a number of gene transcripts. Adenylosuccinate synthase like 1 (ADSSL1) displayed a significant increase in CpG DNA methylation at following acute stimulus (1.15 ± 0.16 ; $P = 0.009$) that was retained after 7-weeks of loading (1.21 ± 0.002 ; $P = 0.001$; Figure 5.6 B), compared to baseline. However, at the expression level, acute resistance exercise stimulus failed to evoke a significant change in mRNA expression ($P > 0.05$; Figure 5.6 A). However, upon continuous exposure to resistance load (loading), gene expression showed an inverse relationship with DNA methylation, displaying a reduction in expression compared to baseline control (0.75 ± 0.14 ; $P = 0.013$). Comparably, chromosome 11 open reading frame 24 (C11orf24) displayed a similar inverse, time-dependent relationship between DNA methylation and gene expression. Indeed, following acute resistance exercise stimulus, C11orf24 displayed a significant reduction in CpG DNA methylation (0.77 ± 0.01 ; $P = 0.022$) that was not met with a significant change in mRNA expression levels (1.16 ± 0.026 ; $P > 0.05$; Figure 5.6 A) compared to baseline. However, upon repeated exposure, relative CpG DNA methylation remained significantly reduced (0.82 ± 0.01 ; $P = 0.018$; Figure 5.6 B), compared to baseline, and was met with an increase in mRNA expression that approached significance, at the same condition (loading 1.62 ± 0.35 ; P value = 0.08; Figure 5.6 B and A, respectively).

More interestingly, both cohesin subunit SA-1 (STAG1) and TNF receptor associated factor 1 (TRAF1) display significant reductions in CpG-specific DNA methylation

following acute exposure to resistance stimulus (0.87 ± 0.03 , $P = 0.008$, and 0.91 ± 0.02 , $P = 0.003$, respectively; Figure 5.7) that remains significantly low following repeated chronic exposure to resistance load stimulus. Indeed, during loading, both genes maintained this significant reduction in CpG DNA methylation (0.87 ± 0.011 ; $P = 0.0002$ and 0.88 ± 0.01 , $P = 0.0004$; Figure 5.7) in STAG1 and TRAF1, respectively, and the subsequent re-encounter with chronic resistance exercise (reloading) continued this hypomethylated state (0.88 ± 0.04 ; $P = 0.0007$ and 0.95 ± 0.03 ; $P = 0.0003$, respectively; Figure 5.7). Importantly, the observed significant reduction in DNA methylation following acute exposure to resistance stimulus produces no significant change ($P > 0.05$ for both transcripts) in STAG1 gene expression (1.05 ± 0.25) and TRAF1 (1.06 ± 0.14), following the same acute resistance exercise stimulus (Figure 5.7). However, in the reloading condition, gene expression in both STAG1 (1.93 ± 0.64 ; $P = 0.007$) and TRAF1 (1.48 ± 0.15 ; $P = 0.007$; Figure 5.7) was significantly increased, where previously reported is a significant reduction in DNA methylation, suggesting an inverse relationship between expression and methylation. Collectively, these data suggest that changes in CpG specific DNA methylation of transcripts ADSSL1, C11orf24, STAG1 and TRAF1 precede any functional changes in gene expression levels upon exposure to resistance exercise stimulus. A similar, but less significant, relationship is observed between changes in CpG methylation following acute RE, and a delayed functional change in gene expression following exposure to reloading for genes GRIK2 and BICC1. Indeed, GRIK2 displayed no significant change in gene expression following acute RE (1.30 ± 0.29) despite displaying a significant reduction ($P = 0.002$) in CpG DNA methylation (0.85 ± 0.05) at the same time point. This hypomethylated profile is maintained through to reloading (0.91 ± 0.04 ; $P = 0.005$), where it is met with the largest increase in GRIK2

gene expression compared to baseline control (1.93 ± 0.5 ; Figure 5.7). Similarly, BICC1 shows a significantly hypomethylated CpG DNA methylation profile following acute RE (0.97 ± 0.002 ; $P = 0.002$) and loading and reloading (0.96 ± 0.004 , $P = 0.002$; 0.94 ± 0.01 , $P < 0.0001$), where after acute RE gene expression does not significantly change (1.17 ± 0.37), but shows its largest increase following continuous reloading exposure (1.58 ± 0.63 ; Figure 5.7).

Collectively, these data suggest that acute RE rapidly modifies CpG DNA methylation of these identified transcripts, even after 30 minutes' post exercise. However, 30 minutes' post exercise is insufficient to induce functional changes in gene expression. Importantly however, genes that were hypomethylated after a single bout of acute resistance exercise were maintained as hypomethylated during loading (ADSSL1 and C11orf24) and reloading (STAG1, TRAF1, BICC1 and GRIK2) and demonstrated an enhanced gene expression after later reloading where the largest increase in lean mass was observed.

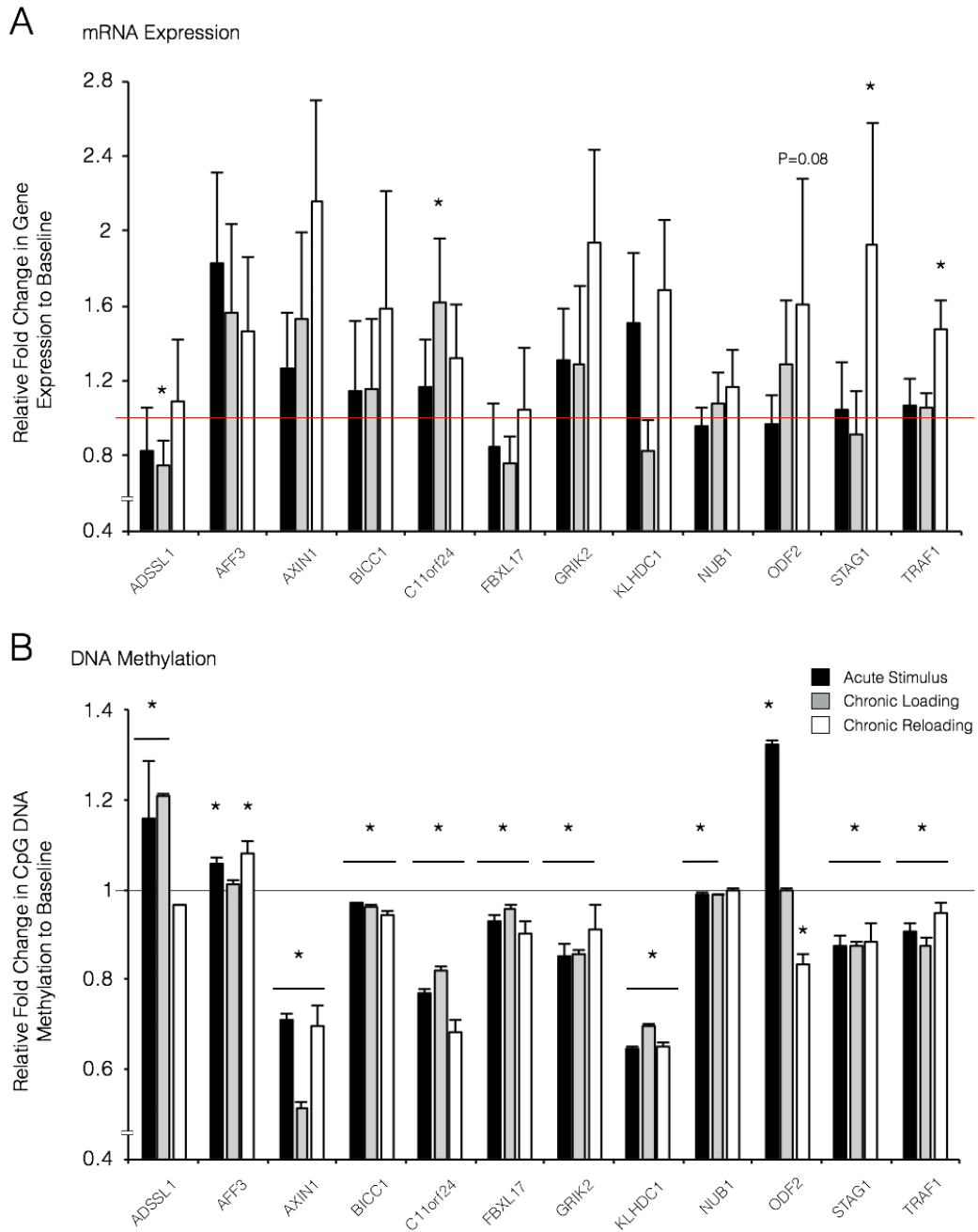


Figure 5.6. Relative fold changes in; **A**) gene expression, and, **B**) CpG DNA methylation in all 12 gene transcripts identified from comparison of methylome data from acute RE vs. 7 weeks loading and reloading analysis. Data represented as means \pm SEM (N=7/8), with significance compared to baseline (red line) indicated by *.

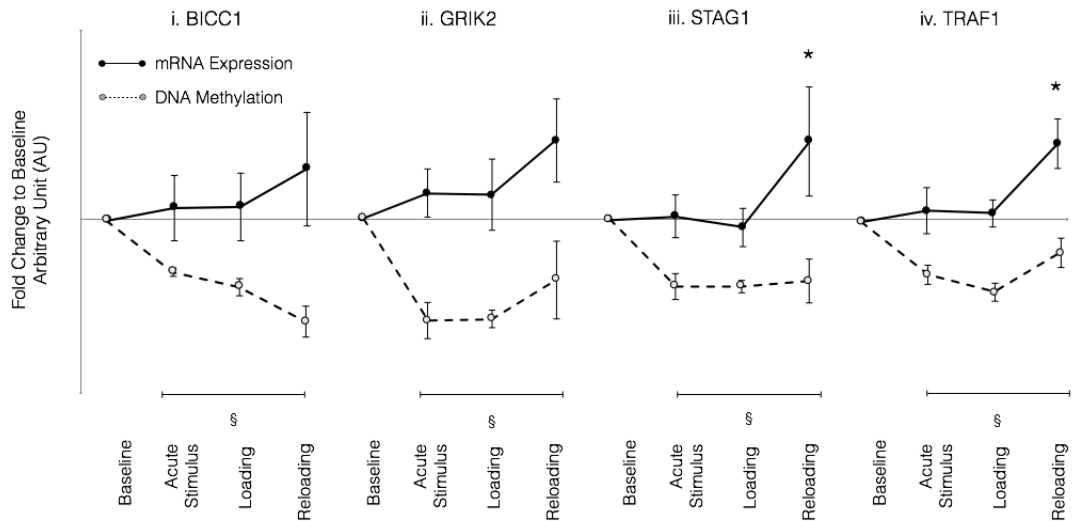


Figure 5.7. Representative schematic identifying early epigenetically modified (DNA methylation, dashed black line) genes after acute RE, that are associated with enhanced gene expression (solid black lines) following reloading. Significance indicated in gene expression (*) and in CpG DNA methylation (§) when compared to baseline.

5.4 Discussion of Findings

5.4.1 Summary

The aim of this chapter was to, for the first time, identify the modifications that occur in the human methylome following exposure to an acute bout of RE, in previously untrained subjects. Further, it was sought to elucidate whether these epigenetic modifications were similar in profile, and in association to changes in gene expression, to those observed following chronic periods of loading and reloading, respectively. In support of the first hypothesis, it was observed that upon exposure to a single bout of resistance exercise, the human methylome is rapidly remodelled to favour a preferential hypomethylated state, a known permissive state for enhanced gene expression (Long et al., 2017). In further support of our hypothesis, and via

comparative bioinformatic analysis, we identify a very strong and significant correlation between epigenetic modifications that occur following acute RE and those associated with chronic loading and reloading time points. Interestingly, the work presented in this chapter also suggested that DNA methylation modifications may precede functional changes in gene expression. Indeed, a number of transcripts displayed significant changes in CpG methylation without significant changes in gene expression following acute RE. However, upon chronic loading and/or reloading exposures, we identified genes GRIK2, TRAF1 BICC1 and STAG1 were hypomethylated after a single bout of acute resistance exercise that were maintained as hypomethylated and had enhanced gene expression after later reloading. Suggesting that these are epigenetically sensitive genes after a single bout of resistance exercise and associated with enhanced gene expression and muscle hypertrophy 22 weeks later.

5.4.2 The human methylome is rapidly altered following single exposure to RE to a preferentially hypomethylated state

Until relatively recently, aberrances in DNA methylation via environmental influences were thought unlikely to occur, due to DNA methylation being believed to be mitotically stable (Reik et al., 2001). However, in direct contrast to this hypothesis, the work presented in this chapter demonstrates that immediately following a single stimulus of resistance exercise, mature human skeletal muscle is rapidly and grossly altered at the epigenetic level. Furthermore, it is also reported that not only is the human methylome highly differentially regulated, it also favours a hypomethylated state that may suggest a transcriptionally permissive status (Long et al., 2017).

Recently published work utilising a combination of high fat feeding and resistance exercise to examine the potential benefits of resistance exercise during high fat feeding periods, Laker et al. (2017) identified that high fat diet alone induced a significant hypermethylation effect, with the concomitant exposure to resistance exercise resulting in a shift towards a preferential hypomethylated state. However, the authors did not examine the beneficial effects of resistance exercise alone, and thus, the findings here are not directly translational given that large epigenetic perturbations have been shown previously following short-term high fat feeding (Jacobsen et al., 2012). Furthermore, the authors acknowledged that muscle samples obtained in their experiment were obtained 48-hrs post the final resistance exercise stimulus, and thus transcriptional behaviour may be low with the authors suggesting that analysis immediately following a resistance exercise stimulus is warranted, given the more dynamic period of transcriptional activity (Barres and Zierath, 2016, Laker et al., 2017). In this regard, the data presented here offers novel findings to support the work presented by Laker et al. (2017), reporting for the first time, the enhanced hypomethylated response of the human methylome immediately following acute resistance exercise alone.

In further support of these findings, a series of intricate studies by Barres et al. (2012) who reported, via use of a number of mammalian exercise models, a significant hypomethylation response of targeted transcripts in the prevailing period following aerobic exercise stimulus. In the first experiment, the authors report that exposure to a single bout of aerobic exercise (80 % VO_2 max maintained until 1674 kJ was expended) induced global hypomethylation of the human genome, that, upon follow up targeted analysis, reported significant reductions in PGC-1 α , TFAM, PDK4 and

PPAR δ immediately or 3-h post exercise cessation (Barres et al., 2012). In the second experiment by the same authors, 60-mins of ex-vivo contraction in an isolated soleus muscle of rodents, produced a hypomethylated response of PGC-1a, PPAR δ , MEF2a, MyoD1 and PDK4 as rapidly as 45-mins post exercise cessation (Barres et al., 2012). Finally, in the last experiment, the authors incubated rodent L6 myotubes in growth media with or without 5mM of supplemented caffeine. Following a time course differentiation experiment, it was observed that expansion in the presence of caffeine induced hypomethylation in genes PGC-1a, TFAM, MEF2a, citrate synthase and PDK4, as rapidly as 60 mins post differentiation (Barres et al., 2012).

Collectively, the novel data demonstrated in this chapter, suggests that acute RE experienced by mature mammalian skeletal muscle evokes large adaptations in DNA methylation, that prefer a hypomethylated response, and thus would preferentially favour a permissive transcriptional genome.

5.4.3 DNA methylation profiles following acute RE are identical to those observed following loading and reloading: highlighting potential DNA methylation biomarkers for later adaptation

Following identification that the human methylome is readily remodelled following acute RE, it was identified that the degree to which these modifications occurred were similar in nature to those observed following 7-weeks loading (Chapter 4). Indeed, the number of statistically differentially regulated CpG sites following acute RE (17,884) was almost identical in number to those modified following 7-weeks loading (17,365). It was therefore sought to investigate how closely regulated these epigenetic modifications between acute and chronic loading (acute RE vs 7-weeks loading and

reloading) were. In support of our hypothesis, it was identified that modifications of a sub-set of differentially regulated CpG sites following acute RE, are almost identical in directional change (i.e. hypo or hypermethylated) to those observed following chronic loading and reloading. Indeed, via comparative bioinformatic analysis of these data sets, it was observed that 26 % of analysed CpG sites following acute RE, portray significantly differentially regulated profiles following loading and reloading (Figure 5.4). More so, a significant correlation is observed ($R = 0.94$, $P < 0.0001$) for the hypo/hypermethylated profile of these CpG sites, when compared to loading and reloading modifications (Figure 5.5). To the authors knowledge, these are the first data to study the acute (acute RE) and long-term (loading and reloading) effects of exposure to same exercise stimulus on DNA methylation modifications in humans.

Through qPCR analysis, we sought to elucidate how functionality relevant the epigenetic modifications following acute RE were, and whether these regulatory alterations were indistinguishable to those observed following more chronic RE periods (loading and reloading). Most interestingly here, it was found that, despite significant changes in CpG DNA methylation following acute RE, there was no observed significant changes in gene expression for any of the analysed transcripts (see Figure 5.6 A and B), collectively suggesting, that DNA methylation modifications may precede detectable changes in gene expression. In further support of this theory, it was observed that where acute RE modifications in CpG DNA methylation orchestrated no significant change in gene expression, but where methylation modifications were retained following continuous loading or reloading, changes in gene expression were observed. Indeed, in genes ADSSL1 and C11orf24, there was a significant and retained reduction in CpG DNA methylation following

acute RE through 7-weeks loading. At the same time points, acute RE produced no significant changes in gene expression, however, upon 7-weeks loading a significant (ADSSL1) and trend for significance (C11orf24) was observed in these transcripts in an inverse manner to changes in methylation (Figure 5.6 A and B). Finally, we identified genes BICC1, STAG1, GRIK2 and TRAF1 that were hypomethylated after a single bout of acute RE that were maintained as hypomethylated during loading and reloading and demonstrated an enhanced gene expression after later reloading (Figure 5.7). The identification of these genes, and their relation to skeletal muscle hypertrophy, is relatively novel. Indeed, BICC1 is an RNA binding protein that has an undermined role in adult skeletal muscle. It has been identified as differentially expressed during prenatal muscle development between two different pig breeds (Murani et al., 2007). RNA binding proteins in general are important in post-transcriptional modifications, suggesting that perhaps reduced DNA methylation and increased gene expression may indicate an increase in post-transcriptional modification after reloading, however this requires further investigation to confirm. STAG1 is fundamental in cell division and part of the cohesin complex, which is required for the cohesion of sister chromatids after DNA replication (Kong et al., 2014). However, to the authors' knowledge there is no specific role for STAG1 identified in adult skeletal muscle hypertrophy. Similarly, GRIK2's role in skeletal muscle is not well defined. On the contrary however, TRAF1 has been widely implicated in skeletal muscle proliferation and differentiation. Indeed, TRAF1 is the TNF receptor-associated factor 1 and together with TRAF2, form the heterodimeric complex required for TNF- α activation of MAPKs, JNK and NF κ B (Pomerantz and Baltimore, 1999). The role of TNF- α in acutely activating satellite cells and cellular proliferation post damaging exercise, is well observed (Foulstone et al., 2004, Li,

2003, Mackey et al., 2007, van de Vyver and Myburgh, 2012). This identification that acute RE induces hypomethylated CpG sites on this transcript, that, following regular RE loading (reloading) induces a significant increase in gene expression is interesting and requires further investigation (Foulstone et al., 2004, Li, 2003). Irrespective of their documented role in skeletal muscle, data presented here suggest that these epigenetically regulated genes (BICC1, GRIK2, TRAF1 and STAG1) were acutely sensitive to hypomethylation after a single bout of resistance exercise, that enhanced gene expression 22 weeks after a period of load-induced hypertrophy, a return of muscle to baseline and later reloading induced hypertrophy. Therefore, the epigenetic regulation of these genes seems to be an early, acute exercise biomarker for later exercise induced adaptation.

In partial support of these findings, comprehensive examination of exercise-induced promoter methylation modifications, and the functional role this plays in regulating gene expression, identified a time-dependent relationship between methylation and gene expression changes (Barres et al., 2012). Indeed, aerobic exercise at 80 % VO₂max (until 1,674 kJ of energy were expended), authors identified a significant hypomethylated promoter region of genes PGC-1 α and PDK4 immediately following exercise cessation, that was related to enhanced gene expression of the same transcripts 3hrs post exercise cessation (Barres et al., 2012). The same authors identify a similar finding in genes PGC-1 α , PDK4 and PPAR- δ following ex-vivo stimulation of rodent soleus muscle (0.3s trains; 25Hz, 0.1ms impulse repeated every 1s for 5-mins, repeated for 4 sets over a 60-min period). Where 45-mins post exercise stimulus, the authors identify significant reduction in promoter methylation of these transcripts, that only purport significant increases in gene expression 180-mins post ex-vivo contraction.

5.5 Summary and Concluding Remarks

The findings in this chapter, firstly, suggest that the human methylome is rapidly remodelled following acute RE that preferentially favours a hypomethylated profile. Furthermore, the data presented here, suggest that a rapid modification in DNA methylation of specific genes may act as an early (30 mins) sensitive DNA methylation biomarker to acute exercise for later adaptive responses to chronic exercise.

Chapter 6:

Thesis Conclusion

6.1 Aims of Thesis

Skeletal muscle mass and plasticity are fundamental for functional performance, maintenance of metabolic health, longevity and quality of life into old age. With this in mind, a large body of biological research has sought to elucidate the molecular mechanisms that regulate muscle mass. Despite recent advances in this field, a complete working understanding of the molecular processes that converge upon skeletal muscle to orchestrate both muscular hypertrophy, and atrophy remain poorly described and inadequately understood.

In this regard, there is a dearth of data and experimental work examining the role of epigenetics in regulating skeletal muscle mass and the adaptive response of mammalian muscle, to both atrophic and hypertrophic encounters. With this in mind, this thesis aimed to elucidate this concept by investigating the DNA methylation response and the functional relevance on gene expression of these modification during periods of atrophy and hypertrophy in mammalian skeletal muscle. The overarching aims of this thesis were therefore to:

1. Investigate the role of DNA methylation in skeletal muscle atrophy using an *in-vivo* tetrodotoxin nerve silencing system in rats to model disuse atrophy over a period of 14 days.
2. elucidate whether these epigenetic modifications were retained or returned to normal with 7 d of full active recovery in the same animals.
3. Investigate whether an epigenetic muscle memory of hypertrophy occurs in human skeletal muscle *in-vivo*, using chronic resistance exercise (loading), followed by cessation of exercise (unloading), and finally a subsequent later

chronic resistance exercise programme (reloading), thus allowing the elucidation of the underlying epigenetic alterations that occur after muscle hypertrophy (loading), a return of muscle back to baseline size (unloading) and memory (reloading) respectively.

4. And finally, explore modifications to genome wide DNA methylation following a single bout of resistance exercise in previously untrained human subjects (acute RE), and correlate these modifications to changes in the DNA methylation and gene expression following chronic resistance exercise induced hypertrophy (loading) and subsequent reloading induced muscle growth (data derived in aim 3 above). Identifying whether these DNA modifications may exist as early acute biological markers of subsequent adaptation to resistance exercise induced muscle hypertrophy.

To realise these aims, in chapter 3 we employed a transcriptome-wide approach in Wistar rats that were subject to atrophy by nerve silencing of the peroneal nerve using tetrodotoxin (TTX) to the hind limb (TTX exposure over 3, 7 and 14D time periods). Furthermore, this model allowed reversal of TTX exposure and the return of normal physical activity to the rodent hind limb, culminating in the partial recovery of skeletal muscle mass over a subsequent 7D period (14D TTX and 7D recovery). The transcriptome-wide analysis allowed for identification of significantly differentially regulated gene transcripts, which were subsequently targeted for DNA methylation analysis. In the second experimental study (chapter 4), an epigenome-wide approach was utilised to examine the human methylome following a 7-week period of resistance exercise (RE) (loading), a subsequent period of exercise cessation (unloading) and a final secondary period of chronic RE loading (reloading). In studying the human

methylome, we were able to investigate over 850,000 DNA CpG sites that were differentially methylated and associated with skeletal muscle loading, unloading and reloading. The most significantly and frequently modified genes between conditions were then followed up for target gene expression analysis at the single gene level. A similar analysis model was utilised in the final experimental study (chapter 5), where previously untrained human subjects underwent a single bout of RE (acute RE) to identify the immediate response of the human methylome following RE. Cross-comparative bioinformatic analysis was performed to understand the relationship between acute and chronic exposures to RE, before specific genes were targeted for further gene expression analysis. With the view to establish whether these DNA modifications may exist as early acute biological markers of later life adaptation to resistance exercise induced muscle hypertrophy.

6.2 DNA methylation is modified following catabolic and anabolic exposure: acute and chronic response of mammalian DNA methylation

It was identified that following both atrophy (aim 1 above; data chapter 3) and loading (aims 3 and 4 above; data chapters 4 and 5), mammalian skeletal muscle demonstrated significant modifications in DNA methylation. Indeed, in chapter 3, the peroneal nerve of rat hind limbs were exposed to treatment of the toxin, tetrodotoxin (TTX), that induced a progressive wasting of the hind limb up to a 14D time point. Following gene arrays (skeletal muscle RNA; 31,000 probe sets, covering over 30,000 transcripts and variants of 28,000 known sequencing gene regions) and the identification of the most statistically differentially regulated genes between conditions, loci-specific pyrosequencing of bisulfite converted DNA from the same animals identified

significant modifications to the promoter methylation profile of important gene transcripts (Myog, Fbxo32, Trim63, Chrna1 and Ampd3) across 3, 7 and 14D exposure. Previously, it was thought that DNA methylation was mitotically stable, and thus environmental factors were not considered a significant vehicle to drive modifications in differentiated adult tissue (Reik et al., 2001). Conversely to this consensus, recent findings have suggested that acute exercise, through mechanisms that currently remain unknown, is able to modify DNA methylation in important regions of gene coding DNA. Indeed, in a series of investigative studies, Barres et al. (2012) utilised aerobic regimen (80% VO₂max until 1674 KJ of energy was expended in humans; 0.3 s trains of 25 Hz, 0.1 ms impulses, repeated every second for 5 mins for 4 sets in *ex-vivo* rodent soleus muscle) in both human and rodent skeletal muscle to examine the effects of exercise on promoter methylation. The authors concluded that acute aerobic exercise is sufficient to rapidly remodel promoter DNA methylation of important metabolic related genes (PGC-1 α , PDK4 and PPAR- δ). Collectively, the findings presented here suggest that exercise is sufficient to modify promoter DNA methylation of important gene transcripts, during relatively acute time periods. Similarly, in chapter 5 of this thesis, we present global regulatory evidence to suggest that the human methylome is rapidly remodelled following just a single bout of resistance exercise (RE) (acute RE). Indeed, in previously untrained human subjects, immediately following (< 30 mins) acute RE, we report 17,884 CpG sites as displaying a significantly differentially regulated methylation profile, with a preferential hypomethylated response in the human methylome (chapter 5). Conclusively, this work suggests that acute exposure to both catabolic (3-14D TTX atrophy remodels promoter methylation of important regulatory genes) and

hypertrophic (acute RE) conditions is sufficient to induce significant modifications to the mammalian DNA methylation.

We also sought to elucidate (aim 3) what large-scale epigenetic modifications are apparent following continuous load induced skeletal muscle hypertrophy after chronic RE (chapter 4) in previously untrained human participants. Indeed, in chapter 4 we identified that, following a 7-week period of load induced hypertrophy, 17,365 CpG sites of the human methylome displayed significantly modified DNA methylation profiles. Furthermore, following a period of exercise cessation (7-weeks unloading), a secondary period of resistance exercise (7-weeks reloading) induced further modifications to the human methylome, where 27,155 CpG sites portrayed statistically differentially methylated profiles. To the authors' knowledge, these data are the first to elucidate the effects that chronic RE exposure has on human skeletal muscle methylome. Similarly, previous work has also suggested that RE induced large-scale modifications to DNA methylation in leukocytes (Denham et al., 2016). Indeed, 8-weeks of RE training (3/week of 3 sets, 8-12 reps at 80 % 1RM) induced over 57,000 differentially methylated CpG sites with an even split between hypo/ (28,987) hypermethylated (28,397) modifications (Denham et al., 2016). Interestingly, following 7-weeks of RE loading, we have shown a similar pattern of change in CpG DNA methylation, where an even distribution of both hypo and hypermethylated sites were observed (9,153 and 8,212, respectively). However, upon exposure to secondary stimulus (reloading), we observed an enhanced hypomethylated profile, where 18,816 CpG sites were hypomethylated compared to 8,339 as hypermethylated (chapter 4; discussed below).

To date however, the precise mechanisms that orchestrate modifications in DNA methylation in mature skeletal muscle, remain elusive. In their work, Barres et al., (2012) initially speculated, and subsequently investigated the role of intracellular calcium (Ca^{2+}) ions in orchestrating the cascade of reactions that demonstrate an addition or removal of a methyl molecular onto promoter DNA sequences (Barres et al., 2012). Nonetheless, these *in-vitro* experiments failed to confirm this hypothesis, and to date, the mechanisms that induce DNA methylation remain unknown and thus, warrant further investigation.

Collectively, the data presented in this thesis, as well as evidence described above, suggests that both anabolic and catabolic environmental encounters, in both an acute and chronic manner, are sufficient to drive significant modifications to mammalian DNA methylation in skeletal muscle. Here, we present novel data that demonstrates this concept in mature mammalian skeletal muscle following both atrophic and hypertrophic stimuli.

6.3 DNA Methylation Displays an Inverse Mirrored Relationship with Changes in Gene Expression During Loss and Growth in Mammalian Skeletal Muscle

Following identification that atrophic and hypertrophic environmental encounters were a driving force for both acute and chronic modifications to mammalian skeletal muscle DNA methylation, we next aimed to understand the functional relevance (in terms of whether the epigenetics lead to changes in the genes being turned on/off) of these modifications (aims 1 and 4, as outlined above). Importantly, in chapters 3 and

4, we identified that where significant modifications to DNA methylation (promoter region and CpG-specific) occurred, these were met with functional changes in gene expression, suggesting a significant role for DNA methylation in regulating the adaptive response of mammalian skeletal muscle during periods of perturbation.

Indeed, in chapter 3 (experimental study 1), we report that following 3D of TTX exposure in rat TA muscle, significant reductions in promoter methylation of the muscle specific basic helix-loop-helix transcription factor Myogenin, was associated with a significant increase in gene expression at the same time point (chapter 3). Furthermore, where 7 and 14D of TTX exposure induced a significant reduction of DNA methylation in the promoter region of *Chrna1*, we also reported an increase in gene expression that attained significance at 14D of TTX exposure (chapter 3). Temporal pattern analysis of the fold-changes in both DNA methylation and gene expression (Figure 3.6 B) during 14D of TTX exposure, further identified an inverse relationship between methylation and gene expression of studied genes. Further work in this model, where TTX cessation induced recovery of ~51 % of skeletal muscle wasting from 14D TTX exposure only, identified a similar relationship between DNA methylation and gene expression. Indeed, in the identified transcripts *Trim63* and most prominently in *Fbxo32* and *Chrna1*, cessation of TTX induced muscle wasting and return to activity in skeletal muscle induced increased DNA methylation that returned back to baseline levels. Importantly, where this increase in methylation was observed, we also observed a reduction in gene expression of these transcripts which was associated, as previously discussed, with the partial recovery of skeletal muscle mass.

This relationship between methylation and gene expression was further identified in chapter 4, where CpG-specific DNA methylation and gene expression of a cluster of identified transcripts displayed an inverse relationship during 7-weeks loading, unloading and reloading, respectively. Indeed, methylome-wide bead array analysis identified the gene cluster consisting of UBR5, BICC1, ODF2, RPL35a, SETD3, C12orf50, PLA2G16, HEG1 and ZFP2, that collectively displayed reduction (hypomethylation) in DNA methylation following loading, that returned to baseline upon exercise cessation (unloading), and displayed a significant ($P = 0.05$) reduction in DNA methylation upon reloading (Figure 4.10B). Importantly, this profile was mirrored by significant changes in gene expression of the same transcripts, across the same conditions (loading, unloading, reloading; Figure 4.10B). More so, in a second cluster of genes including AXIN1, TRAF1, GRIK2 and CAMK4, a similar inverse relationship was observed, whereby initial and maintained hypomethylation was met with an initial and sustained increase in gene expression (Figure 4.11B).

Collectively, these data suggest that there was a strong association between changes in promoter and/or CpG-specific DNA methylation and changes in gene expression during periods of skeletal muscle perturbation. As previously highlighted, such findings have been identified in aerobic exercise models (described above (Barres et al., 2012)) but more recently in a model of RE and high-fat feeding (Laker et al., 2017). Indeed, following short-term RE ($3 \times 8-10$ reps, 3 exercises, 2-days rest between sessions) and high-fat feeding (3.9 g fat/kg fat free mass, equating to 77% of total caloric intake) intervention (total of 9 days), authors reported a total of 54 genes that showed a relationship between DNA methylation modifications (analysed via reduced representative bisulfite sequencing, RBBS) and altered gene expression

(RNA sequencing) (Laker et al., 2017). Despite a strong association between DNA methylation and gene expression being evident, the work described and presented above has characterised the observation of this relationship following skeletal muscle adaptation, thus it shows an association/correlation but not a direct causation. In order to show this causation, experimental models (both in-vitro and in-vivo) utilising over-expression/knockdown of site specific DNA methylation, and analysing the effect on gene functionality and tissue adaptation, must be undertaken.

Nevertheless, there is now a growing number of findings that associate changes in DNA methylation with functional changes in gene expression in mammalian skeletal muscle, suggesting a role for methylation in modulating the adaptive response of this tissue (described above). In this manner, the data presented here adds novel data that supports and extends this field as it is the first to show this relationship during periods of skeletal muscle atrophy, recovery from atrophy and long-term RE induced muscular hypertrophy. The studies are the first to identify a retention of epigenetic information after hypertrophy, even when exercise ceases (discussed directly below).

6.4 Retention and Memory of DNA Methylation in Mammalian Skeletal Muscle

One of the most exciting findings from this research thesis was the identification that, through retention of a hypomethylated profile, human skeletal muscle possesses an epigenetic muscle memory of earlier hypertrophy (chapter 4). After an initial period of RE, where skeletal muscle significantly increased and was met with a similar number of hypo/hypermethylated CpG sites, the global modification of the human

methylome was retained even when skeletal muscle mass returned towards baseline levels. Most importantly however, we identify an enhanced hypomethylated response of the human methylome following secondary exposure to RE loading (reloading; chapter 4), that was associated with the greatest increase of skeletal muscle mass at the whole tissue level. Collectively suggesting that a retention of hypomethylated modifications following RE, that were maintained even during reversal in skeletal muscle mass, allowed for an enhanced hypomethylated profile following a secondary encounter with RE. This enhanced hypomethylated profile was prominent in a cluster of genes targeted for closer analysis. Indeed, genes UBR5, BICC1, ODF2, RPL35a, SETD3, C12orf50, PLA2G16, HEG1 and ZFP2 collectively portrayed an enhanced hypomethylated response following reloading exposure, that was met with the largest increase in gene expression of the same cluster (as described above; Figure 4.10). Correlation analysis identified a significant positive relationship between changes in gene expression and skeletal muscle mass for genes, RPL35a, UBR5, SETD3, PLA2G16 and HEG1, suggesting that these genes, whose behaviour is relatively unstudied in skeletal muscle, may play an important role in skeletal muscle mass regulation. Collectively, these findings imply that, due to a hypomethylated maintenance of previous loading stimulus, secondary exposure to RE evoked an enhanced hypomethylated response that was met with the largest increase in gene expression in transcripts that were identified as highly important for muscle mass adaptation. We concluded that human skeletal muscle possesses an epigenetic ‘memory’ of previous 7 weeks’ load induced hypertrophy. These findings are the first to elucidate such a phenomenon in mature skeletal muscle, however, previous work has insinuated a similar attribute within skeletal muscle cells. Indeed, cells isolated from obese patients and cultured under the influence of an over-supply of lipids,

displayed a significant reduction in the expression of the important fatty acid oxidative (FAO) gene PPAR- δ (Maples and Brault, 2015). Importantly, the authors further identified a distinct dysregulation in multiple CpG sites within close proximity to the transcriptional start site (TSS) of the PPAR- δ gene, of which CpG site 6 (-71 bp from TSS) correlated significantly with mRNA expression (Maples and Brault, 2015). This study implied that epigenetic modifications of the FAO gene, PPAR- δ , acquired during an *in-vivo* encounter (obesity) were remembered and retained *in-vitro*, with these epigenetic modifications being an important mediator in the inability for obese skeletal muscle cells to handle a secondary and similar encounter with stress (lipid over supply). The ability for skeletal muscle cells to retain modified epigenetic signatures has also been shown by our group, as previously discussed (Sharples et al., 2016a). Indeed, it was shown that murine myoblasts, once acutely exposed to the catabolic cytokine TNF- α at an early-life time-point acquired an altered DNA methylation profile of the myogenic regulatory factor, MyoD. Interestingly, this study reported that, following 30 population doublings in the previously exposed cells (TNF- α), the modified DNA methylation profile of MyoD was retained (Sharples et al., 2016a).

Importantly, the study by Sharples et al. (2016a) reported that skeletal muscle cells retained differential DNA methylation profiles following exposure to a catabolic encounter, that maintained a modified pattern for a sustained period of time, following the withdrawal of the stimulus. This retentive attribute of DNA methylation was examined in this thesis, following *in-vivo* exposure to a catabolic stimulus (chapter 3). Indeed, Wistar rats underwent a period of TTX exposure (3, 7 and 14D) that induced progressively increased muscle wasting across this time-course. Importantly,

we identified significant modifications to promoter DNA methylation of genes MyoG, Fbxo32, Trim63 and Chrna1 across this time-course, that were associated with an inverse change in gene expression (as described above). However, the correct assembly of this model allowed for precise cessation of TTX nerve toxin and the return to habitual physical activity for 7D following 14D of muscle wasting (recovery group; chapter 3). This model induced a significant recovery of muscle mass by 51.7% compared to 14D alone, albeit muscle mass not fully returning to baseline control levels. Intriguingly, and contrary to our hypothesis, DNA methylation of the promoter region of the genes (Fbxo32, Trim63 and Chrna1) were not significantly retained following the withdrawal of TTX exposure, and instead, returned to baseline control levels in symmetry to changes in both gene expression and skeletal muscle mass (chapter 3). The reasoning behind this lack of retentive methylation is unclear and was not followed up in this thesis. However, it is plausible that the rodent epigenome may have retained a significant number of differentially methylated CpG sites following 14D TTX induced muscle wasting, but these were over-looked given the specific pyrosequencing analysis utilised within this chapter. Thus, further work of this model, utilising a genome-wide DNA methylation approach (similar to that in chapters 4 and 5), may elucidate a retention of differentially regulated CpG sites.

Collectively, however, work presented from chapters 3 and 4 are interesting, suggesting that DNA methylation may act in both a transient and stable manner during periods of skeletal muscle perturbation. Further explorative work is now needed to understand the mechanisms and functional relevance of these modifications.

6.5 DNA Methylation May Act as an Early Biological Marker for Later Adaptation

Seminal work by Barres et al., (2012) identified that changes in promoter DNA methylation of important metabolic related transcripts in human skeletal muscle, precede those observed in gene expression, partially suggesting that DNA methylation may act as an early marker of later exercise-induced cellular response. In chapter 5, we report similar findings, whereby acute DNA methylation modifications were not directly associated with acute gene expression changes, rather, upon continued loading and reloading (that retained the same modifications to CpG DNA methylation), associated changes in DNA methylation and gene expression were identified. Indeed, following acute RE, ADSLL1 displayed a hypermethylated profile that was identical to that associated following 7-weeks loading, yet, at the gene expression level, acute RE did not generate a significant change. However, upon 7-weeks of repetitive loading, where the hypermethylated profile of ADSLL1 was retained, gene expression was significantly reduced. The opposite (in terms of directionality of change) was observed in C11orf24, whereby acute RE induced a significant hypomethylated response but with no change in gene expression. Upon continued loading however, the maintained hypomethylated response was met with a significant increase in gene expression (Figure 5.6). In continuation of these findings, genes BICC1, STAG1, GRIK2 and TRAF1 displayed significant reductions in DNA methylation (hypomethylation) following acute RE that were not met with detectable changes in gene expression at the same acute time point. However, following reloading (7-weeks reloading), where hypomethylated CpG DNA methylation was significantly retained, these genes displayed their largest increase in gene expression.

It is currently unclear as to the mechanisms that orchestrated this observed response. However, similar findings, that associate significant changes in DNA methylation with a time-dependent and significant change in gene expression in mature skeletal muscle, have previously been acknowledged (Barres et al., 2012). These data raise the tantalising potential for future experimental work to identify this relationship further, with the hypothesis that changes in DNA methylation may precede changes in gene expression, and therefore may act as an early and acutely sensitive bio-marker for later adaptations at a cellular and potentially whole tissue level.

6.6 Future Directions

The work presented in this thesis has uncovered a number of important and interesting findings in the field of skeletal muscle epigenetics. Nonetheless, there still remains a lot of fundamental work that needs to be performed in order for the scientific community to gain a greater understanding as to the importance of epigenetics in regulating skeletal muscle adaptation. With this in mind, and as an artefact to the data derived here, there are a number of future directions stemming from this thesis.

6.6.1 Elucidating whether DNA methylation modifications precede those observed in gene expression during skeletal muscle adaptation

There is a clear association between DNA methylation modifications and changes in the expression of the associated gene, as identified in this thesis. Furthermore, it has been shown that changes in DNA methylation may precede those associated changes in gene expression, in skeletal muscle (Barres et al., 2012). Nonetheless, to the authors knowledge, no data/studies exist that have directly investigated this relationship in a

time-course manner, following changes in skeletal muscle mass. At a molecular level, the mechanistic link between changes in gene expression, protein quantity and enzyme activity are well examined (Perry et al., 2010), resulting in a functional remodelling of the tissue and a progressive skeletal muscle adaptation. However, this model of muscular adaptation bypasses the potential influence of skeletal muscle epigenetics in regulating gene expression, and thus, the down-stream quantity of functional proteins. More so, as previously identified in this thesis (chapter 5), skeletal muscle epigenetics may act as a potential early and sensitive biomarker for later adaptive responses to exercise. Therefore, an investigation to identify if a particular gene, or cluster of genes, is hypo/hypermethylated after acute exercise across differing ranges of exercise intensity in both exercise responders and non-responders for a measurable physiological adaptation to chronic exercise (e.g. muscle size or aerobic capacity). We could perhaps be able to predict, based on an acute DNA methylation assay, if someone would adapt to a chronic exercise program or not.

6.6.2 Do repeated exposures to a catabolic event induce an epigenetic muscle memory

For the first time, this thesis identified that DNA methylation may orchestrate a skeletal muscle memory characteristic in mature tissue, whereby enhanced adaptive responses are observed upon a later encounter with muscle hypertrophy (chapter 4). These findings now need to be further explored to characterise this phenomenon in a number of different environmental approaches. For example, during hospitalisation, humans may experience repeated episodic bouts of acute muscle wasting caused via bed-rest, surgery or their underlying disease state (English and Paddon-Jones, 2010). It is plausible, given the evidence in this thesis, that acute bouts of muscle atrophy

encountered during this period may alter the epigenetic blue-print of crucial muscle mass relating transcripts, and therefore results in a greater reduction in muscle mass upon secondary or even tertiary exposure to a similar stimulus. It is therefore of great clinical importance to elucidate this response in order to further our understanding of this catabolic cyclic paradigm.

A human *in-vivo* model that induces a period of severe muscle wasting, followed by a similar period of muscular recovery, and a final period of skeletal muscle wasting raises a number of ethical and logistical issues however, and thus an extrapolated experimental model would need to be utilised. To over-come such difficulties, a possibility would be to extend the work undertaken in chapter 3 of this thesis. Indeed, Wistar rodents implanted with an osmotic nerve-cuff apparatus could undergo a significant period of disuse-induced atrophy, identical to the model utilised in this chapter (14D TTX exposure). Following correct assembly of the apparatus, where TTX is ceased, 14D of normal habitual activity would commence where it would be expected that skeletal muscle would return to near baseline levels, given that recovery of skeletal muscle in tibialis anterior of rodents in chapter 3 recovered by ~50 % after only 7D (Figure 3.3; chapter 3). Through a secondary minor surgery and a refilling of the assembled osmotic pump in the rats, the nerve cuff would begin to infuse the hind limb with TTX again, thus inducing a secondary period of skeletal muscle wasting (14D). This experiment would create an opposite model of that used in chapter 4 of loading, unloading, reloading in humans by undertaking unloading, loading, unloading in rat skeletal muscle.

6.6.3 Elucidating the role of the newly identified E3 ubiquitin ligase gene, UBR5, in skeletal muscle

Finally, multiple novel and previously unstudied (in mammalian skeletal muscle) transcripts have been identified in the presented work, that, at the expression level, positively correlate with adaptations in skeletal muscle mass (chapters 4 and 5). Our molecular understanding of skeletal muscle targets that generate positive anabolic adaptive responses, is continually advancing and expanding. The novel transcripts identified within this thesis, therefore, may possess a currently un-characterised role in human skeletal muscle size increases after resistance exercise, and thus warrant further investigation. In order to do so, fundamental work needs to be performed to characterise the role of these genes in mature mammalian skeletal muscle. Intriguingly, the E3 ubiquitin ligase protein family member UBR5, whose expression is identified as displaying a positive correlation with increases in muscle mass, also displayed a distinct susceptibility to being modulated by DNA methylation. Typically, E3 ubiquitin ligases, such as those of Murf1/Trim63 and MAFbx/Fbxo32, are associated with increased gene expression during periods of skeletal muscle atrophy (Bodine et al., 2001a), where, in chapter 3, we have also shown that they are also epigenetically regulated. Thus, the identified positive correlation between gene expression of UBR5 and adaptations in skeletal muscle, is counterintuitive, and therefore highly interesting. Evidence provided here, suggests that not only is the expression of UBR5 a novel transcript that correlates positively with skeletal muscle mass development, it is also highly susceptible to aberrancies in DNA methylation. A plethora of future work is required to firstly characterise UBR5's presence in skeletal muscle, but also its role in regulating cellular growth, and to further identify the epigenetic regulation of this transcript.

6.7 Experimental Limitations

It is important to note that despite interesting findings being alluded to throughout this thesis, the explorative work described here is not without limitations. First and foremost, in chapter 3 we utilised a rodent model to characterise the promotor methylation changes in identified important transcripts during a prolonged atrophy and subsequent muscular recovery model. The strain of rat utilised (Wister more details) is an in-bred genetically identical strain of rodent, commonly utilised for in-vivo experimental work. The loci-specific pyrosequencing and high-resolution melt assays utilised within this chapter to elucidate the methylation changes in these transcripts were performed on a small, albeit genetically identical, sample size (N=3). The small sample size used for this section of work may therefore impact the observed data and thus, the biological interpretation of these findings. Future investigations should therefore utilise the data here as a catalyst to further explore these findings in an experimental model utilising greater sample size.

Equally, in chapter 4 and 5, we utilise an in-vivo human model, where voluntary human participants were utilised for both acute and chronic training sessions to explore the aims of these chapters. In these sets of experiments, eight human participants were originally utilised with a high retention rate, where only one participant withdrew in the final stage of chronic training (for reasons unrelated to testing/experimental protocols). Nonetheless, given the high diversity in the human genome (Levy et al., 2007, Venter et al., 2001), this relatively low sample size must be acknowledged as a limitation of the study. Indeed, low sample size in human research adversely effects the likelihood of identifying true statistically significant findings (Dumas-Mallet et al., 2017), and may increase the risk of presenting false

positives (Dumas-Mallet et al., 2017). Furthermore, and with greater specificity to the in-vivo methodologies utilised within these experiments, it has previously been shown that human subjects respond (strength assessment via isometric MVC) to a high inter-individual variability following 9-weeks of progressive RE training (Erskine et al., 2010a). It is therefore plausible that inter-individual differences in the ability for subjects to respond to the RE training prescribed in this thesis may underlie some of the observed findings. However, elucidation of such findings either requires a substantially larger sample size, or a unique demographic of the human population (i.e. monozygotic twin studies) in order to understand the extent to which this is true. Nonetheless, the work offered here is explorative in nature and should therefore be utilised as a catalyst to explore these concepts further, given the interesting findings presented.

The human work presented in chapter 4 utilised two in-vivo methodologies to assess adaptations in muscle strength and mass over time. Both of these methods, isometric MVC assessed via an isokinetic dynamometer and dual-energy X-ray absorptiometry for muscle mass adaptations, are not without limitations. For example, pre-scan nutrient and hydration status has been shown to substantially alter the total and regional lean mass as well as the associated total body mass in individuals, in a repeated measures study (Nana et al., 2012). For isometric MVC tests, diurnal variation is associated with alterations in the torque production of human participants when repeatedly tested, with subjects performing better in the evening compared to morning (Sedliak et al., 2007). The test-retest reliability of the knee extensor isokinetic dynamometry and dual-energy X-ray absorptiometry have both previously been analysed in separate laboratories and been shown to be highly reliable for the

assessment of knee extensor strength and lean mass, respectively (Adsuar et al., 2011, Sole et al., 2007, Bilsborough et al., 2014). However, such a test-retest reliability experiment could have been performed for chapter 4 in order to provide greater confidence that the findings presented are true.

However, given the difficulties in performing these types of studies, the data presented is still of great value to the scientific community and should be utilised as a catalyst to reliably validate and replicate these findings.

6.8 Final Conclusion

This thesis has generated novel findings as to the role DNA methylation plays in regulating skeletal muscle disuse atrophy, acute anabolism, chronic resistance exercise induced hypertrophy and muscle memory.

Chapter 7:

References

- ADHIHETTY, P. J., O'LEARY, M. F., CHABI, B., WICKS, K. L. & HOOD, D. A. 2007. Effect of denervation on mitochondrially mediated apoptosis in skeletal muscle. *J Appl Physiol (1985)*, 102, 1143-51.
- ADSUAR, J. C., OLIVARES, P. R., DEL POZO-CRUZ, B., PARRACA, J. A. & GUSI, N. 2011. Test-retest reliability of isometric and isokinetic knee extension and flexion in patients with fibromyalgia: evaluation of the smallest real difference. *Arch Phys Med Rehabil*, 92, 1646-51.
- AGUER, C., MERCIER, J., MAN, C. Y., METZ, L., BORDENAVE, S., LAMBERT, K., JEAN, E., LANTIER, L., BOUNOUA, L., BRUN, J. F., RAYNAUD DE MAUVERGER, E., ANDREELLI, F., FORETZ, M. & KITZMANN, M. 2010. Intramyocellular lipid accumulation is associated with permanent relocation ex vivo and in vitro of fatty acid translocase (FAT)/CD36 in obese patients. *Diabetologia*, 53, 1151-63.
- AL-SHANTI, N., DURCAN, P., AL-DABBAGH, S., DIMCHEV, G. A. & STEWART, C. E. 2014. Activated lymphocytes secretome inhibits differentiation and induces proliferation of C2C12 myoblasts. *Cell Physiol Biochem*, 33, 117-28.
- AL-SHANTI, N., SAINI, A., FAULKNER, S. H. & STEWART, C. E. 2008. Beneficial synergistic interactions of TNF-alpha and IL-6 in C2 skeletal myoblasts--potential cross-talk with IGF system. *Growth Factors*, 26, 61-73.
- ALDERTON, J. M. & STEINHARDT, R. A. 2000. How calcium influx through calcium leak channels is responsible for the elevated levels of calcium-dependent proteolysis in dystrophic myotubes. *Trends Cardiovasc Med*, 10, 268-72.
- ALLIS, C. D. & JENUWEIN, T. 2016. The molecular hallmarks of epigenetic control. *Nat Rev Genet*, 17, 487-500.
- APPELL, H. J. 1990. Muscular atrophy following immobilisation. A review. *Sports Med*, 10, 42-58.
- ARMSTRONG, R. B. 1990. Initial events in exercise-induced muscular injury. *Med Sci Sports Exerc*, 22, 429-35.
- BAECHLE, T. R., EARLE, R. W. & WATHEN, D. 2008. *Essentials of Strength and Conditioning* Champaign, Ill, Human Kinetics.
- BAEHR, L. M., FURLOW, J. D. & BODINE, S. C. 2011. Muscle sparing in muscle RING finger 1 null mice: response to synthetic glucocorticoids. *J Physiol*, 589, 4759-76.
- BANNISTER, A. J. & KOUZARIDES, T. 2011. Regulation of chromatin by histone modifications. *Cell Res*, 21, 381-95.
- BANSAL, D., MIYAKE, K., VOGEL, S. S., GROH, S., CHEN, C. C., WILLIAMSON, R., MCNEIL, P. L. & CAMPBELL, K. P. 2003. Defective membrane repair in dysferlin-deficient muscular dystrophy. *Nature*, 423, 168-72.
- BARRES, R., OSLER, M. E., YAN, J., RUNE, A., FRITZ, T., CAIDAHL, K., KROOK, A. & ZIERATH, J. R. 2009. Non-CpG methylation of the PGC-1alpha promoter through DNMT3B controls mitochondrial density. *Cell Metab*, 10, 189-98.
- BARRES, R., YAN, J., EGAN, B., TREEBAK, J. T., RASMUSSEN, M., FRITZ, T., CAIDAHL, K., KROOK, A., O'GORMAN, D. J. & ZIERATH, J. R. 2012. Acute exercise remodels promoter methylation in human skeletal muscle. *Cell Metab*, 15, 405-11.

- BARRES, R. & ZIERATH, J. R. 2016. The role of diet and exercise in the transgenerational epigenetic landscape of T2DM. *Nat Rev Endocrinol*, 12, 441-51.
- BATT, J., BAIN, J., GONCALVES, J., MICHALSKI, B., PLANT, P., FAHNESTOCK, M. & WOODGETT, J. 2006. Differential gene expression profiling of short and long term denervated muscle. *Faseb j*, 20, 115-7.
- BAZGIR, B., FATHI, R., REZAZADEH VALOJERDI, M., MOZDZIAK, P. & ASGARI, A. 2017. Satellite Cells Contribution to Exercise Mediated Muscle Hypertrophy and Repair. *Cell J*, 18, 473-484.
- BEKER, F., WEBER, M., FINK, R. H. & ADAMS, D. J. 2003. Muscarinic and nicotinic ACh receptor activation differentially mobilize Ca²⁺ in rat intracardiac ganglion neurons. *J Neurophysiol*, 90, 1956-64.
- BERGER, S. L., KOUZARIDES, T., SHIEKHATTAR, R. & SHILATIFARD, A. 2009. An operational definition of epigenetics. *Genes Dev*, 23, 781-3.
- BERNET, J. D., DOLES, J. D., HALL, J. K., KELLY-TANAKA, K., CARTER, T. A. & OLWIN, B. B. 2014. p38 MAPK signaling underlies a cell autonomous loss of stem cell self-renewal in aged skeletal muscle. *Nat Med*, 20, 265-71.
- BIBIKOVA, M., BARNES, B., TSAN, C., HO, V., KLOTZLE, B., LE, J. M., DELANO, D., ZHANG, L., SCHROTH, G. P., GUNDERSON, K. L., FAN, J. B. & SHEN, R. 2011. High density DNA methylation array with single CpG site resolution. *Genomics*, 98, 288-95.
- BILSBOROUGH, J. C., GREENWAY, K., OPAR, D., LIVINGSTONE, S., CORDY, J. & COUTTS, A. J. 2014. The accuracy and precision of DXA for assessing body composition in team sport athletes. *J Sports Sci*, 32, 1821-8.
- BIRD, A. 2002. DNA methylation patterns and epigenetic memory. *Genes Dev*, 16, 6-21.
- BIRD, A. 2007. Perceptions of epigenetics. *Nature*, 447, 396-8.
- BIRD, A. P. 1986. CpG-rich islands and the function of DNA methylation. *Nature*, 321, 209-13.
- BLAESER, F., HO, N., PRYWES, R. & CHATILA, T. A. 2000. Ca²⁺-dependent Gene Expression Mediated by MEF2 Transcription Factors. *Journal of Biological Chemistry*, 275, 197-209.
- BODINE, S. C. 2013. Disuse-induced muscle wasting. *Int J Biochem Cell Biol*, 45, 2200-8.
- BODINE, S. C. & BAEHR, L. M. 2014. Skeletal muscle atrophy and the E3 ubiquitin ligases MuRF1 and MAFbx/atrogen-1. *Am J Physiol Endocrinol Metab*, 307, E469-84.
- BODINE, S. C., LATRES, E., BAUMHUETER, S., LAI, V. K., NUNEZ, L., CLARKE, B. A., POUYMIROU, W. T., PANARO, F. J., NA, E., DHARMARAJAN, K., PAN, Z. Q., VALENZUELA, D. M., DECHIARA, T. M., STITT, T. N., YANCOPOULOS, G. D. & GLASS, D. J. 2001a. Identification of ubiquitin ligases required for skeletal muscle atrophy. *Science*, 294, 1704-8.
- BODINE, S. C., STITT, T. N., GONZALEZ, M., KLINE, W. O., STOVER, G. L., BAUERLEIN, R., ZLOTCHENKO, E., SCRIMGEOUR, A., LAWRENCE, J. C., GLASS, D. J. & YANCOPOULOS, G. D. 2001b. Akt/mTOR pathway is a crucial regulator of skeletal muscle hypertrophy and can prevent muscle atrophy in vivo. *Nat Cell Biol*, 3, 1014-9.

- BOGDANOVIC, O. & VEENSTRA, G. J. 2009. DNA methylation and methyl-CpG binding proteins: developmental requirements and function. *Chromosoma*, 118, 549-65.
- BONALDO, P. & SANDRI, M. 2013. Cellular and molecular mechanisms of muscle atrophy. *Dis Model Mech*, 6, 25-39.
- BOYES, G. & JOHNSTON, I. 1979. Muscle fibre composition of rat vastus intermedius following immobilisation at different muscle lengths. *Pflugers Arch*, 381, 195-200.
- BRUNET, A., BONNI, A., ZIGMOND, M. J., LIN, M. Z., JUO, P., HU, L. S., ANDERSON, M. J., ARDEN, K. C., BLENIS, J. & GREENBERG, M. E. 1999. Akt promotes cell survival by phosphorylating and inhibiting a Forkhead transcription factor. *Cell*, 96, 857-68.
- BRUUSGAARD, J. C., JOHANSEN, I. B., EGNER, I. M., RANA, Z. A. & GUNDERSEN, K. 2010. Myonuclei acquired by overload exercise precede hypertrophy and are not lost on detraining. *Proc Natl Acad Sci U S A*, 107, 15111-6.
- BUETOW, L. & HUANG, D. T. 2016. Structural insights into the catalysis and regulation of E3 ubiquitin ligases. *Nat Rev Mol Cell Biol*, 17, 626-42.
- CALLAGHAN, M. J., RUSSELL, A. J., WOOLLATT, E., SUTHERLAND, G. R., SUTHERLAND, R. L. & WATTS, C. K. 1998. Identification of a human HECT family protein with homology to the Drosophila tumor suppressor gene hyperplastic discs. *Oncogene*, 17, 3479-91.
- CAMPOS, G. E., LUECKE, T. J., WENDELN, H. K., TOMA, K., HAGERMAN, F. C., MURRAY, T. F., RAGG, K. E., RATAMESS, N. A., KRAEMER, W. J. & STARON, R. S. 2002. Muscular adaptations in response to three different resistance-training regimens: specificity of repetition maximum training zones. *Eur J Appl Physiol*, 88, 50-60.
- CANTINI, M. & CARRARO, U. 1995. Macrophage-released factor stimulates selectively myogenic cells in primary muscle culture. *J Neuropathol Exp Neurol*, 54, 121-8.
- CHAZAUD, B., BRIGITTE, M., YACOUB-YOUSSEF, H., ARNOLD, L., GHERARDI, R., SONNET, C., LAFUSTE, P. & CHRETIEN, F. 2009. Dual and beneficial roles of macrophages during skeletal muscle regeneration. *Exerc Sport Sci Rev*, 37, 18-22.
- COHEN, S., BRAULT, J. J., GYGI, S. P., GLASS, D. J., VALENZUELA, D. M., GARTNER, C., LATRES, E. & GOLDBERG, A. L. 2009. During muscle atrophy, thick, but not thin, filament components are degraded by MuRF1-dependent ubiquitylation. *J Cell Biol*, 185, 1083-95.
- COHEN, T. J., WADDELL, D. S., BARRIENTOS, T., LU, Z., FENG, G., COX, G. A., BODINE, S. C. & YAO, T. P. 2007. The histone deacetylase HDAC4 connects neural activity to muscle transcriptional reprogramming. *J Biol Chem*, 282, 33752-9.
- COLQUHOUN, D. & SIVILOTTI, L. G. 2004. Function and structure in glycine receptors and some of their relatives. *Trends Neurosci*, 27, 337-44.
- CONG, H., SUN, L., LIU, C. & TIEN, P. 2011. Inhibition of atrogen-1/MAFbx expression by adenovirus-delivered small hairpin RNAs attenuates muscle atrophy in fasting mice. *Hum Gene Ther*, 22, 313-24.
- COOPER, R. R. 1972. Alterations during immobilization and regeneration of skeletal muscle in cats. *J Bone Joint Surg Am*, 54, 919-53.

- CORNELISON, D. D., OLWIN, B. B., RUDNICKI, M. A. & WOLD, B. J. 2000. MyoD(-/-) satellite cells in single-fiber culture are differentiation defective and MRF4 deficient. *Dev Biol*, 224, 122-37.
- CORNELISON, D. D. & WOLD, B. J. 1997. Single-cell analysis of regulatory gene expression in quiescent and activated mouse skeletal muscle satellite cells. *Dev Biol*, 191, 270-83.
- CROSS, D. A., ALESSI, D. R., COHEN, P., ANDJELKOVICH, M. & HEMMING, B. A. 1995. Inhibition of glycogen synthase kinase-3 by insulin mediated by protein kinase B. *Nature*, 378, 785-9.
- DAVIS, P., WITCZAK, C. & BRAULT, J. 2015. AMP Deaminase 3 Accelerates Protein Degradation in C2C12 Myotubes. *The FASEB Journal*, 29.
- DE BOER, M. D., MAGANARIS, C. N., SEYNNES, O. R., RENNIE, M. J. & NARICI, M. V. 2007. Time course of muscular, neural and tendinous adaptations to 23 day unilateral lower-limb suspension in young men. *J Physiol*, 583, 1079-91.
- DELANEY, C., GARG, S. K. & YUNG, R. 2015. Analysis of DNA Methylation by Pyrosequencing. *Methods Mol Biol*, 1343, 249-64.
- DENHAM, J., MARQUES, F. Z., BRUNS, E. L., O'BRIEN, B. J. & CHARCHAR, F. J. 2016. Epigenetic changes in leukocytes after 8 weeks of resistance exercise training. *Eur J Appl Physiol*, 116, 1245-53.
- DESHAIES, R. J. & JOAZEIRO, C. A. 2009. RING domain E3 ubiquitin ligases. *Annu Rev Biochem*, 78, 399-434.
- DESPLANCHES, D., MAYET, M. H., SEMPORE, B. & FLANDROIS, R. 1987. Structural and functional responses to prolonged hindlimb suspension in rat muscle. *J Appl Physiol (1985)*, 63, 558-63.
- DIRKS, M. L., WALL, B. T., SNIJDERS, T., OTTENBROS, C. L., VERDIJK, L. B. & VAN LOON, L. J. 2014. Neuromuscular electrical stimulation prevents muscle disuse atrophy during leg immobilization in humans. *Acta Physiol (Oxf)*, 210, 628-41.
- DUMAS-MALLET, E., BUTTON, K. S., BORAUD, T., GONON, F. & MUNAFO, M. R. 2017. Low statistical power in biomedical science: a review of three human research domains. *R Soc Open Sci*, 4, 160254.
- DUPONT SALTER, A. C., RICHMOND, F. J. & LOEB, G. E. 2003. Effects of muscle immobilization at different lengths on tetrodotoxin-induced disuse atrophy. *IEEE Trans Neural Syst Rehabil Eng*, 11, 209-17.
- DWYER, C. M. & STICKLAND, N. C. 1992. Does the anatomical location of a muscle affect the influence of undernutrition on muscle fibre number? *J Anat*, 181 (Pt 2), 373-6.
- EDDINS, M. J., VARADAN, R., FUSHMAN, D., PICKART, C. M. & WOLBERGER, C. 2007. Crystal structure and solution NMR studies of Lys48-linked tetraubiquitin at neutral pH. *J Mol Biol*, 367, 204-11.
- EGAN, B. & ZIERATH, J. R. 2013. Exercise metabolism and the molecular regulation of skeletal muscle adaptation. *Cell Metab*, 17, 162-84.
- EGERMAN, M. A. & GLASS, D. J. 2014. Signaling pathways controlling skeletal muscle mass. *Crit Rev Biochem Mol Biol*, 49, 59-68.
- EGGER, G., JEONG, S., ESCOBAR, S. G., CORTEZ, C. C., LI, T. W., SAITO, Y., YOO, C. B., JONES, P. A. & LIANG, G. 2006. Identification of DNMT1 (DNA methyltransferase 1) hypomorphs in somatic knockouts suggests an essential role for DNMT1 in cell survival. *Proc Natl Acad Sci U S A*, 103, 14080-5.

- EGNER, I. M., BRUUSGAARD, J. C., EFTESTOL, E. & GUNDERSEN, K. 2013. A cellular memory mechanism aids overload hypertrophy in muscle long after an episodic exposure to anabolic steroids. *J Physiol*, 591, 6221-30.
- ENGLISH, K. L. & PADDON-JONES, D. 2010. Protecting muscle mass and function in older adults during bed rest. *Curr Opin Clin Nutr Metab Care*, 13, 34-9.
- EOM, G. H., KIM, K.-B., KIM, J. H., KIM, J.-Y., KIM, J.-R., KEE, H. J., KIM, D.-W., CHOE, N., PARK, H.-J., SON, H.-J., CHOI, S.-Y., KOOK, H. & SEO, S.-B. 2011. Histone Methyltransferase SETD3 Regulates Muscle Differentiation. *Journal of Biological Chemistry*, 286, 34733-34742.
- ERSKINE, R. M., JONES, D. A., WILLIAMS, A. G., STEWART, C. E. & DEGENS, H. 2010a. Inter-individual variability in the adaptation of human muscle specific tension to progressive resistance training. *Eur J Appl Physiol*, 110, 1117-25.
- ERSKINE, R. M., JONES, D. A., WILLIAMS, A. G., STEWART, C. E. & DEGENS, H. 2010b. Resistance training increases in vivo quadriceps femoris muscle specific tension in young men. *Acta Physiol (Oxf)*, 199, 83-9.
- FAHEY, A. J., BRAMELD, J. M., PARR, T. AND BUTTERY, P. J. 2005 The effect of maternal undernutrition before muscle differentiation on the muscle fiber development of the newborn lamb. *American Society of Animal Science*, 83, 2564-2571.
- FIGEAC, N. & ZAMMIT, P. S. 2015. Coordinated action of Axin1 and Axin2 suppresses beta-catenin to regulate muscle stem cell function. *Cell Signal*, 27, 1652-65.
- FISHER, A. G. 2012. *Transcriptional Profiling to Identify Therapeutic Targets Influencing Skeletal Muscle Atrophy*. Ph.D, University of Liverpool.
- FISHER, A. G., SEABORNE, R. A., HUGHES, T. M., GUTTERIDGE, A., STEWART, C., COULSON, J. M., SHARPLES, A. P. & JARVIS, J. C. 2017. Transcriptomic and epigenetic regulation of disuse atrophy and the return to activity in skeletal muscle. *Faseb j*.
- FOULSTONE, E. J., HUSER, C., CROWN, A. L., HOLLY, J. M. & STEWART, C. E. 2004. Differential signalling mechanisms predisposing primary human skeletal muscle cells to altered proliferation and differentiation: roles of IGF-I and TNFalpha. *Exp Cell Res*, 294, 223-35.
- FOULSTONE, E. J., MEADOWS, K. A., HOLLY, J. M. & STEWART, C. E. 2001. Insulin-like growth factors (IGF-I and IGF-II) inhibit C2 skeletal myoblast differentiation and enhance TNF alpha-induced apoptosis. *J Cell Physiol*, 189, 207-15.
- FOULSTONE, E. J., SAVAGE, P. B., CROWN, A. L., HOLLY, J. M. & STEWART, C. E. 2003a. Adaptations of the IGF system during malignancy: human skeletal muscle versus the systemic environment. *Horm Metab Res*, 35, 667-74.
- FOULSTONE, E. J., SAVAGE, P. B., CROWN, A. L., HOLLY, J. M. & STEWART, C. E. 2003b. Role of insulin-like growth factor binding protein-3 (IGFBP-3) in the differentiation of primary human adult skeletal myoblasts. *J Cell Physiol*, 195, 70-9.
- FROMMER, M., MCDONALD, L. E., MILLAR, D. S., COLLIS, C. M., WATT, F., GRIGG, G. W., MOLLOY, P. L. & PAUL, C. L. 1992. A genomic sequencing protocol that yields a positive display of 5-methylcytosine residues in individual DNA strands. *Proc Natl Acad Sci U S A*, 89, 1827-31.
- FRONTERA, W. R. & OCHALA, J. 2015. Skeletal muscle: a brief review of structure and function. *Calcif Tissue Int*, 96, 183-95.

- FRY, A. C. 2004. The Role of Resistance Exercise Intensity on Muscle Fibre Adaptations. *Sports Medicine*, 34, 663-679.
- FUKS, F., HURD, P. J., WOLF, D., NAN, X., BIRD, A. P. & KOUZARIDES, T. 2003. The methyl-CpG-binding protein MeCP2 links DNA methylation to histone methylation. *J Biol Chem*, 278, 4035-40.
- FURUYAMA, T., KITAYAMA, K., YAMASHITA, H. & MORI, N. 2003. Forkhead transcription factor FOXO1 (FKHR)-dependent induction of PDK4 gene expression in skeletal muscle during energy deprivation. *Biochem J*, 375, 365-71.
- GAROFANO, A., CZERNICHOW, P. & BREANT, B. 1998. Postnatal somatic growth and insulin contents in moderate or severe intrauterine growth retardation in the rat. *Biol Neonate*, 73, 89-98.
- GINGRAS, A. R., LIU, J. J. & GINSBERG, M. H. 2012. Structural basis of the junctional anchorage of the cerebral cavernous malformations complex. *J Cell Biol*, 199, 39-48.
- GINIATULLIN, R., NISTRI, A. & YAKEL, J. L. 2005. Desensitization of nicotinic ACh receptors: shaping cholinergic signaling. *Trends Neurosci*, 28, 371-8.
- GIRVEN, M., DUGDALE, H. F., OWENS, D. J., HUGHES, D. C., STEWART, C. E. & SHARPLES, A. P. 2016. l-glutamine Improves Skeletal Muscle Cell Differentiation and Prevents Myotube Atrophy After Cytokine (TNF-alpha) Stress Via Reduced p38 MAPK Signal Transduction. *J Cell Physiol*, 231, 2720-32.
- GLOVER, E. I., PHILLIPS, S. M., OATES, B. R., TANG, J. E., TARNOPOLSKY, M. A., SELBY, A., SMITH, K. & RENNIE, M. J. 2008. Immobilization induces anabolic resistance in human myofibrillar protein synthesis with low and high dose amino acid infusion. *J Physiol*, 586, 6049-61.
- GOLDBERG, A. L. 1969. Protein turnover in skeletal muscle. II. Effects of denervation and cortisone on protein catabolism in skeletal muscle. *J Biol Chem*, 244, 3223-9.
- GOMES, M. D., LECKER, S. H., JAGOE, R. T., NAVON, A. & GOLDBERG, A. L. 2001. Atrogin-1, a muscle-specific F-box protein highly expressed during muscle atrophy. *Proc Natl Acad Sci U S A*, 98, 14440-5.
- GOPALAKRISHNAN, S., VAN EMBURGH, B. O. & ROBERTSON, K. D. 2008. DNA methylation in development and human disease. *Mutat Res*, 647, 30-8.
- GROHMANN, M., FOULSTONE, E., WELSH, G., HOLLY, J., SHIELD, J., CROWNE, E. & STEWART, C. 2005a. Isolation and validation of human prepubertal skeletal muscle cells: maturation and metabolic effects of IGF-I, IGFBP-3 and TNFalpha. *J Physiol*, 568, 229-42.
- GROHMANN, M., SABIN, M., HOLLY, J., SHIELD, J., CROWNE, E. & STEWART, C. 2005b. Characterization of differentiated subcutaneous and visceral adipose tissue from children the influences of TNF- α and IGF-I. *Journal of lipid research*, 46, 93-103.
- HALES, C. N. & BARKER, D. J. 1992. Type 2 (non-insulin-dependent) diabetes mellitus: the thrifty phenotype hypothesis. *Diabetologia*, 35, 595-601.
- HAN, Y., WANG, C., PARK, J. S. & NIU, L. 2010. Channel-opening kinetic mechanism for human wild-type GluK2 and the M867I mutant kainate receptor. *Biochemistry*, 49, 9207-16.

- HAUSCHKA, E. O., ROY, R. R. & EDGERTON, V. R. 1988. Periodic weight support effects on rat soleus fibers after hindlimb suspension. *J Appl Physiol* (1985), 65, 1231-7.
- HOLECEK, M. 2012. Muscle wasting in animal models of severe illness. *Int J Exp Pathol*, 93, 157-71.
- HOPPELER, H., LUTHI, P., CLAASSEN, H., WEIBEL, E. R. & HOWALD, H. 1973. The ultrastructure of the normal human skeletal muscle. A morphometric analysis on untrained men, women and well-trained orienteers. *Pflugers Arch*, 344, 217-32.
- HU, G., WANG, X., SAUNDERS, D. N., HENDERSON, M., RUSSELL, A. J., HERRING, B. P. & ZHOU, J. 2010. Modulation of myocardin function by the ubiquitin E3 ligase UBR5. *J Biol Chem*, 285, 11800-9.
- HUGHES, V. A., FRONTERA, W. R., WOOD, M., EVANS, W. J., DALLAL, G. E., ROUBENOFF, R. & FIATARONE SINGH, M. A. 2001. Longitudinal muscle strength changes in older adults: influence of muscle mass, physical activity, and health. *J Gerontol A Biol Sci Med Sci*, 56, B209-17.
- HURASKIN, D., EIBER, N., REICHEL, M., ZIDEK, L. M., KRAVIC, B., BERNKOPF, D., VON MALTZAHN, J., BEHRENS, J. & HASHEMOLHOSSEINI, S. 2016. Wnt/beta-catenin signaling via Axin2 is required for myogenesis and, together with YAP/Taz and Tead1, active in Ila/Ilx muscle fibers. *Development*, 143, 3128-42.
- IBEBUNJO, C., CHICK, J. M., KENDALL, T., EASH, J. K., LI, C., ZHANG, Y., VICKERS, C., WU, Z., CLARKE, B. A., SHI, J., CRUZ, J., FOURNIER, B., BRACHAT, S., GUTZWILLER, S., MA, Q., MARKOVITS, J., BROOME, M., STEINKRAUSS, M., SKUBA, E., GALARNEAU, J. R., GYGI, S. P. & GLASS, D. J. 2013. Genomic and proteomic profiling reveals reduced mitochondrial function and disruption of the neuromuscular junction driving rat sarcopenia. *Mol Cell Biol*, 33, 194-212.
- INSKIP, H. M., GODFREY, K. M., MARTIN, H. J., SIMMONDS, S. J., COOPER, C. & SAYER, A. A. 2007. Size at birth and its relation to muscle strength in young adult women. *J Intern Med*, 262, 368-74.
- IRIZARRY, R. A., BOLSTAD, B. M., COLLIN, F., COPE, L. M., HOBBS, B. & SPEED, T. P. 2003a. Summaries of Affymetrix GeneChip probe level data. *Nucleic Acids Res*, 31, e15.
- IRIZARRY, R. A., HOBBS, B., COLLIN, F., BEAZER-BARCLAY, Y. D., ANTONELLIS, K. J., SCHERF, U. & SPEED, T. P. 2003b. Exploration, normalization, and summaries of high density oligonucleotide array probe level data. *Biostatistics*, 4, 249-64.
- ITO, S., D'ALESSIO, A. C., TARANOVA, O. V., HONG, K., SOWERS, L. C. & ZHANG, Y. 2010. Role of Tet proteins in 5mC to 5hmC conversion, ES-cell self-renewal and inner cell mass specification. *Nature*, 466, 1129-33.
- IVEY, F. M., ROTH, S. M., FERRELL, R. E., TRACY, B. L., LEMMER, J. T., HURLBUT, D. E., MARTEL, G. F., SIEGEL, E. L., FOZARD, J. L., JEFFREY METTER, E., FLEG, J. L. & HURLEY, B. F. 2000. Effects of age, gender, and myostatin genotype on the hypertrophic response to heavy resistance strength training. *J Gerontol A Biol Sci Med Sci*, 55, M641-8.
- JACOBSEN, S. C., BRONS, C., BORK-JENSEN, J., RIBEL-MADSEN, R., YANG, B., LARA, E., HALL, E., CALVANESE, V., NILSSON, E., JORGENSEN, S. W., MANDRUP, S.,

- LING, C., FERNANDEZ, A. F., FRAGA, M. F., POULSEN, P. & VAAG, A. 2012. Effects of short-term high-fat overfeeding on genome-wide DNA methylation in the skeletal muscle of healthy young men. *Diabetologia*, 55, 3341-9.
- JAENISCH, R. & BIRD, A. 2003. Epigenetic regulation of gene expression: how the genome integrates intrinsic and environmental signals. *Nat Genet*, 33 Suppl, 245-54.
- JARVIS, J. C. & SALMONS, S. 1991. A family of neuromuscular stimulators with optical transcutaneous control. *J Med Eng Technol*, 15, 53-7.
- JAWORSKI, K., AHMADIAN, M., DUNCAN, R. E., SARKADI-NAGY, E., VARADY, K. A., HELLERSTEIN, M. K., LEE, H. Y., SAMUEL, V. T., SHULMAN, G. I., KIM, K. H., DE VAL, S., KANG, C. & SUL, H. S. 2009. AdPLA ablation increases lipolysis and prevents obesity induced by high-fat feeding or leptin deficiency. *Nat Med*, 15, 159-68.
- JEJURIKAR, S. S., HENKELMAN, E. A., CEDERNA, P. S., MARCELO, C. L., URBANCHEK, M. G. & KUZON, W. M., JR. 2006. Aging increases the susceptibility of skeletal muscle derived satellite cells to apoptosis. *Exp Gerontol*, 41, 828-36.
- JIN, B., TAO, Q., PENG, J., SOO, H. M., WU, W., YING, J., FIELDS, C. R., DELMAS, A. L., LIU, X., QIU, J. & ROBERTSON, K. D. 2008. DNA methyltransferase 3B (DNMT3B) mutations in ICF syndrome lead to altered epigenetic modifications and aberrant expression of genes regulating development, neurogenesis and immune function. *Hum Mol Genet*, 17, 690-709.
- JIN, B., YAO, B., LI, J. L., FIELDS, C. R., DELMAS, A. L., LIU, C. & ROBERTSON, K. D. 2009. DNMT1 and DNMT3B modulate distinct polycomb-mediated histone modifications in colon cancer. *Cancer Res*, 69, 7412-21.
- JONES, P. A. & BAYLIN, S. B. 2007. The epigenomics of cancer. *Cell*, 128, 683-92.
- JONES, P. L., VEENSTRA, G. J., WADE, P. A., VERMAAK, D., KASS, S. U., LANDSBERGER, N., STROUBOULIS, J. & WOLFFE, A. P. 1998. Methylated DNA and MeCP2 recruit histone deacetylase to repress transcription. *Nat Genet*, 19, 187-91.
- KANEHISA, M., FURUMICHI, M., TANABE, M., SATO, Y. & MORISHIMA, K. 2017. KEGG: new perspectives on genomes, pathways, diseases and drugs. *Nucleic Acids Res*, 45, D353-d361.
- KANEHISA, M. & GOTO, S. 2000. KEGG: kyoto encyclopedia of genes and genomes. *Nucleic Acids Res*, 28, 27-30.
- KANEHISA, M., SATO, Y., KAWASHIMA, M., FURUMICHI, M. & TANABE, M. 2016. KEGG as a reference resource for gene and protein annotation. *Nucleic Acids Res*, 44, D457-62.
- KIDO, K., ATO, S., YOKOKAWA, T., MAKANAE, Y., SATO, K. & FUJITA, S. 2016. Acute resistance exercise-induced IGF1 expression and subsequent GLUT4 translocation. *Physiol Rep*, 4.
- KING-HIMMELREICH, T. S., SCHRAMM, S., WOLTERS, M. C., SCHMETZER, J., MOSER, C. V., KNOTHE, C., RESCH, E., PEIL, J., GEISSLINGER, G. & NIEDERBERGER, E. 2016. The impact of endurance exercise on global and AMPK gene-specific DNA methylation. *Biochem Biophys Res Commun*, 474, 284-90.
- KLEAVELAND, B., ZHENG, X., LIU, J. J., BLUM, Y., TUNG, J. J., ZOU, Z., SWEENEY, S. M., CHEN, M., GUO, L., LU, M. M., ZHOU, D., KITAJEWSKI, J., AFFOLTER, M., GINSBERG, M. H. & KAHN, M. L. 2009. Regulation of cardiovascular

- development and integrity by the heart of glass-cerebral cavernous malformation protein pathway. *Nat Med*, 15, 169-76.
- KONG, X., BALL, A. R., PHAM, H. X., ZENG, W., CHEN, H. Y., SCHMIESING, J. A., KIM, J. S., BERNS, M. & YOKOMORI, K. 2014. Distinct Functions of Human Cohesin-SA1 and Cohesin-SA2 in Double-Strand Break Repair. *Mol Cell Biol*, 34, 685-98.
- KRAEMER, W. J., FLECK, S. J. & DESCHENES, M. R. 2012. *Exercise Physiology: Integrating Theory and Application* Philadelphia Lippincott Williams & Wilkins.
- KUANG, E., QI, J. & RONAI, Z. 2013. Emerging roles of E3 ubiquitin ligases in autophagy. *Trends Biochem Sci*, 38, 453-60.
- KUANG, S., KURODA, K., LE GRAND, F. & RUDNICKI, M. A. 2007. Asymmetric self-renewal and commitment of satellite stem cells in muscle. *Cell*, 129, 999-1010.
- LAKER, R. C., GARDE, C., CAMERA, D. M., SMILES, W. J., ZIERATH, J. R., HAWLEY, J. A. & BARRES, R. 2017. Transcriptomic and epigenetic responses to short-term nutrient-exercise stress in humans. *Sci Rep*, 7, 15134.
- LAKER, R. C., LILLARD, T. S., OKUTSU, M., ZHANG, M., HOEHN, K. L., CONNELLY, J. J. & YAN, Z. 2014. Exercise prevents maternal high-fat diet-induced hypermethylation of the Pgc-1alpha gene and age-dependent metabolic dysfunction in the offspring. *Diabetes*, 63, 1605-11.
- LANE, S. C., CAMERA, D. M., LASSITER, D. G., ARETA, J. L., BIRD, S. R., YEO, W. K., JEACOCKE, N. A., KROOK, A., ZIERATH, J. R., BURKE, L. M. & HAWLEY, J. A. 2015. Effects of sleeping with reduced carbohydrate availability on acute training responses. *J Appl Physiol (1985)*, 119, 643-55.
- LAPLANTE, M. & SABATINI, D. M. 2012. mTOR signaling in growth control and disease. *Cell*, 149, 274-93.
- LE GRAND, F. & RUDNICKI, M. A. 2007. Skeletal muscle satellite cells and adult myogenesis. *Curr Opin Cell Biol*, 19, 628-33.
- LECKER, S. H., JAGOE, R. T., GILBERT, A., GOMES, M., BARACOS, V., BAILEY, J., PRICE, S. R., MITCH, W. E. & GOLDBERG, A. L. 2004. Multiple types of skeletal muscle atrophy involve a common program of changes in gene expression. *Faseb j*, 18, 39-51.
- LEONHARDT, H., PAGE, A. W., WEIER, H. U. & BESTOR, T. H. 1992. A targeting sequence directs DNA methyltransferase to sites of DNA replication in mammalian nuclei. *Cell*, 71, 865-73.
- LESCAUDRON, L., PELTEKIAN, E., FONTAINE-PERUS, J., PAULIN, D., ZAMPIERI, M., GARCIA, L. & PARRISH, E. 1999. Blood borne macrophages are essential for the triggering of muscle regeneration following muscle transplant. *Neuromuscul Disord*, 9, 72-80.
- LEVY, S., SUTTON, G., NG, P. C., FEUK, L., HALPERN, A. L., WALENZ, B. P., AXELROD, N., HUANG, J., KIRKNESS, E. F., DENISOV, G., LIN, Y., MACDONALD, J. R., PANG, A. W., SHAGO, M., STOCKWELL, T. B., TSIAMOURI, A., BAFNA, V., BANSAL, V., KRAVITZ, S. A., BUSAM, D. A., BEESON, K. Y., MCINTOSH, T. C., REMINGTON, K. A., ABRIL, J. F., GILL, J., BORMAN, J., ROGERS, Y. H., FRAZIER, M. E., SCHERER, S. W., STRAUSBERG, R. L. & VENTER, J. C. 2007. The diploid genome sequence of an individual human. *PLoS Biol*, 5, e254.

- LEXELL, J., TAYLOR, C. C. & SJOSTROM, M. 1988. What is the cause of the ageing atrophy? Total number, size and proportion of different fiber types studied in whole vastus lateralis muscle from 15- to 83-year-old men. *J Neurol Sci*, 84, 275-94.
- LI, Y. P. 2003. TNF-alpha is a mitogen in skeletal muscle. *Am J Physiol Cell Physiol*, 285, C370-6.
- LI, Y. P., CHEN, Y., JOHN, J., MOYLAN, J., JIN, B., MANN, D. L. & REID, M. B. 2005. TNF-alpha acts via p38 MAPK to stimulate expression of the ubiquitin ligase atrogin1/MAFbx in skeletal muscle. *Faseb J*, 19, 362-70.
- LI, Y. P., LECKER, S. H., CHEN, Y., WADDELL, I. D., GOLDBERG, A. L. & REID, M. B. 2003. TNF-alpha increases ubiquitin-conjugating activity in skeletal muscle by up-regulating UbcH2/E220k. *Faseb J*, 17, 1048-57.
- LI, Y. P. & REID, M. B. 2000. NF-kappaB mediates the protein loss induced by TNF-alpha in differentiated skeletal muscle myotubes. *Am J Physiol Regul Integr Comp Physiol*, 279, R1165-70.
- LIAO, L., SONG, M., LI, X., TANG, L., ZHANG, T., ZHANG, L., PAN, Y., CHOUCANE, L. & MA, X. 2017. E3 Ubiquitin Ligase UBR5 Drives the Growth and Metastasis of Triple-Negative Breast Cancer. *Cancer Res*, 77, 2090-2101.
- LINDHOLM, M. E., MARABITA, F., GOMEZ-CABRERO, D., RUNDQVIST, H., EKSTROM, T. J., TEGNER, J. & SUNDBERG, C. J. 2014. An integrative analysis reveals coordinated reprogramming of the epigenome and the transcriptome in human skeletal muscle after training. *Epigenetics*, 9, 1557-69.
- LONG, M. D., SMIRAGLIA, D. J. & CAMPBELL, M. J. 2017. The Genomic Impact of DNA CpG Methylation on Gene Expression; Relationships in Prostate Cancer. *Biomolecules*, 7.
- LONG, X., CREEMERS, E. E., WANG, D. Z., OLSON, E. N. & MIANO, J. M. 2007. Myocardin is a bifunctional switch for smooth versus skeletal muscle differentiation. *Proc Natl Acad Sci U S A*, 104, 16570-5.
- LUNYAK, V. V., BURGESS, R., PREFONTAINE, G. G., NELSON, C., SZE, S. H., CHENOWETH, J., SCHWARTZ, P., PEVZNER, P. A., GLASS, C., MANDEL, G. & ROSENFELD, M. G. 2002. Corepressor-dependent silencing of chromosomal regions encoding neuronal genes. *Science*, 298, 1747-52.
- MABLY, J. D., MOHIDEEN, M. A., BURNS, C. G., CHEN, J. N. & FISHMAN, M. C. 2003. heart of glass regulates the concentric growth of the heart in zebrafish. *Curr Biol*, 13, 2138-47.
- MACKEY, A. L., KJAER, M., DANDANELL, S., MIKKELSEN, K. H., HOLM, L., DOSSING, S., KADI, F., KOSKINEN, S. O., JENSEN, C. H., SCHRODER, H. D. & LANGBERG, H. 2007. The influence of anti-inflammatory medication on exercise-induced myogenic precursor cell responses in humans. *J Appl Physiol (1985)*, 103, 425-31.
- MACLAREN, D. & MORTON, J. P. 2011. *Biochemistry for Sport and Exercise Metabolism*, London, UK, Wiley.
- MACPHERSON, P. C. D., WANG, X. & GOLDMAN, D. 2011. Myogenin Regulates Denervation-Dependent Muscle Atrophy in Mouse Soleus Muscle. *J Cell Biochem*, 112, 2149-59.

- MAIER, A., CROCKETT, J. L., SIMPSON, D. R., SAUBERT, C. I. & EDGERTON, V. R. 1976. Properties of immobilized guinea pig hindlimb muscles. *Am J Physiol*, 231, 1520-6.
- MAKSIMOVIC, J., GORDON, L. & OSHLACK, A. 2012. SWAN: Subset-quantile within array normalization for illumina infinium HumanMethylation450 BeadChips. *Genome Biol*, 13, R44.
- MALLINSON, J. E., SCULLEY, D. V., CRAIGON, J., PLANT, R., LANGLEY-EVANS, S. C. & BRAMELD, J. M. 2007. Fetal exposure to a maternal low-protein diet during mid-gestation results in muscle-specific effects on fibre type composition in young rats. *Br J Nutr*, 98, 292-9.
- MANSFIELD, E., HERSPERGER, E., BIGGS, J. & SHEARN, A. 1994. Genetic and molecular analysis of hyperplastic discs, a gene whose product is required for regulation of cell proliferation in *Drosophila melanogaster* imaginal discs and germ cells. *Dev Biol*, 165, 507-26.
- MAPLES, J. M. & BRAULT, J. J. 2015. Lipid exposure elicits differential responses in gene expression and DNA methylation in primary human skeletal muscle cells from severely obese women. 47, 139-46.
- MARTARELLI, D., CATALANO, A., PROCOPIO, A., ORECCHIA, S., LIBENER, R. & SANTONI, G. 2006. Characterization of human malignant mesothelioma cell lines orthotopically implanted in the pleural cavity of immunodeficient mice for their ability to grow and form metastasis. *BMC Cancer*, 6, 130.
- MCCABE, M. T., BRANDES, J. C. & VERTINO, P. M. 2009. Cancer DNA methylation: molecular mechanisms and clinical implications. *Clin Cancer Res*, 15, 3927-37.
- MEADOWS, K. A., HOLLY, J. M. & STEWART, C. E. 2000. Tumor necrosis factor-alpha-induced apoptosis is associated with suppression of insulin-like growth factor binding protein-5 secretion in differentiating murine skeletal myoblasts. *J Cell Physiol*, 183, 330-7.
- MEADOWS, S. M., WARKMAN, A. S., SALANGA, M. C., SMALL, E. M. & KRIEG, P. A. 2008. The myocardin-related transcription factor, MASTR, cooperates with MyoD to activate skeletal muscle gene expression. *Proc Natl Acad Sci U S A*, 105, 1545-50.
- MICHEL, R. N. & GARDINER, P. F. 1990. To what extent is hindlimb suspension a model of disuse? *Muscle Nerve*, 13, 646-653.
- MIDRIO, M. 2006. The denervated muscle: facts and hypotheses. A historical review. *Eur J Appl Physiol*, 98, 1-21.
- MIKKELSEN, U. R., LANGBERG, H., HELMARK, I. C., SKOVGAARD, D., ANDERSEN, L. L., KJAER, M. & MACKEY, A. L. 2009. Local NSAID infusion inhibits satellite cell proliferation in human skeletal muscle after eccentric exercise. *J Appl Physiol (1985)*, 107, 1600-11.
- MORESI, V., WILLIAMS, A. H., MEADOWS, E., FLYNN, J. M., POTTHOFF, M. J., MCANALLY, J., SHELTON, J. M., BACKS, J., KLEIN, W. H., RICHARDSON, J. A., BASSEL-DUBY, R. & OLSON, E. N. 2010. Myogenin and class II HDACs control neurogenic muscle atrophy by inducing E3 ubiquitin ligases. *Cell*, 143, 35-45.
- MURANI, E., MURANIOVA, M., PONSUKSILI, S., SCHELLANDER, K. & WIMMERS, K. 2007. Identification of genes differentially expressed during prenatal

- development of skeletal muscle in two pig breeds differing in muscularity. *BMC Dev Biol*, 7, 109.
- NAN, X., CAMPOY, F. J. & BIRD, A. 1997. MeCP2 is a transcriptional repressor with abundant binding sites in genomic chromatin. *Cell*, 88, 471-81.
- NAN, X., NG, H. H., JOHNSON, C. A., LAHERTY, C. D., TURNER, B. M., EISENMAN, R. N. & BIRD, A. 1998. Transcriptional repression by the methyl-CpG-binding protein MeCP2 involves a histone deacetylase complex. *Nature*, 393, 386-9.
- NANA, A., SLATER, G. J., HOPKINS, W. G. & BURKE, L. M. 2012. Effects of daily activities on dual-energy X-ray absorptiometry measurements of body composition in active people. *Med Sci Sports Exerc*, 44, 180-9.
- NARICI, M. V. & MAFFULLI, N. 2010. Sarcopenia: characteristics, mechanisms and functional significance. *Br Med Bull*, 95, 139-59.
- NAVE, B. T., OUWENS, M., WITHERS, D. J., ALESSI, D. R. & SHEPHERD, P. R. 1999. Mammalian target of rapamycin is a direct target for protein kinase B: identification of a convergence point for opposing effects of insulin and amino-acid deficiency on protein translation. *Biochem J*, 344 Pt 2, 427-31.
- NICKS, D. K., BENEKE, W. M., KEY, R. M. & TIMSON, B. F. 1989. Muscle fibre size and number following immobilisation atrophy. *J Anat*, 163, 1-5.
- NIKAWA, T., ISHIDOH, K., HIRASAKA, K., ISHIHARA, I., IKEMOTO, M., KANO, M., KOMINAMI, E., NONAKA, I., OGAWA, T., ADAMS, G. R., BALDWIN, K. M., YASUI, N., KISHI, K. & TAKEDA, S. 2004. Skeletal muscle gene expression in space-flown rats. *Faseb j*, 18, 522-4.
- NITERT, M. D., DAYEH, T., VOLKOV, P., ELGZYRI, T., HALL, E., NILSSON, E., YANG, B. T., LANG, S., PARIKH, H., WESSMAN, Y., WEISHAUPT, H., ATTEMA, J., ABELS, M., WIERUP, N., ALMGREN, P., JANSSON, P. A., RONN, T., HANSSON, O., ERIKSSON, K. F., GROOP, L. & LING, C. 2012. Impact of an exercise intervention on DNA methylation in skeletal muscle from first-degree relatives of patients with type 2 diabetes. *Diabetes*, 61, 3322-32.
- PADDON-JONES, D. & RASMUSSEN, B. B. 2009. Dietary protein recommendations and the prevention of sarcopenia. *Curr Opin Clin Nutr Metab Care*, 12, 86-90.
- PEREIRA, M. G., DYAR, K. A., NOGARA, L., SOLAGNA, F., MARABITA, M., BARALDO, M., CHEMELLO, F., GERMINARIO, E., ROMANELLO, V., NOLTE, H. & BLAAUW, B. 2017. Comparative Analysis of Muscle Hypertrophy Models Reveals Divergent Gene Transcription Profiles and Points to Translational Regulation of Muscle Growth through Increased mTOR Signaling. *Front Physiol*, 8, 968.
- PERRY, C. G., LALLY, J., HOLLOWAY, G. P., HEIGENHAUSER, G. J., BONEN, A. & SPIRIET, L. L. 2010. Repeated transient mRNA bursts precede increases in transcriptional and mitochondrial proteins during training in human skeletal muscle. *J Physiol*, 588, 4795-810.
- PETERSON, M. D., PISTILLI, E., HAFF, G. G., HOFFMAN, E. P. & GORDON, P. M. 2011. Progression of volume load and muscular adaptation during resistance exercise. *Eur J Appl Physiol*, 111, 1063-71.
- PETRELLA, J. K., KIM, J. S., MAYHEW, D. L., CROSS, J. M. & BAMMAN, M. M. 2008. Potent myofiber hypertrophy during resistance training in humans is associated with satellite cell-mediated myonuclear addition: a cluster analysis. *J Appl Physiol (1985)*, 104, 1736-42.

- PHILIPPOU, A., PAPAGEORGIOU, E., BOGDANIS, G., HALAPAS, A., SOURLA, A., MARIDAKI, M., PISSIMISSIS, N. & KOUTSILIERIS, M. 2009. Expression of IGF-1 isoforms after exercise-induced muscle damage in humans: characterization of the MGF E peptide actions in vitro. *In Vivo*, 23, 567-75.
- PHILLIPS, B. E., WILLIAMS, J. P., GUSTAFSSON, T., BOUCHARD, C., RANKINEN, T., KNUDSEN, S., SMITH, K., TIMMONS, J. A. & ATHERTON, P. J. 2013. Molecular networks of human muscle adaptation to exercise and age. *PLoS Genet*, 9, e1003389.
- PHILLIPS, S. M. 2014. A brief review of critical processes in exercise-induced muscular hypertrophy. *Sports Med*, 44 Suppl 1, S71-7.
- PIDSLEY, R., ZOTENKO, E., PETERS, T. J., LAWRENCE, M. G., RISBRIDGER, G. P., MOLLOY, P., VAN DJIK, S., MUHLHAUSLER, B., STIRZAKER, C. & CLARK, S. J. 2016. Critical evaluation of the Illumina MethylationEPIC BeadChip microarray for whole-genome DNA methylation profiling. *Genome Biol*, 17, 208.
- POMERANTZ, J. L. & BALTIMORE, D. 1999. NF-kappaB activation by a signaling complex containing TRAF2, TANK and TBK1, a novel IKK-related kinase. *Embo j*, 18, 6694-704.
- PORTER, M. M., VANDERVOORT, A. A. & LEXELL, J. 1995. Aging of human muscle: structure, function and adaptability. *Scand J Med Sci Sports*, 5, 129-42.
- PRADHAN, S., BACOLLA, A., WELLS, R. D. & ROBERTS, R. J. 1999. Recombinant human DNA (cytosine-5) methyltransferase. I. Expression, purification, and comparison of de novo and maintenance methylation. *J Biol Chem*, 274, 33002-10.
- PROBST, A. V., DUNLEAVY, E. & ALMOUZNI, G. 2009. Epigenetic inheritance during the cell cycle. *Nat Rev Mol Cell Biol*, 10, 192-206.
- RAMASWAMY, S., NAKAMURA, N., SANSAL, I., BERGERON, L. & SELLERS, W. R. 2002. A novel mechanism of gene regulation and tumor suppression by the transcription factor FKHR. *Cancer Cell*, 2, 81-91.
- RAMSAHOYE, B. H., BINISZKIEWICZ, D., LYKO, F., CLARK, V., BIRD, A. P. & JAENISCH, R. 2000. Non-CpG methylation is prevalent in embryonic stem cells and may be mediated by DNA methyltransferase 3a. *Proc Natl Acad Sci U S A*, 97, 5237-42.
- RANTANEN, T. 2003. Muscle strength, disability and mortality. *Scand J Med Sci Sports*, 13, 3-8.
- RANTANEN, T., AVLUND, K., SUOMINEN, H., SCHROLL, M., FRANDIN, K. & PERTTI, E. 2002. Muscle strength as a predictor of onset of ADL dependence in people aged 75 years. *Aging Clin Exp Res*, 14, 10-5.
- RANTANEN, T., GURALNIK, J. M., FOLEY, D., MASAKI, K., LEVEILLE, S., CURB, J. D. & WHITE, L. 1999. Midlife hand grip strength as a predictor of old age disability. *Jama*, 281, 558-60.
- RAUE, U., TRAPPE, T. A., ESTREM, S. T., QIAN, H. R., HELVERING, L. M., SMITH, R. C. & TRAPPE, S. 2012. Transcriptome signature of resistance exercise adaptations: mixed muscle and fiber type specific profiles in young and old adults. *J Appl Physiol (1985)*, 112, 1625-36.
- REIK, W., DEAN, W. & WALTER, J. 2001. Epigenetic reprogramming in mammalian development. *Science*, 293, 1089-93.

- RENNIE, M. J., SELBY, A., ATHERTON, P., SMITH, K., KUMAR, V., GLOVER, E. L. & PHILIPS, S. M. 2010. Facts, noise and wishful thinking: muscle protein turnover in aging and human disuse atrophy. *Scand J Med Sci Sports*, 20, 5-9.
- RIGGS, A. D. & XIONG, Z. 2004. Methylation and epigenetic fidelity. *Proc Natl Acad Sci U S A*, 101, 4-5.
- ROBERTSON, K. D. 2005. DNA methylation and human disease. *Nat Rev Genet*, 6, 597-610.
- ROMANICK, M., THOMPSON, L. V. & BROWN-BORG, H. M. 2013. Murine models of atrophy, cachexia, and sarcopenia in skeletal muscle. *Biochim Biophys Acta*, 1832, 1410-20.
- ROMMEL, C., BODINE, S. C., CLARKE, B. A., ROSSMAN, R., NUNEZ, L., STITT, T. N., YANCOPOULOS, G. D. & GLASS, D. J. 2001. Mediation of IGF-1-induced skeletal myotube hypertrophy by PI(3)K/Akt/mTOR and PI(3)K/Akt/GSK3 pathways. *Nat Cell Biol*, 3, 1009-13.
- RONN, T., VOLKOV, P., DAVEGARDH, C., DAYEH, T., HALL, E., OLSSON, A. H., NILSSON, E., TORNBERG, A., DEKKER NITERT, M., ERIKSSON, K. F., JONES, H. A., GROOP, L. & LING, C. 2013. A six months exercise intervention influences the genome-wide DNA methylation pattern in human adipose tissue. *PLoS Genet*, 9, e1003572.
- ROUNTREE, M. R. & SELKER, E. U. 1997. DNA methylation inhibits elongation but not initiation of transcription in *Neurospora crassa*. *Genes Dev*, 11, 2383-95.
- SAINI, A., AL-SHANTI, N., FAULKNER, S. H. & STEWART, C. E. 2008. Pro- and anti-apoptotic roles for IGF-I in TNF-alpha-induced apoptosis: a MAP kinase mediated mechanism. *Growth Factors*, 26, 239-53.
- SAINI, A., AL-SHANTI, N., SHARPLES, A. P. & STEWART, C. E. 2012. Sirtuin 1 regulates skeletal myoblast survival and enhances differentiation in the presence of resveratrol. *Exp Physiol*, 97, 400-18.
- SAINI, A., AL-SHANTI, N. & STEWART, C. 2010. C2 skeletal myoblast survival, death, proliferation and differentiation: regulation by Adra1d. *Cell Physiol Biochem*, 25, 253-62.
- SANDRI, M., SANDRI, C., GILBERT, A., SKURK, C., CALABRIA, E., PICARD, A., WALSH, K., SCHIAFFINO, S., LECKER, S. H. & GOLDBERG, A. L. 2004. Foxo transcription factors induce the atrophy-related ubiquitin ligase atrogin-1 and cause skeletal muscle atrophy. *Cell*, 117, 399-412.
- SANDSMARK, D. K., PELLETIER, C., WEBER, J. D. & GUTMANN, D. H. 2007. Mammalian target of rapamycin: master regulator of cell growth in the nervous system. *Histol Histopathol*, 22, 895-903.
- SARTORI, R., SCHIRWIS, E., BLAAUW, B., BORTOLANZA, S., ZHAO, J., ENZO, E., STANTZOU, A., MOUISEL, E., TONIOLO, L., FERRY, A., STRICKER, S., GOLDBERG, A. L., DUPONT, S., PICCOLO, S., AMTHOR, H. & SANDRI, M. 2013. BMP signaling controls muscle mass. *Nat Genet*, 45, 1309-18.
- SARWAR, R., NICLOS, B. B. & RUTHERFORD, O. M. 1996. Changes in muscle strength, relaxation rate and fatigability during the human menstrual cycle. *J Physiol*, 493 (Pt 1), 267-72.
- SAYER, A. A., SYDDALL, H., MARTIN, H., PATEL, H., BAYLIS, D. & COOPER, C. 2008. The developmental origins of sarcopenia. *J Nutr Health Aging*, 12, 427-32.

- SAYER, A. A., SYDDALL, H. E., GILBODY, H. J., DENNISON, E. M. & COOPER, C. 2004. Does sarcopenia originate in early life? Findings from the Hertfordshire cohort study. *J Gerontol A Biol Sci Med Sci*, 59, M930-4.
- SCANLON, T. C., FRAGALA, M. S., STOUT, J. R., EMERSON, N. S., BEYER, K. S., OLIVEIRA, L. P. & HOFFMAN, J. R. 2014. Muscle architecture and strength: adaptations to short-term resistance training in older adults. *Muscle Nerve*, 49, 584-92.
- SCHIAFFINO, S. & MAMMUCARI, C. 2011. Regulation of skeletal muscle growth by the IGF1-Akt/PKB pathway: insights from genetic models. *Skelet Muscle*, 1, 4.
- SCHMITTGEN, T. D. & LIVAK, K. J. 2008. Analyzing real-time PCR data by the comparative CT method. *Nature Protocols*, 3, 1101-1108.
- SCHOENFELD, B. J. 2010. The mechanisms of muscle hypertrophy and their application to resistance training. *J Strength Cond Res*, 24, 2857-72.
- SCHOENFELD, B. J. 2012. Does exercise-induced muscle damage play a role in skeletal muscle hypertrophy? *J Strength Cond Res*, 26, 1441-53.
- SCOTT, P. H. & LAWRENCE, J. C., JR. 1998. Attenuation of mammalian target of rapamycin activity by increased cAMP in 3T3-L1 adipocytes. *J Biol Chem*, 273, 34496-501.
- SEDLIAK, M., FINNI, T., CHENG, S., KRAEMER, W. J. & HAKKINEN, K. 2007. Effect of time-of-day-specific strength training on serum hormone concentrations and isometric strength in men. *Chronobiol Int*, 24, 1159-77.
- SERRANO, A. L., BAEZA-RAJA, B., PERDIGUERO, E., JARDI, M. & MUNOZ-CANOVES, P. 2008. Interleukin-6 is an essential regulator of satellite cell-mediated skeletal muscle hypertrophy. *Cell Metab*, 7, 33-44.
- SHARPLES, A. P., AL-SHANTI, N. & STEWART, C. E. 2010. C2 and C2C12 murine skeletal myoblast models of atrophic and hypertrophic potential: relevance to disease and ageing? *J Cell Physiol*, 225, 240-50.
- SHARPLES, A. P., POLYDOROU, I., HUGHES, D. C., OWENS, D. J., HUGHES, T. M. & STEWART, C. E. 2016a. Skeletal muscle cells possess a 'memory' of acute early life TNF-alpha exposure: role of epigenetic adaptation. *Biogerontology*, 17, 603-17.
- SHARPLES, A. P., STEWART, C. E. & SEABORNE, R. A. 2016b. Does skeletal muscle have an 'epi'-memory? The role of epigenetics in nutritional programming, metabolic disease, aging and exercise. *Aging Cell*, 15, 603-16.
- SHARPLES, A. P., STEWART, C. E. & SEABORNE, R. A. 2016c. Does skeletal muscle have an 'epi'-memory? The role of epigenetics in nutritional programming, metabolic disease, aging and exercise. *Aging Cell*, n/a-n/a.
- SIMARD, C., LACAILLE, M. & VALLIERES, J. 1987. Effects of hypokinesia/hypodynamia on contractile and histochemical properties of young and old rat soleus muscle. *Exp Neurol*, 97, 106-14.
- SNOECK, A., REMACLE, C., REUSENS, B. & HOET, J. J. 1990. Effect of a low protein diet during pregnancy on the fetal rat endocrine pancreas. *Biol Neonate*, 57, 107-18.
- SOLE, G., HAMREN, J., MILOSAVLJEVIC, S., NICHOLSON, H. & SULLIVAN, S. J. 2007. Test-retest reliability of isokinetic knee extension and flexion. *Arch Phys Med Rehabil*, 88, 626-31.

- STEVENS, L., BASTIDE, B., HEDOU, J., CIENIEWSKI-BERNARD, C., MONTEL, V., COCHON, L., DUPONT, E. & MOUNIER, Y. 2013. Potential regulation of human muscle plasticity by MLC2 post-translational modifications during bed rest and countermeasures. *Arch Biochem Biophys*, 540, 125-32.
- STEWART, C. E., NEWCOMB, P. V. & HOLLY, J. M. 2004. Multifaceted roles of TNF- α in myoblast destruction: a multitude of signal transduction pathways. *J Cell Physiol*, 198, 237-47.
- TAJBAKHSH, S., BOBER, E., BABINET, C., POURNIN, S., ARNOLD, H. & BUCKINGHAM, M. 1996. Gene targeting the myf-5 locus with nlacZ reveals expression of this myogenic factor in mature skeletal muscle fibres as well as early embryonic muscle. *Dev Dyn*, 206, 291-300.
- TANG, H. & GOLDMAN, D. 2006. Activity-dependent gene regulation in skeletal muscle is mediated by a histone deacetylase (HDAC)-Dach2-myogenin signal transduction cascade. *Proc Natl Acad Sci U S A*, 103, 16977-82.
- TANG, H., MACPHERSON, P., MARVIN, M., MEADOWS, E., KLEIN, W. H., YANG, X. J. & GOLDMAN, D. 2009. A histone deacetylase 4/myogenin positive feedback loop coordinates denervation-dependent gene induction and suppression. *Mol Biol Cell*, 20, 1120-31.
- TANG, W. W., DIETMANN, S., IRIE, N., LEITCH, H. G., FLOROS, V. I., BRADSHAW, C. R., HACKETT, J. A., CHINNERY, P. F. & SURANI, M. A. 2015. A Unique Gene Regulatory Network Resets the Human Germline Epigenome for Development. *Cell*, 161, 1453-67.
- TEMPLETON, G. H., PADALINO, M. & MOSS, R. 1986. Influences of inactivity and indomethacin on soleus phosphatidylethanolamine and size. *Prostaglandins*, 31, 545-59.
- TONNA, S., EL-OSTA, A., COOPER, M. E. & TIKELLIS, C. 2010. Metabolic memory and diabetic nephropathy: potential role for epigenetic mechanisms. *Nat Rev Nephrol*, 6, 332-41.
- TORTORA, G. J. & GRABOWSKI, S. R. 2003. *Principles of Anatomy of Physiology*, New York, USA, John Wiley & Sons.
- TRACY, B. L., IVEY, F. M., HURLBUT, D., MARTEL, G. F., LEMMER, J. T., SIEGEL, E. L., METTER, E. J., FOZARD, J. L., FLEG, J. L. & HURLEY, B. F. 1999. Muscle quality. II. Effects Of strength training in 65- to 75-yr-old men and women. *J Appl Physiol (1985)*, 86, 195-201.
- TRAPPE, S., TRAPPE, T., GALLAGHER, P., HARBER, M., ALKNER, B. & TESCH, P. 2004. Human single muscle fibre function with 84 day bed-rest and resistance exercise. *J Physiol*, 557, 501-13.
- TRASLER, J., DENG, L., MELNYK, S., POGRIBNY, I., HIOU-TIM, F., SIBANI, S., OAKES, C., LI, E., JAMES, S. J. & ROZEN, R. 2003. Impact of Dnmt1 deficiency, with and without low folate diets, on tumor numbers and DNA methylation in Min mice. *Carcinogenesis*, 24, 39-45.
- TROY, A., CADWALLADER, A. B., FEDOROV, Y., TYNER, K., TANAKA, K. K. & OLWIN, B. B. 2012. Coordination of satellite cell activation and self-renewal by Par-complex-dependent asymmetric activation of p38 α /beta MAPK. *Cell Stem Cell*, 11, 541-53.
- TSUJI, S., WASHIMI, K., KAGEYAMA, T., YAMASHITA, M., YOSHIHARA, M., MATSUURA, R., YOKOSE, T., KAMEDA, Y., HAYASHI, H., MOROHOSHI, T.,

- TSUURA, Y., YUSA, T., SATO, T., TOGAYACHI, A., NARIMATSU, H., NAGASAKI, T., NAKAMOTO, K., MORIWAKI, Y., MISAWA, H., HIROSHIMA, K., MIYAGI, Y. & IMAI, K. 2017. HEG1 is a novel mucin-like membrane protein that serves as a diagnostic and therapeutic target for malignant mesothelioma. *Sci Rep*, 7, 45768.
- VAN DE VYVER, M. & MYBURGH, K. H. 2012. Cytokine and satellite cell responses to muscle damage: interpretation and possible confounding factors in human studies. *J Muscle Res Cell Motil*, 33, 177-85.
- VENTER, J. C., ADAMS, M. D., MYERS, E. W., LI, P. W., MURAL, R. J., SUTTON, G. G., SMITH, H. O., YANDELL, M., EVANS, C. A., HOLT, R. A., GOCAYNE, J. D., AMANATIDES, P., BALLEW, R. M., HUSON, D. H., WORTMAN, J. R., ZHANG, Q., KODIRA, C. D., ZHENG, X. H., CHEN, L., SKUPSKI, M., SUBRAMANIAN, G., THOMAS, P. D., ZHANG, J., GABOR MIKLOS, G. L., NELSON, C., BRODER, S., CLARK, A. G., NADEAU, J., MCKUSICK, V. A., ZINDER, N., LEVINE, A. J., ROBERTS, R. J., SIMON, M., SLAYMAN, C., HUNKAPILLER, M., BOLANOS, R., DELCHER, A., DEW, I., FASULO, D., FLANIGAN, M., FLOREA, L., HALPERN, A., HANNENHALLI, S., KRAVITZ, S., LEVY, S., MOBARRY, C., REINERT, K., REMINGTON, K., ABU-THREIDEH, J., BEASLEY, E., BIDDICK, K., BONAZZI, V., BRANDON, R., CARGILL, M., CHANDRAMOULISWARAN, I., CHARLAB, R., CHATURVEDI, K., DENG, Z., DI FRANCESCO, V., DUNN, P., EILBECK, K., EVANGELISTA, C., GABRIELIAN, A. E., GAN, W., GE, W., GONG, F., GU, Z., GUAN, P., HEIMAN, T. J., HIGGINS, M. E., JI, R. R., KE, Z., KETCHUM, K. A., LAI, Z., LEI, Y., LI, Z., LI, J., LIANG, Y., LIN, X., LU, F., MERKULOV, G. V., MILSHINA, N., MOORE, H. M., NAIK, A. K., NARAYAN, V. A., NEELAM, B., NUSSKERN, D., RUSCH, D. B., SALZBERG, S., SHAO, W., SHUE, B., SUN, J., WANG, Z., WANG, A., WANG, X., WANG, J., WEI, M., WIDES, R., XIAO, C., YAN, C., et al. 2001. The sequence of the human genome. *Science*, 291, 1304-51.
- VOISIN, S., EYNON, N., YAN, X. & BISHOP, D. J. 2015. Exercise training and DNA methylation in humans. *Acta Physiol (Oxf)*, 213, 39-59.
- WADDINGTON, C. H. 1953. Epigenetics and Evolution. *Symp Soc Exp Biol*, 7, 186-199.
- WALL, B. T., DIRKS, M. L. & VAN LOON, L. J. 2013a. Skeletal muscle atrophy during short-term disuse: implications for age-related sarcopenia. *Ageing Res Rev*, 12, 898-906.
- WALL, B. T., SNIJDERS, T., SENDEN, J. M., OTTENBROS, C. L., GIJSEN, A. P., VERDIJK, L. B. & VAN LOON, L. J. 2013b. Disuse impairs the muscle protein synthetic response to protein ingestion in healthy men. *J Clin Endocrinol Metab*, 98, 4872-81.
- WANG, Z., WANG, D. Z., PIPES, G. C. & OLSON, E. N. 2003. Myocardin is a master regulator of smooth muscle gene expression. *Proc Natl Acad Sci U S A*, 100, 7129-34.
- WARD, S. S. & STICKLAND, N. C. 1991. Why are slow and fast muscles differentially affected during prenatal undernutrition? *Muscle Nerve*, 14, 259-67.
- WILLIAMS, P. E. & GOLDSPINK, G. 1984. Connective tissue changes in immobilised muscle. *J Anat*, 138, 343-50.
- WILSON, S. J., ROSS, J. J. & HARRIS, A. J. 1988. A critical period for formation of secondary myotubes defined by prenatal undernourishment in rats. *Development*, 102, 815-21.

- WOO, M., ISGANAITIS, E., CERLETTI, M., FITZPATRICK, C., WAGERS, A. J., JIMENEZ-CHILLARON, J. & PATTI, M. E. 2011. Early life nutrition modulates muscle stem cell number: implications for muscle mass and repair. *Stem Cells Dev*, 20, 1763-9.
- WU, H., NAYA, F. J., MCKINSEY, T. A., MERCER, B., SHELTON, J. M., CHIN, E. R., SIMARD, A. R., MICHEL, R. N., BASSEL-DUBY, R., OLSON, E. N. & WILLIAMS, R. S. 2000. MEF2 responds to multiple calcium-regulated signals in the control of skeletal muscle fiber type. *Embo j*, 19, 1963-73.
- YASUDA, N., GLOVER, E. I., PHILLIPS, S. M., ISFORT, R. J. & TARNOPOLSKY, M. A. 2005. Sex-based differences in skeletal muscle function and morphology with short-term limb immobilization. *J Appl Physiol (1985)*, 99, 1085-92.
- YATES, D. T., CLARKE, D. S., MACKO, A. R., ANDERSON, M. J., SHELTON, L. A., NEARING, M., ALLEN, R. E., RHOADS, R. P. & LIMESAND, S. W. 2014. Myoblasts from intrauterine growth-restricted sheep fetuses exhibit intrinsic deficiencies in proliferation that contribute to smaller semitendinosus myofibres. *J Physiol*, 592, 3113-25.
- YIN, H., PRICE, F. & RUDNICKI, M. A. 2013. Satellite cells and the muscle stem cell niche. *Physiol Rev*, 93, 23-67.
- YLIHARSILA, H., KAJANTIE, E., OSMOND, C., FORSEN, T., BARKER, D. J. & ERIKSSON, J. G. 2007. Birth size, adult body composition and muscle strength in later life. *Int J Obes (Lond)*, 31, 1392-9.
- YU, X. M. & HALL, Z. W. 1991. Extracellular domains mediating epsilon subunit interactions of muscle acetylcholine receptor. *Nature*, 352, 64-7.
- ZAMMIT, P. S., GOLDING, J. P., NAGATA, Y., HUDON, V., PARTRIDGE, T. A. & BEAUCHAMP, J. R. 2004. Muscle satellite cells adopt divergent fates: a mechanism for self-renewal? *J Cell Biol*, 166, 347-57.

Chapter 8:

Appendices

Appendix 1.

Title: Does skeletal muscle have an ‘epi’-memory? The role of epigenetics in nutritional programming, metabolic disease, ageing and exercise.

Journal: Aging Cell (impact factor 6.34)

Volume: 15

Issue: 4

Pages: 603-615



REVIEW

Does skeletal muscle have an 'epi'-memory? The role of epigenetics in nutritional programming, metabolic disease, aging and exercise

Adam P. Sharples, Claire E. Stewart and Robert A. Seaborne

Stem Cells, Ageing and Molecular Physiology (SCAMP) Research Unit, Exercise Metabolism and Adaptation Research Group (EMARG), Research Institute for Sport and Exercise Sciences (RISES), Liverpool John Moores University, Liverpool, UK

Summary

Skeletal muscle mass, quality and adaptability are fundamental in promoting muscle performance, maintaining metabolic function and supporting longevity and healthspan. Skeletal muscle is programmable and can 'remember' early-life metabolic stimuli affecting its function in adult life. In this review, the authors pose the question as to whether skeletal muscle has an 'epi'-memory? Following an initial encounter with an environmental stimulus, we discuss the underlying molecular and epigenetic mechanisms enabling skeletal muscle to adapt, should it re-encounter the stimulus in later life. We also define skeletal muscle memory and outline the scientific literature contributing to this field. Furthermore, we review the evidence for early-life nutrient stress and low birth weight in animals and human cohort studies, respectively, and discuss the underlying molecular mechanisms culminating in skeletal muscle dysfunction, metabolic disease and loss of skeletal muscle mass across the lifespan. We also summarize and discuss studies that isolate muscle stem cells from different environmental niches *in vivo* (physically active, diabetic, cachectic, aged) and how they reportedly remember this environment once isolated *in vitro*. Finally, we will outline the molecular and epigenetic mechanisms underlying skeletal muscle memory and review the epigenetic regulation of exercise-induced skeletal muscle adaptation, highlighting exercise interventions as suitable models to investigate skeletal muscle memory in humans. We believe that understanding the 'epi'-memory of skeletal muscle will enable the next generation of targeted therapies to promote muscle growth and reduce muscle loss to enable healthy aging.

Key words: ageing; aging; aging muscle; beta-catenin; cellular programming; developmental programming; DNA methylation; epigenetics; exercise; fibre number; fibre type; foetal programming; forkhead box; healthspan; histone acetylation; histone deacetylation; histone modification; insulin-like growth factor; lifespan; metabolic programming; muscle memory; muscle precursor cell; muscle stem cell; myf5;

myoblast; myocyte; myoD; myogenesis; myogenin; myogenic regulatory factor; MRF4; NFkB; nutritional programming; obesity; sarcopenia; tumour necrosis factor alpha; type II diabetes; myostatin.

Scope and aims of the review

For the purposes of this review, the author defines skeletal muscle memory as:

The capacity of skeletal muscle to respond differently to environmental stimuli in an adaptive or maladaptive manner if the stimuli have been previously encountered.

We therefore suggest that skeletal muscle memory refers to both cellular and tissue retention of prior environmental stimuli or stress such as those from acute or chronic exercise, muscle damage/injury, disease or changes in nutrients which culminate in altered behaviour, if the stimulus is re-encountered. Ultimately, this is important for skeletal muscle because if the environment encountered is an anabolic or positive one, muscle may respond to these later-life stimuli with additive muscle growth or healthy maintenance across the lifespan; however, if the environment is catabolic or negative, it may become more susceptible to muscle mass loss in later life. This therefore has important consequences, as sufficient quantity and quality of skeletal muscle are required not only to sustain performance in elite sport but also to enhance lifespan and promote healthspan into older age [recently reviewed in Sharples *et al.* (2015b)].

Historically, the term 'programming' has been used to define similar processes of 'memory' in cells or tissues. Programming however, can evoke a slightly different perception in the minds of scientists even within similar biological fields. For example, programming in embryonic stem cell biology refers to the programme that controls pluripotency in embryonic stem (ES) cells, and reprogramming is a human intervention whereby adult cells are returned to pluripotent embryonic-like states, where any previous environmental encounters experienced during development or with age are essentially re-set. This is therefore somewhat distinct from tissue or cells retaining information after a stimulus or stress in readiness for future stimuli that when re-encountered may bring about further adaptation, or maladaptation. Metabolic or nutrient programming is another example of a phenomenon linked, yet somewhat distinct to what we define as skeletal muscle memory above. This usually refers to a change in nutritional stimuli such as global calorie or protein restriction or a high-fat diet that changes physiology and metabolism of the organism during development that is usually then fixed into older postnatal age. Therefore, these adaptations continue even without confrontation with the same stimulus/stress that initiated them. The majority of work in the metabolic programming field is undertaken using *in utero* studies, therefore also

Correspondence

Dr Adam Philip Sharples, Stem Cells, Ageing and Molecular Physiology (SCAMP) Research Unit, Exercise Metabolism and Adaptation Research Group (EMARG), Research Institute for Sport and Exercise Sciences (RISES), Liverpool John Moores University, Liverpool, UK. Tel.: +447812732670; e-mails: a.sharples@ljmu.ac.uk; a.p.sharples@googlemail.com

Accepted for publication 24 March 2016

© 2016 The Authors. *Aging Cell* published by the Anatomical Society and John Wiley & Sons Ltd. This is an open access article under the terms of the Creative Commons Attribution License, which permits use, distribution and reproduction in any medium, provided the original work is properly cited.

1

termed foetal or developmental programming, where the offspring encounter different environmental stimuli during pregnancy and the phenotypes postbirth (sometimes into adulthood or old age) are dependent on these earlier life occurrences. This field provided some of the earliest evidence to suggest that skeletal muscle was programmable and evolved into the research field encompassing foetal origins of health and disease. Given that this particular field is beginning to examine the molecular and epigenetic mechanisms of these phenomena and provide insights into the concept of muscle memory defined above, this literature is reviewed below.

In addition to the skeletal muscle being programmable, there is also now emerging evidence that suggests even after short-term environmental stimuli, skeletal muscle can retain molecular information in order to be primed for future plasticity following encounters with the same stimulus. Just as we do when we suddenly recall a past childhood memory after being in contact with the same or similar stimuli in adulthood, we propose that skeletal muscle could behave within a similar conceptual framework *via* distinct molecular mechanisms. We suggest that epigenetics, in particular, could mechanistically underpin muscle memory as defined above; therefore, we present the term muscle 'epi'-memory in this review to capture this notion.

Epigenetics is defined as the study of changes in organisms caused by the modification of gene expression rather than the alteration of the genetic code itself (Oxford Dictionary, 2015). Because environmental stimuli, stresses or encounters cause modifications in gene expression, turning genes on or off, and muscle memory is defined as the capacity for skeletal muscle to respond or adapt differently to environmental stimuli if encountered previously, it suggests that epigenetics could mechanistically underpin skeletal muscle memory. Epigenetic modifications can be extremely transient, for example after a simple bout of acute metabolic stress (high-intensity aerobic exercise) (Barres *et al.*, 2012), or obstinately stable, termed genetic inheritance, even being passed to daughter generations of cells (Hansen *et al.*, 2008; Ng & Gurdon, 2008; Petruk *et al.*, 2012). Critically, it has been reported that epigenetic DNA marks maintained in germlines and even RNAs can be transferred to the next generation in mammals (Anway *et al.*, 2005; Campos *et al.*, 2014; Gapp *et al.*, 2014; Liebers *et al.*, 2014; Grandjean *et al.*, 2015; Sharma *et al.*, 2016), contributing to 'heritable' metabolic disease (Grandjean *et al.*, 2015; Chen *et al.*, 2016; Donkin *et al.*, 2016). This evidence firmly points to epigenetics playing an important role in the retention of information into later life. Finally, our group has recently shown that skeletal muscle cells retain epigenetically modified DNA 'tags' (methyl groups) as a result of early-life inflammatory stress and that they seemingly retain this information until later in their proliferative lifespan *in vitro* (Sharples *et al.*, 2015a), a concept that is discussed later in this review (and depicted in Fig. 1). We therefore believe that skeletal muscle memory is underpinned by epigenetic modifications ('epi'-memory).

Therefore, in this review, we will; (i) outline the emergence of scientific evidence contributing to the notion of skeletal muscle memory including metabolic/foetal programming studies and the underlying molecular mechanisms; (ii) discuss the importance of memory/programming in metabolic disease and the underlying molecular mechanisms; (iii) review the data within epidemiological research where aging cohort studies support skeletal muscle programming in humans; (iv) summarize and discuss the evidence for muscle memory from animal tissue models and where muscle stem cells have been isolated under different environmental niches *in vivo*, for example physically active, diabetic, cachexic and aged, and how they 'memorize' this environment once isolated *in vitro*; (v) finally, we will outline the proposed molecular and

epigenetic mechanisms underlying skeletal muscle memory and review the epigenetic regulation of exercise-induced skeletal muscle adaptation, highlighting exercise interventions as suitable models to investigate skeletal muscle memory.

Emergence of evidence for skeletal muscle memory

Early-life nutrient restriction and the programming of skeletal muscle fibre number, composition and size

The Dutch famine (1944–1945), affecting women in the first trimester of pregnancy, was associated with an increased prevalence of coronary heart disease, raised lipids and obesity in the offspring. Severe malnourishment during late gestation was also related to impaired glucose tolerance of the offspring into adult life (Ravelli *et al.*, 1998, 1999; Roseboom *et al.*, 2000a,b). The influence of this catastrophic event was only fully realized in the late 1990s as these children were tracked into adulthood; it had, however, been observed some 16 years previously that malnutrition during pregnancy in rats reduced general cell numbers in the offspring (McLeod *et al.*, 1972). These studies resulted in a programme of research in the field of foetal/developmental programming (later also defined as metabolic/nutritional programming), with basic and clinical scientists examining how these early-life encounters impacted health and function or dysfunction into adulthood and old age. Follow-up animal studies have reported nutritional programming in the liver (Gluckman *et al.*, 2007), kidney, lung (Brameld *et al.*, 2000; Yakubu *et al.*, 2007a,b), adipose tissue (Budge *et al.*, 2003), the brain (Guzman-Quevedo *et al.*, 2013) and even skeletal muscle. More recently, a smaller subgroup of individuals (150 men and women) from the Dutch famine birth cohort (aged 68) were reported to display increased mortality and were more frequently admitted to hospital for age-related disease. In the same study, at the organ/system level, the authors demonstrated larger increases in levels of aging biomarkers in the brain, bone, skeletal muscle and the eye. At the cellular level, increased inflammation, oxidative stress and decreased telomere length of DNA, a hallmark of cellular senescence, were evident (de Rooij & Roseboom, 2013). Overall, this evidence has led to the emergence of the notion that, even decades later, organs, tissues and even cells can be programmed as a result of early-life foetal environmental encounters.

Skeletal muscle tissue is the largest metabolic organ. Therefore, skeletal muscle was an early target of assessment in metabolic programming studies. It is important to note that the gestational nutritional manipulations implemented in experiments detailed in this review occur at different times and for differing durations, and this may impact on data interpretation when attempting to compare across experiments or to draw conclusions. It is therefore important to understand the time course of developing skeletal muscle in the different mammalian models used. It is also important to appreciate that the majority of studies in the mammalian developmental programming field are undertaken in sheep due to their similar pregnancies to humans. The first fibres formed in skeletal muscle development and growth are called primary muscle fibres and in mammals begin to develop at 32 days during gestation and continue to form up to approximately 38 days. Primary myofibres have myofibrils that are peripherally located and surround an axial core of nuclei and cytoplasm (Beermann *et al.*, 1978). Secondary fibres then use the primary fibres as a scaffold and develop after 38–62 days (Wilson *et al.*, 1992). They are derived from PAX7-positive precursor cells that become activated myoblasts that terminally fuse/differentiate into myotubes and subsequently mature into muscle fibres parallel to the primary fibres, and go

on to make up the majority of skeletal muscle. This process is driven by a dramatic downregulation of PAX7 and sequential activation of muscle-specific myogenic regulatory factors (MRFs), myf5 (proliferation), myoD (early fusion), myogenin (fusion) and mrf4 (late fusion/myotube maturation) (as reviewed in Sabourin & Rudnicki, 2000; Maltin *et al.*, 2001). This is followed by an advancement of tertiary myofibre development from 62 days (Wilson *et al.*, 1992). In rodents, the primary fibres develop at 14–16 days, secondary fibres around 17–19 days (Wilson *et al.*, 1988) and tertiary formation thereafter. Generally, the primary fibres become slow (type I/oxidative), whereas secondary fibres become fast fibres (type IIa: fast, mixed oxidative and glycolytic and type IIb: fast, glycolytic) (Draeger *et al.*, 1987).

To the authors' knowledge, it was first observed that prenatal nutrition negatively affected skeletal muscle fibre growth and composition in the offspring, where a 30% reduction in total calories consumed reduced the number of fast fibres in both the soleus and lumbrical muscles of newborn rats (Wilson *et al.*, 1988). Importantly, re-feeding of the mothers during lactation was unable to restore fibre number in the soleus of restricted offspring vs. controls, yet was able to restore fibre number in the lumbrical muscle (Wilson *et al.*, 1988). This suggested that fibre number within the rat soleus was fixed into older age, but this effect was fibre type dependent. It was later confirmed in other species (guinea pig) that 40–60% total nutrient restriction throughout gestation reduced birth weight of the offspring and reduced myofibre number in the biceps brachii by 20–26% (Ward & Stickland, 1991; Dwyer & Stickland, 1994; Dwyer *et al.*, 1995). Together with a reduction in fibre number, it has been demonstrated that global nutrient restriction during pregnancy can also impact on the composition (fibre type) and size of the fibre. In ewes, 50% globally reduced maternal nutrition between 30–70 days of gestation resulted in fewer fast and increased slow fibre numbers in the vastus lateralis, 14 days postpartum, vs. relevant controls, an observation notwithstanding in the group restricted at 30–70 days or between 55–95 days (Fahey *et al.*, 2005). Furthermore, 50% nutrient restriction in the conception period (minus 6–18 days of gestation) reduced myofibre number of the mid-gestation foetus but had no effect on foetal weight (Quigley *et al.*, 2005). Therefore, it appears that the impact of nutrient restrictions on fibre type, composition and size is gestation dependent, with a general view that earlier restriction impacts fibre number, mid-gestation impacts fibre composition (predominantly fast fibres) and later restriction impacts muscle size and weight. However, to complicate this observation, it has been subsequently shown that a similar, yet longer phase of global restriction (50%) in ewes between 28 and 70 days of gestation actually increased fast myosin type IIb isoforms, albeit on a background of reduced total myofibre number, in the longissimus dorsi of 8-month-old offspring (Zhu *et al.*, 2006). It is therefore worth postulating that adaptations are dependent on timing, duration, degree of restriction and the muscles impacted, for example, the triceps brachii (both slow- and fast-twitch myofibres) suffer reduced fibre and capillary density in the offspring of restricted ewes in response to restricted maternal diet vs. no change in the soleus (majority slow-twitch myofibres) under the same conditions (Costello *et al.*, 2008). Coupled with altered fibre number, composition and muscle size, reduced maternal nutrition during 28–78 days of gestation in ewes results in increases in fat mass (both subcutaneous and visceral) and reduced lean mass in the offspring (Ford *et al.*, 2007). The translation to human studies however, is somewhat compounded, in that women who are lean and on a restricted diet during pregnancy are generally speaking also equivalently lean and restricted pre-pregnancy. Therefore, to simulate this situation, researchers investigated the impact of low (excessively lean) maternal body scores (LBS) before and throughout gestation in ewes vs. high body score (HBS) ewes (obese) (Costello *et al.*,

2013). Here, bioptic samples highlighted impairments in the skeletal muscle of the offspring produced by LBS mothers, including reductions in total myofibre density, fast fibre size and capillary-to-myofibre ratio (Costello *et al.*, 2013), observations similar to those in nutrient-restricted studies. While questions remain and specifics need to be determined, overall, it is clear that as a consequence of nutrient restriction *in utero*, skeletal muscle demonstrates the alterations in fibre number, composition and size, which prevail into later life, despite normal feeding patterns.

Maternal protein restriction and skeletal muscle programming

The majority of the studies above manipulated nutritional intake *via* a 40–60% global reduction in food consumed. Some studies have also altered specific macronutrients to measure the impact of individual nutritional components on metabolic programming. With respect to skeletal muscle, as protein feeding is important in protein synthesis and muscle maintenance across the lifespan, a particular interest has focused on protein-restricted rodent maternal diets, where rats that had their protein intake restricted (9% vs. 18% in controls as a proportion of total matched calories from protein) during mid-pregnancy (8–14 days in rats), demonstrated significantly reduced muscle fibre number and density in their 4-week-old offspring (Mallinson *et al.*, 2007). As with the restriction of total energy, these observations were fibre type and muscle group dependent where the number and density of fast-twitch fibres in the soleus were found to be reduced in the offspring after early (0–7 days), mid (8–14 days)- and late (15–22 days) restriction, whereas in the gastrocnemius, only a reduction in the density of slow-twitch fibres occurred at mid (8–14 days)-restriction (Mallinson *et al.*, 2007). A more recent study suggested that a more severe maternal protein restriction at mid (7–14 days)-gestation (6% of total calories from protein vs. 17% in control group) reduced type I fibre diameter by 20% together with a reduction in type IIa fibres by 5%, while type IIb fibres actually increased by 5% vs. the aged matched control group in aged rat offspring (365 days old) (Confortim *et al.*, 2015). Finally, in the same study it was shown that protein restriction during gestation results in a reduction in size of neuromuscular junctions; as age-related decline in muscle is associated with denervation (Confortim *et al.*, 2015), these fascinating findings suggest an important role for early-life encounters on muscle size and function into old age, which is discussed later in this review. Therefore once again, although there are some discrepancies in the specific fibre-type changes following protein restriction, on a background of differences in muscle groups studied, timing of protein restriction and sampling of the offspring, it is clear that the general consensus is that muscle size is reduced following maternal protein restriction. The important role of protein per se has been illustrated in guinea pig models, where all dietary components were reduced to 60% of the *ad libitum* level, but pregnant mothers were supplemented with protein, to the same level as controls during gestation. It was reported that muscle fibre number in the offspring returned back to the level of the *ad libitum*-fed controls (Dwyer & Stickland, 1994). This however, is also observed when carbohydrates are supplemented back, but not fat (Dwyer & Stickland, 1994), suggesting that at least in this study, the different macronutrients have an equal role in the programming of fibre number. Further, supplementing with higher protein (55% vs. 20% in control) during rat gestation and weaning reduces birth weight by 7% by a reduction in adipose tissue (31%) (Desclee de Maredsous *et al.*, 2016). Overall these studies suggest that programming due to protein restriction may be somewhat reversible by protein feeding during gestation or lactation.

Proposed molecular mechanisms of reduced muscle size under maternal nutrient restriction

Although a vast number of studies contribute to what we know about morphological and compositional adaptations of skeletal muscle into adulthood and following early-life nutrient stress, there are few studies to investigate the potential molecular mechanisms of metabolic programming. However, fetuses of globally (50%) nutrient-restricted mothers have a reduced activity of protein synthetic pathways, including a reduced activation of mammalian target of rapamycin (mTOR) at Ser2448 and ribosomal protein S6 (p70S6K) at Ser235/336 with corresponding reductions in fibre size and the number of secondary fibres (Zhu *et al.*, 2004). The alterations in protein activity in this study reportedly occurred without the change in the total levels of the signalling proteins, energy sensing activity (e.g. 5' adenosine monophosphate-activated protein kinase/AMPK) or protein degradative signalling (Zhu *et al.*, 2004). However, reductions in upstream protein kinase B (PKB or Akt) total protein levels were observed in offspring from LBS mothers (Costello *et al.*, 2013). Further, upstream of this intracellular signalling, it has also been observed that restricted global maternal nutrition (60%) altered gene expression of the ligand, insulin-like growth factor II (IGF-II), in the skeletal muscle of sheep fetuses sampled at 80 days gestation (Brameld *et al.*, 2000). In this study, IGF-I was found to be not altered locally in the skeletal muscle, but was reduced in production by the liver. It may be hypothesized that greater IGF-II may have actually led to earlier and enhanced differentiation in muscle during gestation, causing a disruption of myofibre number. This, however, is only speculative as overexpression of IGF-II by our group has been shown to have this role in adult muscle cells (Stewart *et al.*, 1996) and not as yet, developing muscle tissue. Alternatively, this could be due to a compensatory mechanism to attempt to promote mesoderm growth (Morali *et al.*, 2000) in the face of nutrient restriction, especially when it has been previously observed in work by our group that IGF-1R knockout increased circulating IGF-II and the mice were 25–30% larger vs. controls (Lau *et al.*, 1994). A recent study suggested that the reduction in muscle size seen in the offspring of rat mothers subjected to protein restriction (8% total calories vs. 20% total calories) was also due to the reductions in amino acid response (AAR) pathway-related genes and an elevation of autophagy-related genes. Interestingly, in this study, the authors alluded to the concept of muscle memory stating that the muscle at 38 days postpartum had 'memorized' the early-life low-protein environment (Wang *et al.*, 2015). Furthermore, a low-protein maternal diet in pigs increased the gene expression of the ligand myostatin and its receptor (activin type II receptor) in 35-day-old offspring (Liu *et al.*, 2015). Myostatin is a potent negative regulator of muscle mass (McPherron & Lee, 1997); therefore, these studies add to the growing data set, suggesting that alterations in protein synthetic/degradative pathways *in utero* impact on muscle composition in later life (Liu *et al.*, 2015).

It has also been proposed that glucose-restricted sheep (40%) have decreased protein accretion, driven not by reductions in protein synthesis, a finding that is in opposition to Zhu *et al.*, (2004) and Costello *et al.* (2013), but by an increase in protein degradation via the skeletal muscle ubiquitin-proteasome pathway (Brown *et al.*, 2014). In this study, increased mRNA production of atrogen 1 (MAFbx1) and muscle ring finger 1 (MuRF1) (Brown *et al.*, 2014) were reported, both ubiquitin ligases important in the tagging of proteins for degradation. No alterations, however, were observed in autosome-lysosome pathways, for example mRNA for cathepsin L1, BCL2/adenovirus E1B 19-kDa protein-interacting protein (*BNIP3*) or beclin 1. It is also worth mentioning when trying to account for these potential discrepancies that the

muscle of these offspring in studies by Costello *et al.* (2013) and Zhu *et al.*, (2014) were sampled after gestation into adulthood, whereas the study by Brown *et al.* (2014) sampled 8-week-old fetuses. Furthermore, the studies by Costello *et al.*, 2013 and Zhu *et al.*, 2014 showed a reduction in protein synthetic signalling, via the manipulation of total nutritional content across all macronutrients, whereas glucose was the only nutrient restricted when ubiquitin-proteasome pathway was impaired (Brown *et al.*, 2014). Therefore, with the caveat that not all studies investigated protein degradation, it would perhaps be suitable to hypothesize that a reduction in other macronutrients (e.g. protein, as this usually makes up the other largest macronutrient to be restricted) may, as expected, drive the reductions in protein synthesis (e.g. via mTOR), whereas the reductions in glucose (carbohydrate) may drive increases in protein degradation, something that has previously been observed in starvation in the skeletal muscle cells via the activation of forkhead box (FOXO) transcription factors leading to the activation of atrogen 1 gene expression and subsequent protein degradation (Sandri *et al.*, 2004). However, the role of FOXO in nutritional programming requires further investigation in skeletal muscle during nutrient restriction. To the authors' knowledge, it has only been investigated in the offspring of maternally obese sheep who are overnourished. Here, sheep consumed 150% of the recommended global nutrient intake for 60 days prior to conception and 75 days into gestation at which point the foetal muscle was sampled (Tong *et al.*, 2009). The sampled muscle demonstrated increased FOXO3a and nuclear factor kappa light chain enhancer of activated B cells (NF- κ B) signalling (via increased I κ B kinase (IKK β) and p65 activity). Due to FOXO's role in mediating NF- κ B-driven inflammation (van der Horst & Burgering, 2007) in the skeletal muscle [reviewed in Li *et al.* (2008)] and obesity [reviewed in Tornatore *et al.* (2012)], as well as its role in quiescence mammalian cells (Bowerman, 2005) and muscle atrophy (Sandri *et al.*, 2004), the authors hypothesized that FOXO could be involved in the reduction of myogenesis observed in the foetal muscle of obese mothers. Indeed, they found that the foetal muscle had reduced fibre size and reductions in MRFs controlling myogenesis via the reduced content of myoD and myogenin as well as the intermediate protein filament desmin and, in an earlier study by the same group, increased adipogenesis (Zhu *et al.*, 2008). This drop in myogenesis was observed with reduced beta-catenin, which has been shown to be involved in the activation of transcription of the above MRFs (Cossu & Borello, 1999). As FOXO diverts beta-catenin away from the nucleus where it is unable to form an active transcription complex with members of the TCF family of transcription factors involved in the transcription of the MRFs (Almeida *et al.*, 2007), these findings suggested that FOXO may be involved in mediating the reductions in myogenesis and fibre size in the foetal muscle. Although protein degradation was not directly analysed in this study, the observations point to a potentially important role for FOXO in the programming effect in skeletal muscle following early-life nutrient stress. NF- κ B's signalling has also been shown to be involved in atrophy of skeletal muscle via protein degradation (reviewed in Jackman & Kandarian, 2004; Bakkar *et al.*, 2008), but also plays a role in early muscle cell survival where NF- κ B inhibition in the presence of an apoptotic dose of tumour necrosis factor- α (TNF- α) exacerbates cell death (Stewart *et al.*, 2004). Furthermore, as both NF- κ B and FOXO have been linked with cell survival instead of growth, that is, shifting cellular function towards oxidative stress resistance and DNA repair (Brunet *et al.*, 2004; Greer & Brunet, 2005; Wang *et al.*, 2007), and are associated with lifespan extension (Giannakou *et al.*, 2004; Alic *et al.*, 2014), these molecules could be fundamental in programming and perhaps memory, particularly impacting in later life where impaired DNA

repair and oxidative stress are linked with the muscle loss and sarcopenia (reviewed in Jackson & McArdle, 2011). This is especially relevant when maternal obesity in ewes has been shown to increase fibrogenesis vs. skeletal muscle tissue accretion in the foetal skeletal muscle (Tong *et al.*, 2009), a hall mark of sarcopenia, and one of the fundamental causes of reduced muscle force and quality (force per cross-sectional area of muscle) (reviewed in Serrano & Munoz-Canoves, 2010; Mann *et al.*, 2011). It is also worth noting that as well as protein restriction, high-fat gestational rodent feeding and postpartum rodent feeding have been shown to reduce protein synthetic signalling via p70S6 kinase 1 and 4E binding protein-1 phosphorylation while also manipulating FOXO and NF- κ B action. Overall, these studies suggest that the mechanisms for reduced muscle size following maternal nutrient restriction involve reductions in protein synthetic signalling and increases in protein degradative signalling, with the latter perhaps more likely when carbohydrates alone are restricted. High-fat diets are also detrimental to muscle size via reduced myogenic cues, reduced protein synthetic signalling, increased protein degradation and enhanced inflammation.

Nutrient/metabolic programming and the impact on metabolism and metabolic disease

Metabolic programming is also clinically important, as it has been suggested that early-life stress-induced alterations in skeletal muscle fibre type and size may predispose individuals to metabolic abnormalities such as obesity (Tanner *et al.*, 2002) and type II diabetes (Marin *et al.*, 1994). Indeed, nutrient restriction during mid- and late gestation (but not early gestation) results in glucose intolerance in response to an intravenous glucose tolerance test (IGTT) (Gardner *et al.*, 2005; Ford *et al.*, 2007). It is worth noting that in this study this phenomena may not have not been due to muscle tissue but may have been a result of reduced adipose tissue disposal of glucose via reductions in insulin-responsive glucose transporter 4 (GLUT4), an observation that was not found in the skeletal muscle. However, the glucose intolerance observed was not related to insulin deficiency as insulin area under the curve in response to an IGTT was actually increased in the offspring of global restricted maternal nourishment (Gardner *et al.*, 2005). Furthermore, in the skeletal muscle specifically, a key enzyme controlling fat oxidation, carnitine palmitoyltransferase-1, has been shown to be reduced by approximately 25% in the skeletal muscle of ewe offspring from nutrient-restricted parents, where intramuscular triglyceride content (IMTG) was also found to be increased contributing to an increased fat deposition (Zhu *et al.*, 2006). As increased IMTG content predisposes insulin resistance in the skeletal muscle (Phillips *et al.*, 1996; Krssak *et al.*, 1999), these findings are suggestive of an increased likelihood of diabetes. Furthermore, rats considered small for their gestational age (Deng *et al.*, 2014) and humans with low birth weight (Ozanne *et al.*, 2005) can also develop insulin resistance and glucose intolerance. Indeed, it was observed that in Danish low birth weight men, levels of GLUT4 protein abundance and insulin signalling [protein kinase C zeta (PKC ζ) and the p85a/p110b subunits of phosphoinositol-3-kinase] were found to be reduced in their skeletal muscle (Ozanne *et al.*, 2005), overall pointing to an altered glucose handling and a predisposition to type II diabetes in response to early foetal environmental encounters. To relate this altered phenotype of low birth weight in humans to foetal nutrient restriction, in the same study, rats were exposed to low-protein diets during gestation and lactation, where the rats exhibited changes similar to the Danish men with low birth weights (Ozanne *et al.*, 2005). Later studies have also confirmed the above findings, where gestational low protein (6% vs. 20% in control) in rats led to insulin resistance in adult offspring by involving an inadequate insulin-

induced phosphorylation of the Insulin receptor, insulin receptor substrate-1 (IRS-1) and Akt substrate of 160 kDa (AS160) as well as an impaired GLUT4 translocation and the corresponding increases in glucose and insulin levels when subjected to an IGTT (Blesson *et al.*, 2014). Indeed, maternal low protein (8%) and postnatal high diets (45%) in the rats have been shown to increase the risk of type II diabetes by decreasing skeletal muscle oxidative respiration, via increased sirtuin 3 (Sirt3), and potentially by decreasing the activity of succinate dehydrogenase (SDH) (Claycombe *et al.*, 2015). Protein restriction in maternal rat and subsequent acute fasting of the resulting offspring can also alter the metabolic properties of faster muscle fibres (EDL vs. soleus) (Aragao *et al.*, 2014). It was observed in this study that fasting in the offspring on a background of maternal protein restriction reduced the gene expression of lipid metabolism regulators peroxisome proliferator-activated receptors alpha (PPAR α), PPAR δ and peroxisome proliferator-activated receptor gamma coactivator 1-alpha (PGC-1 α – an important regulator of mitochondrial biogenesis and carbohydrate/lipid metabolism) to the same extent as nonfasted controls in their slow-twitch (soleus) muscles, yet, in faster fibres (EDL) control animals were protected from fasting-induced reductions in gene expression, whereas the protein-restricted group demonstrated impairments, a phenomenon that the authors described as metabolic 'inflexibility' (Aragao *et al.*, 2014). However, it was clear that in this study the fast-twitch muscle was able to retain information from early-life encounters with nutrient stress and was subsequently more susceptible to later-life stress of the same kind, demonstrating skeletal muscle memory.

Overall, to substantiate that nutritional programming influences metabolic inadequacies; hypertension, insulin resistance and obesity have been observed in the adult offspring of obese C57BL/6J mice (Samuelsson *et al.*, 2008; Shelley *et al.*, 2009). Also, the skeletal muscles from foetuses from obese sheep have blunted insulin and AMPK signalling as well as an increased inflammatory cytokine tumour necrosis factor-alpha (TNF- α), in their plasma, suggesting the development of insulin resistance in these offspring (Zhu *et al.*, 2008). Somewhat counterintuitively however, high-fat diets during gestation in pigs have been seen to increase myofibre cross-sectional area (Fainberg *et al.*, 2014). However, pigs are encouraged to eat high-fat diets once born, and therefore, it may be suggested that their mothers may offer some kind of protection for their foetuses, as high-fat diets during pregnancy in other mammalian and human studies seem to have only negative consequences for metabolic disease risk (Khan *et al.*, 2005; Srinivasan *et al.*, 2006; Elahi *et al.*, 2009). An important recent study in mice has also shown that high-fat diets during both gestation and lactation result in insulin resistance and obesity in the offspring, with increased inflammation originating in the adipose tissue (Kruse *et al.*, 2015). An observation confirmed a background of genetic deletion of gastric inhibitory polypeptide receptor (GIPR) that has previously been shown to prevent high-fat diet-induced obesity (Kruse *et al.*, 2015). However, if prenatal high-fat diets are followed by normal diets consumed after pregnancy, it seems that offspring may not develop obesity but type II diabetes via increased cytokine activation, inflammation and mitochondrial dysfunction (Latouche *et al.*, 2014). These alarming effects of early-life nutritional stress have culminated in the recent UK guidelines in the importance of maternal weight and diet in influencing the risk of obesity and type II diabetes in humans (NICE 2010).

Programming in human muscle memory: Evidence from epidemiological studies and relevance to sarcopenia

Together with metabolic disorders, in human aging cohort studies, low birth weight and malnutrition have been associated with the decline in

the skeletal muscle mass, low strength and slower gait speed in men and women into old age (Sayer *et al.*, 2004b, 2008; Sayer & Cooper, 2005; Patel *et al.*, 2010, 2011, 2012, 2014). This leads to the earlier onset of the geriatric disorder known as sarcopenia and is therefore perhaps suggestive that sarcopenia may have origins in foetal and early life. Indeed, the reductions in muscle size and strength have been strongly associated with birth weight independently of height and weight and even when social class, physical activity, smoking and alcohol are adjusted for (Sayer *et al.*, 2004b). Furthermore, birth weight has shown a positive association with adult body mass index and fat-free mass, but not with measures of adult fat mass (Sayer *et al.*, 2004a), again indicating that lean body mass reductions in old age, a hall mark of sarcopenia, can be somewhat determined in early life. These impairments in muscle function are associated with earlier onset of disability, morbidity and mortality (Laukkanen *et al.*, 1995; Rantanen *et al.*, 1999, 2002; Rantanen, 2003; Gale *et al.*, 2007). The mechanisms of these early-life environmental differences and their impact on muscle mass and strength in these cohort studies have begun to be investigated using a cross-sectional design investigating those with lower vs. higher grip strength or lean body mass. Lower transcript expression of vitamin D receptor and interferon gamma in skeletal muscle tissue was associated with higher lean mass and lower gene expression of interleukin 6 (IL-6), tumour necrosis factor-alpha (TNF- α) and interleukin-1 receptor (IL1R1) in community-dwelling older men (Patel *et al.*, 2014). Furthermore, lower myostatin was also associated with higher grip strength in community-dwelling older men, whereas lower IL-6 in the serum was associated with lower strength (Patel *et al.*, 2014), suggesting overall that the inflammation and catabolic/protein degradative regulators are found to be increased in aged cohorts who have reduced strength and lean body mass, observed previously to be correlated with low birth weight. Although epigenetics is considered an important modulator of these foetal origins of metabolism, and studies in other animal models and tissues are beginning to take place, for example reviewed in Saffery (2014), there are limited epigenetic studies into the early-life origins of sarcopenia. This may be partly due to the expensive nature of the genome-wide type analysis and access to these human cohorts as well as complex, expensive-equivalent aging studies in animal models. There is, however, an important study to date that characterizes the methylome and transcriptome of aged, but disease-free, skeletal muscle vs. young adults (Zykovich *et al.*, 2014). These types of studies need to be conducted in the skeletal muscle of maternal nutrient-restricted offspring into old age and human cohort studies that have early-life malnourishment or low birth weights in order to distinguish important epigenetic mechanisms of the foetal origins of health and disease. It is also important that future studies assess the epigenetic response of these animals or human cohorts to a later-life nutrient, muscle growth or loss stimuli in order to address the mechanisms of muscle memory.

Muscle cellular memory: Evidence from animal tissue models and muscle-derived stem cells from humans under different environmental niches

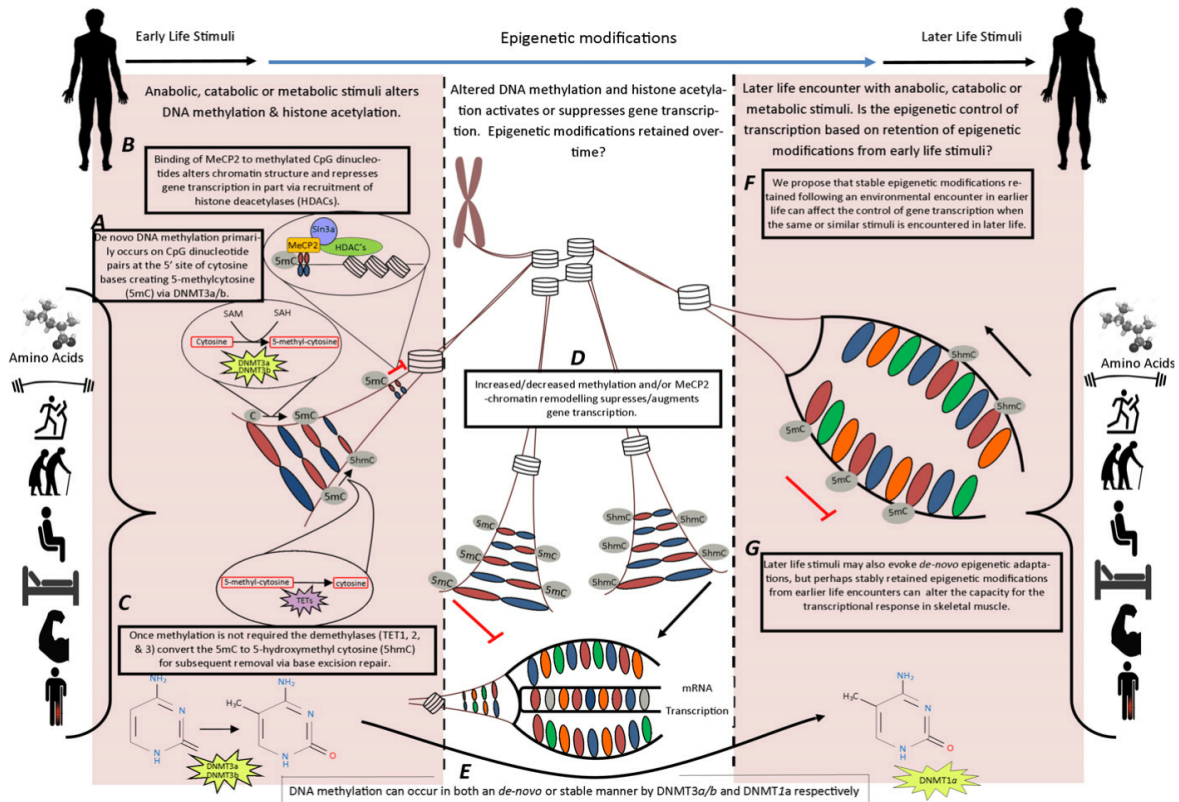
Memory from positive anabolic/growth encounters

In 2010, an important study in mice suggested that the increased muscle nuclei in fibres (myonuclei) acquired *via* a mechanical overload stimulus are retained even when a subsequent period of denervation-induced muscle loss was encountered vs. controls (Bruusgaard *et al.*, 2010). These studies were expanded by the same group in 2013, whereby testosterone was administered to mice for 3 months, enabling robust

muscle hypertrophy that was accompanied by an increase in myonuclei (Bruusgaard *et al.*, 2010; Egner *et al.*, 2013; Gundersen, 2016). These myonuclei were subsequently retained during muscle size losses following a period of testosterone withdrawal. Most importantly, when mechanical overload was presented to the animals that had received an earlier encounter of testosterone vs. controls, they exhibited a 31% increase in muscle cross-sectional area vs. control mice that showed no growth in the same period of time (Bruusgaard *et al.*, 2010; Egner *et al.*, 2013). This study therefore alludes to a mechanism whereby muscle has the capacity to adapt to a muscle growth stimulus (overload) with a positive adaptation if hypertrophic stimuli (testosterone) have been encountered previously, in line with our definition of muscle memory in this review. More evidence for memory of positive environments comes from studies that derived muscle 'stem' or precursor cells from humans. These studies are important as skeletal muscle tissue is terminally differentiated or postmitotic; therefore, skeletal muscle has its own resident stem cell population known as satellite cells that have mitotic potential and therefore contribute to muscle regeneration, repair and turnover *via* the process of proliferation, migration and fusion into the existing fibres (reviewed in Sharples & Stewart, 2011). Populations of the mitotic cells also self-renew to allow the replenishment of the stem cell pool for future regenerative bouts (Troy *et al.*, 2012). Importantly, a recent study derived these muscle stem cells from active and inactive (sedentary) individuals. The cells derived from active humans displayed an improved ability to uptake glucose and were somewhat protected from palmitate-induced insulin resistance vs. cells isolated from sedentary humans (Green *et al.*, 2013; Valencia & Spangenburg, 2013). These types of cellular studies are also important as they suggest that muscle cells retain molecular information even after isolation outside of their environmental niches. Also, as these cells have mitotic and self-renewal capabilities, they may be fundamental in passing epigenetic modifications onto daughter populations of cells and therefore involved in regulating skeletal muscle memory, something that is discussed below with respect to epigenetics regulating muscle stem cell self-renewal into old age.

Memory from negative catabolic encounters from disease, inflammation and nutrient stress

In the same vein as the studies above regarding the memory of positive environments, earlier work from our group has shown that human muscle stem cells derived from the skeletal muscle biopsies of patients with cancer, display memory of the environment from which they were derived. These cells exhibit inappropriate proliferation vs. aged matched cells derived from the muscle biopsies of healthy control patients (Foulstone *et al.*, 2003). While at an endocrine level, the IGF system between the groups was not different, at a cellular level, inappropriate IGFBP-3 expression by the muscle cells derived from the patients with cancer was associated with dysregulated cell retrieval and behaviour (Foulstone *et al.*, 2003). These were the first reported studies to identify dysregulated local expression of the IGF system in human skeletal muscle stem cells and associated memory of the derived muscle milieu. Since these earlier studies it has been demonstrated that myotubes grown from muscle-derived cells isolated from obese humans have greater intramyocellular lipid contents due to the membrane relocation of fatty acid translocase (FAT/CD36) (Aguer *et al.*, 2010). More recently, this concept has been confirmed and discussed by four further papers (three original works and one review), again collectively suggesting that muscle-derived cells retain a 'memory' of negative encounters once isolated from different environmental niches, where (i)



Acute epigenetic modification by existing myonuclei in terminally differentiated fibres? Stable epigenetic modification passed onto daughter cells via self-renewing satellite cells incorporated into fibres?

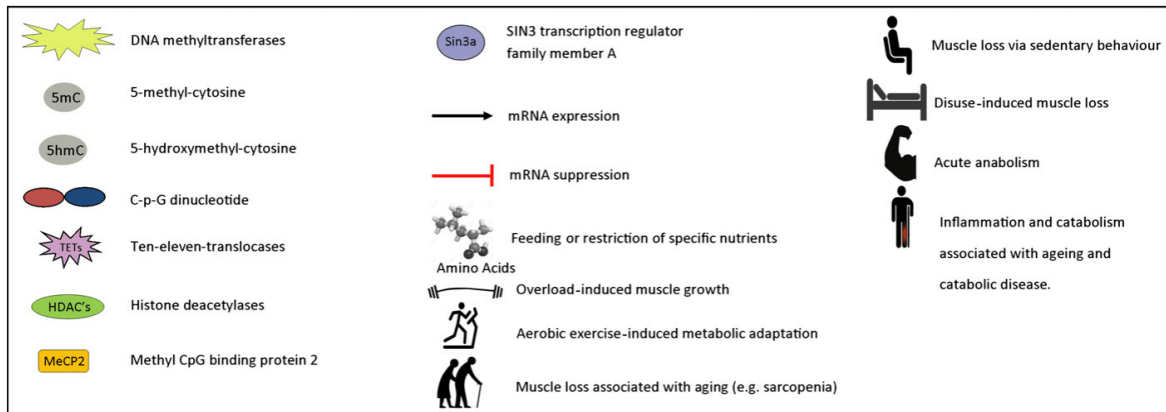


Fig. 1 A proposed schematic representation of skeletal muscle 'epi'-memory.

muscle-derived cells from obese patients do not respond to lipid oversupply with the same gene expression signatures vs. control (Maples & Braut, 2015); (ii) muscle-derived cells from intrauterine growth-restricted sheep foetuses exhibit deficiencies in proliferation vs. controls (Yates *et al.*, 2014); (iii) skeletal muscle stem cells isolated from prenatal

50% global nutrient-restricted mice offspring or early postnatal high-fat diet (60% of total calories from fat) offspring have a reduced number of muscle precursor cells and a 32% decrease in the capacity of these cells to regenerate after injury (Woo *et al.*, 2011). Interestingly, in the same study it was reported that a high-fat diet also evoked reductions in the

number of muscle stem cells retrieved from skeletal muscle tissue and was associated with larger reductions (44%) in regeneration (chow 16% vs. high-fat diet 9%), suggesting that the environment in which the muscle cells were derived could be remembered and subsequently affect the muscle repair and regeneration in later life (Woo *et al.*, 2011); (iv) finally, the vast majority of aged muscle stem cells isolated from aged animals and humans or those replicatively aged in culture have an impaired or delayed differentiation/regenerative capacity (Allen *et al.*, 1982; Charge *et al.*, 2002; Lorenzon *et al.*, 2004; Lees *et al.*, 2006; Carlson & Conboy, 2007; Lancioni *et al.*, 2007; Bigot *et al.*, 2008; Hidestrand *et al.*, 2008; Pietrangelo *et al.*, 2009; Beccafico *et al.*, 2010; Sharples *et al.*, 2010, 2011, 2012; Kandalla *et al.*, 2011; Merritt *et al.*, 2013; Zwetsloot *et al.*, 2013) or display delayed differentiation (Corbu *et al.*, 2010). Very few studies showed no impact of age on differentiation of the isolated muscle stem cells (Shefer *et al.*, 2006; Alsharidah *et al.*, 2013); where even these studies reported aged muscle to have fewer stem cells to begin with (Shefer *et al.*, 2006). Furthermore, the ability of these cells to self-renew, depleting the stem cell pool (Bigot *et al.*, 2015), appears to be impaired with age, a process that may be epigenetically regulated (discussed below). Importantly, all of these studies highlight that the epigenetic regulation of muscle 'stem' cells with mitotic potential could be important in the concept of muscle memory with respect to metabolic function, muscle repair and regeneration in skeletal muscle tissue.

Epigenetics underpins programming and gives muscle an 'Epi-memory'

Epigenetics translated means 'above genetics' and is defined as changes in gene activity and expression as a result of transient or stable structural modifications (primarily to DNA or histones, but also post-transcriptional modification of RNA) without altering the genetic code. The modifications are caused directly to DNA *via* methylation, or at the level of the surrounding core histones (H2A, H2B, H3 and H4). Histones have long N-terminal tails, meaning that they are readily prone to methylation (me), acetylation (ac), phosphorylation (p), ubiquitination (ub), SUMOylation, ADP-ribosylation and finally citrullination (reviewed in Bannister & Kouzarides, 2011). DNA methylation and histone modification result in alterations in gene transcription. DNA methylation primarily occurs on CpG dinucleotide pairs at the 5' site of cytosine bases creating 5-methylcytosine (5mC). This usually leads to gene suppression when occurring within a promoter region of a gene *via* blocking the access of RNA polymerase after the enlistment of methyl CpG binding domain (MBD) proteins (Bogdanovic & Veenstra, 2009). Other DNA methylation that occurs at intragenic sites, however, has an extremely variable impact on gene transcription, only when intragenic methylation leads to repressing the function of long-range gene enhancers and it has been shown to more consistently suppress gene expression (Weber *et al.*, 2007; Schmidl *et al.*, 2009), and intragenic methylation can also be involved in modulating alternative splicing of the gene (Shukla *et al.*, 2011; Sati *et al.*, 2012; Maunakea *et al.*, 2013). The process of DNA methylation and demethylation is controlled by DNA methyltransferases (DNMTs) and demethylases, called the ten-eleven translocation (TET) enzymes. De novo methylation is controlled by methyltransferases DNMT3a and DNMT3b, whereas DNMT1 maintains methylation (Trasler *et al.*, 2003). Once methylation is not required, TET1, 2 and 3 convert the 5mC to 5-hydroxymethyl cytosine (5hmC) for the subsequent removal *via* base excision repair (Tahiliani *et al.*, 2009; Ito *et al.*, 2010). Histone modifications, however, are more complex than DNA methylation in their action to activate or suppress gene transcription. Generally,

histone methylation of lysine 4 of histone H3 (H3K4me3) is associated with an increased gene expression as is acetylation of numerous lysine residues of histones H3 and H4 (acetyl H3 and acetyl H4), whereas trimethylation of lysines 9 and 27 of histone H3 (H3K9me 2/3 and H3K27me3) and lysine 20 of histone H4 (H4K20me3) is involved in gene suppression (reviewed in Schuettengruber *et al.*, 2011). Acetylation of histones is controlled by the histone acetyltransferases (HATs) such as K-Lysine acetyltransferase 2A (KAT2A or GCN5), P300/CBP-associated factor (PCAF), CREB-binding protein (CBP), p300, K-Lysine acetyltransferase 5 (Tip60) and male absent on the first (MOF), that add acetyl groups to/from target histones. In contrast, deacetylases (HDACs) remove acetyl groups, including the class I (HDAC 1-3 and 8), class II (HDAC 4-7, 9-10), class III (Sirt1-7) and class IV HDACs (HDAC11). As described above, acetylation of histones leads to active transcription, and HATs therefore have been associated with active gene expression and the HDACs gene suppression (reviewed in Wang *et al.*, 2009). For the purposes of this review, the above summarized mechanisms are currently those that are studied with respect to skeletal muscle memory. For a more detailed role of histone modifications in modulating gene expression, this is reviewed extensively in Bannister & Kouzarides (2011).

Despite epigenetic modifications underpinning gene expression operating following changes in environmental stimuli (reviewed in Bhutani *et al.*, 2011), there are few studies to investigate the potential epigenetic modulation of skeletal muscle cell memory. Currently, there are more extensive data that exist regarding the epigenetic control of muscle stem cells and the process of myogenesis and muscle stem cell function (reviewed in Dilworth & Blais, 2011; Segales *et al.*, 2015; Laker & Ryall, 2016), including work by ourselves on the class III HDAC sirtuin 1 (Saini *et al.*, 2012). However, a very recent study has investigated the underlying epigenetics in muscle-derived cells of obese patients where lipid oversupply in these cells induced increased DNA methylation of PPAR δ with the subsequent greater suppression of PPAR δ gene expression vs. nonobese controls (Maples & Brault, 2015). Despite the subjects in the control group not being aged matched with the obese group, where the obese group were on average almost 7 years older, this study implies that epigenetic modification of lipid metabolism genes after encountering a negative metabolic environment (obesity) was retained once isolated in culture, and that epigenetic regulation of lipid metabolism genes were important mediators of metabolic function when a similar later-life environment (lipid oversupply) was encountered. At the tissue level, another study to investigate the potential epigenetic mechanisms underpinning metabolic programming as a consequence of maternal protein restriction vs. controls (8% vs. 20%) suggested that the reduction in PGC-1 α gene expression in the offspring's skeletal muscle was underpinned by increases in its own promoter methylation (Zeng *et al.*, 2013). Furthermore, early (postnatal) high-carbohydrate diets reduced Glut4 transcription in the skeletal muscle of the adult offspring (100 days postgestation) *via* epigenetic modifications including an increased methylation of the Glut4 promoter and acetylation of H2 variant (H2A.Z) and H4, importantly highlighting a novel epigenetic mechanism contributing to early-life nutrient stress that is associated with later-life adult insulin resistance and obesity (Raychaudhuri *et al.*, 2014). In humans, the relationship between nutrient stress and the potential epigenetic modulation of diabetes and obesity was also investigated where only 5 days of a high-fat feeding (50% extra calories distributed as 60% fat vs. controls with no extra calorie consumption and diet made up of 35% fat) reportedly altered DNA methylation of over 6508 genes of 14475 genes studied (Jacobsen *et al.*, 2012). Interestingly, there was a slow reversibility of DNA methylation when the high-fat diet was switched back to the control diet for 6-8 weeks, where

out of the top 10% of altered genes post the high-fat diet, only 66% of these genes had a methylation status in the opposite direction, with only 5% of these significant (Jacobsen *et al.*, 2012). Importantly this study suggests that methylation could be retained and the implication that CpG methylation could perhaps be preserved or built up over time after multiple high-fat diet periods. De novo vs. maintained methylation, as discussed above, is controlled by DNMTs that also increased post the high-fat diet in the same study, where both de novo regulating DNMT3a and maintaining DNMT1 mRNA increased (Jacobsen *et al.*, 2012). The authors did not study the activity of these enzymes that may also underpin the maintenance of methylation some 6–8 weeks later.

Importantly, our group has shown that skeletal muscle cells have an increased susceptibility to the impaired differentiation after encountering TNF- α inflammatory stress in later proliferative life if the cells have experienced an earlier, acute TNF- α stress (Sharples *et al.*, 2015a), suggestive of a morphological memory of catabolic stress in myoblasts. Importantly, in this study, the muscle cells that experienced even an acute cytokine stress in early life retained elevated myoD methylation even after 30 population doublings (Sharples *et al.*, 2015a). This study therefore suggests an important epigenetic mechanism *via* the retention of DNA methylation of important myogenic regulatory genes throughout proliferative lifespan in the muscle cells following early-life inflammatory stress. The de novo and maintenance of this methylation *via* modulating DNMTs and TETs now requires further investigation in this model. It has previously been shown in developing xenopus embryo's that memory of myoDs active gene state can persist through 24 cell divisions in the absence of transcription (Ng & Gurdon 2008). Interestingly, rather than methylation of the myoD promoter, this epigenetic memory was regulated by the association of histone H3.3 with the myoD promoter (Ng & Gurdon 2008), where histone H3.3 requires future investigation in adult muscle cell models of memory such as those described by Sharples *et al.*, (2015a) above. As chronic TNF- α is increased in the circulation (Greive *et al.*, 2001; Bruunsgaard & Pedersen, 2003; Bruunsgaard *et al.*, 2003a,b) and in that produced by skeletal muscle tissue in aged individuals (Greive *et al.*, 2001; Leger *et al.*, 2008) as well as being associated with sarcopenia and muscle loss (reviewed in (Saini *et al.*, 2006; Sharples *et al.*, 2015b), these studies suggest a potential important mechanism for muscle memory's involvement in muscle loss with age. Furthermore, recent pioneering research deriving aged human muscle stem cells showed impairments in the ability of these cells to self-renew (Bigot *et al.*, 2015), as described above, a process that is required to replenish the stem cell pool across the lifespan. In this study was reported that elderly muscle stem cells once isolated in culture demonstrated significantly lower proportion of reserve (PAX7-expressing) cells and an impaired ability for these cells to be incorporated as satellite cells when engrafted back into immunodeficient mice vs. young human muscle stem cells (Bigot *et al.*, 2015). Importantly, these cells also had higher global DNA methylation (assessed *via* whole DNA methylome array). Importantly, by using a demethylation agent, 5-aza-20-deoxycytidine (5AZA) in culture, aged muscle stem cells improved their self-renewal capacity. Of particular interest, the authors reported that increased DNA methylation of sprouty1 (or SPYR1 a known regulator of self-renewal/quiescence) corresponded with the reduced SPYR1 transcription (Bigot *et al.*, 2015). By knocking down SPYR1 to 5% using small interfering RNA (siRNA), even in the presence of global demethylation *via* 5AZA treatment, the capacity to self-renew in these cells was completely abolished, confirming the important role of epigenetically regulated SPYR1 in the loss of the muscle stem cell pool with age. This manuscript now opens up the possibility of epigenetic characteristics being 'reset' in aged muscle to restore normal function

where self-renewal is fundamental to the capacity of muscle to respond to repeated regenerative bouts across the lifespan, demonstrating a clear clinical translation. Earlier work also suggested that increased senescence in isolated muscle stem cells from aged mice, characterized by an increased in p16INK4, was controlled epigenetically by the polycomb protein 1/H2A ubiquitination (PRC1/H2Aub) and the subsequent loss in repressive function of P16INK4a gene expression (Sousa-Victor *et al.*, 2014), importantly, also suggesting that, together with DNA methylation, histone modifications can also be retained by muscle cells once isolated from their niches that may subsequently affect their function into old age. Overall, these studies strongly suggest that epigenetic modifications are retained throughout the lifespan and can affect skeletal muscle function in later life. Importantly, these types of epigenetic modifications could be targeted therapeutically in future to 'reset' skeletal muscle loss associated with aging or perhaps even diseases such as cachexia.

Epigenetics of exercise adaptation and exercise interventions as a suitable model to investigate skeletal muscle memory

Muscle memory originally entered scientific literature synonymous to motor learning, where the learning of a motor task involves consolidating a specific movement pattern through repetition. Within exercise or strength and conditioning settings, muscle 'memory' is largely an anecdotal phrase used to describe the ability of adult human skeletal muscle to respond more advantageously to stimuli that have already been encountered in the past, where applied practitioners often describe the ability of individual muscle to respond more quickly, for example after injury or the off-season, to an environmental stimulus, such as a period of resistance or aerobic training that has already been experienced in the past. There is currently evidence that muscle responds morphologically and functionally differently following retraining (i.e. following an earlier period of exercise and cessation/detraining of exercise), especially postresistance exercise (Staron *et al.*, 1991; Taaffe & Marcus, 1997; Henwood & Taaffe, 2008; Taaffe *et al.*, 2009), that myonuclei are retained after prior anabolic hormonal/exercise encounters (Bruunsgaard *et al.*, 2010; Egner *et al.*, 2013; Gundersen, 2016) and finally that epigenetic modification occurs in the skeletal muscle following exercise (reviewed in Ntanasis-Stathopoulos *et al.*, 2013; Goto *et al.*, 2015). However, the epigenetic mechanisms for exercise-induced muscle memory still require further investigation.

Most notably, with respect to exercise-induced epigenetic adaptations, 60 min of acute high-intensity cycling exercise (75% VO_2 max/maximal aerobic capacity) induced histone acetylation of H3 in skeletal muscle, a process that was found to be controlled by the removal of the HDACs from the nucleus (McGee *et al.*, 2009). Furthermore, following initial studies suggesting that PGC-1 α hypermethylation resulted in associated reductions in mitochondrial content in patients with type 2 diabetes (Barres *et al.*, 2009), it has subsequently been observed that there was reduced DNA methylation of PGC-1 α , mitochondrial transcription factor A (TFAM) and pyruvate dehydrogenase lipoamide kinase isozyme 4 (PDK4) (all associated with mitochondrial biogenesis) immediately post acute aerobic exercise at 80% of maximal aerobic capacity (until 1674 KJ was expended) and a reduction in PPAR δ methylation 3 h post exercise, corresponding with reductions in their own gene expression (3 h post exercise for PGC-1 α , PDK4 and PPAR- δ , immediately post for TFAM) (Barres *et al.*, 2012). Lower exercise intensities (40% vs. 80% VO_2 max until 1674 KJ was expended) were, however, found to evoke no methylation changes in the above-mentioned genes (Barres *et al.*, 2012). More, recently 120 min of steady-state exercise

(60% Vo_2 peak) reportedly increased methylation in the promoter of fatty acid-binding protein 3 (FABP3) after 4 h of recovery resulting in the impaired mRNA transcription (Lane *et al.*, 2015). Furthermore, suppression of DNA methylation was also associated with increased basal mRNA levels of the PGC-1 α promoter A after exercise but not the PGC-1 α promoter B where this was controlled by the methylation of lysine 4 on histone 3 (H3K4me3) (Lochmann *et al.*, 2015). With respect to chronic exercise, 6 months of supervised aerobic exercise 3 \times 1 h per week (varied intensity) changed the methylation of several genes associated with metabolism (Nitert *et al.*, 2012). These included increases in DNA methylation of runt-related transcription factor 1 (*RUNX1*) and myocyte-specific enhancer factor 2A (*MEF2A*), transcription factors involved in exercise-induced changes in Glut4 expression influencing glucose uptake in skeletal muscle (Smith *et al.*, 2007, 2008). Furthermore, in the same study, methylation of NADH dehydrogenase ubiquinone 1 subunit C2 (*NDUFC2*) increased, encoding an enzyme that is part of the respiratory chain (Olsson *et al.*, 2011), as well as observed alterations in the methylation of adiponectin receptors 1 and 2 and bradykinin receptor (*BDKRB2*), which are both involved in regulating metabolism in the skeletal muscle (Taguchi *et al.*, 2000; Yamauchi *et al.*, 2003). Together with epigenetic alterations at the tissue level, epigenetic modifications are observed in satellite cells after exercise-induced activation (Fujimaki *et al.*, 2014). Increased Wnt/ β -catenin signalling post exercise caused histone modifications promoting gene activation such as H3K4me2 and H3Ac together with corresponding decreases in gene suppressing H3K9me2 on Myf5 and myoD gene promoters that subsequently led to observed exit from the quiescent states in satellite cells and increased number of dividing satellite cells post exercise (Fujimaki *et al.*, 2014). Most notably, exercise in obese mothers (mice) rescued hypermethylation of PGC-1 α and corresponding reductions in mRNA levels of PGC-1 α , Glut4, Cox4 and CytoC together with the loss in metabolic function in later life of the offspring that was a consequence of the obese *in utero* environment in the nonexercise group (Laker *et al.*, 2014). Collectively, the above studies fascinatingly suggest that both acute and chronic exercise stimuli can cause epigenetic modifications in skeletal muscle, with the later studies suggesting that an exercise stimulus in the parents can be 'remembered' by the offspring. However, it remains to be seen whether these exercise-induced methylation changes can be retained, or over what period they are lost before a further acute or chronic exercise encounter is required to have the same or accumulative effect. There are currently little or no studies into epigenetic modulation post acute anabolic stimuli such as that of acute resistance exercise or those induced by muscle hypertrophy *via* chronic resistance exercise. To the authors' knowledge, there are also no studies investigating the epigenetic mechanisms underlying muscle adaptation to prior encounters with muscle growth or loss associated with resistance exercise or metabolic adaptation associated with aerobic exercise. Importantly, studies are required to understand skeletal muscle memory of muscle loss encounters associated with disuse or inactivity, or following nutrient feeding, for example via amino acid administration, or nutrient stress, for example CHO restriction or calorie restriction. Finally, it is unknown whether the skeletal muscle can retain any increase or suppression of methylation if a similar exercise stimulus is encountered in later life, or more stably retain these changes following chronic exercise. As exercise stimuli are routinely undertaken in human skeletal muscle adaptation studies, we propose that exercise *via* exposure to 'earlier life' training followed by the cessation of training (detraining) back to baseline and then followed by subsequent retraining would be a suitable model to investigate the epigenetic adaptation of skeletal muscle memory at the tissue and cellular level. Finally, it will be fundamental to

experimentally determine the importance of epigenetic modifications using the memory evoking models described above in both terminally differentiated muscle fibres/tissue and satellite cells that do have mitotic potential. As muscle tissue is postmitotic, it could be assumed that epigenetic modifications would be more transient and perhaps important for more acute adaptation. On the other hand, satellite cells can proliferate, self-renew and potentially pass on epigenetic modifications to daughter populations (Sharples *et al.*, 2015a); therefore once incorporated into tissue as myonuclei, this would perhaps implicate a role for satellite cells in memory of the muscle tissue later in life. These notions require important future attention to determine the epigenetic adaptation of skeletal muscle memory and the importance of these modifications both at the cellular and tissue level (depicted in Fig. 1).

Conclusion

Skeletal muscle memory is defined as 'The capacity of skeletal muscle to respond differently to environmental stimuli in an adaptive or maladaptive manner if the stimuli have been previously encountered.' Based on the evidence from metabolic programming studies in animal models, epidemiological evidence in humans as well as a suggested retention of epigenetic information in skeletal muscle cells isolated from different environmental niches or over daughter populations, we suggest that; memory in skeletal muscle is underpinned by epigenetic modifications (epi-memory). The future study of epigenetic modifications during periods of muscle growth, loss, and regrowth, as well as during metabolic disease and aging across the lifespan, has the potential to pave the way for future understanding into the mechanisms of skeletal muscle adaptation and plasticity and potentially provide novel therapeutic targets for ameliorating muscle loss conditions.

Funding info

No funding information provided.

Conflict of interest

None declared.

References

- Aguer C, Mercier J, Man CY, Metz L, Bordenave S, Lambert K, Jean E, Lantier L, Bounoua L, Brun JF, Raynaud de Mauverger E, Andreelli F, Foretz M, Kitzmann M (2010) Intramyocellular lipid accumulation is associated with permanent relocation *ex vivo* and *in vitro* of fatty acid translocase (FAT)/CD36 in obese patients. *Diabetologia* **53**, 1151–1163.
- Alic N, Tullet JM, Niccoli T, Broughton S, Hoddinott MP, Slack C, Gems D, Partridge L (2014) Cell-nonautonomous effects of dFOXO/DAF-16 in aging. *Cell Rep.* **6**, 608–616.
- Allen RE, McAllister PK, Masak KC, Anderson GR (1982) Influence of age on accumulation of alpha-actin in satellite-cell-derived myotubes *in vitro*. *Mech. Ageing Dev.* **18**, 89–95.
- Almeida M, Han L, Martin-Millan M, O'Brien CA, Manolagas SC (2007) Oxidative stress antagonizes Wnt signaling in osteoblast precursors by diverting β -catenin from T cell factor- to forkhead box O-mediated transcription. *J. Biol. Chem.* **282**, 27298–27305.
- Alsharidah M, Lazarus NR, George TE, Agle CC, Velloso CP, Harridge SD (2013) Primary human muscle precursor cells obtained from young and old donors produce similar proliferative, differentiation and senescent profiles in culture. *Ageing Cell*, **12**, 333–344.
- Anway MD, Cupp AS, Uzumcu M, Skinner MK (2005) Epigenetic transgenerational actions of endocrine disruptors and male fertility. *Science* **308**, 1466–1469.

- Aragao RD, Guzman-Quevedo O, Perez-Garcia G, Manhaes-de-Castro R, Bolanos-Jimenez F (2014) Maternal protein restriction impairs the transcriptional metabolic flexibility of skeletal muscle in adult rat offspring. *Br. J. Nutr.*, **112**, 328–337.
- Bakkar N, Wang J, Ladner KJ, Wang H, Dahlman JM, Carathers M, Acharyya S, Rudnicki MA, Hollenbach AD, Guttridge DC (2008) IKK/NF-kappaB regulates skeletal myogenesis via a signaling switch to inhibit differentiation and promote mitochondrial biogenesis. *J. Cell Biol.* **180**, 787–802.
- Bannister AJ, Kouzarides T (2011) Regulation of chromatin by histone modifications. *Cell Res.* **21**, 381–395.
- Barres R, Osler ME, Yan J, Rune A, Fritz T, Caidahl K, Krook A, Zierath JR (2009) Non-CpG methylation of the PGC-1alpha promoter through DNMT3B controls mitochondrial density. *Cell Metab.* **10**, 189–198.
- Barres R, Yan J, Egan B, Trebak JT, Rasmussen M, Fritz T, Caidahl K, Krook A, O'Gorman DJ, Zierath JR (2012) Acute exercise remodels promoter methylation in human skeletal muscle. *Cell Metab.* **15**, 405–411.
- Beccafico S, Riuzzi F, Puglielli C, Mancinelli R, Fulle S, Sorci G, Donato R (2010) Human muscle satellite cells show age-related differential expression of S100B protein and RAGE. *Age (Dordr.)*, **33**, 523–541.
- Beermann DH, Cassens RG, Hausman GJ (1978) A second look at fiber type differentiation in porcine skeletal muscle. *J. Anim. Sci.* **46**, 125–132.
- Bhutani N, Burns DM, Blau Helen M (2011) DNA demethylation dynamics. *Cell* **146**, 866–872.
- Bigot A, Jacquemin V, Debaqç-Chainiaux F, Butler-Browne GS, Toussaint O, Furling D, Mouly V (2008) Replicative aging down-regulates the myogenic regulatory factors in human myoblasts. *Biol. Cell* **100**, 189–199.
- Bigot A, Duddy WJ, Ouandaogo ZG, Negroni E, Mariot V, Ghimbovski S, Harmon B, Wielgosik A, Loiseau C, Devaney J, Dumonceaux J, Butler-Browne G, Mouly V, Duguez S (2015) Age-associated methylation suppresses SPRY1, leading to a failure of re-quietance and loss of the reserve stem cell pool in elderly muscle. *Cell Rep.* **13**, 1172–1182.
- Blesson CS, Sathishkumar K, Chinnathambi V, Yallampalli C (2014) Gestational protein restriction impairs insulin-regulated glucose transport mechanisms in gastrocnemius muscles of adult male offspring. *Endocrinology* **155**, 3036–3046.
- Bogdanovic O, Veenstra GJ (2009) DNA methylation and methyl-CpG binding proteins: developmental requirements and function. *Chromosoma* **118**, 549–565.
- Bowerman B (2005) Cell biology. Oxidative stress and cancer: a beta-catenin convergence. *Science* **308**, 1119–1120.
- Brameld JM, Mostyn A, Dandrea J, Stephenson TJ, Dawson JM, Buttery PJ, Symonds ME (2000) Maternal nutrition alters the expression of insulin-like growth factors in fetal sheep liver and skeletal muscle. *J. Endocrinol.* **167**, 429–437.
- Brown LD, Thorn SR, O'Meara MC, Lavezzi JR, Rozance PJ (2014) A physiological increase in insulin suppresses muscle-specific ubiquitin ligase gene activation in fetal sheep with sustained hypoglycemia. *Physiol. Rep.* **2**, e12045.
- Brunet A, Sweeney LB, Sturgill JF, Chua KF, Greer PL, Lin Y, Tran H, Ross SE, Mostoslavsky R, Cohen HY (2004) Stress-dependent regulation of FOXO transcription factors by the SIRT1 deacetylase. *Science* **303**, 2011–2015.
- Brunsgaard H, Pedersen BK (2003) Age-related inflammatory cytokines and disease. *Immunol. Allergy Clin. North Am.* **23**, 15–39.
- Brunsgaard H, Andersen-Ranberg K, Hjelmborg JB, Pedersen BK, Jeune B (2003a) Elevated levels of tumor necrosis factor alpha and mortality in centenarians. *Am. J. Med.* **115**, 278–283.
- Brunsgaard H, Ladelund S, Pedersen AN, Schroll M, Jorgensen T, Pedersen BK (2003b) Predicting death from tumour necrosis factor-alpha and interleukin-6 in 80-year-old people. *Clin. Exp. Immunol.* **132**, 24–31.
- Brunsgaard JC, Johansen IB, Egnér IM, Rana ZA, Gundersen K (2010) Myonuclei acquired by overload exercise precede hypertrophy and are not lost on detraining. *Proc. Natl Acad. Sci. USA* **107**, 15111–15116.
- Budge H, Dandrea J, Mostyn A, Evens Y, Watkins R, Sullivan C, Ingleton P, Stephenson T, Symonds ME (2003) Differential effects of fetal number and maternal nutrition in late gestation on prolactin receptor abundance and adipose tissue development in the neonatal lamb. *Pediatr. Res.* **53**, 302–308.
- Campos EI, Stafford JM, Reinberg D (2014) Epigenetic inheritance: histone bookmarks across generations. *Trends Cell Biol.* **24**, 664–674.
- Carlson ME, Conboy IM (2007) Loss of stem cell regenerative capacity within aged niches. *Aging Cell* **6**, 371–382.
- Charge SB, Brack AS, Hughes SM (2002) Aging-related satellite cell differentiation defect occurs prematurely after Ski-induced muscle hypertrophy. *Am. J. Physiol. Cell Physiol.* **283**, C1228–C1241.
- Chen Q, Yan M, Cao Z, Li X, Zhang Y, Shi J, Feng GH, Peng H, Zhang X, Zhang Y, Qian J, Duan E, Zhai Q, Zhou Q (2016) Sperm tsRNAs contribute to intergenerational inheritance of an acquired metabolic disorder. *Science* **351**, 397–400.
- Claycombe KJ, Roemmich JN, Johnson L, Vomhof-DeKrey EE, Johnson WT (2015) Skeletal muscle Sirt3 expression and mitochondrial respiration are regulated by a prenatal low-protein diet. *J. Nutr. Biochem.* **26**, 184–189.
- Confortim HD, Jeronimo LC, Centenaro LA, Felipe PP, Brancalho RM, Michelin MS, Torrejais MM (2015) Effects of aging and maternal protein restriction on the muscle fibers morphology and neuromuscular junctions of rats after nutritional recovery. *Micron (Oxford, England: 1993)* **71**, 7–13.
- Corbu A, Scaramozza A, Badiali-DeGiorgi L, Tarantino L, Papa V, Rinaldi R, D'Alessandro R, Zavatta M, Laus M, Lattanzi G, Cenacchi G (2010) Satellite cell characterization from aging human muscle. *Neurol. Res.* **32**, 63–72.
- Cossu G, Borello U (1999) Wnt signaling and the activation of myogenesis in mammals. *EMBO J.* **18**, 6867–6872.
- Costello PM, Rowlerson A, Astaman NA, Anthony FE, Sayer AA, Cooper C, Hanson MA, Green LR (2008) Peri-implantation and late gestation maternal undernutrition differentially affect fetal sheep skeletal muscle development. *J. Physiol.* **586**, 2371–2379.
- Costello PM, Hollis LJ, Cripps RL, Bearpark N, Patel HP, Sayer AA, Cooper C, Hanson MA, Ozanne SE, Green LR (2013) Lower maternal body condition during pregnancy affects skeletal muscle structure and GLUT-4 protein levels but not glucose tolerance in mature adult sheep. *Reprod. Sci. (Thousand Oaks, Calif.)* **20**, 1144–1155.
- Deng HZ, Deng H, Cen CQ, Chen KY, Du ML (2014) Post-receptor crosstalk between growth hormone and insulin signal in rats born small for gestational age with catch-up growth. *PLoS One* **9**, e100459.
- Desclee de Maredsous C, Oozeer R, Barbillon P, Mary-Huard T, Deltel C, Blachier F (2016) High-protein exposure during gestation or lactation or after weaning has a period-specific signature on rat pup weight, adiposity, food intake, and glucose homeostasis up to 6 weeks of age. *J. Nutr.* **146**, 21–29.
- Dilworth FJ, Blais A (2011) Epigenetic regulation of satellite cell activation during muscle regeneration. *Stem Cell Res. Ther.* **2**, 18.
- Donkin I, Verstehey S, Ingerslev LR, Qian K, Mechta M, Nordkap L, Mortensen B, Appel EV, Jorgensen N, Kristiansen VB, Hansen T, Workman CT, Zierath JR, Barres R (2016) Obesity and bariatric surgery drive epigenetic variation of spermatozoa in humans. *Cell Metab.* **23**, 369–378.
- Draeger A, Weeds AG, Fitzsimons RB (1987) Primary, secondary and tertiary myotubes in developing skeletal muscle: a new approach to the analysis of human myogenesis. *J. Neurol. Sci.* **81**, 19–43.
- Dwyer CM, Stickland NC (1994) Supplementation of a restricted maternal diet with protein or carbohydrate alone prevents a reduction in fetal muscle fibre number in the guinea-pig. *Br. J. Nutr.* **72**, 173–180.
- Dwyer CM, Madgwick AJ, Ward SS, Stickland NC (1995) Effect of maternal undernutrition in early gestation on the development of fetal myofibres in the guinea-pig. *Reprod. Fertil. Dev.* **7**, 1285–1292.
- Egnér IM, Bruusgaard JC, Eftestol E, Gundersen K (2013) A cellular memory mechanism aids overload hypertrophy in muscle long after an episodic exposure to anabolic steroids. *J. Physiol.* **591**, 6221–6230.
- Elahi MM, Cagampang FR, Mukhtar D, Anthony FW, Ohri SK, Hanson MA (2009) Long-term maternal high-fat feeding from weaning through pregnancy and lactation predisposes offspring to hypertension, raised plasma lipids and fatty liver in mice. *Br. J. Nutr.* **102**, 514–519.
- Fahey AJ, Brameld JM, Parr T, Buttery PJ (2005) The effect of maternal undernutrition before muscle differentiation on the muscle fiber development of the newborn lamb. *J. Anim. Sci.* **83**, 2564–2571.
- Fainberg HP, Almond KL, Li D, Rauch C, Bikker P, Symonds ME, Mostyn A (2014) Impact of maternal dietary fat supplementation during gestation upon skeletal muscle in neonatal pigs. *BMC Physiol.* **14**, 6.
- Ford SP, Hess BW, Schwoppe MM, Nijland MJ, Gilbert JS, Vonnahme KA, Means WJ, Han H, Nathanielsz PW (2007) Maternal undernutrition during early to mid-gestation in the ewe results in altered growth, adiposity, and glucose tolerance in male offspring. *J. Anim. Sci.* **85**, 1285–1294.
- Foulstone EJ, Savage PB, Crown AL, Holly JM, Stewart CE (2003) Adaptations of the IGF system during malignancy: human skeletal muscle versus the systemic environment. *Horm. Metab. Res.* **35**, 667–674.
- Fujimaki S, Hidaka R, Asashima M, Takemasa T, Kuwabara T (2014) Wnt protein-mediated satellite cell conversion in adult and aged mice following voluntary wheel running. *J. Biol. Chem.* **289**, 7399–7412.
- Gale CR, Martyn CN, Cooper C, Sayer AA (2007) Grip strength, body composition, and mortality. *Int. J. Epidemiol.* **36**, 228–235.
- Gapp K, Jawaid A, Sarkies P, Bohacek J, Pelczar P, Prados J, Farinelli L, Miska E, Mansuy IM (2014) Implication of sperm RNAs in transgenerational inheritance of the effects of early trauma in mice. *Nat. Neurosci.* **17**, 667–669.

- Gardner DS, Tingey K, Van Bon BW, Ozanne SE, Wilson V, Dandrea J, Keisler DH, Stephenson T, Symonds ME (2005) Programming of glucose-insulin metabolism in adult sheep after maternal undernutrition. *Am. J. Physiol. Regul. Integr. Comp. Physiol.* **289**, R947–R954.
- Giannakou ME, Goss M, Junger MA, Hafen E, Leevers SJ, Partridge L (2004) Long-lived *Drosophila* with overexpressed dFOXO in adult fat body. *Science* **305**, 361.
- Gluckman PD, Lillycrop KA, Vickers MH, Pleasants AB, Phillips ES, Beedle AS, Burdge GC, Hanson MA (2007) Metabolic plasticity during mammalian development is directionally dependent on early nutritional status. *Proc. Natl Acad. Sci. USA* **104**, 12796–12800.
- Goto S, Kawakami K, Naito H, Katamoto S, Radak Z (2015) Epigenetic Modulation of Gene Expression by Exercise. In *Nutrition, Exercise and Epigenetics: Ageing Interventions*. (Yu BP, ed.). New York, USA: Springer International Publishing, pp. 85–100.
- Grandjean V, Foure S, De Abreu DA, Derieppe MA, Remy JJ, Rassoulzadegan M (2015) RNA-mediated paternal heredity of diet-induced obesity and metabolic disorders. *Sci. Rep.* **5**, 18193.
- Green CJ, Bunprajun T, Pedersen BK, Scheele C (2013) Physical activity is associated with retained muscle metabolism in human myotubes challenged with palmitate. *J. Physiol.* **591**, 4621–4635.
- Greer EL, Brunet A (2005) FOXO transcription factors at the interface between longevity and tumor suppression. *Oncogene* **24**, 7410–7425.
- Greive JS, Cheng B, Rubin DC, Yarasheski KE, Semenovich CF (2001) Resistance exercise decreases skeletal muscle tumor necrosis factor alpha in frail elderly humans. *FASEB J.* **15**, 475–482.
- Gundersen K (2016) Muscle memory and a new cellular model for muscle atrophy and hypertrophy. *J. Exp. Biol.* **219**, 235–242.
- Guzman-Quevedo O, Da Silva Aragao R, Perez Garcia G, Matos RJ, de Sa Braga Oliveira A, Manhaes de Castro R, Bolanos-Jimenez F (2013) Impaired hypothalamic mTOR activation in the adult rat offspring born to mothers fed a low-protein diet. *PLoS One* **8**, e74990.
- Hansen KH, Bracken AP, Pasini D, Dietrich N, Gehani SS, Monrad A, Rappsilber J, Lerdrup M, Helin K (2008) A model for transmission of the H3K27me3 epigenetic mark. *Nat. Cell Biol.* **10**, 1291–1300.
- Henwood TR, Taaffe DR (2008) Detraining and retraining in older adults following long-term muscle power or muscle strength specific training. *J. Gerontol. A Biol. Sci. Med. Sci.* **63**, 751–758.
- Hidestrand M, Richards-Malcolm S, Gurley CM, Nolen G, Grimes B, Waterstrat A, Zant GV, Peterson CA (2008) Sca-1-expressing nonmyogenic cells contribute to fibrosis in aged skeletal muscle. *J. Gerontol. A Biol. Sci. Med. Sci.* **63**, 566–579.
- van der Horst A, Burgering BM (2007) Stressing the role of FoxO proteins in lifespan and disease. *Nat. Rev. Mol. Cell Biol.* **8**, 440–450.
- Ito S, D'Alessio AC, Taranova OV, Hong K, Sowers LC, Zhang Y (2010) Role of Tet proteins in 5mC to 5hmC conversion, ES-cell self-renewal and inner cell mass specification. *Nature* **466**, 1129–1133.
- Jackman RW, Kandarian SC (2004) The molecular basis of skeletal muscle atrophy. *Am. J. Physiol. Cell Physiol.* **287**, C834–C843.
- Jackson MJ, McArdle A (2011) Age-related changes in skeletal muscle reactive oxygen species generation and adaptive responses to reactive oxygen species. *J. Physiol.* **589**, 2139–2145.
- Jacobsen SC, Brons C, Bork-Jensen J, Ribel-Madsen R, Yang B, Lara E, Hall E, Calvanese V, Nilsson E, Jorgensen SW, Mandrup S, Ling C, Fernandez AF, Fraga MF, Poulsen P, Vaag A (2012) Effects of short-term high-fat overfeeding on genome-wide DNA methylation in the skeletal muscle of healthy young men. *Diabetologia* **55**, 3341–3349.
- Kandalla PK, Goldspink G, Butler-Browne G, Mouly V (2011) Mechano Growth Factor E peptide (MGF-E), derived from an isoform of IGF-1, activates human muscle progenitor cells and induces an increase in their fusion potential at different ages. *Mech. Ageing Dev.* **132**, 154–162.
- Khan IY, Dekou V, Douglas G, Jensen R, Hanson MA, Poston L, Taylor PD (2005) A high-fat diet during rat pregnancy or suckling induces cardiovascular dysfunction in adult offspring. *Am. J. Physiol. Regul. Integr. Comp. Physiol.* **288**, R127–R133.
- Krssak M, Falk Petersen K, Dresner A, DiPietro L, Vogel SM, Rothman DL, Roden M, Shulman GI (1999) Intramyocellular lipid concentrations are correlated with insulin sensitivity in humans: a 1H NMR spectroscopy study. *Diabetologia* **42**, 113–116.
- Kruse M, Keyhani-Nejad F, Isken F, Nitz B, Kretschmer A, Reischl E, de Las Heras Gala T, Osterhoff MA, Grallert H, Pfeiffer AF (2015) A high fat diet during mouse pregnancy and lactation targets GIP-regulated metabolic pathways in adult male offspring. *Diabetes*, **65**, 574–584.
- Laker RC, Ryall JG (2016) DNA methylation in skeletal muscle stem cell specification, proliferation, and differentiation. *Stem Cells Int.* **2016**, 9.
- Laker RC, Lillard TS, Okutsu M, Zhang M, Hoehn KL, Connelly JJ, Yan Z (2014) Exercise prevents maternal high-fat diet-induced hypermethylation of the Pgc-1alpha gene and age-dependent metabolic dysfunction in the offspring. *Diabetes* **63**, 1605–1611.
- Lancioni H, Lucentini L, Palomba A, Fulle S, Micheli MR, Panara F (2007) Muscle actin isoforms are differentially expressed in human satellite cells isolated from donors of different ages. *Cell Biol. Int.* **31**, 180–185.
- Lane SC, Camera DM, Lassiter DG, Areta JL, Bird SR, Yeo WK, Jeacocke NA, Krook A, Zierath JR, Burke LM, Hawley JA (2015) Effects of sleeping with reduced carbohydrate availability on acute training responses. *J. Appl. Physiol.* (1985) **119**, 643–655.
- Latouche C, Heywood SE, Henry SL, Ziemann M, Lazarus R, El-Osta A, Armitage JA, Kingwell BA (2014) Maternal overnutrition programs changes in the expression of skeletal muscle genes that are associated with insulin resistance and defects of oxidative phosphorylation in adult male rat offspring. *J. Nutr.* **144**, 237–244.
- Lau MM, Stewart CE, Liu Z, Bhatt H, Rotwein P, Stewart CL (1994) Loss of the imprinted IGF2/cation-independent mannose 6-phosphate receptor results in fetal overgrowth and perinatal lethality. *Genes Dev.* **8**, 2953–2963.
- Laukkanen P, Heikkinen E, Kauppinen M (1995) Muscle strength and mobility as predictors of survival in 75–84-year-old people. *Age Ageing* **24**, 468–473.
- Lees SJ, Rathbone CR, Booth FW (2006) Age-associated decrease in muscle precursor cell differentiation. *Am. J. Physiol. Cell Physiol.* **290**, C609–C615.
- Leger B, Derave W, De Bock K, Hespel P, Russell AP (2008) Human sarcopenia reveals an increase in SOCS-3 and myostatin and a reduced efficiency of Akt phosphorylation. *Rejuvenation Res.* **11**, 163–175B.
- Li H, Malhotra S, Kumar A (2008) Nuclear factor-kappa B signaling in skeletal muscle atrophy. *J. Mol. Med.* (Berlin, Germany) **86**, 1113–1126.
- Liebers R, Rassoulzadegan M, Lyko F (2014) Epigenetic regulation by heritable RNA. *PLoS Genet.* **10**, e1004296.
- Liu X, Pan S, Li X, Sun Q, Yang X, Zhao R (2015) Maternal low-protein diet affects myostatin signaling and protein synthesis in skeletal muscle of offspring piglets at weaning stage. *Eur. J. Nutr.* **54**, 971–979.
- Lochmann TL, Thomas RR, Bennett JP Jr, Taylor SM (2015) Epigenetic modifications of the PGC-1alpha promoter during exercise induced expression in mice. *PLoS One* **10**, e0129647.
- Lorenz P, Bandi E, de Guarrini F, Pietrangelo T, Schafer R, Zweyer M, Wernig A, Ruzzier F (2004) Ageing affects the differentiation potential of human myoblasts. *Exp. Gerontol.* **39**, 1545–1554.
- Mallinson JE, Sculley DV, Craigon J, Plant R, Langley-Evans SC, Brameld JM (2007) Fetal exposure to a maternal low-protein diet during mid-gestation results in muscle-specific effects on fibre type composition in young rats. *Br. J. Nutr.* **98**, 292–299.
- Maltin CA, Delday MI, Sinclair KD, Steven J, Sneddon AA (2001) Impact of manipulations of myogenesis in utero on the performance of adult skeletal muscle. *Reproduction* (Cambridge, England) **122**, 359–374.
- Mann CJ, Perdiguero E, Kharraz Y, Aguilar S, Pessina P, Serrano AL, Munoz-Canoves P (2011) Aberrant repair and fibrosis development in skeletal muscle. *Skeletal Muscle* **1**, 21.
- Maples JM, Brault JJ (2015) Lipid exposure elicits differential responses in gene expression and DNA methylation in primary human skeletal muscle cells from severely obese women. *Physiol. Genomics* **47**, 139–146.
- Marin P, Andersson B, Krotkiewski M, Bjorntorp P (1994) Muscle fiber composition and capillary density in women and men with NIDDM. *Diabetes Care* **17**, 382–386.
- Maunakea AK, Chepelev I, Cui K, Zhao K (2013) Intragenic DNA methylation modulates alternative splicing by recruiting MeCP2 to promote exon recognition. *Cell Res.* **23**, 1256–1269.
- McGee SL, Fairlie E, Garnham AP, Hargreaves M (2009) Exercise-induced histone modifications in human skeletal muscle. *J. Physiol.* **587**, 5951–5958.
- McLeod KI, Goldrick RB, Whyte HM (1972) The effect of maternal malnutrition on the progeny in the rat. Studies on growth, body composition and organ cellularity in first and second generation progeny. *Aust. J. Exp. Biol. Med. Sci.* **50**, 435–446.
- McPherron AC, Lee SJ (1997) Double muscling in cattle due to mutations in the myostatin gene. *Proc. Natl Acad. Sci. USA* **94**, 12457–12461.
- Merritt EK, Stec MJ, Thalacker-Mercer A, Windham ST, Cross JM, Shelley DP, Tuggle SC, Kosek DJ, Kim JS, Bamman MM (2013) Heightened muscle inflammation susceptibility may impair regenerative capacity in aging humans. *J. Appl. Physiol.*, **115**, 937–948.
- Morali OG, Jouneau A, McLaughlin KJ, Thiery JP, Larue L (2000) IGF-II promotes mesoderm formation. *Dev. Biol.* **227**, 133–145.
- Ng RK, Gurdon JB (2008) Epigenetic inheritance of cell differentiation status. *Cell Cycle* **7**, 1173–1177.

Appendix 2.

Title: The transcriptomic and epigenetic regulation of disuse atrophy and the return to activity in skeletal muscle.

Journal: The Official Publication of the Federation of American Societies for Experimental Biology (impact factor 5.498)

Volume: 31

Issue: 12

Pages: 5268-5282

Transcriptomic and epigenetic regulation of disuse atrophy and the return to activity in skeletal muscle

Andrew G. Fisher,^{*,1} Robert A. Seaborne,^{†,‡,1} Thomas M. Hughes,[§] Alex Gutteridge,[¶] Claire Stewart,[†] Judy M. Coulson,^{||} Adam P. Sharples,^{†,‡,2} and Jonathan C. Jarvis^{‡,3}

^{*}Institute for Ageing and Chronic Disease and ^{||}Department of Cellular and Molecular Physiology, Institute of Translational Medicine, University of Liverpool, Liverpool, United Kingdom; [†]Institute for Science and Technology in Medicine, Keele University Medical School, Keele University, Staffordshire, United Kingdom; [‡]Stem Cells, Ageing and Molecular Physiology Research Unit, Exercise Metabolism and Adaptation Research Group, Research Institute for Sport and Exercise Sciences, Liverpool John Moores University, Liverpool, United Kingdom; [§]Instituto de Física y Astronomía, Universidad de Valparaíso, Valparaíso, Chile; and [¶]Pfizer, Tadworth, United Kingdom

ABSTRACT: Physical inactivity and disuse are major contributors to age-related muscle loss. Denervation of skeletal muscle has been previously used as a model with which to investigate muscle atrophy following disuse. Although gene regulatory networks that control skeletal muscle atrophy after denervation have been established, the transcriptome in response to the recovery of muscle after disuse and the associated epigenetic mechanisms that may function to modulate gene expression during skeletal muscle atrophy or recovery have yet to be investigated. We report that silencing the tibialis anterior muscle in rats with tetrodotoxin (TTX)—administered to the common peroneal nerve—resulted in reductions in muscle mass of 7, 29, and 51% with corresponding reductions in muscle fiber cross-sectional area of 18, 42, and 69% after 3, 7, and 14 d of TTX, respectively. Of importance, 7 d of recovery, during which rodents resumed habitual physical activity, restored muscle mass from a reduction of 51% after 14 d TTX to a reduction of only 24% compared with sham control. Returning muscle mass to levels observed at 7 d TTX administration (29% reduction). Transcriptome-wide analysis demonstrated that 3714 genes were differentially expressed across all conditions at a significance of $P \leq 0.001$ after disuse-induced atrophy. Of interest, after 7 d of recovery, the expression of genes that were most changed during TTX had returned to that of the sham control. The 20 most differentially expressed genes after microarray analysis were identified across all conditions and were cross-referenced with the most frequently occurring differentially expressed genes between conditions. This gene subset included myogenin (MyoG), Hdac4, Ampd3, Trim63 (MuRF1), and acetylcholine receptor subunit $\alpha 1$ (Chrna1). Transcript expression of these genes and Fboxo32 (MAFbx), because of its previously identified role in disuse atrophy together with Trim63 (MuRF1), were confirmed by real-time quantitative RT-PCR, and DNA methylation of their promoter regions was analyzed by PCR and pyrosequencing. MyoG, Trim63 (MuRF1), Fboxo32 (MAFbx), and Chrna1 demonstrated significantly decreased DNA methylation at key time points after disuse-induced atrophy that corresponded with significantly increased gene expression. Of importance, after TTX cessation and 7 d of recovery, there was a marked increase in the DNA methylation profiles of Trim63 (MuRF1) and Chrna1 back to control levels. This also corresponded with the return of gene expression in the recovery group back to baseline expression observed in sham-operated controls. To our knowledge, this is the first study to demonstrate that skeletal muscle atrophy in response to disuse is accompanied by dynamic epigenetic modifications that are associated with alterations in gene expression, and that these epigenetic modifications and gene expression profiles are reversible after skeletal muscle returns to normal activity.—Fisher, A. G., Seaborne, R. A., Hughes, T. M., Gutteridge, A., Stewart, C., Coulson, J. M., Sharples, A. P., Jarvis, J. C. Transcriptomic and epigenetic regulation of disuse atrophy and the return to activity in skeletal muscle. *FASEB J.* 31, 000–000 (2017). www.fasebj.org

ABBREVIATIONS: Chrna1, acetylcholine receptor subunit $\alpha 1$; CSA, cross-sectional area; DNMT, *de novo* methyltransferase; dNTP, deoxynucleotide; Hdac4, histone deacetylase 4; HRM-PCR, high-resolution melt PCR; MyoG, myogenin; nAChR, nicotinic acetyl choline receptor; qRT-PCR, quantitative RT-PCR; TA, tibialis anterior; TAC, Transcriptome Analysis Console; TTX, tetrodotoxin

¹ These authors contributed equally to this work.

² Correspondence: Institute for Science and Technology in Medicine, Keele University, Guy Hilton Research Centre, Thornburrow Dr., Staffordshire ST4 7QB, United Kingdom. E-mail: a.p.sharples@gmail.com

³ Correspondence: Research Institute for Sport and Exercise, Sciences, Liverpool John Moores University, Byrom St. Campus, Liverpool L3 3AF, United Kingdom. E-mail: J.C.Jarvis@ljmu.ac.uk

doi: 10.1096/fj.201700089RR

This article includes supplemental data. Please visit <http://www.fasebj.org> to obtain this information.

Skeletal muscle is the most abundant tissue in the mammalian body and, therefore, maintenance of its structure and function are important to health across the lifespan. The global maintenance of skeletal muscle mass is governed by a fine balance between muscle protein synthesis and degradation. Skeletal muscle undergoes rapid loss—atrophy—during disuse and inactivity (1–4); catabolic/inflammatory disease states, such as cancer cachexia (5, 6), sepsis (7), chronic heart failure (8), and obesity (9); as well as with denervation after, for example, spinal cord injury (10) or during aging (sarcopenia) (11). To investigate the underlying time course and mechanisms of skeletal muscle atrophy, such models as denervation *via* nerve section (12), tetrodotoxin (TTX) injection (13), limb suspension (14), spaceflight (15), and chronic overuse (16, 17) have been implemented. Within these models, large alterations in gene regulatory networks may orchestrate the altered balance between protein synthesis and degradation during muscle wasting (18). Under such conditions, these regulatory networks are altered to favor the breakdown of skeletal muscle proteins, predominantly *via* the ubiquitin-proteasome pathway (19–21). Whereas gene regulatory networks that control skeletal muscle atrophy have been somewhat elucidated, the role of epigenetic alterations in modulating gene expression during skeletal muscle atrophy has received less attention. Furthermore, there are few studies that have investigated the transcriptomic and epigenetic change that underlies the recovery of skeletal muscle after a return to normal physical activity after a period of disuse.

Epigenetic control of gene expression occurs primarily as a result of the modification to DNA or chromatin/histones as well as post-transcriptional modification of RNA (22). It has recently been suggested that denervation-induced atrophy results in the differential expression of genes that are associated with chromatin remodeling (23). Recent *in vitro* evidence also suggests that epigenetic mechanisms may influence regeneration and myotube atrophy (24). Skeletal muscle cells that have encountered the atrophic stimulus of the inflammatory cytokine, TNF- α , during their early proliferative life are more susceptible to TNF- α later in their proliferative life, and demonstrate impaired differentiation and regeneration compared with matched, untreated controls (24). Of importance, in this study, a retention of DNA methylation of the myogenic regulatory factor, MyoD was evident over 30 population doublings in muscle cells that receive a single acute (24-h) cytokine stress in early life (24). This study, therefore, points to a potentially important epigenetic mechanism that underlies the susceptibility to loss of muscle mass (25). Furthermore, recent studies that investigated 44 muscle-specific genes reported that where low methylation occurred, gene enhancer activity increased (26). Despite this, it has not been confirmed *in vivo* whether the modulation of gene expression *via* DNA methylation is a mechanism that regulates skeletal muscle disuse atrophy.

In the present study, we used TTX to silence the nerve to evoke disuse-induced muscle atrophy. TTX inhibits the firing of action potentials by binding to the voltage-gated sodium channel in nerve cell membranes, which blocks the throughput of sodium ions; therefore, the muscles that are

innervated by the blocked nerve cannot be activated to contract (27). This model has the advantage over nerve section in that TTX causes a complete, but reversible, block of sodium channels and, thus, reversible nerve and muscle inactivity. In this study, to investigate both disuse and recovery, TTX was delivered over a preset period after which normal nerve activity resumed. After nerve silencing, DNA microarray technology was used to investigate the temporal genome-wide transcript expression profiles associated with progressive atrophy at 3, 7, and 14 d of disuse. Nerve block was then released, habitual activity resumed, and gene expression profiles were monitored after 7 d of recovery. Finally, DNA methylation within the promoter regions of genes was measured *via* pyrosequencing for genes that demonstrated—*via* microarray and confirmatory real-time quantitative RT-PCR (qRT-PCR)—the most significant alterations in expression across all conditions and that were most frequently differentially expressed across all pairwise comparisons. The aim of this investigation was, therefore, to elucidate the epigenetic control of gene expression after disuse atrophy and a return to normal physical activity in skeletal muscle. We hypothesized that disuse atrophy would be controlled by differential DNA methylation and corresponding changes in gene expression, and that these alterations perhaps would be transient and dynamic in nature and, therefore, reversible as normal muscle activity resumes.

MATERIALS AND METHODS

Animals

Ethics approval was obtained and experimental procedures were conducted with the permissions within a project license granted under the British Home Office Animals (Scientific Procedures) Act 1986. Male Wistar rats that weighed between 350–450 g were housed in controlled conditions of 20°C and 45% relative humidity, with food and water available *ad libitum*. Animals were assigned to 5 groups that included 1 control group and 3 TTX-exposed groups for periods of 3, 7, and 14 d, including a 14-d TTX exposure plus 7-d active recovery group. Experimental groups are detailed below and represented schematically in Fig. 1.

Experimental groups

The left common peroneal nerve was exposed to TTX over preset time courses. Groups ($n = 6$) consisted of 3, 7, and 14-d TTX exposure and 14 d of TTX followed by 7 d of natural active recovery. To control TTX exposure, a miniosmotic pump (Mini Osmotic Pump 2002; Alzet, Cupertino, CA, USA) was implanted subcutaneously in the scapular region of animals under TTX conditions. Delivery tubes were subcutaneously channeled to a silicone rubber cuff that was carefully placed around the common peroneal nerve of the left hind limb. Implantation was performed in-house as a modification of a published design (28). The osmotic pump efficiently delivered 0.5 μ l/h TTX (350 μ g/ml in sterile 0.9% saline) to the nerve cuff, which allowed the common peroneal nerve to be exposed to TTX so that the ankle dorsiflexor muscles—tibialis anterior (TA) and extensor digitorum longus—were silenced but normal voluntary plantarflexion was maintained. The general welfare and mobility of group-housed rats were minimally affected. Correct assembly and loading of the osmotic pump and nerve cuff was planned so

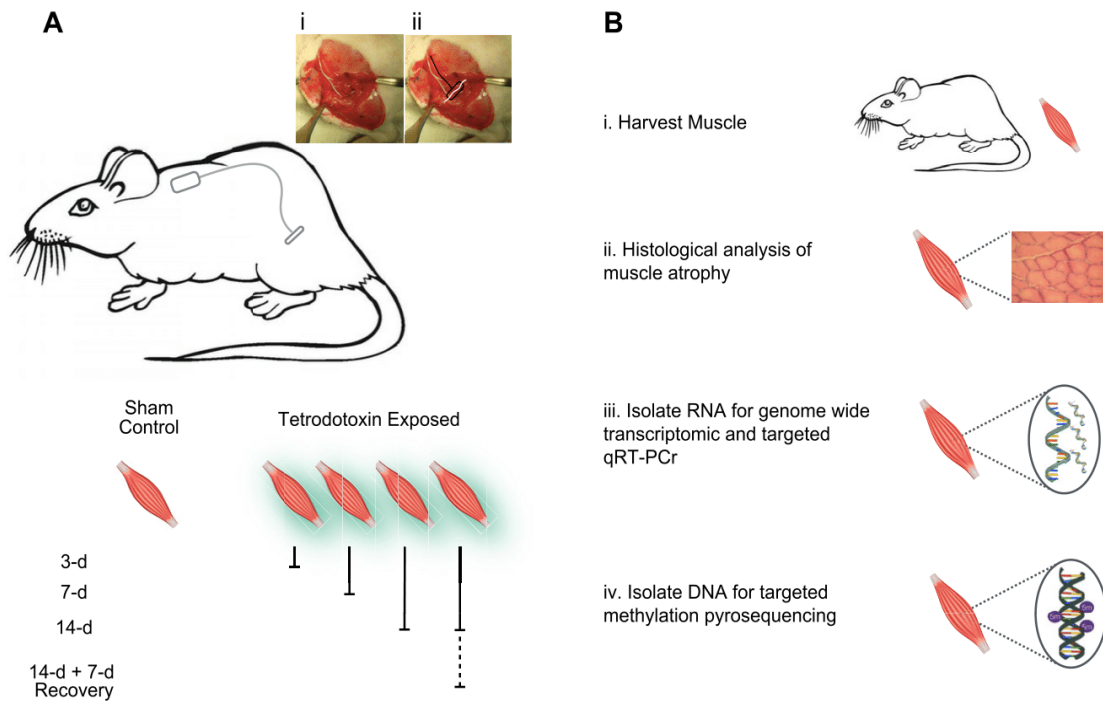


Figure 1. Schematic representation of the TTX muscle atrophy model and subsequent muscle sample preparation for morphologic, transcriptomic, and epigenetic analysis. *A*) Display of physiologic location of TTX administration pump. Real image of osmotic pump location and assembly within the left hindlimb of the rodent (*i*), and a representation overview of the osmotic pump assembly (*ii*; black lines show osmotic pump unit and delivery tube to nerve cuff unit and white line displays the synaptic nerve). *B*) Muscle sample preparation for downstream analysis: treated (left) and untreated contralateral control (right; $n = 6$).

that TTX administration would terminate after 14 d, which allowed the recovery of hindlimb function from d 14 to 21 within the 14-d TTX + 7-d recovery group.

Morphology and histology for muscle size (mass and cross-sectional area)

At the end of each experimental time course, all animals were humanely euthanized with increasing CO₂ concentration and cervical dislocation. For morphologic and histologic purposes, muscle was harvested from control and experimental groups ($n = 6$), weighed, and divided into pieces, and a transverse portion from the midbelly of the muscle was frozen in melting isopentane, cryostat sectioned (~10 μm), and stained with hematoxylin and eosin. For each muscle sample, 5 images were obtained at random. By using ImageJ 1.45i software (National Institutes of Health, Bethesda, MD, USA), each photograph was overlaid with an 8 × 8 grid with which to make an unbiased selection of fibers. Ten fibers were selected for counting for each field of view at the first 10 intersections of the grid that fell within a fiber. Magnification of each section was calibrated from an image of a stage graticule. Cross-sectional area (CSA) was estimated from precise diameter measurements that were taken by selecting 2 points across the minimum diameter and assuming a circular cross-section. Mean TA mass for all control and experimental groups was expressed as a percentage of whole animal body mass (428 ± 45 g) to normalize for interindividual differences in animal size ($n = 6$). Mean CSA of TA muscle fiber was expressed as percent change from the untreated contralateral

control limb for each animal ($n = 6$). All data are presented as means ± SD, unless otherwise stated.

Transcriptome analysis

We conducted microarray analyses to compare genome-wide transcript expression from 3-, 7-, 14-d TTX and 14-d TTX + 7-d recovery ($n = 4$ for each group). Untreated control samples were also used for quality control of microarray analysis and were excluded from the final analysis. Frozen muscle samples were sent to AROS Applied Biotechnology (Aarhus, Denmark), where RNA was isolated *via* AROS Standard Operating Procedures. More than 30,000 rat transcripts and 28,000 variants were examined *via* Affymetrix GeneChip Rat Genome 230 2.0 Array (Affymetrix, High Wycombe, United Kingdom). Raw data files (CEL) were normalized *via* the MAS 5.0 signal method (29, 30), and CHP files were subsequently analyzed for significantly differential gene expression from microarray data [Transcriptome Analysis Console (TAC); Affymetrix]. TAC software was used to create hierarchical clustering heatmaps of the most differentially expressed genes.

RNA isolation and primer design for real-time qRT-PCR

RNA was extracted from frozen muscle tissue ($n = 6$ for all sample groups) and frozen in RNA storage solution (Qiagen, Manchester, United Kingdom). Samples (~20 mg) were immersed and homogenized in Trizol (Thermo Fischer Scientific, Waltham,

MA, USA), and RNA was extracted according to the manufacturer's instructions. Quantities and quality of RNA were assessed by 260/280 UV spectroscopy (Thermo Fisher Scientific). Isolated RNA produced an average 260/280 ratio of 1.99 (\pm 0.02). Primers were designed with Primer-Basic Local Alignment Search Tool (BLAST) (National Center for Biotechnology Information, Bethesda, MD, USA). All designed primers were between 20 and 21 bp in length and, where possible, had a guanine-cytosine content of 50–55%. The software program, netprimer, predicted the efficiency of the primer products, estimating the probability of primer dimer or hairpin formation. Primers were manufactured by Sigma-Aldrich (St. Louis, MO, USA) and resuspended in either Tris-EDTA buffer or RNA-free water (Sigma-Aldrich) as a 100- μ M stock suspension. Details of primer assays are provided in Table 1.

Real-time qRT-PCR

Real-time qRT-PCR was performed by using either HotStart Taq Master Mix Kit (Qiagen) and an iQ5 Thermocycler (Bio-Rad, Hercules, CA, USA) or QuantiFast SYBR Green RT-PCR one-step kit on a Rotorgene 3000Q (Qiagen). cDNA synthesis for subsequent PCR on the iQ5 Thermocycler was performed as follows: 1 μ g RNA was diluted in 12 μ l of RNA-free water, and 1 μ l of oligo dT primer (Thermo Fisher Scientific) was incubated at 70°C for 10 min and subsequently snap-cooled on ice to enable binding of the primer. A reaction mix—4 μ l of 5 \times buffer, 2 μ l DTT, 1 μ l deoxynucleotides (dNTPs)—were added per RNA sample and incubated at 42°C for 2 min. One microliter of Superscript II Reverse Transcriptase (Thermo Fisher Scientific) was then added and the reaction mix was incubated for an additional 50 min at 42°C. This reaction was inhibited by then heating to 70°C for 15 min. As a control, reactions were prepared in parallel with those previously described for each RNA sample, without the inclusion of the reverse-transcriptase enzyme so that mRNA would not be reverse transcribed into cDNA. These negative control primers were used to confirm that the products amplified by PCR were indeed derived from cDNA. For real-time qPCR using HotStart Taq Master Mix Kit on the iQ5 Thermocycler, reactions were as follows: 3 μ l cDNA, 15 μ l Hotstar Taq Master Mix, and 1.5 μ l each of forward and reverse primer and 9 μ l of RNase-free water, totaling 30 μ l for reactions. For real-time qPCR using QuantiFast SYBR Green RT-PCR One-Step Kit on a Rotorgene 3000Q, reactions were as follows: 9.5 μ l RNA sample (7.3 ng/ μ l = 70 ng total RNA in the reaction), 0.15 μ l of forward primer, 0.15 μ l of reverse primer, 0.20 μ l of reverse transcriptase mix, and 10 μ l of SYBR Green buffer (QuantiFast SYBR Green RT-PCR One-Step Kit; Qiagen), totaling 20 μ l. For the QuantiFast SYBR Green RT-PCR One-Step Kit, reverse transcription cycles were performed in the same tube/reaction before PCR as follows: hold 50°C for 10 min (reverse transcription/cDNA synthesis), followed by 95°C for 5 min (transcriptase inactivation and initial denaturation step), before 40 PCR cycles of 95°C for 10 s (denaturation) and

60°C for 30 s (annealing and extension). Finally, melt curve analyses were performed to identify any primer dimer formation or nonspecific amplification. All melt curves produced single reproducible melt temperatures across all experimental samples. All relative mRNA expression was quantified by using the C_t ($\Delta\Delta C_t$) method (31) against a known reference gene, RPIIb (polr2b) and/or Rn18s. Average C_t values for RPIIb and Rn18s were 20.08 (\pm 0.59) and 15.80 (\pm 0.39), respectively, across all experimental conditions.

DNA isolation and bisulfite conversion

To elucidate methylation profiles, DNA was extracted from frozen muscle tissue by using a commercially available DNA isolation kit (DNA Blood and Muscle Kit; Qiagen) according to manufacturer instructions. For methylation analysis *via* high-resolution melt PCR (HRM-PCR), bisulfite conversion of 2 μ g DNA was performed by using InnuConvert All-in-One Bisulfite Conversion kits (AJ Innuscreen GmbH, Berlin, Germany). For DNA methylation by PCR and pyrosequencing (see Materials and Methods), 500 ng DNA was bisulfite converted by using a Zymo Research EZ Methylation Kit (Zymo Research, Irvine, CA, USA).

DNA methylation by PCR and pyrosequencing

Assays for pyrosequencing were purchased from epigenDX (Hopkinton, MA, USA; summarized in Fig. 2 and Table 2). After bisulfite conversion, PCR reactions were designed depending on the specific DNA methylated region of interest and the size of the product as per the manufacturer's instructions; however, a typical reaction was performed as follows: 3 μ l of 10 \times PCR buffer (containing 15 mM MgCl₂), 0.2 μ l of 10 mM dNTPs, 1.8 μ l of 25 mM MgCl₂, 0.6 μ l of 10 mM dNTPs, 0.15 μ l HotStar Taq Polymerase, 1 μ l of bisulfite-treated DNA, and 0.2 μ M of forward and reverse primer (Table 2). One primer was biotin-labeled and HPLC-purified to facilitate the purification of the final PCR product using Sepharose beads. After an initial denaturation incubation at 95°C for 15 min, 45 cycles of denaturation at 95°C for 30 s, 63°C for 30 s (annealing), and 68°C for 30 s (extension) were performed, with all PCR cycles followed by a final 5 min at 68°C. PCR products were then bound to Streptavidin Sepharose HP (GE Healthcare Life Sciences, Waukesha, WI, USA), after which the immobilized PCR products were purified, washed, denatured with a 0.2- μ M NaOH solution, and rewashed using the Pyrosequencing Vacuum Prep Tool (Qiagen) as per manufacturer instructions. After annealing with 0.5 μ M sequencing primer, purified single-stranded PCR products were sequenced by using the PSQ96 HS System (Qiagen) according to manufacturer instructions. The methylation status of each CpG site was determined individually as an artificial C/T single-nucleotide polymorphism using QCpG software (Qiagen). The methylation

TABLE 1. Primer assay design for real-time qRT-PCR

Gene	Accession No.	Primer, 5'–3'		Primer length (bp)	Optimum annealing temperature (°C)	Product length (bp)
		Forward	Reverse			
<i>Trim63</i>	NM_080903	GGAGGAGTTTACTGAAGAGG	GACACACTTCCCTATGGTGCC	20	61	180
<i>Fbxo32</i>	NM_133521	CTTGTCTGACAAAGGGCAGC	TGAAAGTGAGACGGAGCAGC	20	61	184
<i>Ampd3</i>	NM_031544	ACGCTTGCTGGTCGGTTTAG	TGGCTTCTCTGTCCGATG	20	60	197
<i>Hdac4</i>	XM_343629.4	GCAGCCAAACTTCTCCAGCA	TTGACATTGAAACCCACGCC	20	61	212
<i>MyoG</i>	NM_017115.2	GCCATCCAGTACATTGAGCG	CATATCCTCCACCGTGATGC	20	61	267
<i>Chna1</i>	NM_024485.1	TGTCATCAACACACACCACC	CTGCAATGTACTTCCACACC	20	61	269

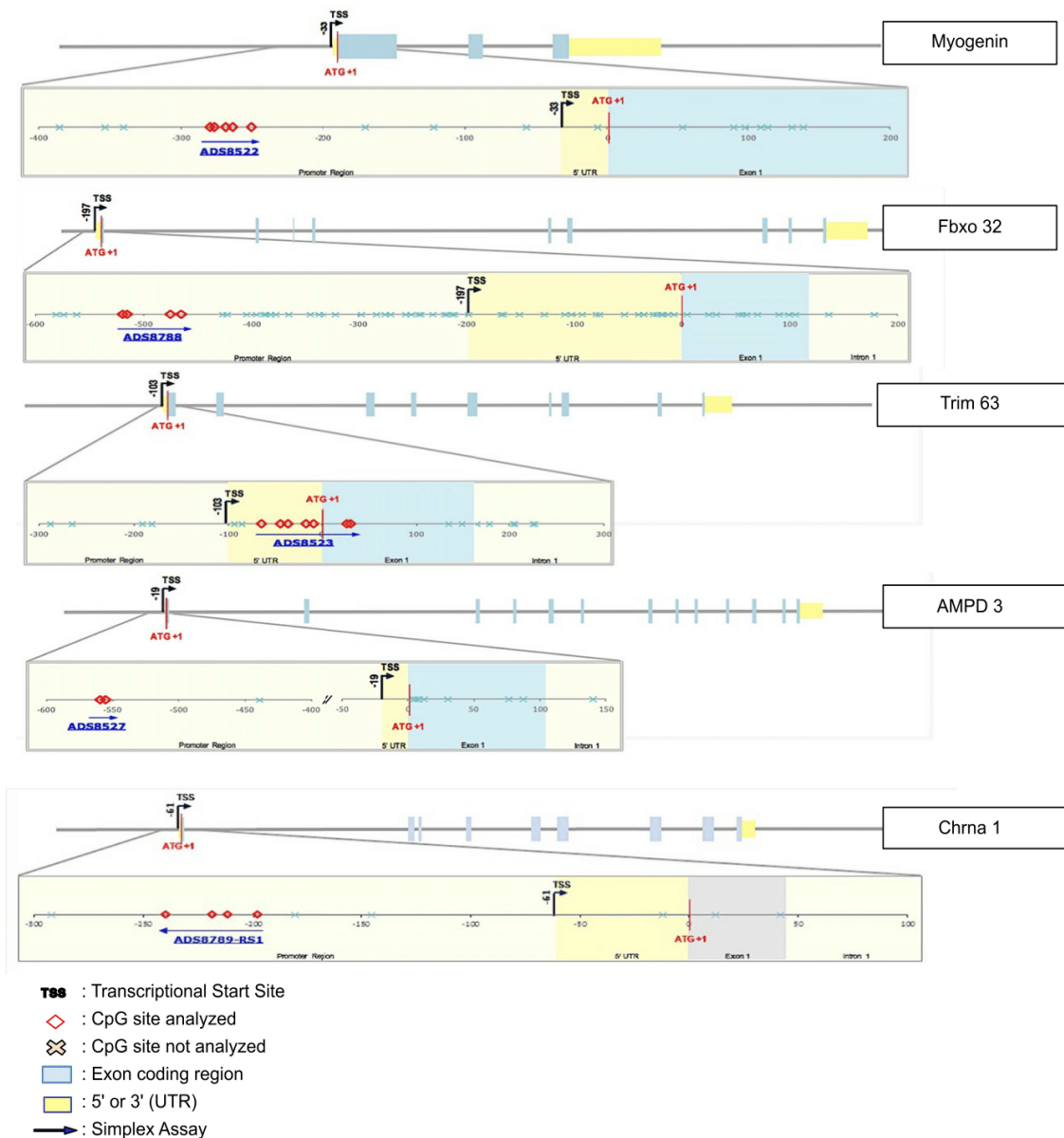


Figure 2. Gene map of CpG islands for loci-specific pyrosequencing for quantification of DNA methylation *via* pyrosequencing. In descending order: MyoG, Fbxo32 (MAFbx), Trim63 (MuRF1), Ampd3, and Chrna1. URT, untranslated region.

level at each CpG site was calculated as the percentage of methylated alleles divided by the sum of all methylated and unmethylated alleles. The mean methylation level was calculated by using the methylation levels of all measured CpG sites within the targeted region of each gene. Each experiment included non-CpG cytosines as internal control to detect the incomplete bisulfite conversion of the input DNA. In addition, a series of unmethylated and methylated DNA strands were included as a control after each PCR. Furthermore, PCR bias testing was performed by mixing unmethylated control DNA with *in vitro* methylated DNA at different ratios (0, 5, 10, 25, 50, 75, and 100%), followed by bisulfite modification, PCR, and pyrosequencing analysis. All supporting information for gene assays, including assay sequence, chromosomal CpG island locations, position from the ATG start

codon and transcriptional start site, and CpG number are given in Fig. 2 and Table 2.

HRM-PCR for total DNA methylation

HRM-PCR for CpG methylation was performed as previously described (24). In brief, 20 ng DNA was subjected to HRM-PCR using EpiTect HRM-PCR kits and Rotorgene 3000Q (Qiagen) with Rotorgene software. All primer concentrations for gene CpG assays and EpiTect HRM master mix volumes were used in accordance with manufacturer instructions. HDAC4 (Qiagen) was designed to amplify a product length of 140–190 bp (Table 3). PCR cycles were performed as follows: 10 s at 95°C (denaturation), 30 s at 55°C (annealing), and 10 s at 72°C

TABLE 2. Description of targeted DNA methylation assays for loci-specific pyrosequencing analysis

Gene	CpG	Position from ATG codon	Position from TSS	Chromatin location	Sequence to analyze
<i>MyoG</i>	CpG-9	-280 to -251	-247 to -218	Chr13: 51126212-51126241	AGTYGAYGGTTTTTGGATTGTTGTTATAGGAGTGTGTTGGG
	CpG-8	-280	-247	Chr13: 51126212	
	CpG-7	-277	-244	Chr13: 51126215	
	CpG-6	-269	-236	Chr13: 51126223	
	CpG-5	-264	-231	Chr13: 51126228	
<i>Trim63</i>		-251	-218	Chr13: 51126241	ATTYGAGTGGGATTTTTTTTATTGTTGGTGTGAYGTAGGTGG AAGAGATAGTYGTAGTTTTYGAAGTAATATGGATTATAA ATTTGGTTTGATTTTGGAYGGAAATG
		-63 to +30	+40 to +133	Chr5: 152533388-152533481	
	CpG-5	-64	40	Chr5: 152533388	
	CpG-4	-44	60	Chr5: 152533408	
	CpG-3	-36	68	Chr5: 152533416	
<i>Amphd3</i>	CpG-2	-17	87	Chr5: 152533435	GYGGGYGTATGGGTG
	CpG-1	-9	95	Chr5: 152533443	
	CpG1	26	129	Chr5: 152533447	
	CpG2	30	133	Chr5: 152533481	
	CpG-10	-559 to -555	-540 to -536	Chr1: 175585557-175585561	
	CpG-9	-559	-540	Chr1: 175585557	
<i>Fbxo32</i>		-555	-536	Chr1: 175585561	TAYGTTYGATAGGGGAGTAGGGGAGGTGTAAGAGGTGTTA GGGTATYGAGGGTTAGYGGGATATTTGG
		-519 to -465	-322 to -268	Chr7: 98098536-98098590	
	CpG-49	-519	-322	Chr7: 98098590	
	CpG-48	-515	-318	Chr7: 98098586	
	CpG-47	-475	-278	Chr7: 98098546	
<i>Chma1</i>	CpG-46	-465	-268	Chr7: 98098536	TCTRACTCATATTAACRTAAACCRATAAACCTATAAAAAATCTACATA AATCRTAAACCAAAAAAC
		-198 to -240	-137 to -179	Chr3: 60460861-60460903	
	CpG-7	-240	-179	Chr3: 60460903	
	CpG-6	-219	-158	Chr3: 60460882	
	CpG-5	-212	-151	Chr3: 60460875	
	-198	-137	Chr3: 60460861		

TSS, transcription start site.

TABLE 3. HDAC4 DNA methylation via HRM-PCR

Gene	CpG no.	GeneGlobe no.	Chromatin location	Sequence to analyze	Product length (bp)
<i>Hdac4</i>	1	PM00599046	Chr9: 91389151–91391341	GGGCGCGCAAGAGCGCAGACTGTGAC GGGGGCCCGGT	190
	2	PM00599053	Chr9: 91390077–91391147	GCGCCCGCAAGCGGGGTGGCTGTT GGGCTATTGTAGGGCGGA	138
	3	PM00599060	Chr9: 91389052–91391220	GCTAGCGCCTGGAGAGTCTCGGTAC GCCCGC	168
	4	PM00599067	Chr9: 91389477–91391621	GCTTTGGGTGCGCCGCCACCGCTCCC GGT	144
	5	PM00599074	Chr9: 91389472–91391621	CGTTGCTGTGGCGGAGGTGTAGGCTT TGGGTGCGCCGCCACCGCTCCC	149

(extension) for a maximum of 55 cycles. After PCR, an HRM analysis was performed with 0.1°C increments from 65°C to 95°C. Fluorescence *vs.* melt temperature was used to create a standard curve using rat methylated DNA standards that represented 100, 75, 50, 25, 10, 5, and 0% methylation. All samples were run in duplicate and were normalized to 0% methylated control and averaged to produce a single curve. The relationship between the area under the curve—determined *via* each standard curve—and the corresponding percentage methylation curve of specific gene loci was determined by using the best-fitting fourth-order polynomial relation. This relationship was subsequently used to quantify the percent methylation from the integrated raw melt curves of the experimental samples. Calculations were performed by using a Python-based program, MethylCal, that was developed for this purpose in-house [used previously (24)].

Statistical analyses

All statistical analyses of morphologic data were performed *via* either R software (v.2.13.1; <http://www.R-project.org>) or SPSS (v.22.0; SPSS, Chicago, IL, USA). Morphologic (muscle mass and CSA) comparisons between experimental and control conditions were assessed *via* 1-way between-group ANOVA. Microarray data were analyzed for statistical comparisons *via* 1-way between-group ANOVA within the TAC software. Targeted real-time qRT-PCR was analyzed by using a 1-way between-group ANOVA (with Tukey's *post hoc* tests). DNA methylation data sets were analyzed by using a 2-way between-group ANOVA (with Tukey's *post hoc* tests), which allowed comparison of experimental conditions and individual CpG islands. A follow-up 1-way ANOVA between CpG islands at each experimental condition was used to identify significant differences in the DNA methylation status of each CpG island within the same experimental condition. Finally, Student's *t* tests were used to identify significant differences in CpG methylation between experimental conditions and control. All statistical analyses for DNA methylation were performed on absolute values, with figures representing data as mean \pm SD to relevant control. Differences were considered statistically significant at values of $P \leq 0.05$.

RESULTS

Skeletal muscle disuse and recovery evokes considerable, yet reversible, muscle atrophy

Exposure to TTX produced an average of $7.0 \pm 2.4\%$ loss in TA muscle mass at 3 d, $28.7 \pm 5.1\%$ at 7 d, and $50.7 \pm 2.7\%$ loss after 14 d that resulted in statistical significance at all

time points *vs.* the unoperated right TA ($P < 0.001$; Fig. 3) and a significant difference between paired comparisons of 3 and 7 d, 3 and 14 d, 7 and 14 d ($P < 0.001$). After 14 d of TTX exposure followed by 7 d of cessation in the recovery group, muscle mass significantly recovered by 51.7% *vs.* 14 d of denervation ($P = 0.001$; Fig. 3). Seven days of recovery did not completely restore muscle mass, as muscle mass was still significantly lower than control ($P < 0.001$; Fig. 3), and total muscle mass was equivalent to levels at 7 d of TTX administration, which suggests that rates of loss over 7 d were similar to rates of recovery. We therefore report significant skeletal muscle atrophy of the TA muscles with disuse and a 51.7% recovery of muscle mass after 7 d of cessation of TTX administration and the return of normal habitual physical activity *vs.* 14 d of TTX induced-denervation.

Exposure to TTX produced a progressive reduction in mean muscle fiber CSA of $17.95 \pm 12.06\%$ at 3 d, $42.09 \pm 6.17\%$ at 7 d, and $68.94 \pm 2.97\%$ at 14 d of TTX exposure, with 7 and 14 d of TTX being significantly reduced *vs.* control ($P = 0.003$ and $P < 0.001$, respectively; Fig. 4). Similar to TA muscle mass, upon TTX cessation, the 14-d TTX + 7-d recovery group muscle CSA significantly recovered compared with 14 d of TTX alone, with an increase of 62.6% in CSA compared with 14 d of TTX alone ($P = 0.002$; Fig. 4); therefore, there was significant atrophy of individual skeletal muscle fibers in TA muscles after denervation, and a 51.7% recovery of muscle mass and a 62.6% recovery of muscle CSA after 7 d of cessation of TTX administration and a return to normal habitual physical activity.

Gene expression microarrays identify important gene regulatory networks involved in muscle atrophy and recovery

After confirming a significant reduction in muscle mass, the temporal transcriptome profile that accompanied muscle atrophy was investigated ($n = 4$). The dendrogram from the hierarchical clustering of probe sets across the genome identified 3714 genes that demonstrated highly significant differential expression across all conditions with a value of $P \leq 0.001$ (Fig. 5A). It also demonstrated that there was high clustering similarity for the 3-, 7-, and 14-d TTX groups, which were dissimilar to the sham-operated controls and the recovery group that also

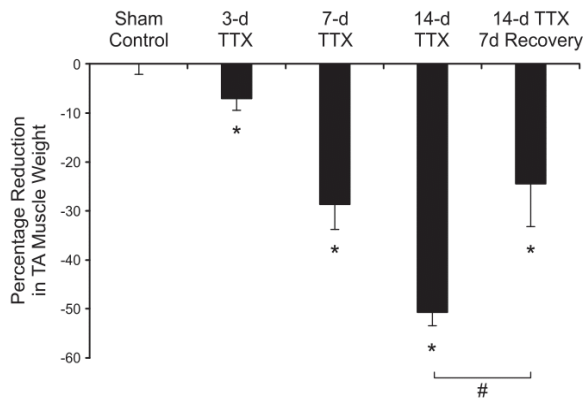


Figure 3. Quantification of muscle atrophy (muscle mass) *in vivo* after TTX-induced nerve block. Data shown for 3, 7, and 14 d of treatment, and TTX nerve block + 7 d of active recovery (7-d Recovery). Mean TA mass for all control and experimental groups were expressed as a percentage difference of whole-animal body mass (428 ± 45 g) to normalize for interindividual differences in animal size. All data are presented as means \pm sd for $n = 6$ in each condition. *Statistically significant *vs.* sham control ($P < 0.05$); #statistically significant *vs.* 14-d TTX ($P < 0.05$).

demonstrated high clustering similarity (Fig. 5A and Supplemental 1A). This suggested that disuse-induced atrophy evoked a considerable change in the expression of a large number of genes that were returned to levels similar to those in sham controls on the cessation of nerve block in the recovery group (Fig. 5A). Despite the top 20 genes showing recovery to control sham levels, 846 genes were still significantly differentially expressed ($P < 0.05$) in the recovery group compared with sham control (Supplemental 1I). Additional analyses were performed by using unsupervised hierarchical clustering of the top 20 most differentially expressed genes (Fig. 5B and Supplemental 2). This analysis confirmed that these top 20 genes that were most differentially expressed in TTX groups returned to sham control after 7 d of recovery. Furthermore, the top 500 genes that were up-regulated by TTX administration could be grouped into 3 distinct clusters on the basis of their temporal behavior: an immediate and sustained increase in expression (Fig. 5C), a delayed, but progressive, increase in expression (Fig. 5D), and, finally, an immediate increase in expression that declined over the time course (Fig. 5E), which suggested that dynamic and coordinated gene expression occurred across a large number of genes as a result of disuse, and that there was a return to control levels in the recovery group.

Regulated genes identified by microarray and ranked by significance of change

Transcriptome-wide data were analyzed to compare conditions in 6 pairwise comparisons [sham *vs.* 3 d (Supplemental 1C), 7 d (Supplemental 1D), and 14 d (Supplemental 1E); and Recovery *vs.* 3 d (Supplemental 1F), 7 d (Supplemental 1G), and 14 d (Supplemental 1H)] to identify the genes that were among the most significantly affected in the experimental

groups. Trim 63 (MuRF1), myogenin (MyoG), and Ampd3 were identified as being the most frequently occurring genes that were most differentially expressed across these paired comparisons and that also appeared in the top 20 differentially expressed genes across all conditions (Fig. 5B and Supplemental 1B). Ampd3 appeared in 4 of 6 of these paired comparisons (Supplemental 1C, F–H). Previous studies have also suggested that overexpression of Ampd3 increases protein degradation in C2C12 myotubes (32); therefore, we sought to further elucidate its transcriptional and epigenetic role in denervation-induced atrophy in the present study. The E3 ubiquitin ligase, Trim63, appeared in 3 of 6 paired comparisons (Supplemental 1C, F, H) and has been previously strongly associated with muscle atrophy *in vitro* and *in vivo* (33–37), as has been its protein family member, Fbxo32 (Mafbx). We therefore extended the analysis of this change by qRT-PCR and loci-specific pyrosequencing for the role of DNA methylation in TTX-induced atrophy and recovery. The muscle-specific basic helix-loop-helix myogenic regulatory factor, MyoG, was also identified in 3 of 6 paired comparisons (Supplemental Fig. 1C–E) and has previously been identified as a key transcript in the regulation of denervation-dependent muscular atrophy in rodent models (38). Of importance, the class II histone deacetylase 4 (Hdac4) also appeared within the top 20 most statistically differentially expressed genes across all probe sets (Fig. 5B and Supplemental 1B) and was the most statistically differentially expressed gene when comparing sham control with 3-d TTX atrophy probe sets (Supplemental 1C). Hdac4 is a known upstream regulatory factor of MyoG activity (36, 39), and, thus, both Hdac4 and MyoG genes were identified as warranting additional targeted analysis. Additionally, a neuromuscular junction-associated gene that was significantly altered and that also appeared in the top 20 most differentially expressed genes included the acetylcholine receptor subunit $\alpha 1$ (Chrna1; Fig. 5B). This gene also appeared in 2 of 6 paired comparisons of most differentially expressed genes (Supplemental 1D, E). Chrna1 plays a crucial role in acetylcholine binding and the channel-gating activity within the neuromuscular junction pathway (40) and has been previously identified *via* transcriptome analysis as the most differentially expressed gene in skeletal muscle loss observed in age-related muscle loss/denervation (41). After the identification of key gene transcripts, quantification of gene expression was elucidated *via* follow-up real-time qRT-PCR to confirm and further profile the transcriptional responses, and DNA methylation analyses were performed *via* pyrosequencing to assess the DNA methylation status of the gene promoter region in response to disuse-induced muscle atrophy and recovery.

Changes in gene expression after disuse-induced atrophy are returned to control levels after recovery

Confirmation of microarray gene expression by qRT-PCR demonstrated that MyoG, Hdac4, Trim63, and Fbxo32 were significantly increased at 3 d of TTX exposure compared with control ($P < 0.05$), with Hdac4 and Fbxo32

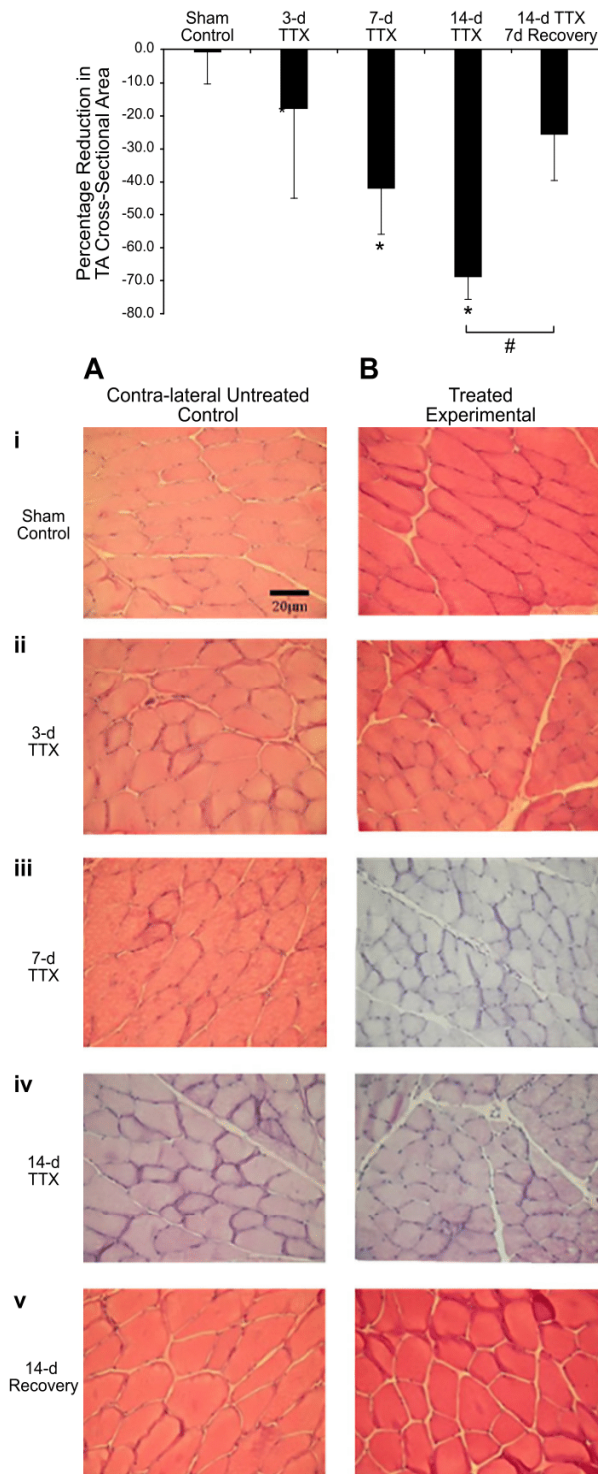
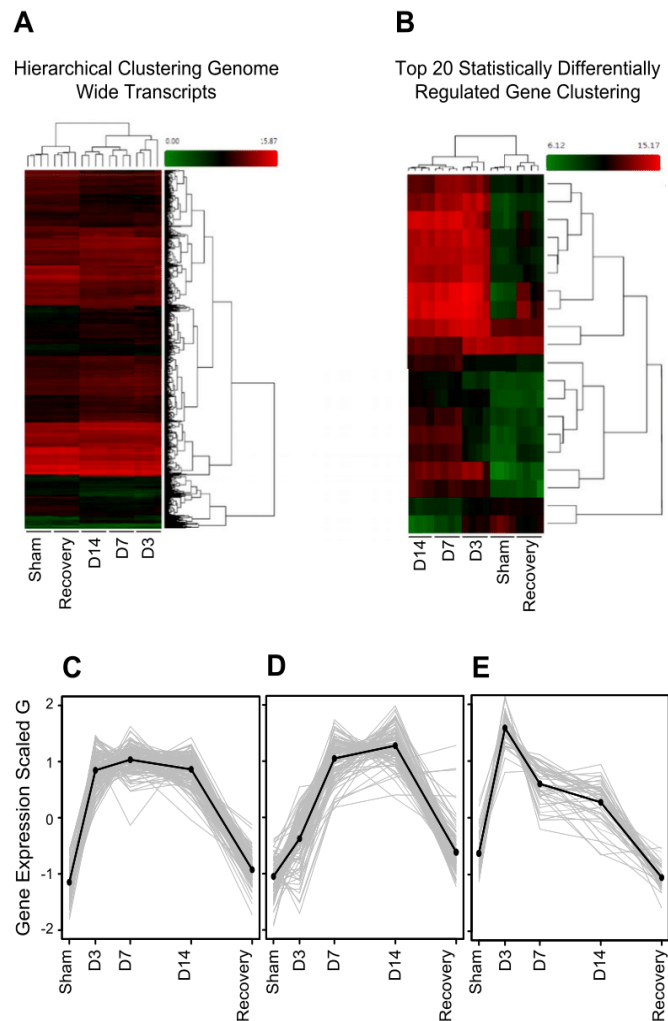


Figure 4. Muscle fiber CSA after TTX-induced atrophy and recovery. Mean CSA of the TA muscle was expressed as a percent change from untreated contralateral control limb for each animal. *A, B* Hematoxylin and eosin-stained sections of untreated (*A*) and treated (*B*) TA muscle of control (*i*), 3-d TTX exposed (*ii*), 7-d TTX exposed (*iii*), 14-d TTX exposed (*iv*), and 14-d TTX exposed with 7-d recovery (*v*). *Statistically significant *vs.* sham control ($P < 0.05$); # statistically significant *vs.* 14-d TTX ($P < 0.05$).

(Fig. 6A) remaining elevated at 7 d of TTX exposure. By 14 d, mean levels for Hdac4, MyoG, Trim63, and Fbxo32 were not significantly different, that suggested an elevation of these genes at 3 and 7 d in response to disuse. In contrast, whereas significant changes in Atp2b3 expression were not detected (Fig. 6A), Chrna1 expression was significantly

elevated at 3, 7, and 14 d (177.5-fold increase *vs.* control; $P = 0.016$; Fig. 6A). After TTX cessation and 7 d of recovery, it was also confirmed *via* qRT-PCR that Hdac4, MyoG, Trim63, Fbxo32, and Chrna1 gene expression had all returned to sham control levels, as demonstrated in the microarray data.

Figure 5. Transcriptome analysis indicated a highly dynamic gene expression response to progressive muscular atrophy that returns to expression levels in the sham control upon muscle recovery. *A)* Hierarchical clustering heatmaps of probe set expression across the rodent genome identified 3714 genes that were highly statistically significantly ($P \leq 0.001$) expressed across all conditions, with 3-, 7-, and 14-d TTX atrophy being differentially expressed compared with sham control and 14-d TTX + 7-d recovery. *B)* This observation was confirmed in analysis of the top 20 statistically differentially expressed genes across all conditions. Similar clustering occurred within 3-, 7-, and 14-d of TTX exposure which was distinctly dissimilar to the clustering observed in the sham control and 7-day recovery group. *C–E)* Top 500 most statistically differentially expressed genes grouped into 3 distinct temporal expression patterns: an immediate and sustained increase in expression (*C*); delayed, but progressive, increase in expression (*D*); or an immediate increase in expression that declined over the time course (*E*). Of note, all gene clusterings return to sham control expression levels upon TTX cessation and 7 d of recovery.



Changes in DNA methylation were associated with altered gene expression in disuse-induced atrophy and recovery

Loci-specific pyrosequencing of individual CpG islands within gene promoters revealed significant alterations in the DNA methylation of key genes that were identified after microarray analysis and confirmatory real-time qRT-PCR that corresponded with significant increases in gene transcription. After 3 d of TTX exposure, there was a significant reduction ($P = 0.011$) of DNA methylation in the MyoG gene promoter (Fig. 6B) and a concomitant significant increase ($P = 0.011$) in MyoG gene expression (Fig. 6A), both of which then returned to baseline levels during the remaining 14 d (all gene expression/DNA methylation overlap relationships are schematically represented in Fig. 6C). The DNA methylation profile of the Chrna1 gene promoter progressively decreased relative to control, with 7 and 14 d of TTX treatment attaining significance compared with sham control ($P = 0.035$ and $P < 0.001$, respectively). This corresponded with the increased expression of this gene over the 14-d denervation period

(Fig. 6A, C). As with Chrna1, Trim63 displayed a significant reduction in methylation at 7 and 14 d of TTX exposure ($P = 0.035$ and $P < 0.001$, respectively; Fig. 6B, C), which coincided with a stable increase in mRNA expression at the same time points (Fig. 6A, C). Fbxo32 demonstrated a decreasing trend in DNA methylation at specific time points, attaining significance at 14 d of TTX exposure ($P = 0.021$; Fig. 6B, C), with gene expression data demonstrating significant increases at 3 ($P = 0.037$) and 7 d ($P = 0.038$) atrophy (Fig. 6A, C). Of importance, after TTX cessation, there was recovery in the DNA methylation profiles of Trim63, Fbxo32, and Chrna1, which returned to sham control levels ($P > 0.05$). This was in conjunction with an observed recovery of gene expression of the same genes upon TTX cessation (Fig. 6C). We observed no differences in DNA methylation for Ampd3 after TTX administration or recovery (Fig. 6B). Furthermore, after initial total percent of methylation within the total amplicon/product *via* HRM-PCR for Hdac4, we were unable to identify methylation greater than that of the 0% methylation control for all conditions, and, therefore, pyrosequencing for loci-specific DNA methylation was not performed for Hdac4.

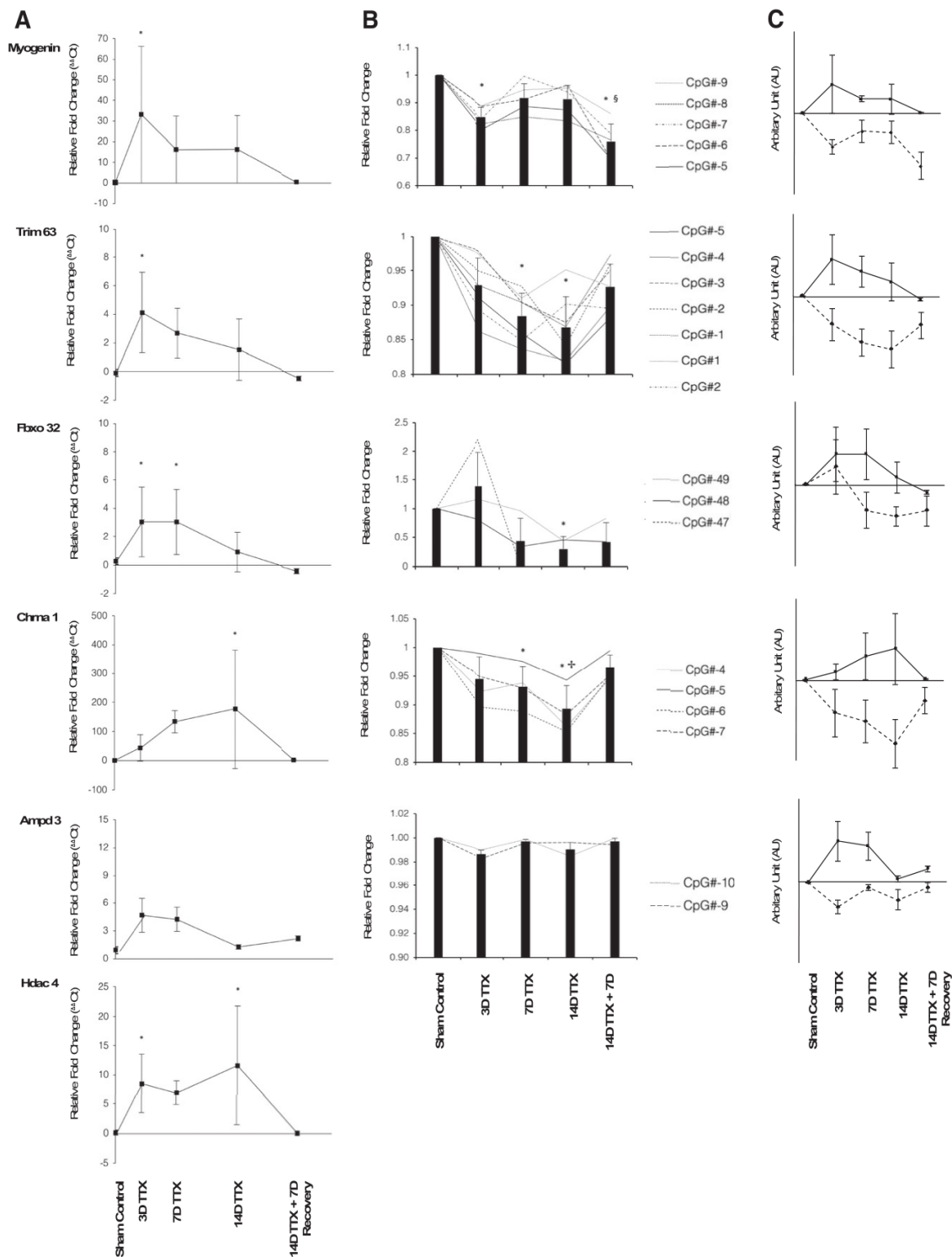


Figure 6. Relative fold change of gene expression and DNA methylation of a subset of identified gene transcripts. *A*) Relative fold change in mRNA expression of genes MyoG, Trim63, Fbxo32, Chrna1, Ampd3, and Hdac4 (in descending order). All genes are presented as means \pm SD ($n = 6$), Ampd3 ($n = 3$). Statistically significant changes in fold difference compared with sham control group are indicated *via* *. Sham control group is represented with triangle icon. All TTX-treated groups are represented with a square icon. *B*) Mean methylation data presented as relative fold change compared with sham control for genes: MyoG, Trim63, Fbxo32, Chrna1, and Ampd3 (in descending order). Mean percentage data (black column bars) are the average taken from each CpG island of the respective gene, analyzed *via* loci-specific pyrosequencing. Individual CpG island methylation percentages are (continued on next page)

DISCUSSION

Summary

The aim of this investigation was to elucidate the epigenetic control of gene expression after skeletal muscle disuse-induced atrophy after 3, 7, and 14 d of nerve block with TTX. First, we observed a 7, 29, and 51% loss of muscle at 3, 7, and 14 d of disuse, with 7 d of recovery resulting in a 51.7% restoration of total muscle mass that had been lost after 14 d of disuse. Muscle mass was therefore similar after 7 d of disuse or 14 d of disuse followed by 7 d of normal activity. Muscle atrophy was further confirmed with fiber cross-sectional area data in which a similar pattern of progressive loss of 18, 42, and 69% was observed after 3, 7, and 14 d of TTX, respectively. Seven days of recovery restored 63% of muscle cross-sectional area *vs.* 14 d of disuse-induced atrophy alone. Our original hypothesis was supported, in that disuse-induced atrophy was associated with reduced DNA methylation and enhanced gene expression. Both DNA methylation and gene expression were partially returned to baseline after 7 d of recovery from nerve block. Of importance, after gene expression microarray analysis, we found that 3714 genes were significantly differentially regulated ($P \leq 0.001$) across all TTX groups, and that these genes were returned in the recovery group to levels that were observed in sham control. Specifically, by identifying the top 20 most differentially expressed genes in the atrophy and recovery groups and cross-referencing with the most frequently occurring significantly regulated genes for between-group pairwise comparisons, we identified a key subset of influential genes: MyoG, Hdac4, Trim63 (Murf1), Ampd3, and Chrna1. These genes—together with Fbxo32 (Mafbx), because of its previously defined role with Trim63 (Murf1) in muscle atrophy—were then analyzed *via* real-time qRT-PCR to confirm microarray gene expression data for these genes as well as loci-specific DNA methylation of the promoter regions by pyrosequencing. All of these genes—MyoG, Hdac4, Trim63/Murf1, Ampd3, Chrna1, and Fbxo32/Mafbx—have been identified previously *via* transcriptome-wide analysis of disuse-induced atrophy after neuromuscular blocker α -cobrototoxin treatment (42). In this investigation, we have identified novel data that suggest that MyoG, Trim63 (Murf1), Fbxo32 (Mafbx), and Chrna1 demonstrate reduced DNA methylation at specific time points after disuse-induced atrophy that corresponded with increases in gene expression at the same time points. Of importance, after TTX cessation and 7 d of recovery, during which normal habitual physical activity was resumed, there was a return of DNA methylation for Trim63, Fbxo32, and Chrna1 to sham control levels. This also corresponded

with the return of gene expression to that of baseline sham control levels. Because the reduced DNA methylation within promoter or enhancer regions of genes can lead to enhanced gene expression as a result of reduced methylation, which allows access for RNA polymerase to enable transcription (43), our data suggest that atrophy and recovery of skeletal muscle after disuse is associated with dynamic and transient epigenetic modifications that correspond with altered gene expression.

Dynamic and transient DNA methylation after atrophy and recovery of muscle mass

Interestingly, 51.7% of total muscle mass loss after 14 d was restored after 7 d of recovery, yet, importantly, gene expression was returned fully to baseline after 7 d, which suggests—as perhaps would be expected because of the time required for transcription, translation, and protein incorporation—a time lag between gene expression and the physiological restoration of muscle mass. The findings in this study, however, suggest that reduced DNA methylation that corresponded with increased gene expression of MyoG, Trim63 (Murf1), Fbxo32 (Mafbx), and Chrna1 are dynamic and transient events, in which decreases in DNA methylation at 3, 7, and 14 d of TTX-induced atrophy correspond with increases in gene expression that, in turn, are returned to baseline (Trim63/Murf1 and Chrna1) within just 7 d after the removal of the TTX block. DNA methylation has previously been reported to be mitotically stable and, as such, environmental factors were previously believed to be unable to induce significant alterations in DNA methylation at both acute and chronic time points (44). Furthermore, our previous data suggest that even after acute catabolic stress, DNA methylation can be stably retained across several population doublings of muscle cells *in vitro* (24); however, we demonstrate here that DNA methylation does respond at a rate that allows for its participation in the adaptive control of gene expression and therefore adds additional weight to previous findings in support of transient alterations of DNA methylation in skeletal muscle, for example, as previously after an acute bout of aerobic exercise (24, 45). Our data therefore add support to previous findings demonstrating transient alterations of skeletal muscle DNA methylation.

Although not identified in this study, it will be important in future studies to investigate DNA methyltransferase activity. The DNA methyltransferases (DNMT3a/3b) are involved in the initial incorporation of methyl groups to cytosine residues and the creation of 5-methylcytosine to increase DNA methylation. Maintenance DNA methyltransferase (DNMT1) is involved in retaining the methyl tag on the DNA strand (46). The dynamic and transient observation of DNA methylation in this study is perhaps

visualized as individual lines. DNA methylation data presented as means \pm SD for $n = 3$. *Statistically significant reductions compared with the sham control group; [§]significant reduction compared with 7- and 14-d TTX atrophy; [†]significant reduction in DNA methylation compared with 3-d TTX-exposed experimental group (B). C) An overlap schematic represents the relationship between DNA methylation and mRNA expression of key transcripts (arbitrary units). bHLH muscle specific basic helix-loop-helix; H&E, hematoxylin and eosin; MRF, myogenic regulatory factor.

suggestive of high DNMT3a/3b activity in which initial and rapid increases in DNA methylation are observed; however, we do not report a significant retention of DNA methylation upon TTX cessation (14-d TTX + 7-d recovery), which would perhaps suggest that DNMT1 did not maintain the methylation status of some of these genes during muscle recovery. It has previously been reported that increases in both types of DNMT are observed after a high-fat diet that induces increases in DNA methylation of 6508 genes (47). Additional work is needed to confirm similar findings in atrophying muscle and to elucidate the response of DNA methyltransferases upon the reversible insult. Finally, it would be important to undertake 14 d of recovery in future experiments to assess whether muscle mass can be returned fully to baseline control levels and to examine the transcriptomic and epigenetic responses during this period.

DNA methylation correlates with important changes in skeletal muscle gene expression after disuse-induced atrophy and with the return of gene expression to baseline during recovery

As suggested above, MyoG, Trim63, Fbxo32, and Chrn1 demonstrated decreased DNA methylation after disuse-induced atrophy that corresponded with increased gene expression. Of importance, after TTX cessation and 7 d of recovery, during which normal habitual physical activity was resumed, DNA methylation of Trim63 and Chrn1 returned to sham control levels as the suppressed levels of gene expression recovered. The muscle-specific basic helix-loop-helix transcriptional factor and member of the myogenic regulatory factors, MyoG, is commonly associated with the coordination of skeletal muscle development/myogenesis or skeletal muscle regeneration and, specifically, the differentiation/fusion of skeletal muscle cells (48). Here, we report a significant induction of gene expression for this transcription factor upon disuse-induced muscle atrophy. Because expression of this protein is usually associated with muscle regeneration, this may reflect a compensatory mechanism in an unsuccessful attempt to halt atrophy or to respond to a return of activity. The role of MyoG as a transcription factor has previously been linked with the regulation of the ubiquitin E3 ligases, Trim63 and Fbxo32, and associated muscle atrophy (34). We provide novel data that suggest that the DNA methylation profile of this transcript is altered in an inverse fashion to its mRNA expression. Indeed, at 3, 7, and 14 d, we observed a significant reduction in MyoG DNA methylation and an increase in MyoG transcript expression; therefore, we suggest that increased MyoG gene expression is regulated by reduced MyoG DNA methylation.

Previous studies have also reported that MyoG gene expression is under the regulatory control of class II Hdacs (34, 35). In partial support of this notion, we report a significant increase in Hdac4 gene expression at 3 and 14 d of TTX exposure; however, we did not measure protein abundance or the phosphorylation/deacetylation status of Hdac4. Indeed, the initial screening of Hdac4 DNA

methylation *via* HRM-PCR was unable to detect a notable change, with global gene percentage methylation indicating no methylation above 0% methylated controls. Therefore, additional work at the protein and histone levels is needed to elucidate the epigenetic regulation of Hdacs during periods of loss and recovery of muscle mass, as its altered gene expression after denervation does not seem to be controlled *via* DNA methylation. Furthermore, despite a return of MyoG gene expression to control levels after 7 d of recovery, DNA methylation continued to reduce in the recovery group. This suggested that while reduced DNA methylation may have been important in increased gene expression during denervation-induced atrophy, DNA methylation was not controlling the gene expression of MyoG during recovery.

As previously suggested, downstream transcriptional targets of MyoG have also been shown to be highly induced in rodents during periods of muscle loss caused by denervation, immobilization, and unloading (49, 50). Trim63 is an E3 ubiquitin ligase and a member of the RING zinc finger family of proteins that directs the polyubiquitination of proteins to target them for proteolysis. With catabolic stimuli, such as diabetes, cancer, denervation, unloading, and glucocorticoid or cytokine treatment, its expression has consistently been demonstrated to increase (50, 51). Previous studies have also suggested that upon denervation, Northern blot analysis identified a significant increase in Trim63 and Fbxo32 after 3 d of muscle atrophy, that continued through to 7 d (50). Here, we report a significant increase in Trim63 and Fbxo32 gene expression *via* real-time qRT-PCR compared with control levels in parallel with a reduction in DNA methylation. This suggests an important role for epigenetic control of these ubiquitin ligases in the resulting protein degradation and muscle loss that has been observed in this study. We note that DNA methylation of both of these ubiquitin ligases increased to control levels with corresponding decreases in gene expression to the sham control level, which also suggests that the reductions in DNA methylation during atrophy can be dynamically regulated.

Furthermore, Chrn1 makes up the majority of the muscle-specific nicotinic acetyl choline receptor (nAChR) in adult skeletal muscle (52) and plays a crucial role in initiating the opening of the nAChR channels and the transfer of positively charged ions (53). We reported a progressive increase in gene expression resulting in a cumulative significant fold change after 14 d of TTX exposure. This alteration in gene expression was met with a parallel progressive reduction in DNA methylation with significance being observed at both 7 and 14 d after TTX-induced atrophy. An observation similar to previous work (54), in which a significant increase in Chrn1 activity was observed as a result of sarcopenia. nAChRs are made up of 5 isoforms in human skeletal muscle, in which the subunit Chrn1 is most dominant. These isoforms function to create an acetylcholine cluster around the neuromuscular central pore, in which they house target binding sites predominantly located at the α -subunit in the extracellular domain near the N terminus. Upon contact of a chemical messenger to the binding site, all present subunits undergo a conformational change that results in the opening

of the nAChR channel (55). Upon denervation, however, no action potential messages are received and, therefore, it is possible that the reduced DNA methylation and increased transcriptional response—although we do not provide evidence of protein levels—may increase as a compensatory mechanism that is understood to increase the chance of forming new end plates. This response is equivalent to that observed after nerve section and it seems, therefore, to be a response to the lack of activity rather than the physical absence or damage to the nerve. Further, upon TTX cessation and muscle recovery, we report a return of Chrn1 DNA methylation and gene expression back towards sham control levels.

Finally, it is important to note that MyoG, ubiquitin ligases, and Chrn1 have been identified as major regulators of muscle regeneration, protein degradation, and function, respectively, and that the present study identified these genes as being the most frequently occurring, differentially expressed genes across comparisons by using a nonselective transcriptome-wide approach in a novel model of osmotically administered TTX-induced atrophy. Therefore, these data further consolidate the important role for epigenetics in the regulation of these genes in disuse-induced atrophy and the recovery of skeletal muscle following a return to activity.

CONCLUSIONS

MyoG, Trim63, Fbxo32, and Chrn1, but not Ampd3, demonstrate decreased DNA methylation after disuse-induced atrophy that correspond with increased gene expression and muscle atrophy. Importantly, after TTX cessation and 7 d of recovery, there was increased DNA methylation of Trim63 and Chrn1 to control levels that also corresponded with the return of gene expression to that of baseline in sham controls. Overall, this suggests that the atrophy and recovery of skeletal muscle after disuse is controlled by the dynamic and transient epigenetic regulation of gene expression. FJ

ACKNOWLEDGMENTS

This work was supported by an integrative mammalian biology studentship from the UK Medical Research Council [to A.G.F. (via J.C.J.)], as well as by a Doctoral Training Alliance funded studentship and GlaxoSmithKline [to R.A.S. (via A.P.S.)]. The authors declare no conflicts of interest.

AUTHOR CONTRIBUTIONS

A. G. Fisher, R. A. Seaborne, J. M. Coulson, A. P. Sharples, and J. C. Jarvis designed research; A. G. Fisher, R. A. Seaborne, T. M. Hughes, A. Gutteridge, C. Stewart, J. M. Coulson, A. P. Sharples, and J. C. Jarvis analyzed data; A. G. Fisher, R. A. Seaborne, J. M. Coulson, A. P. Sharples, and J. C. Jarvis performed research; A. G. Fisher, R. A. Seaborne, C. Stewart, A. P. Sharples, and J. C. Jarvis wrote the paper; and T. M. Hughes contributed analytic tools.

REFERENCES

- Ferrando, A. A., Lane, H. W., Stuart, C. A., Davis-Street, J., and Wolfe, R. R. (1996) Prolonged bed rest decreases skeletal muscle and whole body protein synthesis. *Am. J. Physiol.* **270**, E627–E633
- LeBlanc, A. D., Schneider, V. S., Evans, H. J., Pientok, C., Rowe, R., and Spector, E. (1992) Regional changes in muscle mass following 17 weeks of bed rest. *J. Appl. Physiol.* (1985) **73**, 2172–2178
- Gibson, J. N., Halliday, D., Morrison, W. L., Stoward, P. J., Hornsby, G. A., Watt, P. W., Murdoch, G., and Rennie, M. J. (1987) Decrease in human quadriceps muscle protein turnover consequent upon leg immobilization. *Clin. Sci. (Lond.)* **72**, 503–509
- Deitrick, J. E. (1948) The effect of immobilization on metabolic and physiological functions of normal men. *Bull. N. Y. Acad. Med.* **24**, 364–375
- Acharyya, S., Ladner, K. J., Nelsen, L. L., Damrauer, J., Reiser, P. J., Swoap, S., and Guttridge, D. C. (2004) Cancer cachexia is regulated by selective targeting of skeletal muscle gene products. *J. Clin. Invest.* **114**, 370–378
- Tan, B. H., and Fearon, K. C. (2008) Cachexia: prevalence and impact in medicine. *Curr. Opin. Clin. Nutr. Metab. Care* **11**, 400–407
- Hasselgren, P. O., and Fischer, J. E. (1998) Sepsis: stimulation of energy-dependent protein breakdown resulting in protein loss in skeletal muscle. *World J. Surg.* **22**, 203–208
- Strassburg, S., Springer, J., and Anker, S. D. (2005) Muscle wasting in cardiac cachexia. *Int. J. Biochem. Cell Biol.* **37**, 1938–1947
- Kalyani, R. R., Corriere, M., and Ferrucci, L. (2014) Age-related and disease-related muscle loss: the effect of diabetes, obesity, and other diseases. *Lancet Diabetes Endocrinol.* **2**, 819–829
- Giangregorio, L., and McCartney, N. (2006) Bone loss and muscle atrophy in spinal cord injury: epidemiology, fracture prediction, and rehabilitation strategies. *J. Spinal Cord Med.* **29**, 489–500
- Janssen, I., Heymsfield, S. B., and Ross, R. (2002) Low relative skeletal muscle mass (sarcopenia) in older persons is associated with functional impairment and physical disability. *J. Am. Geriatr. Soc.* **50**, 889–896
- Batt, J., Bain, J., Goncalves, J., Michalski, B., Plant, P., Fahnstock, M., and Woodgett, J. (2006) Differential gene expression profiling of short and long term denervated muscle. *FASEB J.* **20**, 115–117
- Dupont Salter, A. C., Richmond, F. J., and Loeb, G. E. (2003) Effects of muscle immobilization at different lengths on tetrodotoxin-induced disuse atrophy. *IEEE Trans. Neural Syst. Rehabil. Eng.* **11**, 209–217
- De Boer, M. D., Maganaris, C. N., Seynnes, O. R., Rennie, M. J., and Narici, M. V. (2007) Time course of muscular, neural and tendinous adaptations to 23 day unilateral lower-limb suspension in young men. *J. Physiol.* **583**, 1079–1091
- Nikawa, T., Ishidoh, K., Hirasaka, K., Ishihara, I., Ikemoto, M., Kano, M., Kominami, E., Nonaka, I., Ogawa, T., Adams, G. R., Baldwin, K. M., Yasui, N., Kishi, K., and Takeda, S. (2004) Skeletal muscle gene expression in space-flown rats. *FASEB J.* **18**, 522–524
- Jarvis, J. C., and Salmons, S. (1991) A family of neuromuscular stimulators with optical transcutaneous control. *J. Med. Eng. Technol.* **15**, 53–57
- Jarvis, J. C., Mokrusch, T., Kwende, M. M., Sutherland, H., and Salmons, S. (1996) Fast-to-slow transformation in stimulated rat muscle. *Muscle Nerve* **19**, 1469–1475
- Bonaldo, P., and Sandri, M. (2013) Cellular and molecular mechanisms of muscle atrophy. *Dis. Model. Mech.* **6**, 25–39
- Eddins, M. J., Varadan, R., Fushman, D., Pickart, C. M., and Wolberger, C. (2007) Crystal structure and solution NMR studies of Lys48-linked tetraubiquitin at neutral pH. *J. Mol. Biol.* **367**, 204–211
- Sandri, M., Sandri, C., Gilbert, A., Skurc, C., Calabria, E., Picard, A., Walsh, K., Schiaffino, S., Lecker, S. H., and Goldberg, A. L. (2004) Foxo transcription factors induce the atrophy-related ubiquitin ligase atrogin-1 and cause skeletal muscle atrophy. *Cell* **117**, 399–412
- Lecker, S. H., Jagoe, R. T., Gilbert, A., Gomes, M., Baracos, V., Bailey, J., Price, S. R., Mitch, W. E., and Goldberg, A. L. (2004) Multiple types of skeletal muscle atrophy involve a common program of changes in gene expression. *FASEB J.* **18**, 39–51
- Jaenisch, R., and Bird, A. (2003) Epigenetic regulation of gene expression: how the genome integrates intrinsic and environmental signals. *Nat. Genet.* **33** (Suppl), 245–254
- Magnusson, C., Svensson, A., Christerson, U., and Tägerud, S. (2005) Denervation-induced alterations in gene expression in mouse skeletal muscle. *Eur. J. Neurosci.* **21**, 577–580
- Sharples, A. P., Polydorou, I., Hughes, D. C., Owens, D. J., Hughes, T. M., and Stewart, C. E. (2016) Skeletal muscle cells possess a

- 'memory' of acute early life TNF- α exposure: role of epigenetic adaptation. *Biogerontology* **17**, 603–617
25. Sharples, A. P., Stewart, C. E., and Seaborne, R. A. (2016) Does skeletal muscle have an 'epi'-memory? The role of epigenetics in nutritional programming, metabolic disease, aging and exercise. *Aging Cell* **15**, 603–616
 26. Ehrlich, K. C., Paterson, H. L., Lacey, M., and Ehrlich, M. (2016) DNA hypomethylation in intragenic and intergenic enhancer chromatin of muscle-specific genes usually correlates with their expression. *Yale J. Biol. Med.* **89**, 441–455
 27. Buffelli, M., Pasino, E., and Cangiano, A. (1997) Paralysis of rat skeletal muscle equally affects contractile properties as does permanent denervation. *J. Muscle Res. Cell Motil.* **18**, 683–695
 28. Michel, R. N., and Gardiner, P. F. (1990) To what extent is hindlimb suspension a model of disuse? *Muscle Nerve* **13**, 646–653
 29. Irizarry, R. A., Bolstad, B. M., Collin, F., Cope, L. M., Hobbs, B., and Speed, T. P. (2003) Summaries of affymetrix geneChip probe level data. *Nucleic Acids Res.* **31**, e15
 30. Irizarry, R. A., Hobbs, B., Collin, F., Beazer-Barclay, Y. D., Antonellis, K. J., Scherf, U., and Speed, T. P. (2003) Exploration, normalization, and summaries of high density oligonucleotide array probe level data. *Biostatistics* **4**, 249–264
 31. Schmittgen, T. D., and Livak, K. J. (2008) Analyzing real-time PCR data by the comparative C_T method. *Nat. Protoc.* **3**, 1101–1108
 32. Davis, P., Witczak, C., and Brault, J. (2015) AMP deaminase 3 accelerates protein degradation in C2C12 myotubes. *FASEB J.* **29**
 33. Cohen, S., Brault, J. J., Gygi, S. P., Glass, D. J., Valenzuela, D. M., Gartner, C., Latres, E., and Goldberg, A. L. (2009) During muscle atrophy, thick, but not thin, filament components are degraded by MuRF1-dependent ubiquitylation. *J. Cell Biol.* **185**, 1083–1095
 34. Cohen, T. J., Waddell, D. S., Barrientos, T., Lu, Z., Feng, G., Cox, G. A., Bodine, S. C., and Yao, T. P. (2007) The histone deacetylase HDAC4 connects neural activity to muscle transcriptional reprogramming. *J. Biol. Chem.* **282**, 33752–33759
 35. Tang, H., and Goldman, D. (2006) Activity-dependent gene regulation in skeletal muscle is mediated by a histone deacetylase (HDAC)-Dach2-myogenin signal transduction cascade. *Proc. Natl. Acad. Sci. USA* **103**, 16977–16982
 36. Tang, H., Macpherson, P., Marvin, M., Meadows, E., Klein, W. H., Yang, X. J., and Goldman, D. (2009) A histone deacetylase 4/myogenin positive feedback loop coordinates denervation-dependent gene induction and suppression. *Mol. Biol. Cell* **20**, 1120–1131
 37. Tang, W. W., Dietmann, S., Irie, N., Leitch, H. G., Floros, V. I., Bradshaw, C. R., Hackett, J. A., Chinnery, P. F., and Surani, M. A. (2015) A unique gene regulatory network resets the human germline epigenome for development. *Cell* **161**, 1453–1467
 38. Macpherson, P. C. D., Wang, X., and Goldman, D. (2011) Myogenin regulates denervation-dependent muscle atrophy in mouse soleus muscle. *J. Cell. Biochem.* **112**, 2149–2159
 39. Moresi, V., Williams, A. H., Meadows, E., Flynn, J. M., Potthoff, M. J., McAnally, J., Shelton, J. M., Backs, J., Klein, W. H., Richardson, J. A., Basse-Duby, R., and Olson, E. N. (2010) Myogenin and class II HDACs control neurogenic muscle atrophy by inducing E3 ubiquitin ligases. *Cell* **143**, 35–45
 40. Yu, X. M., and Hall, Z. W. (1991) Extracellular domains mediating epsilon subunit interactions of muscle acetylcholine receptor. *Nature* **352**, 64–67
 41. Ibejunjo, C., Chick, J. M., Kendall, T., Eash, J. K., Li, C., Zhang, Y., Vickers, C., Wu, Z., Clarke, B. A., Shi, J., Cruz, J., Fournier, B., Brachet, S., Gutzwiller, S., Ma, Q., Markovits, J., Broome, M., Steinkrauss, M., Skuba, E., Galarnau, J. R., Gygi, S. P., and Glass, D. J. (2013) Genomic and proteomic profiling reveals reduced mitochondrial function and disruption of the neuromuscular junction driving rat sarcopenia. *Mol. Cell. Biol.* **33**, 194–212
 42. Llano-Diez, M., Gustafson, A.-M., Olsson, C., Goransson, H., and Larsson, L. (2011) Muscle wasting and the temporal gene expression pattern in a novel rat intensive care unit model. *BMC Genomics* **12**, 602
 43. Bogdanović, O., and Veenstra, G. J. (2009) DNA methylation and methyl-CpG binding proteins: developmental requirements and function. *Chromosoma* **118**, 549–565
 44. Reik, W., Dean, W., and Walter, J. (2001) Epigenetic reprogramming in mammalian development. *Science* **293**, 1089–1093
 45. Barrès, R., Yan, J., Egan, B., Treebak, J. T., Rasmussen, M., Fritz, T., Caidahl, K., Krook, A., O'Gorman, D. J., and Zierath, J. R. (2012) Acute exercise remodels promoter methylation in human skeletal muscle. *Cell Metab.* **15**, 405–411
 46. Trasler, J., Deng, L., Melnyk, S., Pogribny, I., Hiou-Tim, F., Sibani, S., Oakes, C., Li, E., James, S. J., and Rozen, R. (2003) Impact of Dnmt1 deficiency, with and without low folate diets, on tumor numbers and DNA methylation in Min mice. *Carcinogenesis* **24**, 39–45
 47. Jacobsen, S. C., Brøns, C., Bork-Jensen, J., Ribel-Madsen, R., Yang, B., Lara, E., Hall, E., Calvanese, V., Nilsson, E., Jørgensen, S. W., Mandrup, S., Ling, C., Fernandez, A. F., Fraga, M. F., Poulsen, P., and Vaag, A. (2012) Effects of short-term high-fat overfeeding on genome-wide DNA methylation in the skeletal muscle of healthy young men. *Diabetologia* **55**, 3341–3349
 48. Le Grand, F., and Rudnicki, M. A. (2007) Skeletal muscle satellite cells and adult myogenesis. *Curr. Opin. Cell Biol.* **19**, 628–633
 49. Bodine, S. C., and Baehr, L. M. (2014) Skeletal muscle atrophy and the E3 ubiquitin ligases MuRF1 and MAFbx/atrogen-1. *Am. J. Physiol. Endocrinol. Metab.* **307**, E469–E484
 50. Bodine, S. C., Latres, E., Baumhueter, S., Lai, V. K., Nunez, L., Clarke, B. A., Poueymirou, W. T., Panaro, F. J., Na, E., Dharmarajan, K., Pan, Z. Q., Valenzuela, D. M., DeChiara, T. M., Stitt, T. N., Yancopoulos, G. D., and Glass, D. J. (2001) Identification of ubiquitin ligases required for skeletal muscle atrophy. *Science* **294**, 1704–1708
 51. Goldberg, A. L. (1969) Protein turnover in skeletal muscle. II. Effects of denervation and cortisone on protein catabolism in skeletal muscle. *J. Biol. Chem.* **244**, 3223–3229
 52. Giniatullin, R., Nistri, A., and Yakel, J. L. (2005) Desensitization of nicotinic ACh receptors: shaping cholinergic signaling. *Trends Neurosci.* **28**, 371–378
 53. Beker, F., Weber, M., Fink, R. H., and Adams, D. J. (2003) Muscarinic and nicotinic ACh receptor activation differentially mobilize Ca^{2+} in rat intracardiac ganglion neurons. *J. Neurophysiol.* **90**, 1956–1964
 54. Ibejunjo, C. (2013) Genomic and proteomic profiling reveals reduced mitochondrial function and disruption of the neuromuscular junction driving rat sarcopenia. *Mol. Cell. Biol.* **33**, 194–212
 55. Colquhoun, D., and Sivilotti, L. G. (2004) Function and structure in glycine receptors and some of their relatives. *Trends Neurosci.* **27**, 337–344

Received for publication March 15, 2017.
Accepted for publication July 25, 2017.

- Shelley P, Martin-Gronert MS, Rowleson A, Poston L, Heales SJ, Hargreaves IP, McConnell JM, Ozanne SE, Fernandez-Twinn DS (2009) Altered skeletal muscle insulin signaling and mitochondrial complex II-III linked activity in adult offspring of obese mice. *Am. J. Physiol. Regul. Integr. Comp. Physiol.* **297**, R675–R681.
- Shukla S, Kavak E, Gregory M, Imashimizu M, Shutinoski B, Kashlev M, Oberdoerffer P, Sandberg R, Oberdoerffer S (2011) CTCF-promoted RNA polymerase II pausing links DNA methylation to splicing. *Nature* **479**, 74–79.
- Smith JAH, Collins M, Grobler LA, Magee CJ, Ojuka EO (2007) Exercise and CaMK activation both increase the binding of MEF2A to the Glut4 promoter in skeletal muscle in vivo. *Am. J. Physiol. – Endocrinol. Metabol.* **292**, E413–E420.
- Smith JAH, Kohn TA, Chetty AK, Ojuka EO (2008) CaMK activation during exercise is required for histone hyperacetylation and MEF2A binding at the MEF2 site on the Glut4 gene. *Am. J. Physiol. – Endocrinol. Metabol.* **295**, E698–E704.
- Sousa-Victor P, Gutarra S, Garcia-Prat L, Rodriguez-Ubreva J, Ortet L, Ruiz-Bonilla V, Jardi M, Ballestar E, Gonzalez S, Serrano AL, Perdiguerro E, Munoz-Canoves P (2014) Geriatric muscle stem cells switch reversible quiescence into senescence. *Nature* **506**, 316–321.
- Srinivasan M, Katewa SD, Palaniyappan A, Pandya JD, Patel MS (2006) Maternal high-fat diet consumption results in fetal malprogramming predisposing to the onset of metabolic syndrome-like phenotype in adulthood. *Am. J. Physiol. Endocrinol. Metab.* **291**, E792–E799.
- Staron RS, Leonardi MJ, Karapondo DL, Malicky ES, Falkel JE, Hagerman FC, Hikida RS (1991) Strength and skeletal muscle adaptations in heavy-resistance-trained women after detraining and retraining. *J. Appl. Physiol.* (1985) **70**, 631–640.
- Stewart CE, James PL, Fant ME, Rotwein P (1996) Overexpression of insulin-like growth factor-II induces accelerated myoblast differentiation. *J. Cell. Physiol.* **169**, 23–32.
- Stewart CE, Newcomb PV, Holly JM (2004) Multifaceted roles of TNF-alpha in myoblast destruction: a multitude of signal transduction pathways. *J. Cell. Physiol.* **198**, 237–247.
- Taaffe DR, Marcus R (1997) Dynamic muscle strength alterations to detraining and retraining in elderly men. *Clin. Physiol.* **17**, 311–324.
- Taaffe DR, Henwood TR, Nalls MA, Walker DG, Lang TF, Harris TB (2009) Alterations in muscle attenuation following detraining and retraining in resistance-trained older adults. *Gerontology* **55**, 217–223.
- Taguchi T, Kishikawa H, Motoshima H, Sakai K, Nishiyama T, Yoshizato K, Shirakami A, Toyonaga T, Shirontani T, Araki E, Shichiri M (2000) Involvement of bradykinin in acute exercise-induced increase of glucose uptake and GLUT-4 translocation in skeletal muscle: studies in normal and diabetic humans and rats. *Metabolism* **49**, 920–930.
- Tahiliani M, Koh KP, Shen Y, Pastor WA, Bandukwala H, Brudno Y, Agarwal S, Iyer LM, Liu DR, Aravind L, Rao A (2009) Conversion of 5-methylcytosine to 5-hydroxymethylcytosine in mammalian DNA by MLL partner TET1. *Science* **324**, 930–935.
- Tanner CJ, Barakat HA, Dohm GL, Pories WJ, MacDonald KG, Cunningham PR, Swanson MS, Houmard JA (2002) Muscle fiber type is associated with obesity and weight loss. *Am. J. Physiol. Endocrinol. Metab.* **282**, E1191–E1196.
- Tong JF, Yan X, Zhu MJ, Ford SP, Nathanielsz PW, Du M (2009) Maternal obesity downregulates myogenesis and beta-catenin signaling in fetal skeletal muscle. *Am. J. Physiol. Endocrinol. Metab.* **296**, E917–E924.
- Tornatore L, Thotakura AK, Bennett J, Moretti M, Franzoso G (2012) The nuclear factor kappa B signaling pathway: integrating metabolism with inflammation. *Trends Cell Biol.* **22**, 557–566.
- Trasler J, Deng L, Melnyk S, Pogribny I, Hiou-Tim F, Sibani S, Oakes C, Li E, James SJ, Rozen R (2003) Impact of Dnmt1 deficiency, with and without low folate diets, on tumor numbers and DNA methylation in Min mice. *Carcinogenesis* **24**, 39–45.
- Troy A, Cadwallader AB, Fedorov Y, Tyner K, Tanaka KK, Olwin BB (2012) Coordination of satellite cell activation and self-renewal by Par-complex-dependent asymmetric activation of p38alpha/beta MAPK. *Cell Stem Cell* **11**, 541–553.
- Valencia AP, Spangenburg EE (2013) Remembering those 'lazy' days—imprinting memory in our satellite cells. *J. Physiol.* **591**, 4371.
- Wang F, Nguyen M, Qin F, Tong Q (2007) SIRT2 deacetylates FOXO3a in response to oxidative stress and caloric restriction. *Aging Cell* **6**, 505–514.
- Wang Z, Zang C, Cui K, Schones DE, Barski A, Peng W, Zhao K (2009) Genome-wide mapping of HATs and HDACs reveals distinct functions in active and inactive genes. *Cell* **138**, 1019–1031.
- Wang H, Wilson GJ, Zhou D, Lezmi S, Chen X, Layman DK, Pan YX (2015) Induction of autophagy through the activating transcription factor 4 (ATF4)-dependent amino acid response pathway in maternal skeletal muscle may function as the molecular memory in response to gestational protein restriction to alert offspring to maternal nutrition. *Br. J. Nutr.* **114**, 519–532.
- Ward SS, Stickland NC (1991) Why are slow and fast muscles differentially affected during prenatal undernutrition? *Muscle Nerve* **14**, 259–267.
- Weber M, Hellmann I, Stadler MB, Ramos L, Paabo S, Rebhan M, Schubeler D (2007) Distribution, silencing potential and evolutionary impact of promoter DNA methylation in the human genome. *Nat. Genet.* **39**, 457–466.
- Wilson SJ, Ross JJ, Harris AJ (1988) A critical period for formation of secondary myotubes defined by prenatal undernourishment in rats. *Development* **102**, 815–821.
- Wilson SJ, McEwan JC, Sheard PW, Harris AJ (1992) Early stages of myogenesis in a large mammal: formation of successive generations of myotubes in sheep tibialis cranialis muscle. *J. Muscle Res. Cell Motil.* **13**, 534–550.
- Woo M, Isganaitis E, Cerletti M, Fitzpatrick C, Wagers AJ, Jimenez-Chillaron J, Patti ME (2011) Early life nutrition modulates muscle stem cell number: implications for muscle mass and repair. *Stem Cells Dev.* **20**, 1763–1769.
- Yakubu DP, Mostyn A, Hyatt MA, Kurlak LO, Budge H, Stephenson T, Symonds ME (2007a) Ontogeny and nutritional programming of mitochondrial proteins in the ovine kidney, liver and lung. *Reproduction* (Cambridge, England) **134**, 823–830.
- Yakubu DP, Mostyn A, Wilson V, Pearce S, Alves-Guerra MC, Pecqueur C, Miroux B, Budge H, Stephenson T, Symonds ME (2007b) Different effects of maternal parity, cold exposure and nutrient restriction in late pregnancy on the abundance of mitochondrial proteins in the kidney, liver and lung of postnatal sheep. *Reproduction* (Cambridge, England) **133**, 1241–1252.
- Yamauchi T, Kamon J, Ito Y, Tsuchida A, Yokomizo T, Kita S, Sugiyama T, Miyagishi M, Hara K, Tsunoda M, Murakami K, Ohteki T, Uchida S, Takekawa S, Waki H, Tsuno NH, Shibata Y, Terauchi Y, Froguel P, Tobe K, Koyasu S, Taira K, Kitamura T, Shimizu T, Nagai R, Kadowaki T (2003) Cloning of adiponectin receptors that mediate antidiabetic metabolic effects. *Nature* **423**, 762–769.
- Yates DT, Clarke DS, Macko AR, Anderson MJ, Shelton LA, Nearing M, Allen RE, Rhoads RP, Limesand SW (2014) Myoblasts from intrauterine growth-restricted sheep fetuses exhibit intrinsic deficiencies in proliferation that contribute to smaller semitendinosus myofibres. *J. Physiol.*, **592**, 3113–3125.
- Zeng Y, Gu P, Liu K, Huang P (2013) Maternal protein restriction in rats leads to reduced PGC-1alpha expression via altered DNA methylation in skeletal muscle. *Mol. Med. Rep.* **7**, 306–312.
- Zhu MJ, Ford SP, Nathanielsz PW, Du M (2004) Effect of maternal nutrient restriction in sheep on the development of fetal skeletal muscle. *Biol. Reprod.* **71**, 1968–1973.
- Zhu MJ, Ford SP, Means WJ, Hess BW, Nathanielsz PW, Du M (2006) Maternal nutrient restriction affects properties of skeletal muscle in offspring. *J. Physiol.* **575**, 241–250.
- Zhu MJ, Han B, Tong J, Ma C, Kimzey JM, Underwood KR, Xiao Y, Hess BW, Ford SP, Nathanielsz PW, Du M (2008) AMP-activated protein kinase signalling pathways are down regulated and skeletal muscle development impaired in fetuses of obese, over-nourished sheep. *J. Physiol.* **586**, 2651–2664.
- Zwetsloot KA, Childs TE, Gilpin LT, Booth FW (2013) Non-passaged muscle precursor cells from 32-month old rat skeletal muscle have delayed proliferation and differentiation. *Cell Prolif.* **46**, 45–57.
- Zykovich A, Hubbard A, Flynn JM, Tarnopolsky M, Fraga MF, Kerksick C, Ogborn D, MacNeil L, Mooney SD, Melov S (2014) Genome-wide DNA methylation changes with age in disease-free human skeletal muscle. *Aging Cell* **13**, 360–366.

Appendix 3.

Title: Human Skeletal Muscle Possesses an Epigenetic Memory of Hypertrophy.

Journal: Scientific Reports (impact factor 4.259)

Volume: 8

Issue: 1

Pages: 1898

SCIENTIFIC REPORTS

OPEN

Human Skeletal Muscle Possesses an Epigenetic Memory of Hypertrophy

Robert A. Seaborne^{1,2}, Juliette Strauss², Matthew Cocks², Sam Shepherd², Thomas D. O'Brien², Ken A. van Someren³, Phillip G. Bell³, Christopher Murgatroyd⁴, James P. Morton², Claire E. Stewart² & Adam P. Sharples^{1,2}

Received: 31 October 2017
Accepted: 16 January 2018
Published online: 30 January 2018

It is unknown if adult human skeletal muscle has an epigenetic memory of earlier encounters with growth. We report, for the first time in humans, genome-wide DNA methylation (850,000 CpGs) and gene expression analysis after muscle hypertrophy (loading), return of muscle mass to baseline (unloading), followed by later hypertrophy (reloading). We discovered increased frequency of hypomethylation across the genome after reloading (18,816 CpGs) versus earlier loading (9,153 CpG sites). We also identified AXIN1, GRIK2, CAMK4, TRAF1 as hypomethylated genes with enhanced expression after loading that maintained their hypomethylated status even during unloading where muscle mass returned to control levels, indicating a memory of these genes methylation signatures following earlier hypertrophy. Further, UBR5, RPL35a, HEG1, PLA2G16, SETD3 displayed hypomethylation and enhanced gene expression following loading, and demonstrated the largest increases in hypomethylation, gene expression and muscle mass after later reloading, indicating an epigenetic memory in these genes. Finally, genes; GRIK2, TRAF1, BICC1, STAG1 were epigenetically sensitive to acute exercise demonstrating hypomethylation after a single bout of resistance exercise that was maintained 22 weeks later with the largest increase in gene expression and muscle mass after reloading. Overall, we identify an important epigenetic role for a number of largely unstudied genes in muscle hypertrophy/memory.

Numerous studies demonstrate that skeletal muscle can be programmed, where early life exposure to environmental stimuli lead to a sustained alteration of skeletal muscle phenotype in later life [reviewed in ref.¹]. This has been demonstrated in mammalian models in which reduced nutrient availability during gestation impairs skeletal muscle fibre number, composition (fast/slow fibre proportions) and size of the offspring¹. Epidemiological studies in human ageing cohorts also suggest that low birth weight and gestational malnutrition are strongly associated with reduced skeletal muscle size, strength and gait speed in older age^{2,3}. Driven by encounters with the environment, foetal programming in skeletal muscle has been attributed in part to epigenetics^{4,5}, which refers to alterations in gene expression as a result of non-genetic structural modifications of DNA and/or histones⁶. Despite these compelling data, it is unknown if adult skeletal muscle possesses the capacity to respond differently to environmental stimuli in an adaptive or maladaptive manner if the stimuli have been encountered previously, a concept recently defined as skeletal muscle memory¹, or if this process is epigenetically regulated. Indeed, it is known that skeletal muscle cells retain information or 'remember' the stem cell niche of the donor once derived *in-vitro* from physically active⁷ obese^{8,9} and sarcopenic individuals [recently reviewed in ref.¹]. Our group were the first to demonstrate this phenomenon, where human muscle stem cells derived from the skeletal muscle of cancer patients exhibited overactive proliferation versus age matched control cells¹⁰. These studies collectively suggest that skeletal muscle cells could be epigenetically regulated, as they appear to not only retain information from the environmental niche from which they originated, but also to pass this molecular 'signature' onto future daughter cell progeny *in-vitro*. Furthermore, we have recently reported that mouse skeletal muscle cells (C2C12),

¹Institute for Science and Technology in Medicine (ISTM), School of Medicine, Keele University, Staffordshire, United Kingdom. ²Research Institute for Sport and Exercise Sciences, Liverpool John Moores University, Liverpool, United Kingdom. ³Department of Sport, Exercise and Rehabilitation, Northumbria University, Newcastle upon Tyne, United Kingdom. ⁴School of Healthcare Science, Manchester Metropolitan University, Manchester, United Kingdom. Correspondence and requests for materials should be addressed to A.P.S. (email: a.p.sharples@googlemail.com)

following an early-life inflammatory stress, pass molecular information onto future generations (30 cellular divisions), through a process of DNA methylation¹¹. Importantly, the cells that encountered catabolic inflammatory stress in their earlier proliferative life had impaired differentiation capacity when encountering the same inflammatory stress in later proliferative life¹¹. It has therefore been proposed that a memory and susceptibility of skeletal muscle to repeated encounters with inflammation may be controlled by epigenetic modifications such as DNA methylation, a phenomenon we have termed skeletal muscle 'epi-memory'¹.

Mouse skeletal muscle *in-vivo* also appears to possess a memory from the anabolic growth steroid sex hormone, testosterone. Where testosterone induced hypertrophy over a period of 3 months, resulted in enhanced incorporation of myonuclei within muscle fibres^{12,13}. These myonuclei were retained even following testosterone withdrawal and the return of muscle mass to baseline^{12,13}. Most notably the mice exposed to earlier life testosterone, exhibited a 31% increase in muscle cross-sectional area following mechanical loading versus control mice that failed to grow in the same period of time^{12,13}. This suggests an enhanced response to load induced muscle hypertrophy when earlier life growth from testosterone had been encountered, and therefore corresponds with the previously highlighted definition of muscle memory by Sharples *et al.*¹. However, epigenetics has not been studied in this model, and specifically genome-wide DNA methylation has not been investigated after adult human skeletal muscle growth (hypertrophy) alone, or in skeletal muscle that has experienced later growth, to investigate if skeletal muscle possesses an epigenetic memory from earlier life encounters with hypertrophy.

To provide parallel insights into the effect of the environment on genome-wide methylation changes in skeletal muscle, recent studies have suggested that even an acute period of increased fat intake can alter the human DNA methylome of CpGs in over 6,500 genes¹⁴. Like previous studies demonstrating rapid and dynamic alterations in DNA methylation in skeletal muscle tissue after acute metabolic stress (aerobic exercise)^{15,16} or disuse atrophy in rats¹⁷, this study also suggested that large scale epigenetic modifications can occur very rapidly in skeletal muscle, after only 5 days of high fat feeding. However, the authors also demonstrated a maintenance of methylation following cessation of the high fat diet¹⁴. Where after 8 weeks of returning to a normal diet, not all of the altered methylation, particularly hypermethylation, was fully returned to baseline control levels¹⁴. This therefore suggests that in response to an acute negative environmental stress, DNA methylation could be retained and accumulated over time. Indeed, human skeletal muscle cells isolated from aged donors demonstrated a genome wide hypermethylated profile versus young adult tissue¹⁸. Therefore, because DNA methylation, particularly within promoter or enhancer regions of genes, generally leads to suppressed gene expression¹⁹, accumulation of high DNA methylation (hypermethylation) following a high fat diet and/or ageing could lead to universally suppressed gene expression. It may therefore be hypothesised that positive environmental encounters, such as muscle growth stimuli, may induce a hypomethylated state (low DNA methylation) of important target transcripts or loci associated with cellular growth and as a result, lead to enhanced gene expression when exposed to later life anabolic encounters.

To test this hypothesis, we aimed to investigate an epigenetic memory of earlier hypertrophy in adult human skeletal muscle using a within measures design, by investigating genome wide DNA methylation of over 850,000 CpG sites after: (1) Resistance exercise induced muscle growth (loading), followed by; (2) cessation of resistance exercise to return muscle back towards baseline levels (unloading), and; (3) a subsequent later period of resistance exercise induced muscle hypertrophy (reloading). This allowed us to assess the epigenetic regulation of skeletal muscle; (a) hypertrophy; (b) a return of muscle back to baseline and, (c) memory of previous encounters with hypertrophy, respectively. Importantly, these investigations for the first time identified an increased frequency of hypomethylation across the genome during later reloading where lean muscle mass increases were enhanced compared to earlier loading. We also detected genes; AXIN1, GRIK 2, CAMK4 and TRAF1 displayed increasing DNA hypomethylation together with enhanced gene expression across loading, unloading and reloading. Where hypomethylation of these genes was maintained even during unloading where muscle mass returned back to baseline, indicating an epigenetic memory of earlier muscle growth. Furthermore, UBR5, RPL35a, HEG1 and PLA2G16 previously unstudied in skeletal muscle, together with SETD3 displayed hypomethylation and enhanced gene expression following loading versus baseline and displayed even larger increases in both hypomethylation and gene expression after later reloading, also indicating an epigenetically regulated memory leading to enhanced gene expression during reloading. Gene expression of this cluster also strongly and positively correlated with increased muscle mass across all conditions, confirming these transcripts to be novel resistance exercise induced- hypertrophy genes in skeletal muscle. Finally, we identified genes GRIK2, TRAF1 (identified above), BICC1 and STAG1 were hypomethylated after a single bout of acute resistance exercise that were maintained as hypomethylated, and had enhanced gene expression after later reloading. Suggesting that these are epigenetically sensitive genes after a single bout of resistance exercise and associated with enhanced muscle hypertrophy 22 weeks later.

Methods

Human Participants and Ethical Approval. Eight healthy males gave written, informed consent to participate in the study, following successful completion of a readiness to exercise questionnaire and a pre-biopsy screening as approved by a physician. One participant withdrew from the study at experimental week 17 of 21, for reasons unrelated to this investigation. However, consent allowed samples to be analysed prior to withdrawal, therefore for this participant, this included all conditions excluding the final reloading condition (for details see below). Ethical approval was granted by the NHS West Midlands Black Country, UK, Research Ethics Committee (NREC approval no. 16/WM/0103), all methods were performed in accordance with the relevant ethical guidelines and regulations.

Experimental Design. Using a within subject design, eight previously untrained male participants (27.6 ± 2.4 yr, 82.5 ± 6.0 kg, 178.1 ± 2.8 cm, means \pm SEM) completed an acute bout of resistance exercise (acute RE), followed by 7 weeks (3d/week) of resistance exercise (loading), 7 weeks of exercise cessation (unloading) and a further period of 7 weeks (3d/week) resistance exercise (re-loading). Graphical representation of experimental

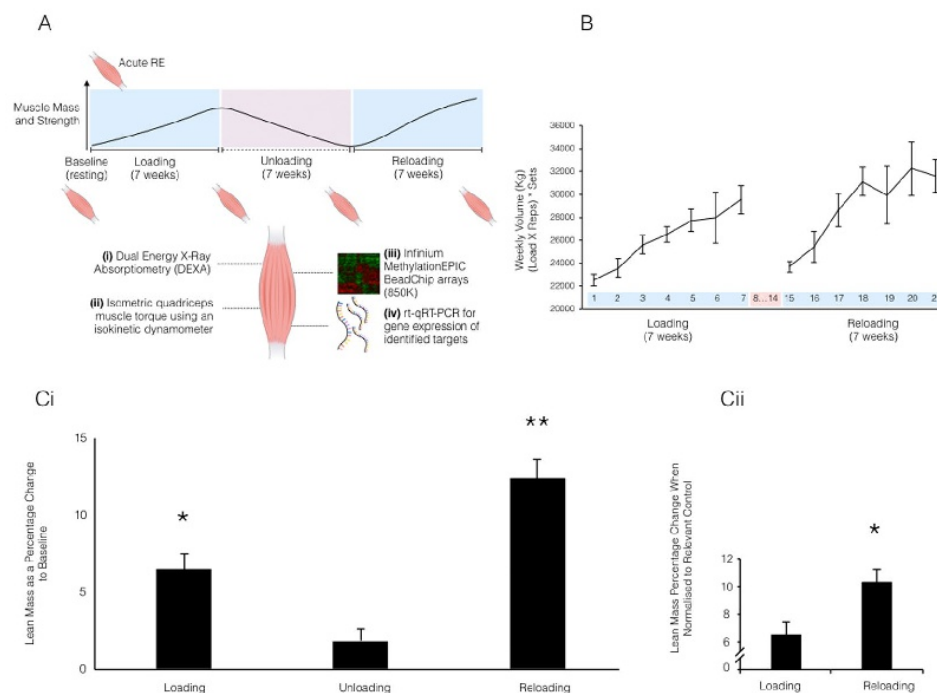


Figure 1. (A) Schematic representation of experimental conditions and types of analysis undertaken across the time-course. The image of a muscle represents the time point for analysis of muscle mass via (i) DEXA and strength via (ii) isometric quadriceps muscle torque using an isokinetic dynamometer. The images of muscle tissue also represent the time point of skeletal muscle biopsy of the Vastus Lateralis, muscle sample preparation for downstream analysis of (iii) Infinium MethylationEPIC BeadChip arrays (850 K CpG sites) methylome wide array (iv) and rt-qRT-PCR for gene expression analysis of important genes identified following methylome wide analysis. (B) Weekly total volume of resistance exercise undertaken by human participants ($n = 7$) during the first 7-week resistance exercise period (loading, weeks 1–7), followed by a 7 week cessation of resistance exercise (unloading, weeks 8–14) and the later second period of 7 weeks resistance exercise (reloading, weeks 15–21). Data represents volume load as calculated by ((load (Kg) x reps) x sets) averaged across 3 resistance exercise sessions per week. Data presented mean \pm SEM. (Ci) Lean lower limb mass changes in human subjects ($n = 7$) after a period of 7 weeks resistance exercise (loading), exercise cessation (unloading) and a subsequent second period of 7 weeks resistance exercise (reloading). Total limb lean mass normalised to baseline (percentage change). Significant change compared to baseline represented by * and significant difference to all other conditions represented by **. (Cii) Total lean mass percentage change when loading is normalised to baseline, and reloading normalised to unloading to account for starting lean mass in both conditions. Pairwise t-test of significance indicated by *. All data presented as mean \pm SEM ($n = 7$).

design is provided in Fig. 1A. Whole-body fan beam dual-energy x-ray absorptiometry (DEXA), strength of the quadriceps via dynamometry and muscle biopsies from the vastus lateralis for RNA and DNA isolation were obtained at baseline, after 7 weeks loading (beginning of week 8), 7 weeks unloading (end of week 14) and 7 weeks reloading (beginning of week 22). A muscle biopsy was also obtained 30 minutes after acute RE prior to 7 weeks loading. Genome-wide analysis of DNA methylation was performed via Illumina EPIC array (850,000 CpG sites-detailed below) for participants across all conditions ($n = 8$ baseline, acute, loading, unloading, $n = 7$ reloading). Rt-qRT-PCR was used to investigate corresponding transcript expression of epigenetically altered genes identified via the genome wide DNA methylation analysis.

Resistance exercise induced muscle hypertrophy: Loading, unloading and reloading.

Untrained male subjects initially performed an exercise familiarization week, in which participants performed all exercises with no/low load to become familiar with the exercise type (detailed below). In the final session of the familiarization week, the load that participants could perform 4 sets of 8–10 repetitions for each exercise was assessed. Due to participants being uncustomized to resistance exercise, assessment was made on competence of lifting technique, range of exercise motion and verbal feedback (participant), and a starting load was set for each participant on an individual basis (mean load for this starting load is included below). Three to four days later, participants then undertook a single bout of lower limb resistance exercise (acute RE, exercises detailed below) followed by biopsies 30 minutes post exercise. Following this single bout of acute RE they then began a chronic resistance exercise program, completing 60-min training sessions (Monday-Wednesday-Friday), for 7 weeks,

with 2 sessions/week focusing on lower limb muscle groups (Monday and Friday) and the third session focusing on upper body muscle groups (Wednesday). Lower limb exercises included, behind head squat, leg press, leg extension, leg curl, Nordic curls, weighted lunges and calf raises. Upper limb exercises included, flat barbell bench press, shoulder press, latissimus pull down, dumbbell row and triceps cable extension. To ensure progression in participants with no previous experience in resistance exercise, a progressive volume model was adopted²⁰ in which investigators regularly assessed competency of sets, reps and load of all exercises. Briefly, exercises were performed for 4 sets of 10 reps in each set, ~90–120 s in between sets and ~3 mins between exercises. When participants could perform 3 sets of 10 repetitions without assistance and with the correct range of motion, load was increased by ~5–10% in the subsequent set and participants continued on this new load until further modifications were required, as similar to that previously described²⁰. Where subjects failed to complete 10 full repetitions (usually for their final sets), they were instructed to reduce the load in order to complete a full repetition range for the subsequent (usually final) set. Total weekly volume load was calculated as the sum of all exercise loads;

$$\text{Total exercise volume (kgs)} = (\text{Exercise load (kgs)} * \text{No. of Reps}) * \text{No. Sets}$$

The acute resistance exercise session resulted in a total load of 8,223 kg (\pm 284 kg). Thereafter, the loading and reloading phases resulted in a progressive increase in training volume (\pm SEM) of 2,257 \pm 639 kg and 2,386 \pm 222 kg respectively per week (Fig. 1B), with the reloading phase displaying a significant ($P = 0.043$) increase in average load. Loading and reloading programs were conducted in an identical manner, with the same exercises, program layout (same exercises on the same day), sets and repetition pattern and rest between sets and exercises. During the 7 week unloading phase, participants were instructed to return to habitual pre-intervention exercise levels and not to perform any resistance training. Regular verbal communication between researcher and participant ensured subjects followed these instructions. A trainer was present at all resistance exercise sessions to enable continued monitoring, provide verbal encouragement and to ensure sufficient progression. No injuries were sustained throughout the exercise intervention.

Lean mass and strength of the lower limbs by dual-energy x-ray absorptiometry (DEXA) and dynamometry. A whole-body fan beam dual-energy x-ray absorptiometry (DEXA; Hologic QDR Series, Discovery A, Bedford, MA, USA) scan was performed after loading, unloading and reloading (depicted in Fig. 1A) to assess lower limb changes in lean mass. All scans were performed and analysed (QDR for Windows, version 12:4:3) by the same trained operator, according to Hologic guidelines. The DEXA scan was automatically analysed via the QDR software and the operator confirmed areas of interest including lower limb positions. Lean mass was calculated on absolute values for each condition, and presented as percentage change compared to baseline. Furthermore, in addition, a separate analysis was undertaken to assess whether later reloading altered lean mass, where loading was normalised to baseline, and reloading was normalised to unloading to account for any residual starting mass (even if non-significant) following the earlier loading period. A pairwise t-test was then used to analyse the percentage increase in lean mass as a consequence of reloading compared to loading. To assess quadriceps muscle strength, *in-vivo* isometric knee extension maximal voluntary contractions (MVC) were performed using an isokinetic dynamometer (IKD; Biodex, New York, USA) to measure peak joint torque. Data presented as percentage increase to baseline (%) using absolute values (Nm), unless otherwise stated. A full description of strength assessment can be found in Supplementary File 1.

Muscle Biopsies and Sample Preparation. At baseline, 30 minutes post acute resistance exercise (RE) and after 7 weeks loading (beginning of week 8), 7 weeks unloading (end of week 14) and 7 weeks reloading (beginning of week 22) (Fig. 1A), a conchotome muscle biopsy was obtained from the vastus lateralis muscle of the quadriceps from each participant, avoiding areas of immediate proximity to previous incisions, before being carefully cleaned and dissected using a sterile scalpel on a sterile petri dish. In the unlikely event of any fibrous/fat tissue, this was removed using a scalpel, leaving only lean tissue. Separate samples were immediately snap frozen in liquid nitrogen before being stored at -80°C for RNA and DNA analysis.

DNA Isolation, Bisulfite Conversion and Methylome Wide BeadChip Arrays. DNA was extracted from frozen tissue samples using a commercially available DNA isolation kit (DNeasy Blood and Tissue Kit, Qiagen, Manchester, UK) in accordance with manufacturer's instructions, before being analysed (Nanodrop, ThermoFisher Scientific, Paisley, UK) for yield (mean \pm SDEV 8.0 $\mu\text{g} \pm$ 4.2) and quality (260/280 ratio of mean \pm SDEV 1.88 \pm 0.09). Five-hundred ng of prepared DNA was bisulfite converted using the EZ-96 DNA Methylation Kit (Zymo Research Corp., CA, USA) following the manufacturer's instructions for use of the DNA in Illumina assays. Infinium MethylationEPIC BeadChip array examined over 850,000 CpG sites of the human epigenome (Infinium MethylationEPIC BeadChip, Illumina, California, United States) and data was analysed in Partek Genomics Suite V.6.6 (Partek Inc. Missouri, USA). Raw data files (.IDAT) were normalised via the Subset-Quantile Within Array Normalisation (SWAN) method, as previously described²¹. Initial quality control steps were undertaken to detect samples within arrays that were identified as outliers. Principal component analysis (PCA) and normalisation histograms detected two observable outliers across all samples. These samples were removed from any further analysis (Supplementary Figure 1A & B). While skeletal muscle tissue samples may contain a small proportion of other non-muscle cells this analysis suggests sample homogeneity was consistent in the experimental groups and therefore downstream analysis was representative of skeletal muscle tissue and its niche. Data sets represent SWAN-normalised beta (β)-values which correspond to the percentage of methylation at each site and are calculated as a ratio of methylated to unmethylated probes²². Differential methylation was subsequently detected across all experimental conditions, and between conditions to identify statistically differentially regulated CpG sites. Fold change in CpG specific DNA methylation and statistical significance

was performed using Partek Genomic Suite V.6.6 software, where statistical significance was obtained following ANOVA (with bonferroni correction) analysis.

Hierarchical Clustering Dendrogram. Unadjusted p-value significance ($P < 0.05$) was used to create a CpG site marker list of standardized beta-values. A standardized expression normalisation was performed to shift CpG sites to mean of zero and scale to a standard deviation of one. Unsupervised hierarchical clustering was performed and dendrograms were constructed to represent differentially methylated CpG loci and statistical clustering of experimental samples. Heatmaps represent expression of CpG loci, where reduced methylation at DNA sites (hypomethylated) are represented in green, increased methylation at DNA sites (hypermethylated) in red, and unchanged sites are represented in black.

Tissue Homogenisation, RNA Isolation and rt-qRT-PCR. Skeletal muscle tissue (~30 mg) was immersed in Tri-Reagent (Sigma-Aldrich, MO, United States) in MagNA Lyser 1.4 mm beaded tubes (MagNA Lyser Green Beads, Roche, Germany) and homogenised for 40 secs at 6 m/s in a MagNA Lyser Homogeniser (Roche, Germany), before being stored on ice for 5 mins. This step was repeated three times to ensure complete disruption of muscle tissue sample. RNA was extracted using standard Tri-Reagent procedure via chloroform/isopropanol extractions and 75% ethanol washing as per manufacturer's instructions. RNA pellets were resuspended in 30 μ l of RNA storage solution (Ambion, Paisley, UK) and analysed (Nanodrop, ThermoFisher Scientific, Paisley, UK) for quantity (mean \pm SDEV; 6671 ± 3986 ng) and an indication of quality (260/280 ratio of mean \pm SDEV, 1.95 ± 0.09). For rt-qRT-PCR using QuantiFast™ SYBR® Green RT-PCR one-step kit on a RotorGene 3000Q, reactions were setup as follows; 9.5 μ l experimental sample (5.26 ng/ μ l totaling 50 ng per reaction), 0.15 μ l of both forward and reverse primer of the gene of interest (100 μ M), 0.2 μ l of QuantiFast RT Mix (Qiagen, Manchester, UK) and 10 μ l of QuantiFast SYBR Green RT-PCR Master Mix (Qiagen, Manchester, UK). Reverse transcription was initiated with a hold at 50 °C for 10 minutes (cDNA synthesis), followed by a 5-minute hold at 95 °C (transcriptase inactivation and initial denaturation), before 40–45 PCR cycles of; 95 °C for 10 sec (denaturation) followed by 60 °C for 30 secs (annealing and extension). Primer sequences are provided in Supplementary File 7. Gene expression analysis was performed on at least $n = 7$ for all genes, unless otherwise stated. All relative gene expression was quantified using the comparative Ct ($\Delta\Delta$ Ct) method. Individual participants own baseline Ct values were used in $\Delta\Delta$ Ct equation as the calibrator using RPL13a as the reference gene. The average Ct value for the reference gene was consistent across all participants and experimental conditions (20.48 ± 0.64 , SDEV) with low variation of 3.17%.

Statistical Analysis. Analysis of exercise volume load was performed via a T-test (MiniTab Version 17.2.1) of average participant load during the loading vs. reloading phases. DEXA and isometric peak torque; for $n = 7$, as well as correlation analysis was analysed via a statistical package for the social sciences software for Microsoft (SPSS, version 23.0, SPSS Inc, Chicago, IL) using a one-way repeated measures ANOVA, where applicable. Pearson correlation of coefficient analysis (two tailed) was conducted for gene expression vs. percentage change of leg lean mass. Methylome wide array data sets ($n = 8$ for baseline, acute RE, loading, unloading, $n = 7$ for reloading) were analysed for significant epigenetically modified CpG sites in Partek Genome Suite (version 6.6). All gene ontology and KEGG signalling pathway^{25–25} analysis was performed in Partek Genomic Suite and Partek Pathway, on generated CpG lists of statistical significance ($P < 0.05$) across conditions (ANOVA) or pairwise comparisons between conditions. In MiniTab Statistical Software (MiniTab Version 17.2.1) follow up rt-qRT-PCR gene expression was analysed using both a MANOVA, to detect for significant interactions across time for identified clusters of genes, and an ANOVA for follow up of individual genes over time. A pairwise t-test was used to analyse gene expression following acute RE vs. baseline. For follow up fold change in CpG DNA methylation analysis was performed via ANOVA in MiniTab Statistical Software (MiniTab Version 17.2.1). Statistical values were considered significant at the level of $P \leq 0.05$. All data represented as mean \pm SEM unless otherwise stated.

Results

Lean leg muscle mass is increased after loading, returns toward baseline during unloading and is further increased after reloading.

Analysis of lower limb lean mass via DEXA, identified a significant increase of 6.5% ($\pm 1.0\%$; $P = 0.013$) in lean mass after 7-wks of chronic loading compared to baseline (20.74 ± 1.11 kg loading vs. 19.47 ± 1.01 kg baseline). Following 7-wks of unloading, lean mass significantly reduced by $4.6\% \pm 0.6\%$ ($P = 0.02$) vs. the 7 weeks loading, back towards baseline levels (unloading, 19.83 ± 1.06 kg), confirmed by no significant difference between unloading and baseline. Subsequently, a significant increase in lean mass of the lower limbs was accrued after the reloading phase of $12.4 \pm 1.3\%$, compared to baseline (reloading, 21.85 ± 2.78 kg, $P = 0.001$, Fig. 1Ci), resulting in an increase of $5.9 \pm 1.0\%$ compared to the earlier period of loading ($P = 0.005$). Pairwise t-test analysis that corrected for any lean mass that was maintained during unloading demonstrated a significant increase in lean muscle mass in the reloading phase (unloading to reloading), compared to the loading phase (baseline to loading) ($P = 0.022$; Fig. 1Cii). Analysis of muscle strength suggested a similar trend. Isometric peak torque increased by $9.3 \pm 3.5\%$ from 296.2 ± 22.1 Nm at baseline to 324.5 ± 27.3 Nm after 7-wks of loading, this difference was not statistically significant (Supplementary Figure 2). Upon 7-wks of unloading, peak torque reduced by $8.3 \pm 2.8\%$ vs. loading, back towards baseline levels. Upon subsequent reloading, a significant $18 \pm 3.6\%$ increase in isometric peak torque production (349.6 ± 27.7 Nm) was observed compared to baseline ($P = 0.015$; Supplementary Figure 2A).

The largest DNA hypomethylation across the genome occurred following reloading. The frequency of statistically ($P < 0.05$) differentially regulated CpGs in each condition was analysed (Fig. 2A; Supplementary File 2B). 17,365 CpG sites were significantly ($P < 0.05$) differentially epigenetically modified following loading induced hypertrophy compared to baseline, with a larger number being hypomethylated (9,153)

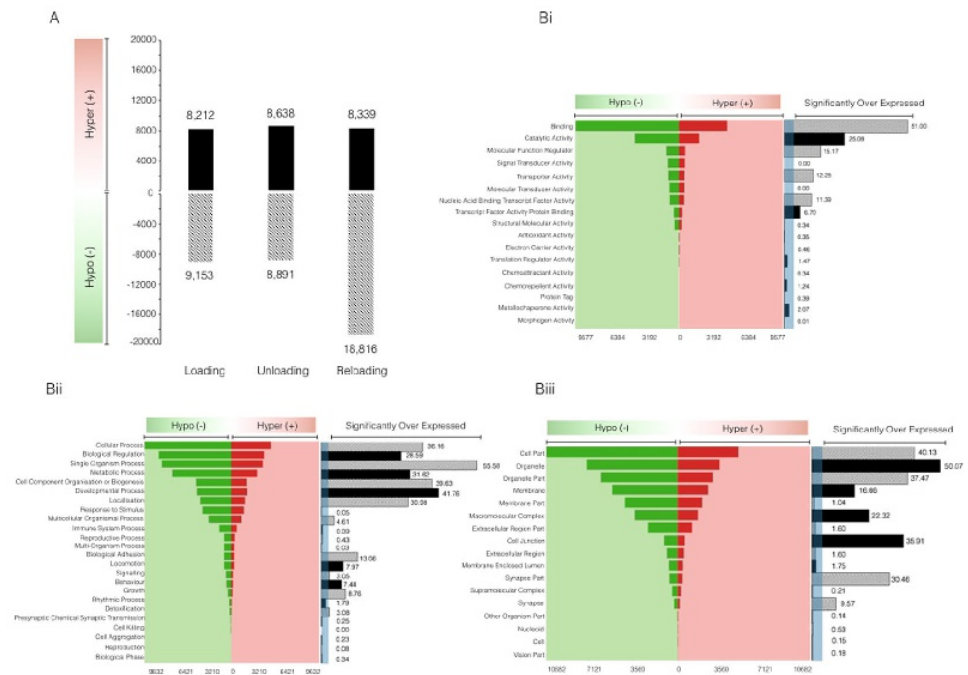


Figure 2. (A) Infinium MethylationEPIC BeadChip arrays (850 K CpG sites) identified an enhanced frequency of hypomethylated CpG sites upon reloading ($n = 7$). (B) Gene ontology analysis using forest plot schematics confirmed an enhanced hypomethylated profile after reloading across various (i) molecular function, (ii) biological processes and (iii) cellular components. Functional groups with a fold enrichment > 3 (as indicated via shaded blue region) represents statistically 'over expressed' (in this case epigenetically modified) KEGG pathways $FDR < 0.05$ ($n = 8$).

compared to hypermethylated (8,212) (Fig. 2A; Supplementary File 2A & B). The frequency of hypomethylated epigenetic modifications was similar to loading after unloading (8,891) (Fig. 2A; Supplementary File 2A & C), where we reported lean muscle mass returned back towards baseline. Importantly, following reloading induced muscle growth we observed an increase in the number of epigenetically modified sites (27,155) and an enhanced number of hypomethylated DNA sites (18,816, Fig. 2A; Supplementary File 2A & D). This increase in hypomethylation coincided with the largest increase in skeletal muscle mass in reloading. By contrast, hypermethylation remained stable (8,339) versus unloading (8,638) and initial loading (8,212). To further analyse the reported increased frequency of hypomethylated genes across the genome following reloading, gene ontologies were analysed for the frequency of hypo and hypermethylated CpG sites. In agreement with our above frequency analysis, the most statistically significant enriched GO terms identified an increased number of hypomethylated CpG sites compared to baseline (Fig. 2Bi–iii). Indeed, the most statistically significantly ($FDR < 0.05$) enriched GO terms were: 1) molecular function GO:0005488 encoding for genes related to 'binding', that displayed 9,577 (68.71%) CpG sites that were hypomethylated following reloading and 4,361 (31.29%) sites as hypermethylated compared to baseline (Fig. 2Bi), and; 2) Biological process GO:0044699 encoding for genes related to 'single-organism processes' that displayed 7,586 (68.57%) hypomethylated CpG sites compared to 3,493 (31.43%) sites profiled as hypermethylated after reloading compared to baseline (Fig. 2Bii). Finally, 3) cellular component, GO:004326 encoding for genes related to 'organelle' reported 7,301 hypomethylated CpG sites following reloading and 3,311 hypermethylated sites, compared to baseline, therefore favouring a majority 68.88% hypomethylated profile (Fig. 2Biii).

Following confirmation that the largest alteration in CpG DNA methylation occurred upon later reloading evoked hypertrophy, we sought to elucidate how the serine/threonine AKT signaling pathway, a critical pathway involved in mammalian growth, proliferation and protein synthesis^{26,27}, was differentially regulated across experimental conditions (Fig. 3, Supplementary Figure 3A and B). Intuitively, we report that the PI3K/AKT pathway was significantly enriched upon all pairwise comparisons of baseline vs. loading, unloading and reloading, respectively ($P < 0.022$; Supplementary Figure 3A, B and Fig. 3A), suggesting that the pathway was significantly epigenetically modified following periods of skeletal muscle perturbation. Importantly, frequency analysis of statistically differentially regulated transcripts (Fig. 3B) attributed to this pathway, reported an enhanced number of differentially regulated CpG sites (444 CpG sites) following reloading (Fig. 3A), compared to loading (264 CpG sites; Supplementary Figure 3A) and unloading (283 CpG sites; Supplementary Figure 3B) alone. In accordance with our previous findings, the enhanced number of statistically differentially regulated CpG sites in this pathway upon reloading is attributed to an enhanced number of hypomethylated (299 CpG sites, 67.3%) compared to hypermethylated (145 sites, 32.7%) CpG sites (Raw data: Supplementary File 3).

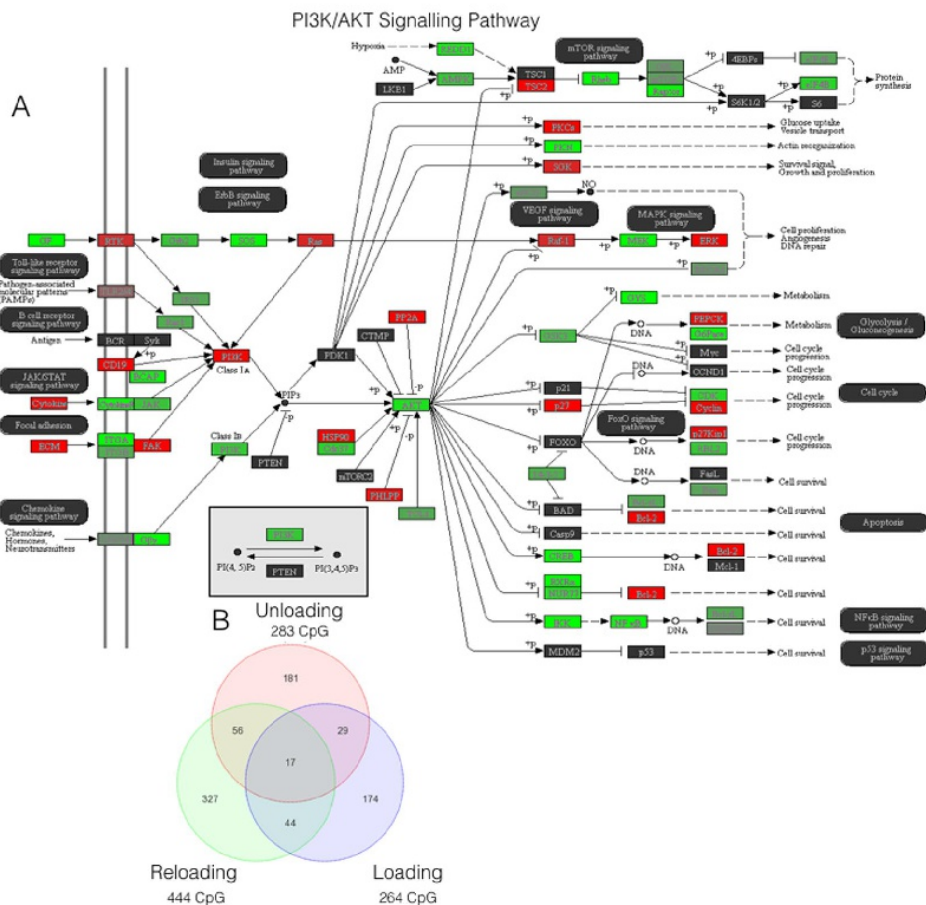


Figure 3. (A) Representation of the DNA methylation modifications that occurred within the PI3K/AKT KEGG pathway following 7 weeks of reloading in human subjects. Signalling analysis performed on statistically differentially regulated CpG sites compared to baseline, with green indicating a hypomethylated fold change and red indicating a hypermethylated change, with strength of colour representing the intensity of fold change^{23–25}. Figure 3b. Venn diagram analysis of the statistically differentially regulated CpG sites attributed to the PI3K/AKT pathway following loading, unloading and reloading, compared to be baseline. Ellipsis reports number of commonly statistically differentially regulated CpG sites across each condition. Analysis confirms an enhanced number of differentially regulated CpG sites upon reloading condition.

Genome-wide DNA methylation analysis identified two clusters of temporal DNA methylation patterns that provide initial evidence of an epigenetic memory. Changes in genome-wide DNA methylation were analysed following loading, unloading and reloading induced muscle adaptation. A dendrogram of the top 500 most statistically epigenetically modified CpG sites across each experimental condition compared to baseline, identified large alterations in DNA methylation profiles (Fig. 4A; Supplementary File 4A). A ranked unsupervised hierarchical clustering analysis demonstrated significant differences between the initial loading (weeks 1–7) vs. all other conditions (Fig. 4A). Closer analysis of the top 500 CpG sites across experimental conditions highlighted a clear temporal trend occurring within different gene clusters. The first cluster (named Cluster A) displayed enhanced hypomethylation with earlier loading-induced hypertrophy. This cluster was methylated at baseline and became hypomethylated after loading, re-methylated with unloading (Fig. 4A) and hypomethylated after reloading. The second temporal trend (named Cluster B) also displayed an enhanced hypomethylated state across the top 500 CpG sites as a result of load induced hypertrophy. As with Cluster A, Cluster B genes were methylated at baseline and became hypomethylated after initial loading. In contrast to Cluster A, Cluster B remained hypomethylated with unloading, even when muscle returned to baseline levels, and this hypomethylation was also maintained/‘remembered’ after reload induced hypertrophy (Cluster B, depicted Fig. 4A). The third temporal trend, named Cluster C, revealed genes as hypomethylated at both baseline and after initial loading, suggesting no epigenetic modification after the first period of hypertrophy in these genes (Cluster C, Fig. 4A). During unloading, genes were hypermethylated and remained in this state during reloading. The final cluster (Cluster D) of genes, were hypomethylated at baseline, became hypermethylated after loading (Cluster D, Fig. 4A), reverted back to a hypomethylated state with

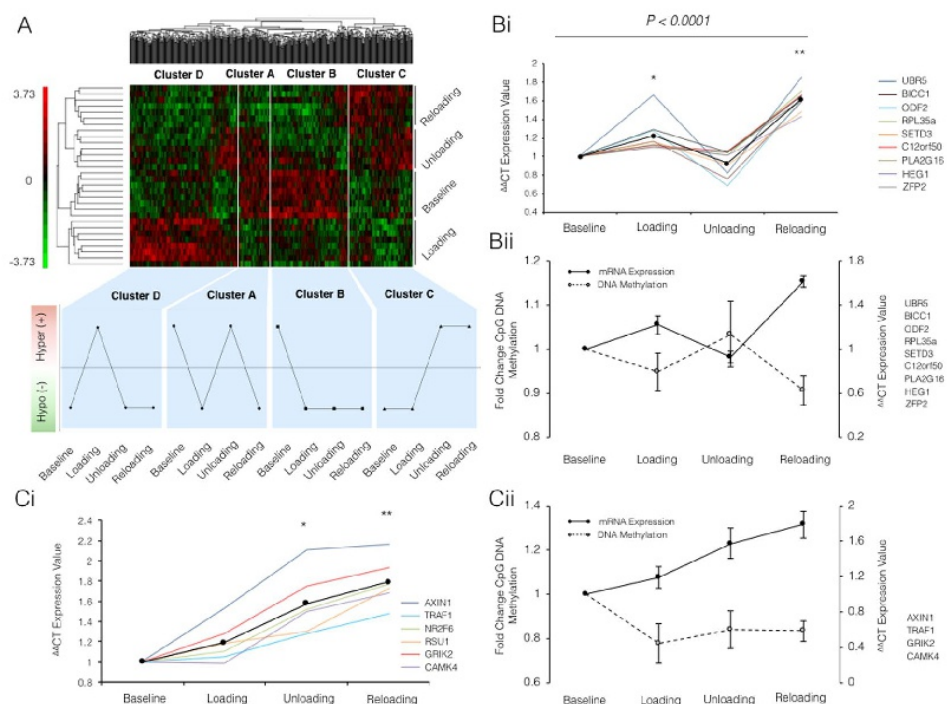


Figure 4. (A) Heat map depicting unsupervised hierarchical clustering of the top 500 statistically differentially regulated CpG loci (columns) and conditions (baseline, loading, unloading and reloading) in previously untrained male participants ($n = 8$). The heat-map colours correspond to standardised expression normalised β -values, with green representing hypomethylation, red hypermethylation and unchanged sites are represented in black. (4B and C) Relative gene expression (i) and schematic representation of CpG DNA methylation and gene expression relationship (ii) in two identified gene clusters from genome wide methylation analysis after a period of 7 weeks resistance exercise (loading), exercise cessation (unloading) and a subsequent secondary period of 7 weeks resistance exercise (reloading). (Bi) Expression of genes that displayed a significant increase compared to baseline (represented by *) upon earlier loading, that returned to baseline during unloading, and displayed enhanced expression after reloading (significantly different to all other conditions **). MANOVA analysis reported a significant effect over the entire time course of the experiment ($P < 0.0001$). (Bii) Representative schematic displaying the inverse relationship between mean gene expression (solid black lines) and CpG DNA methylation (dashed black lines) of grouped transcripts (RPL35a, C12orf50, BICC1, ZFP2, UBR5, HEG1, PLA2G16, SETD3 and ODF2). Data represented as fold change for DNA methylation (left y axis) and gene/mRNA expression (right y axis). (Ci) Clustering of genes that portrayed an accumulative increase in gene expression after loading, unloading and reloading. With the largest increase in gene expression after reloading. Culminating in significance in the unloading (baseline vs. unloading*), and reloading (reloading vs. baseline**). (Cii) Representative schematic displaying the inverse relationship between mean gene expression (solid black lines) and CpG DNA methylation (dashed black lines) of grouped transcripts (AXIN1, TRAF1, GRIK2, CAMK4). All data represented as mean \pm SEM for gene expression ($n = 7$ for UBR5, PLA2G16, AXIN1, GRIK2; $n = 8$ for all others) and CpG DNA methylation ($n = 8$ for baseline, loading and unloading; $n = 7$ for reloading).

unloading and then maintained the hypomethylated state after reloading, reflecting the profile of the baseline targets in the same cluster (Cluster D, Fig. 4A). These two clusters (C&D) did report a maintenance of the DNA methylation profile from unloading to reloading conditions. Cluster C also reported a hypermethylated profile after unloading following a period of loading, that may therefore identify important CpG sites that are hypermethylated when muscle mass is reduced (we therefore include a full list from cluster C that includes the CpG sites significantly modified in loading vs. unloading, Supplementary File 4G). However, both Cluster C&D suggest no retention of epigenetic modifications from the first loading period to the later reloading phase.

Identification of gene expression clusters inversely associated with DNA methylation. To assess whether the changes in DNA methylation affected gene expression, the 100 most significantly differentially modified CpG sites across all conditions were identified and cross referenced with the most frequently occurring (Supplementary File 4B) CpG modifications in pairwise comparisons of all conditions (Supplementary File 4C to H). This identified 48 genes that were then analysed by rt-qRT-PCR to assess gene expression. Forty-six percent of the

top 100 CpG sites were within gene promoter regions with 18% residing in intergenic regions (Supplementary File 5). Interestingly, gene expression analysis identified two distinct clusters of genes that had different transcript profiles. This first cluster included RPL35a, C12orf50, BICC1, ZFP2, UBR5, HEG1, PLA2G16, SETD3 and ODF2 genes that displayed a significant main effect for time ($P < 0.0001$) after MANOVA analysis (Fig. 4Bi). Chromosome locations, reference sequence numbers and gene region section details for these genes can be found in Supplementary File 5. Importantly, this first cluster displayed a mirrored (inverse) temporal pattern to those identified previously in Cluster A above for CpG methylation (in the top 500 differentially regulated CpG sites, Fig. 4A). Where, upon 7-wks of loading, gene expression of this cluster significantly increased (1.22 ± 0.09 , $P = 0.004$) and CpG methylation of the same genes was non-significantly reduced (hypomethylated) (0.95 ± 0.04 Fig. 4Bii). During unloading, methylation returned to baseline (1.03 ± 0.07), which was met by a return to baseline in gene expression (0.93 ± 0.05), as indicated by both CpG methylation and gene expression displaying no significant difference compared to baseline (Fig. 4Bii). Importantly, upon reloading, both CpG methylation and gene expression displayed an enhanced response compared to the baseline and loading time point, respectively. Indeed, upon reloading, this cluster became hypomethylated (0.91 ± 0.03 , $P = 0.05$, Fig. 4Bii). This was met with a significant enhancement (1.61 ± 0.06) in gene expression of the same cluster compared to baseline and loading ($P < 0.001$, Fig. 4Bii).

A second separate gene cluster was identified and included: AXIN1, GRIK2, CAMK4, TRAF1, NR2F6 and RSU1. Although together there was no significant effect of time via MANOVA analysis. ANOVA analysis reported that this cluster displayed increased gene expression after loading (1.19 ± 0.08) that then further increased during unloading (1.58 ± 0.13) resulting in statistical significance ($P = 0.001$) compared to baseline alone. Gene expression was then even further enhanced (1.79 ± 0.09) upon reload induced hypertrophy ($P < 0.0001$; Fig. 4Ci; Chromosome locations, reference sequence numbers, region section details for this cluster of genes can be found in Supplementary File 5). In this cluster we identified an accumulative increase in gene expression, attaining significance at unloading condition (ANOVA; $P = 0.001$) compared to baseline, gene expression was subsequently further increased following reloading conditions (ANOVA; $P < 0.0001$). This temporal gene expression pattern was inversely associated to CpG methylation observed in Cluster B (identified previously in the top 500 differentially regulated CpG sites, Fig. 4A). Closer fold-change analysis of CpG DNA methylation of this gene cluster, identified a distinct inverse relationship with methylation and gene expression of 4 out of 6 of the targets (AXIN1, GRIK2, CAMK4, TRAF1). Where, upon loading, these genes became significantly hypomethylated (0.78 ± 0.09 ; $P = 0.036$) compared to baseline, with this profile being maintained during unloading (0.84 ± 0.09) and reloading (0.83 ± 0.05) conditions, albeit non-significantly. Collectively, we report that a sustained hypomethylated state in 4 out of 6 of the genes in this cluster that correspond to an increased transcript expression of the same genes (Fig. 4Cii).

Identification of a number of novel genes at the expression level associated with skeletal muscle hypertrophy. To ascertain the relationship between skeletal muscle hypertrophy and gene expression, fold change in gene expression was plotted against percentage changes (to baseline) in leg lean mass. Interestingly, in our first cluster of genes identified above (RPL35a, C12orf50, BICC1, ZFP2, UBR5, HEG1, PLA2G16, SETD3 and ODF2), a significant correlation between gene expression and lean mass was observed for genes RPL35a, UBR5, SETD3, PLA2G16 and HEG1 (Fig. 5A & BI–V). Following exposure to 7-wks of load induced hypertrophy, RPL35a gene expression displayed a non-significant increase compared to baseline (1.13 ± 0.23 ; Fig. 5AI), that upon unloading returned back to the baseline levels (1.01 ± 0.21). Upon reloading, the expression of RPL35a increased to $1.70 (\pm 0.44$; Fig. 5AI) compared to baseline ($P = 0.05$). This expression pattern across loading, unloading and reloading conditions corresponded to a significant correlation with percentage changes in skeletal muscle mass ($R = 0.6$, $P = 0.014$; Fig. 5BI), with RPL35a accounting for 36% of the variation in muscle across experimental conditions. Both UBR5 and SETD3 displayed similar percentage accountability for the change in skeletal muscle mass across conditions. Indeed, UBR5 and SETD3 accounted for 33.64% and 32.49% of the variability in skeletal muscle mass, respectively, both portraying strong correlations between their gene expression and the percentage change in lean leg mass (UBR5, $R = 0.58$, $P = 0.018$, Fig. 5BII; SETD3, $R = 0.57$, $P = 0.013$, Fig. 5BII, respectively). Additionally, UBR5 (1.65 ± 0.4 ; Fig. 5BII) and SETD3 (1.16 ± 0.2 ; Fig. 5AIII) both demonstrated non-significant increases in gene expression after 7-wks of loading ($P > 0.05$), with the expression of both genes, UBR5 (0.82 ± 0.27) and SETD3 (0.90 ± 0.15), returning to baseline levels upon 7-wks of unloading (Fig. 5AII and AIII, respectively). Furthermore, upon reloading UBR5 displayed its greatest increase in expression (1.84 ± 0.5 ; Fig. 5AII), demonstrating a trend for significance compared to baseline condition ($P = 0.07$), and a significant increase compared to unloading ($P = 0.035$). Whereas, SETD3 demonstrated a fold increase of $1.48 (\pm 0.25$; Fig. 5AIII) approaching significance compared to baseline ($P = 0.072$) and achieving significance compared to unloading ($P = 0.036$). PLA2G16 also demonstrated a significant correlation between its fold change in gene expression and the percentage change in skeletal muscle mass ($R = 0.55$; $P = 0.027$; Fig. 5BIV), with PLA2G16 accounting for 30.25% of the change in skeletal muscle. Interestingly, across conditions, PLA2G16 demonstrated the greatest significant changes in gene expression. Indeed, loading induced hypertrophy, PLA2G16 displayed a non-significant increase compared to baseline in expression (1.09 ± 0.17 ; Fig. 5AIV), that upon unloading returned back to the baseline levels (1.04 ± 0.25). Importantly, upon reloading, the expression of PLA2G16 significantly increased (1.60 ± 0.18 ; Fig. 5AIV) compared to baseline ($P = 0.026$) and unloading conditions ($P = 0.046$), as well as approaching a significant increase compared to the initial loading stimulus ($P = 0.067$ compared to load; Fig. 5AIV). HEG 1 gene expression exhibited a significant correlation with skeletal muscle mass ($R = 0.53$, $P = 0.05$) with HEG 1 accounting for 28.09% of the changes in muscle mass. However, HEG1 did not demonstrate any significant fold changes in gene expression across the experimental conditions. Furthermore, no significant correlation was observed for the other identified cluster of genes (AXIN1, GRIK2, CAMK4, TRAF1, NR2F6 and RSU1; $P > 0.05$; Data not shown). Collectively, these data suggest that RPL35a, UBR5, SETD3 and PLA2G16 all display a significantly enhanced gene expression upon reloading induced hypertrophy. This suggests, that these genes portray a memory of earlier load induced hypertrophy, by displaying the largest fold increases in gene expression after reload induced growth.

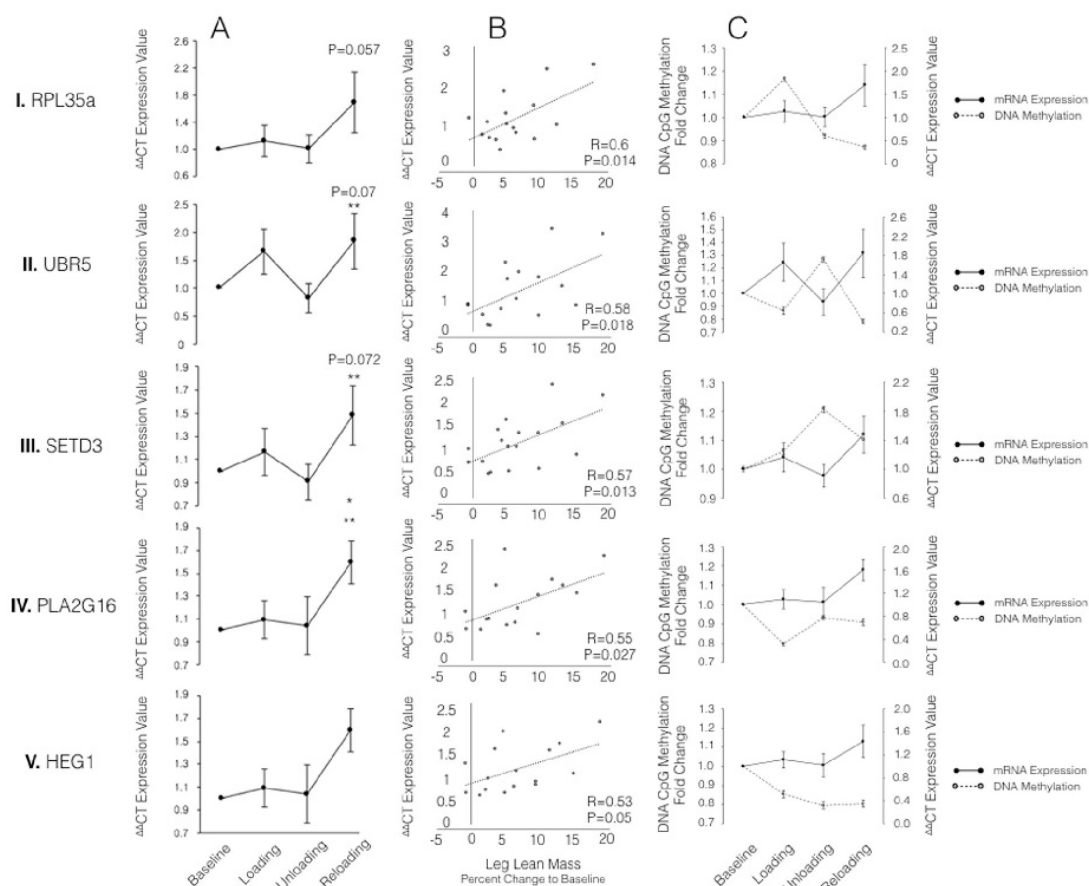


Figure 5. Relative fold changes in: (A) gene expression; (B) correlation between gene expression and lower limb lean mass across experimental conditions, and; (C) schematic representation of relationship between fold changes in CpG DNA methylation (dashed black line; left y axis) and fold change in gene/mRNA expression (solid black line; right y axis) for identified genes: RPL35a (I), UBR5 (II), SETD3 (III), PLA2G16 (IV) and HEG1 (V). Statistical significance compared to baseline and unloading represented by* and** respectively. All significance taken as p less than or equal to 0.05 unless otherwise state on graph. All data presented as mean \pm SEM (n = 7/8).

The E3 Ubiquitin Ligase, UBR5, has enhanced hypomethylation and the largest increase in gene expression during reloading. The HECT E3 ubiquitin ligase gene UBR5 (Fig. 6), for which the CpG identified is located on chromosome 8 (start 103424372) in the promoter region 546 bp from the transcription start site, was identified as being within the top 100 most statistically differentially regulated CpG sites across all pair-wise conditions (loading, unloading and reloading; Fig. 6); but also the transcript that displayed the most distinctive mirrored-inverse relationship with gene expression (Fig. 5CII), after every condition. Following the initial period of 7-weeks of load induced hypertrophy, there was a non-significant increase in UBR5 gene expression (1.65 ± 0.4) versus baseline, which was met with a concomitant (albeit non-significant) reduction in CpG DNA methylation (0.87 ± 0.03). Gene expression returned to baseline control levels after unloading (0.82 ± 0.27) demonstrated by a significant reduction vs. loading ($P = 0.05$) and non-significance versus baseline ($P = \text{N.S.}$; Fig. 5CII). After the same unloading condition, we observed a significant increase in CpG DNA methylation compared to baseline (1.27 ± 0.02 ; $P = 0.013$; Fig. 5CII). Importantly, upon reloading, UBR5 displayed its largest increase in transcript expression, significantly greater compared to unloading (1.84 ± 0.5 vs. 0.82 ± 0.27 , $P = 0.035$) and versus baseline levels to the level of $P = 0.07$. Concomitantly, after the reloading condition, we observed the largest statistically significant reduction in CpG DNA methylation (0.78 ± 0.02) compared to baseline ($P = 0.039$), and unloading ($P \leq 0.05$; Fig. 5CII).

Dynamic changes in DNA methylation after a single acute bout of resistance exercise precede changes in gene expression after loading and reloading. We next wished to ascertain how dynamic and transient DNA methylation of the identified genes were, after a single acute bout of resistance exercise (acute RE).

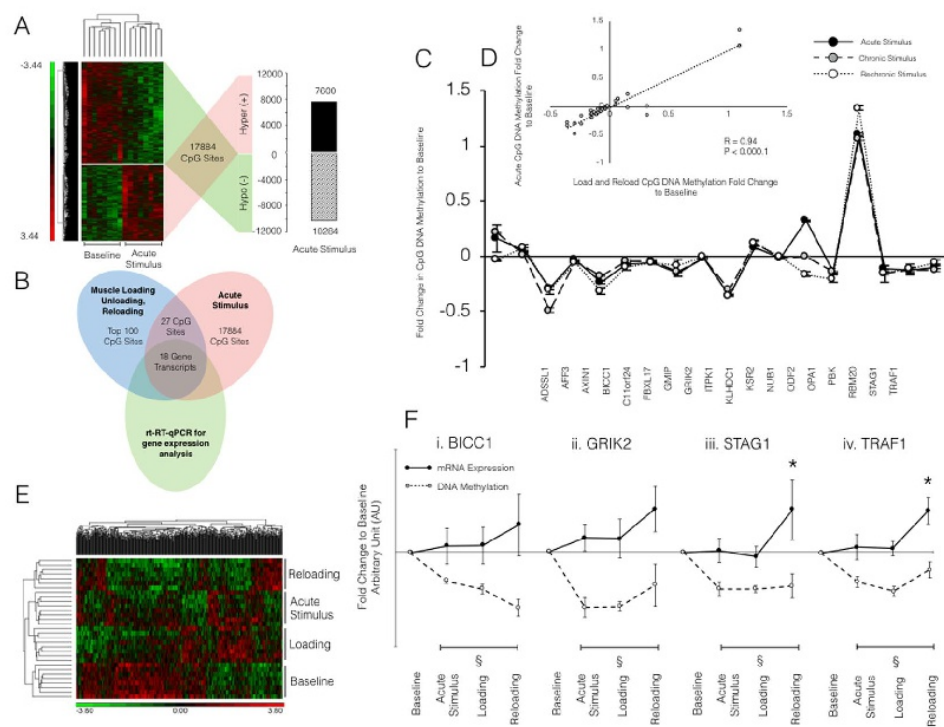


Figure 7. Response of the methylome after acute resistance loading stimulus compared to baseline, 7 weeks loading and 7 weeks reloading: (A) Heat map depicting unsupervised hierarchical clustering of statistically differentially regulated ($P = 0.05$) CpG loci following exposure to acute RE compared to baseline; (B) a Venn diagram depicting the number of CpG sites that were significantly differentially regulated in both methylome analysis experiments (base, loading, unloading and reloading, blue circle; baseline and acute resistance stimulus, red circle), and the amount of genes analysed for gene expression across acute, 7 weeks loading and 7 weeks reloading, respectively; (C) temporal pattern of fold change in DNA CpG methylation of the identified overlapping CpG sites that mapped to relevant gene transcripts; (D) correlation of CpG DNA methylation of acute RE vs. 7 weeks loading and reloading conditions, and (E) Heat map depicting unsupervised hierarchical clustering of statistically differentially regulated ($P = 0.05$) CpG loci following exposure to acute RE compared to baseline, loading and reloading (F) representative schematic displaying the inverse relationship between mean gene expression (solid black lines) and CpG DNA methylation (dashed black lines) of identified transcripts. Significance indicated in gene expression (*) and in CpG DNA methylation (§) when compared to baseline.

during chronic loading, unloading and subsequent reloading conditions. Finally, we analysed fold changes in gene expression of a sub set of the 18 CpG sites identified as overlapping in both sets of methylome analysis experiments (Supplementary Figure 4a) and compared changes in gene expression to changes in CpG DNA methylation (Supplementary Figure 4B). We identified that significant hypomethylation upon acute resistance exercise (Figure 7Fi–vii) was not associated with significant changes in gene expression (Figure 7Fi–vii) in a sub-set of analysed transcripts. However, upon continued loading (chronic loading and reloading conditions), changes in CpG DNA methylation were associated with significant changes in a number of these genes upon the reloading stimulus (Figure 7Fi–vii). Suggesting that these newly identified epigenetically regulated genes (BICC1, GRIK2, TRAF1 and STAG1) were acutely sensitive to hypomethylation after a single bout of resistance exercise, that enhanced gene expression 22 weeks after a period of load induced hypertrophy, a return of muscle to baseline and later reloading induced hypertrophy. Therefore, the epigenetic regulation of these genes seems to be an early, acute exercise biomarker of later muscle hypertrophy.

Discussion

Frequency of genome-wide hypomethylation is the largest after reloading induced hypertrophy where lean muscle mass is enhanced. We aimed to investigate an epigenetic memory of earlier hypertrophy in adult human skeletal muscle using a within measures design, by undertaking: (1) resistance exercise induced muscle growth (loading), followed by; (2) cessation of resistance exercise, to return muscle back towards baseline levels (unloading), and; (3) a subsequent later period of resistance exercise induced muscle hypertrophy (reloading). We first confirmed that we were able to elicit an increase in lean mass of the lower limbs after 7 weeks loading, that returned back to baseline levels after 7 weeks unloading, with 7 weeks reloading evoking the largest

increase in lean mass. Interestingly, after DNA methylation analysis of over 850,000 CpG sites, we identified the largest frequency of hypomethylation (18,816 CpG sites) occurred after reloading where the largest lean mass occurred. Previous studies have suggested that hypermethylation of over 6,500 genes are retained, after an more acute stress of high fat intake (for 5 days) 8 weeks later despite removal of the high fat diet¹⁴, and hypermethylation occurs following early life inflammatory stress in muscle cells and is maintained for over 30 cellular divisions¹¹. The present study also suggested hypomethylation was maintained during unloading (8,891 CpG sites) where muscle mass returned to baseline having being subjected to an earlier period of load induced muscle growth (9,153 CpG sites), then upon reloading the frequency of hypomethylation was enhanced in association with the largest increases in lean mass. Furthermore, bioinformatic analysis of the PI3K/AKT pathway across loading, unloading and reloading conditions, supports the findings of an enhanced hypomethylated state upon secondary exposure to resistance stimulus. Importantly, this pathway is identified as critical for cell proliferation/differentiation, muscle protein synthesis and therefore muscle hypertrophy²⁷, and therefore, it is plausible that the enhanced hypomethylated state of the genes in this pathways would lead to enhanced gene expression and protein levels. However, further analysis is required to investigate the total protein or activity of these pathways in this model. Nonetheless, collectively, these results provide initial evidence for a maintenance/memory of universal hypomethylation. The only other study to demonstrate a memory of prior hypertrophy in skeletal muscle was in rodents following earlier encounters with testosterone administration, where a retention of myonuclei occurred even during testosterone withdrawal and a return of muscle to baseline levels¹³, suggesting a memory at the cellular level. However, these are the first studies to demonstrate that a memory occurs at the epigenetic level within skeletal muscle tissue.

Hypomethylation is maintained from earlier load induced hypertrophy even during unloading where muscle mass returns back towards baseline and is inversely associated with gene expression.

Following the frequency analysis of hypo/hypermethylated sites mentioned above, closer analysis of the top 500 most significantly differentially modified CpG sites across all conditions, identified two epigenetically modified clusters of interest (named Cluster A&B). Cluster B supported the frequency analysis above and demonstrated hypomethylation after load induced hypertrophy that was then maintained following unloading where muscle returned to baseline levels and this hypomethylation was then also maintained after reload induced hypertrophy. This maintenance of hypomethylation during unloading, suggested that the muscle ‘remembered’ the epigenetic modifications that occurred after an earlier period of load induced muscle hypertrophy. As reduced DNA methylation of genes generally leads to enhanced gene expression due to the removal of methylation allowing improved access of the transcriptional machinery and RNA polymerase that enable transcription, and also creating permissive euchromatin^{19,28–30}, this would be suggestive that the earlier period of hypertrophy leads to increased gene expression of this cluster of genes that is then retained during unloading to enable enhanced muscle growth in the later reloading period. To confirm this, in a separate analysis we identified the top 100 most significantly differentially modified CpG sites across all conditions and cross referenced these with the most frequently occurring CpG modifications in all pairwise comparisons of experimental conditions. From this we identified 48 genes that were frequently occurring in all pairwise comparisons and examined gene expression by rt-qRT-PCR. Interestingly, we identified two clusters of genes with distinct temporal expression after loading, unloading and reloading. One of the clusters included AXIN1, GRIK2, CAMK4, TRAF1. Importantly, the majority of these genes demonstrated a mirror/inverse relationship with DNA methylation of the CpG sites within the same genes. Where DNA methylation reduced after loading and remained low into unloading and reloading, gene expression accumulated, demonstrating the highest expression after reloading where the largest increase in lean mass was also demonstrated. Overall, this suggested that these genes were hypomethylated and switched on after the earlier period of load induced hypertrophy, maintained during unloading due to methylation of these genes remaining low, and then upon exposure to a later period of reload induced hypertrophy, these genes were switched on to an even greater extent. Overall, this demonstrates that the methylation and collective responsiveness of these genes are important epigenetic regulators of skeletal muscle memory.

Interestingly, AXIN1 is a component of the beta-catenin destruction complex, where in skeletal muscle cells AXIN1 has been shown to inhibit WNT/ β -catenin signalling and enable differentiation³¹, where treatment with the canonical WNT ligand suppresses differentiation³². Other studies suggested that AXIN2 not AXIN1 is increased after differentiation, however confirmed that the absence of AXIN1 reduced proliferation and myotube formation³². Therefore, together with the present data perhaps suggest an important epigenetic regulation of AXIN1 involved in human skeletal muscle memory and hypertrophy at the tissue level, perhaps due to inhibition of WNT/ β -catenin signaling. GRIK2 (glutamate ionotropic receptor kainate type subunit 2, a.k.a. GluK2) belongs to the kainate family of glutamate receptors, which are composed of four subunits and function as ligand-activated ion channels³³. Although reportedly expressed in skeletal muscle, its role in muscle growth or cellular function has not been determined. CAMK4 is calcium/calmodulin-dependent protein kinase, that via phosphorylation, triggers the CaMKK-CaMK4 signaling cascade and activates several transcription factors, such as MEF2³⁴. MEF2 has been previously associated with a switch to slow fibre types after exercise³⁵ and is hypomethylated after 6 months aerobic exercise³⁶. While resistance exercise has been show to preferentially increase the size of type II faster fibres, chronic innervation even at higher loads can lead to an overall slowing in phenotype [reviewed in ref.³⁷] and therefore this epigenetically regulated gene, although not usually studied during hypertrophy maybe important in fibre type changes in the present study. However, it is unknown how DNA methylation affects the protein levels of CAMK4, and with its role in phosphorylation, would be important to ascertain in the future. Furthermore, fibre type properties were not analyzed in the present study and therefore require further investigation. TRAF1 is the TNF receptor-associated factor 1 and together with TRAF2 form the heterodimeric complex required for TNF- α activation of MAPKs, JNK and NF κ B³⁸. In skeletal muscle, acute TNF exposure activates proliferation via activation of MAPKs such as ERK and P38 MAPK^{39–41}. Therefore, acutely elevated systemic TNF- α following

damaging exercise such as resistance exercise correlates positively with satellite cell activation *in-vivo* after damaging exercise^{42,43}, yet chronic administration *in-vitro* inhibits differentiation, promotes myotube atrophy^{40,44} and muscle wasting *in-vivo*⁴⁴. Indeed, exposure to early life TNF- α during an early proliferative age in mouse C2C12s results in maintenance of hypermethylation in the myoD promoter after 30 divisions and an increased susceptibility to reduced differentiation and myotube atrophy when muscle cells encounter TNF- α in later proliferative life¹¹. Suggesting a role for DNA methylation in retention of memory following earlier periods of high inflammation. Because resistance exercise evokes increases in TNF- α in the systemic circulation and has been shown increase locally in muscle at the protein level (discussed above), these data collectively suggest an interesting epigenetic role for TNF and TRAF1 in the epigenetic memory of earlier load induced muscle hypertrophy.

Identification of novel genes with the largest hypomethylation during reloading that are associated with enhanced gene expression.

The second DNA methylation cluster determined in the top 500 differentially modified CpG sites across all conditions, identified a cluster of genes (named Cluster A) that was methylated at baseline and also became hypomethylated after loading (similar to Cluster B above), then, upon unloading, genes reverted back to a methylated state, and after reloading switched back to hypomethylated. Therefore, while not demonstrating an epigenetic memory per se, if hypomethylation was further enhanced and was associated with enhanced gene expression in reloading versus loading would also support an epigenetic memory. Further gene expression analysis identified a cluster of genes that demonstrated a mirror/inverse temporal pattern of gene expression versus their DNA methylation pattern. These genes included RPL35a, C12orf50, BICC1, ZFP2, UBR5, HEG1, PLA2G16, SETD3 and ODF2, that demonstrated hypomethylation of DNA after load induced growth and an increase in gene expression. Subsequently, then both DNA methylation and gene expression returned back to baseline levels (in opposite directions) and after reload induced muscle growth DNA was hypomethylated again with an associated increase in gene expression. Importantly, during reloading, gene expression was further enhanced versus loading, suggesting that an earlier period of load induced growth was enough to produce enhanced gene expression when reload induced muscle growth was encountered later, again suggesting a skeletal muscle memory at both the epigenetic and resultant transcript level. Statistical analysis identified the genes RPL35a, UBR5, SETD3 and PLA2G16 as having significantly enhanced expression upon reloading. Importantly, these four genes, plus HEG1, displayed significant correlations between their gene expression and the percentage change in lean mass, suggesting for the first time, a role for these four genes in regulating adult human load induced skeletal muscle growth. Interestingly, SET Domain Containing 3 (SETD3) is a H3K4/H3K36 methyltransferase, is abundant in skeletal muscle, and has been shown to be recruited to the myogenin promoter, with MyoD, to promote its expression⁴⁵. Furthermore, overexpression of SETD3 in C2C12 murine myoblasts, evokes increases in myogenin, muscle creatine kinase, and Myf6 (or MRF4) gene expression. Inhibition via shRNA in a myoblasts also impairs muscle cell differentiation⁴⁵, suggesting a role for SETD3 in regulating skeletal muscle regeneration. However, less is known regarding the role of PLA2G16 in skeletal muscle. PLA2G16 is a member of the superfamily of phospholipase A enzymes, whose predominant localization is in adipose tissue. PLA2G16 is known to regulate adipocyte lipolysis in an autocrine/paracrine manner, via interactions with prostaglandin and EP3 in a G-protein-mediated pathway⁴⁶. Indeed, ablation of PLA2G16 (referred to as Adpla), prevents obesity during periods high fat feeding in mouse models, indicated via significantly less adipose tissue and triglyceride content, compared to relevant controls⁴⁶. However, to date no known research has elucidated the role of PLA2G16 in skeletal muscle and therefore, this requires future experimentation. Finally, HEG1 homology 1 (HEG1), initially reported as the *heart of glass* gene, is recognised for its role in regulating the zebrafish heart growth. HEG1 is a transmembrane receptor that has been reported to be fundamental in the development of both the heart and blood vessels⁴⁷. However, a recent study reported a distinct role for HEG1 in regulating malignant cell growth⁴⁸. Tsuji, *et al.*⁴⁸ and colleagues reported that gene silencing of HEG1 in human MPM cell line, a cell lineage that develop mesothelioma tumours, significantly reduced the survival and proliferation of mesothelioma cells, suggesting a role for HEG1 in regulating cellular growth. However, no known research has examined the role of HEG1 in regulating adult skeletal muscle growth.

In the present study UBR5 displayed the most distinctive inverse relationship between DNA hypomethylation and increased gene expression following loading and reloading. With the largest increase in hypomethylation and gene expression after reloading where the largest increase in lean mass was observed. UBR5 is a highly conserved homologue of the drosophila tumour suppressor hyperplastic discs (HYD), and in the mammalian genome refers to a protein that is a member of the HECT-domain E3 ubiquitin-ligase family⁴⁹. E3 ubiquitin ligases play an integral role in the ubiquitin - proteasome pathway, providing the majority of substrate recognition for the attachment of ubiquitin molecules onto targeted proteins, preferentially modifying them for targeted autophagy/breakdown⁵⁰. Indeed, extensive work has identified a distinct role of a number of E3 ubiquitin ligases such as MuRF1, MAFbx and MUSA1 in muscle atrophy^{51,52}. Furthermore, we have recently demonstrated that reduced DNA methylation and increased gene expression of MuRF1 and MAFbx are associated with disuse atrophy in rats following nerve silencing of the hind limbs via tetrodotoxin exposure¹⁷. A process that is reversed upon a return to habitual physical activity and a partial recovery of skeletal muscle mass¹⁷, suggesting a role for DNA methylation in regulating the transcript behavior of a number of ubiquitin ligases during periods of skeletal muscle atrophy and recovery. However, there have been no studies that the authors are aware of, examining the role of UBR5 in skeletal muscle atrophy or growth. Given the role of ubiquitin ligases in skeletal muscle, counterintuitively, we report that the expression of the E3 ubiquitin ligase, UBR5, is increased during earlier periods of skeletal muscle hypertrophy and are even further enhanced in later reload induced muscle growth. We further report that the methylation profile of this E3 ubiquitin ligase portrays an inversed relationship with gene expression, supporting a role for DNA epigenetic modifications in regulating its expression, as previously suggested¹⁷. However, in support of its role in positively impacting on muscle, UBR5 has also been shown to promote smooth muscle

differentiation through its ability to stabilize myocardin proteins⁵³. While myocardin is only expressed in smooth and cardiac muscle, it is considered the master regulator of smooth muscle gene expression⁵⁴ and a known transcription factor that upregulates smooth muscle myosin heavy chains (MYHCs), actin and desmin. It therefore possesses a similar role to the myogenic regulatory factors during early differentiation (Mrf5 and MyoD), during fusion (myogenin) and during myotube hypertrophy (adult MYHC's). Interestingly, it has previously been observed that myocardin-related transcription factors (MRTF) interact with the myogenic regulatory factor, MyoD, to activate skeletal muscle specific gene expression⁵⁵, suggesting a potential cross-talk between muscle specific regulatory factors, enabling skeletal muscle adaptations^{55,56}. Therefore, UBR5's expression throughout the time course of skeletal muscle cell differentiation, its role in myotube hypertrophy are required *in-vitro* as well as mammalian overexpression and knock-out of UBR5 to confirm its importance *in-vivo*. Further work is needed to characterize UBR5, as well as other HECT-domain E3 ubiquitin ligase protein members identified in this work via pathway analysis of the ubiquitin mediated proteolysis pathway, in the development of muscle growth to better understand its role in facilitating skeletal muscle hypertrophy.

A single bout of acute resistance exercise evokes hypomethylation of genes that have enhanced gene expression in later reload induced hypertrophy: Novel acutely exercise sensitive DNA methylation biomarkers.

Finally, we identified genes BICC1, STAG1, GRIK2 and TRAF1 were hypomethylated after a single bout of acute resistance exercise that were maintained as hypomethylated during loading (as identified above) and reloading and demonstrated an enhanced gene expression after later reloading. Previous studies have suggested that acute aerobic exercise hypomethylates important genes in metabolic adaptation and mitochondrial biogenesis such as PGC-1 α , mitochondrial transcription factor A (TFAM) and pyruvate dehydrogenase lipoamide kinase isozyme 4 (PDK4) post exercise, and reduces PPAR- δ methylation (hypomethylates) 3 hours post exercise¹⁶, with corresponding increases in gene expression (3 hrs post exercise for PGC-1 α , PDK4 and PPAR- δ , immediately post for TFAM)¹⁶. Interestingly, hypermethylation of PGC 1 α and reduced gene expression, observed in skeletal muscle of the offspring of obese murine mothers, was reversed (hypomethylated) by exercise in the mothers⁴. These data support the role for aerobic exercise in hypomethylating candidate genes. We also identify in the present study that hypomethylation (10,284 CpG sites) is favoured over hypermethylation (7,600 CpG sites) across the genome 30 minutes post an acute bout of resistance exercise, yet without changes in gene expression at this time point. Interestingly, however, hypomethylation of BICC1, STAG1, GRIK2 and TRAF1 after acute RE that was maintained after 7 weeks loading and reloading induced hypertrophy, resulted in significantly enhanced gene expression 22 weeks later. This suggested that DNA methylation of these genes after a single bout of resistance exercise were more sensitive biomarkers than their acutely corresponding gene expression for later load induced hypertrophy. BICC1 is an RNA binding protein that has an undermined role in adult skeletal muscle. It has been identified as differentially expressed during prenatal muscle development between two different pig breeds⁵⁷. RNA binding proteins in general are important in post transcriptional modifications, suggesting that perhaps reduced DNA methylation and increased gene expression may indicate an increase in post-transcriptional modification after reloading, however this requires further investigation to confirm. STAG1 (Cohesin subunit SA-1) is fundamental in cell division and part of the cohesin complex, which is required for the cohesion of sister chromatids after DNA replication⁵⁸. However, to the authors knowledge there is no specific role for STAG1 identified in adult skeletal muscle hypertrophy. GRIK2 and TRAF2 were also identified as being hypomethylated after loading and reloading together with enhanced gene expression. As suggested above, GRIK2's role in skeletal muscle is not well defined. However, TRAF1 has been widely implicated in skeletal muscle cell proliferation and differentiation, as discussed above, and hypomethylation of TRAF1 appears to be both sensitive to acute RE, as well as maintained following repeated loading and reloading induced hypertrophy that resulted in the largest increase in gene expression after reloading, 22 weeks after being detected as hypomethylated after acute RE. Overall, suggesting an important role for TRAF2 in skeletal muscles epigenetic memory of hypertrophy.

Conclusion

We identify that human skeletal muscle possesses an epigenetic memory of earlier acute and chronic anabolic stimuli when encountering later muscle hypertrophy.

References

1. Sharples, A. P., Stewart, C. E. & Seaborne, R. A. Does skeletal muscle have an 'epi'-memory? The role of epigenetics in nutritional programming, metabolic disease, aging and exercise. *Aging cell* **15**, 603–616, <https://doi.org/10.1111/acel.12486> (2016).
2. Patel, H. P. *et al.* Developmental influences, muscle morphology, and sarcopenia in community-dwelling older men. *J Gerontol A Biol Sci Med Sci* **67**, 82–87, <https://doi.org/10.1093/gerona/glr020> (2012).
3. Patel, H. P. *et al.* Lean mass, muscle strength and gene expression in community dwelling older men: findings from the Hertfordshire Sarcopenia Study (HSS). *Calcified tissue international* **95**, 308–316, <https://doi.org/10.1007/s00223-014-9894-z> (2014).
4. Laker, R. C. *et al.* Exercise prevents maternal high-fat diet-induced hypermethylation of the Pgc-1alpha gene and age-dependent metabolic dysfunction in the offspring. *Diabetes* **63**, 1605–1611, <https://doi.org/10.2337/db13-1614> (2014).
5. Zeng, Y., Gu, P., Liu, K. & Huang, P. Maternal protein restriction in rats leads to reduced PGC-1alpha expression via altered DNA methylation in skeletal muscle. *Molecular medicine reports* **7**, 306–312, <https://doi.org/10.3892/mmr.2012.1134> (2013).
6. Jaenisch, R. & Bird, A. Epigenetic regulation of gene expression: how the genome integrates intrinsic and environmental signals. *Nature genetics* **33**, Suppl, 245–254, <https://doi.org/10.1038/ng1089> (2003).
7. Green, C. J., Bunprajun, T., Pedersen, B. K. & Scheele, C. Physical activity is associated with retained muscle metabolism in human myotubes challenged with palmitate. *J Physiol* **591**, 4621–4635, <https://doi.org/10.1113/jphysiol.2013.251421> (2013).
8. Aguer, C. *et al.* Intramyocellular lipid accumulation is associated with permanent relocation *ex vivo* and *in vitro* of fatty acid translocase (FAT)/CD36 in obese patients. *Diabetologia* **53**, 1151–1163, <https://doi.org/10.1007/s00125-010-1708-x> (2010).
9. Maples, J. M. *et al.* Lipid exposure elicits differential responses in gene expression and DNA methylation in primary human skeletal muscle cells from severely obese women. *Physiological genomics* **47**, 139–146, <https://doi.org/10.1152/physiolgenomics.00065.2014> (2015).

10. Foulstone, E. J., Savage, P. B., Crown, A. L., Holly, J. M. & Stewart, C. E. Adaptations of the IGF system during malignancy: human skeletal muscle versus the systemic environment. *Horm Metab Res* **35**, 667–674, <https://doi.org/10.1055/s-2004-814159> (2003).
11. Sharples, A. P. *et al.* Skeletal muscle cells possess a 'memory' of acute early life TNF- α exposure: role of epigenetic adaptation. *Biogerontology* **17**, 603–617, <https://doi.org/10.1007/s10522-015-9604-x> (2016).
12. Egner, I. M., Bruusgaard, J. C., Eftestøl, E. & Gundersen, K. A cellular memory mechanism aids overload hypertrophy in muscle long after an episodic exposure to anabolic steroids. *The Journal of Physiology* **591**, 6221–6230, <https://doi.org/10.1113/jphysiol.2013.264457> (2013).
13. Bruusgaard, J. C., Johansen, I. B., Egner, I. M., Rana, Z. A. & Gundersen, K. Myonuclei acquired by overload exercise precede hypertrophy and are not lost on detraining. *Proc Natl Acad Sci USA* **107**, 15111–15116, <https://doi.org/10.1073/pnas.0913935107> (2010).
14. Jacobsen, S. C. *et al.* Effects of short-term high-fat overfeeding on genome-wide DNA methylation in the skeletal muscle of healthy young men. *Diabetologia* **55**, 3341–3349, <https://doi.org/10.1007/s00125-012-2717-8> (2012).
15. Barres, R. *et al.* Non-CpG methylation of the PGC- α promoter through DNMT3B controls mitochondrial density. *Cell Metab* **10**, 189–198, <https://doi.org/10.1016/j.cmet.2009.07.011> (2009).
16. Barres, R. *et al.* Acute exercise remodels promoter methylation in human skeletal muscle. *Cell Metab* **15**, 405–411, <https://doi.org/10.1016/j.cmet.2012.01.001> (2012).
17. Fisher, A. *et al.* Transcriptomic and Epigenetic Regulation of Disuse Atrophy and the Return to Activity in Skeletal Muscle. *Faseb J* **31**, 5268–5282, <https://doi.org/10.1096/fj.201700089RR> (2017).
18. Bigot, A. *et al.* Age-Associated Methylation Suppresses SPRY1, Leading to a Failure of Re- quiescence and Loss of the Reserve Stem Cell Pool in Elderly Muscle. *Cell reports* **13**, 1172–1182, <https://doi.org/10.1016/j.celrep.2015.09.067> (2015).
19. Bogdanovic, O. & Veenstra, G. J. DNA methylation and methyl-CpG binding proteins: developmental requirements and function. *Chromosoma* **118**, 549–565, <https://doi.org/10.1007/s00412-009-0221-9> (2009).
20. Peterson, M. D., Pistilli, E., Haff, G. G., Hoffman, E. P. & Gordon, P. M. Progression of volume load and muscular adaptation during resistance exercise. *European journal of applied physiology* **111**, 1063–1071, <https://doi.org/10.1007/s00421-010-1735-9> (2011).
21. Maksimovic, J., Gordon, L. & Oshlack, A. SWAN: Subset-quantile within array normalization for illumina infinium HumanMethylation450 BeadChips. *Genome biology* **13**, R44, <https://doi.org/10.1186/gb-2012-13-6-r44> (2012).
22. Pidsley, R. *et al.* Critical evaluation of the Illumina MethylationEPIC BeadChip microarray for whole-genome DNA methylation profiling. *Genome biology* **17**, 208, <https://doi.org/10.1186/s13059-016-1066-1> (2016).
23. Kanehisa, M. & Goto, S. KEGG: kyoto encyclopedia of genes and genomes. *Nucleic acids research* **28**, 27–30 (2000).
24. Kanehisa, M., Furumichi, M., Tanabe, M., Sato, Y. & Morishima, K. KEGG: new perspectives on genomes, pathways, diseases and drugs. *Nucleic acids research* **45**, D353–d361, <https://doi.org/10.1093/nar/gkw1092> (2017).
25. Kanehisa, M., Sato, Y., Kawashima, M., Furumichi, M. & Tanabe, M. KEGG as a reference resource for gene and protein annotation. *Nucleic acids research* **44**, D457–462, <https://doi.org/10.1093/nar/gkv1070> (2016).
26. Egerman, M. A. & Glass, D. J. Signaling pathways controlling skeletal muscle mass. *Critical Reviews in Biochemistry and Molecular Biology* **49**, 59–68, <https://doi.org/10.3109/10409238.2013.857291> (2014).
27. Schiaffino, S. & Mammucari, C. Regulation of skeletal muscle growth by the IGF1-Akt/PKB pathway: insights from genetic models. *Skeletal Muscle* **1**, 4, <https://doi.org/10.1186/2044-5040-1-4> (2011).
28. Fuks, F. *et al.* The methyl-CpG-binding protein MeCP2 links DNA methylation to histone methylation. *The Journal of biological chemistry* **278**, 4035–4040, <https://doi.org/10.1074/jbc.M210256200> (2003).
29. Lunyak, V. V. *et al.* Corepressor-dependent silencing of chromosomal regions encoding neuronal genes. *Science (New York, N.Y.)* **298**, 1747–1752, <https://doi.org/10.1126/science.1076469> (2002).
30. Rountree, M. R. & Selker, E. U. DNA methylation inhibits elongation but not initiation of transcription in *Neurospora crassa*. *Genes & development* **11**, 2383–2395 (1997).
31. Figeac, N. & Zammit, P. S. Coordinated action of Axin1 and Axin2 suppresses beta-catenin to regulate muscle stem cell function. *Cellular signalling* **27**, 1652–1665, <https://doi.org/10.1016/j.celsig.2015.03.025> (2015).
32. Huraskin, D. *et al.* Wnt/beta-catenin signaling via Axin2 is required for myogenesis and, together with YAP/Taz and Tead1, active in Ila/Iix muscle fibers. *Development* **143**, 3128–3142, <https://doi.org/10.1242/dev.139907> (2016).
33. Han, Y., Wang, C., Park, J. S. & Niu, L. Channel-opening kinetic mechanism for human wild-type GluK2 and the M867I mutant kainate receptor. *Biochemistry* **49**, 9207–9216, <https://doi.org/10.1021/bi100819v> (2010).
34. Blaeser, F., Ho, N., Prywes, R. & Chatila, T. A. Ca²⁺-dependent Gene Expression Mediated by MEF2 Transcription Factors. *Journal of Biological Chemistry* **275**, 197–209, <https://doi.org/10.1074/jbc.275.1.197> (2000).
35. Wu, H. *et al.* MEF2 responds to multiple calcium-regulated signals in the control of skeletal muscle fiber type. *Embo j* **19**, 1963–1973, <https://doi.org/10.1093/emboj/19.9.1963> (2000).
36. Nitert, M. D. *et al.* Impact of an exercise intervention on DNA methylation in skeletal muscle from first-degree relatives of patients with type 2 diabetes. *Diabetes* **61**, 3322–3332, <https://doi.org/10.2337/db11-1653> (2012).
37. Fry, A. C. The Role of Resistance Exercise Intensity on Muscle Fibre Adaptations. *Sports Medicine* **34**, 663–679, <https://doi.org/10.2165/00007256-200434100-00004> (2004).
38. Pomerantz, J. L. & Baltimore, D. NF- κ B activation by a signaling complex containing TRAF2, TANK and TBK1, a novel IKK-related kinase. *Embo j* **18**, 6694–6704, <https://doi.org/10.1093/emboj/18.23.6694> (1999).
39. Foulstone, E. J., Huser, C., Crown, A. L., Holly, J. M. & Stewart, C. E. Differential signalling mechanisms predisposing primary human skeletal muscle cells to altered proliferation and differentiation: roles of IGF-I and TNF α . *Exp Cell Res* **294**, 223–235, <https://doi.org/10.1016/j.yexcr.2003.10.034> (2004).
40. Girven, M. *et al.* l-glutamine Improves Skeletal Muscle Cell Differentiation and Prevents Myotube Atrophy After Cytokine (TNF- α) Stress Via Reduced p38 MAPK Signal Transduction. *Journal of cellular physiology* **231**, 2720–2732, <https://doi.org/10.1002/jcp.25380> (2016).
41. Li, Y. P. TNF- α is a mitogen in skeletal muscle. *Am J Physiol Cell Physiol* **285**, C370–376, <https://doi.org/10.1152/ajpcell.00453.2002> (2003).
42. Mackey, A. L. *et al.* The influence of anti-inflammatory medication on exercise-induced myogenic precursor cell responses in humans. *J Appl Physiol* **103**, 425–431, <https://doi.org/10.1152/jappphysiol.00157.2007> (2007).
43. van de Vyver, M. & Myburgh, K. H. Cytokine and satellite cell responses to muscle damage: interpretation and possible confounding factors in human studies. *J Muscle Res Cell Motil* **33**, 177–185, <https://doi.org/10.1007/s10974-012-9303-z> (2012).
44. Li, Y. P. *et al.* TNF- α acts via p38 MAPK to stimulate expression of the ubiquitin ligase atrogin1/MAFbx in skeletal muscle. *Faseb J* **19**, 362–370, <https://doi.org/10.1096/fj.04-2364com> (2005).
45. Eom, G. H. *et al.* Histone Methyltransferase SETD3 Regulates Muscle Differentiation. *Journal of Biological Chemistry* **286**, 34733–34742, <https://doi.org/10.1074/jbc.M110.203307> (2011).
46. Jaworski, K. *et al.* AdPLA ablation increases lipolysis and prevents obesity induced by high-fat feeding or leptin deficiency. *Nature medicine* **15**, 159–168, <https://doi.org/10.1038/nm.1904> (2009).
47. Kleaveland, B. *et al.* Regulation of cardiovascular development and integrity by the heart of glass-cerebral cavernous malformation protein pathway. *Nature medicine* **15**, 169–176, <https://doi.org/10.1038/nm.1918> (2009).
48. Tsuji, S. *et al.* HEG1 is a novel mucin-like membrane protein that serves as a diagnostic and therapeutic target for malignant mesothelioma. *Scientific reports* **7**, 45768, <https://doi.org/10.1038/srep45768> (2017).

49. Callaghan, M. J. *et al.* Identification of a human HECT family protein with homology to the *Drosophila* tumor suppressor gene hyperplastic discs. *Oncogene* **17**, 3479–3491, <https://doi.org/10.1038/sj.onc.1202249> (1998).
50. Buetow, L. & Huang, D. T. Structural insights into the catalysis and regulation of E3 ubiquitin ligases. *Nature reviews. Molecular cell biology* **17**, 626–642, <https://doi.org/10.1038/nrm.2016.91> (2016).
51. Bodine, S. C. *et al.* Identification of ubiquitin ligases required for skeletal muscle atrophy. *Science* **294**, 1704–1708, <https://doi.org/10.1126/science.1065874> (2001).
52. Sartori, R. *et al.* BMP signaling controls muscle mass. *Nature genetics* **45**, 1309–1318, <https://doi.org/10.1038/ng.2772> (2013).
53. Hu, G. *et al.* Modulation of myocardin function by the ubiquitin E3 ligase UBR5. *The Journal of biological chemistry* **285**, 11800–11809, <https://doi.org/10.1074/jbc.M109.079384> (2010).
54. Wang, Z., Wang, D. Z., Pipes, G. C. & Olson, E. N. Myocardin is a master regulator of smooth muscle gene expression. *Proceedings of the National Academy of Sciences of the United States of America* **100**, 7129–7134, <https://doi.org/10.1073/pnas.1232341100> (2003).
55. Meadows, S. M., Warkman, A. S., Salanga, M. C., Small, E. M. & Krieg, P. A. The myocardin-related transcription factor, MASTR, cooperates with MyoD to activate skeletal muscle gene expression. *Proceedings of the National Academy of Sciences of the United States of America* **105**, 1545–1550, <https://doi.org/10.1073/pnas.0703918105> (2008).
56. Long, X., Creemers, E. E., Wang, D. Z., Olson, E. N. & Miano, J. M. Myocardin is a bifunctional switch for smooth versus skeletal muscle differentiation. *Proceedings of the National Academy of Sciences of the United States of America* **104**, 16570–16575, <https://doi.org/10.1073/pnas.0708253104> (2007).
57. Muráni, E., Murániová, M., Ponsuksili, S., Schellander, K. & Wimmers, K. Identification of genes differentially expressed during prenatal development of skeletal muscle in two pig breeds differing in muscularity. *BMC Developmental Biology* **7**, 109, <https://doi.org/10.1186/1471-213x-7-109> (2007).
58. Kong, X. *et al.* Distinct functions of human cohesin-SA1 and cohesin-SA2 in double-strand break repair. *Mol Cell Biol* **34**, 685–698, <https://doi.org/10.1128/mcb.01503-13> (2014).

Acknowledgements

This work was funded by a PhD studentship for Robert A. Seaborne by the Doctoral Training Alliance UK/LJMU/Keele University awarded via Adam P. Sharples (PI). Genome-wide methylation/gene expression studies were funded by a GlaxoSmithKline grant awarded to Adam P. Sharples (PI).

Author Contributions

Sharples conceived experiments, Sharples and Seaborne designed experiments and research methodology, performed the research and data collection, analysed all the data and wrote the manuscript. Sharples, Seaborne, Strauss, Cocks, Shepherd, O'Brien, van Someren, Bell, Murgatroyd, Morton, Stewart provided expertise for sample, data collection and analysis. All authors reviewed the manuscript drafts and inputted corrections, amendments and their expertise.

Additional Information

Supplementary information accompanies this paper at <https://doi.org/10.1038/s41598-018-20287-3>.

Competing Interests: The authors declare that they have no competing interests.

Publisher's note: Springer Nature remains neutral with regard to jurisdictional claims in published maps and institutional affiliations.



Open Access This article is licensed under a Creative Commons Attribution 4.0 International License, which permits use, sharing, adaptation, distribution and reproduction in any medium or format, as long as you give appropriate credit to the original author(s) and the source, provide a link to the Creative Commons license, and indicate if changes were made. The images or other third party material in this article are included in the article's Creative Commons license, unless indicated otherwise in a credit line to the material. If material is not included in the article's Creative Commons license and your intended use is not permitted by statutory regulation or exceeds the permitted use, you will need to obtain permission directly from the copyright holder. To view a copy of this license, visit <http://creativecommons.org/licenses/by/4.0/>.

© The Author(s) 2018